SELF FLOWING REFRACTORY CASTABLES: STUDY OF THE HYDRAULIC BOND AND CERAMIC MATRIX FORMATION

by Florin Esanu

M. A. Sc., Polytechnic University of Bucharest, 1992

A THESIS SUBMITTED IN PARTIAL FULFILLMENT OF THE REQUIREMENTS
FOR THE DEGREE OF DOCTOR OF PHILOSOPHY

THE FACULTY OF GRADUATE STUDIES
DEPARTMENT OF METALS AND MATERIALS ENGINEERING

WE ACCEPT THIS THESIS AS CONFORMING
TO THE REQUIRED STANDARDS

The University of British Columbia

January 2000

In presenting this thesis in partial fulfilment of the requirements for an advanced degree at the University of British Columbia, I agree that the Library shall make it freely available for reference and study. I further agree that permission for extensive copying of this thesis for scholarly purposes may be granted by the head of my department or by his or her representatives. It is understood that copying or publication of this thesis for financial gain shall not be allowed without my written permission.

Department of _METALS AND MATERIALS ENGINEERING_

The University of British Columbia
Vancouver, Canada

Date _NOVEMBER 28, 2000_

DE-6 (2/88)

ABSTRACT

Refractories are *enabling* materials in that their primary function is to facilitate the production of other materials such as metals, glasses, petrochemicals, and cements. They have enabled the utilization of heat to make materials since the Bronze Age. Although, in recent years, a number of studies concerning the many complex variables that determine the rheologic, hydraulic and ceramic properties of Advanced Refractory Castables (ARC) have been performed, the fundamentals of free-flow and of transition from a hydraulic to a ceramic matrix are still only poorly understood.

The aim of this study is to provide a scientific base for understanding the flow behavior of ARC and its influence on the formation of ceramic. For this purpose the flow behavior of a series of low, ultra-low and no cement ARC compositions was analyzed. A method for measuring the viscosity of the binding system of ARC was developed. This method allowed for the first time the study of a direct correlation between the rheology of the matrix and the flow of a castable, and therefore a precise and scientific base for determining the influence of different dispersant additives.

The rheological parameters of ARC compositions for different amounts of water, silica fume purity, content and type of refractory aggregate were correlated with mechanical strength at high temperatures.

Based on the experimental and theoretical work carried out in this study a thorough characterization of the rheology of self-flowing castable refractories was performed. The rheological conditions that allow the early formation of the hydraulic matrix were identified. A new concept of interaction (Flash Flocculation) between the binding system and the spray gunning admixtures was developed. This concept was materialized in a novel type of spray-gunning admixture. Laboratory studies as well as a pilot scale experiment confirmed the superiority of the flash flocculating admixture over the setting accelerators, which are currently used as spray gunning admixtures.

TABLE OF CONTENTS

LIST OF FIGURES

LIST OF TABLES

LIST OF SYMBOLS AND ABBREVIATIONS

ABBREVIATIONS

A1000   Calcined alumina A1000SGD, Alcan

A3000   Calcined alumina A3000FL, Alcan

AC34B5   Calcined Alumina AC 34B5, Pechiney

APA   Amonium Polyacrylate

ARC   Advanced Refractory Castables

ASTM   American Society for Testing and Materials

BS   Binding Sytem

CAC   Calcium Aluminate Cement

CRC   Conventional Refractory Castables

CCS   Cold Compression Strength

CPFT   Cumulative Percent Finer Than

DoE   Design of Experiments

EDS   Energy Dispersive Spectroscopy

FF   Flash Flocculation

FFAS   Flash-Flocculating Admixture Solutions

HAB   Hydraulic Alumina Binder

HMOR   Hot Modulus of Rupture

LCC   Low Cement Castables

MAS   Matrix Advantage Sytems

LS   Modified Ligno-Sulfonate Materials

MOR	Modulus of Rupture
NCC	No Cement Castables
PMS	Sulfonated Melamyneformaldehyde Polymers
PGA	Calcined alumina PGA
PNS	Sulfonated Naphtaleneformaldehyde Polymers
SF1	silica fume Elkem 971U, Elkem Norway
SF2	silica fume Globe Metallurgical, Globe Inc.
SF3	silica fume Duralum AB, Washington Mills Ltd.
SFF	Silica Fume Free (Castables)
SHMP	Sodium Hexametaphosphate
SMA	Sodium Metacrylate
SMC	Shear Modulus Constant
SRC	Shear Rate Constant
SNFC	Sodium Naphtalenesulfonate Formaldehyde Polycondensate
SPA	Sodium Polyacrylate
SPMA	Sodium Polymetacrylate
STPP	Sodium Tripolyphosphate
ULCC	Ultra Low Cement Castables
XRD	X-Ray Diffraction

LATIN SYMBOLS

q	Andreassen exponent
w	water content (wt%)
w_0	normal water content

w/c	water to cement ratio
w/s	water to solid ratio

GREEK SYMBOLS

α	parameter of the central composite design (distance from the center of a composite design to a star point)
η	viscosity
η_o	initial viscosity in Eq. (2) p. 30
η_r	high viscosity characteristic in Eq. (2) p. 30
γ	shear rate
σ_y	yield stress
σ	shear stress
θ	constant depending on the type of admixture in Eq. (1) p.16

ACKNOWLEDGEMENTS

1. INTRODUCTION

Refractories are *enabling* materials in that their primary function is to facilitate the production of other materials such as metals, glasses, petrochemicals, and cements. They have enabled the utilization of heat to make materials since the Bronze Age. Like many other industrial fields, the refractory industry has seen a tremendous technical progress in the 1990's. The steel industry, the major consumer of refractories (> 60% of all refractories used[1]), has completely changed its outlook from production rates to high quality focus. Other refractories consumers such as the aluminum, copper, glass and cement industries have also improved the level of the technology.

As a consequence of these technological changes, the refractories industry has been forced to adapt itself to new operating conditions in those installations where refractories are used. Historically, the driving force for change has been either improved process technology or a desire by the materials producers for higher productivity via longer campaign lives, usually at higher temperatures, achieved by improving the thermomechanical and corrosion-resisting properties of the refractories. More recently factors related to refractories installation have become significant. These factors include labor saving, reduced furnace downtime, alleviation of heavy physical labor, and improvement of working environments in furnace lining installations.

These technological changes are best reflected in the evolution of monolithic refractories. From 1960 to the present there has been a steady increase in the use of monolithic refractories by all refractory-consuming industries at the expense of pre-fired refractories. At least one industry (refining and petrochemical) has moved almost exclusively towards the use of monolithics.

One of the most dramatic increases in the use of refractories occurred with the introduction of Advanced Refractory Castables (ARC). Some of today's ARC represent the most complex refractory formulations, consisting of high-quality precision-sized aggregates, modifying fillers, binders, and a large variety of additives [2].

The versatility of these mixes has created many new applications for refractory products [3-6]. Accordingly to the ASTM C401 definition, a low-cement castable contains between 1.5 and 2.5% CaO, and an ultralow-cement castable, less than 1.5%. For no-cement castables, in order to further reduce the content of CaO, calcium aluminate cement is replaced with a new generation of hydraulic binders (high alumina binders). These refractories, based on the use of a low amount of calcium aluminate cement, have replaced a variety of other monolithics, such as conventional cement castables, plastics, ramming and gunning mixes, as well as many brick compositions. Castable refractories are also widely used because they are easy to apply to any kind of work by trowelling, ramming, casting, vibration casting, or gunning, [7-11].

Any castable refractory may be considered a mix of two components:

- refractory aggregate: the main component (60-85wt.%), consisting of a mixture of refractory grains having sizes over 45 μm;

- binding system (15-40wt%) which contains: the hydraulic binder (high alumina cement or rehydratable alumina), ultrafine powders (microsilica and calcined or reactive alumina), and proprietary mixtures of chemicals, which cumulatively do not exceed 0.3% of the mix. They have different roles in the cement paste rheology and setting process [12].

The essential feature which distinguishes low and ultra-low cement castables from other type of castables, is the presence of the ultrafine components. These ultrafine materials replace part of the cement used in conventional castables. When used with an appropriate dispersant, the ultrafine particles fill the voids between larger particles which would otherwise be filled with

water [13]. Therefore, less water is needed to achieve the casting consistency resulting in a decrease in porosity and increase in bulk density of the installed material. The use of low water content is very important because the performance of a castable is strongly affected by increasing the amount of water for casting. Over-watering by 0.5-1% can reduce strengths in some cases by over 50 % and result in segregation and/or separation when vibrated into place. Self-flowing capability of castables has to be achieved by a cohesive consistency so that the castable could be installed without separation of the fine material or the fluid phase from the coarse aggregate [14].

Due to their nature, castable refractories are complex systems characterized by chemical interactions (generated by the hydraulic binder), colloidal interactions (between the fine particles of the binder system in the presence of water and additives), and solid state or liquid assisted transformations during the firing stage, which generate the ceramic structure [15].

Notwithstanding the excellent progress made in recent years with respect to development of advanced refractory castables, the correlations between the chemical and colloidal interactions occurring during initial stages of processing and their role in development of the ceramic structure are not yet fully understood.

This work was performed in order to examine the influence of the chemistry of hydraulic bond on the development of a ceramic matrix in advanced refractory castables.

2. LITERATURE REVIEW

Conventional refractory castables (CRC) typically contain 15 to 30%* calcium aluminate cement (equivalent to 3 to 11% CaO), which acts as a lubricant in water suspensions and as a binder after hardening to give mechanical strength at room temperatures. The cured strength of conventional castables is due to the formation of the various hydrated phases of the cement. When heated, decomposition of the hydrates causes a decrease in strength between 600°C and 1000°C. At temperatures above 1200°C, the calcium oxide will react with silica and alumina to form low melting point anorthite, and respective gehlenite liquids. These liquids will decrease the bond strength, and the corrosion and erosion resistance at high temperatures. The high cement content in conventional castables also requires a relatively high water content (9-12%) that limits the potential of achieving a low porosity. Practical means of reducing the cement and the water levels consist of :

- proprietary mixtures of chemicals, which improve the rheological behavior of the system and the setting process [12].
- ultrafine reactive powders which replace part of the cement of conventional castables and, when used with an appropriate dispersant, fill the voids between larger particles which would otherwise be filled with water [13].

Low cement castables (LCC) have 4-8% calcium aluminate cement (1.5-2.5% CaO) and similar amount of fume silica and alumina. At this low level of cement content the water for casting ranges from 3.5 wt% (vibcasting) to 6.5 wt% (self flowing), which results in much lower porosity (10-15%) for these products. Even at this lower cement content, though, these castables still have too high a percentage of CaO for developing good hot strength, which

---

* Unless otherwise specified, % is equivalent to wt%.

rapidly decreases at 1200-1400°C. At 1500°C, the Al_2O_3-SiO_2-CaO low cement castables have a hot modulus of rupture near zero [38].

Ultra low cement castables (ULCC) have less than 4% calcium aluminate cement (providing less than 1.5% CaO), and their binder system consists mainly of ultrafine powders such as silica fume and reactive alumina. This type of binder system has the advantage of reduced formation of low melting point liquid phases, resulting in high hot strength and an increase in strength with firing temperature. ULCC's have very good thermo-mechanical properties, but because of the low cement content, the setting times are long, making necessary the use of setting time accelerators. Also, the flow of these castables is very sensitive to minor variations in composition pH, and to the presence of impurities.

No cement castables (NCC) are new materials that use special Hydraulic Alumina Binders (HAB) instead of calcium aluminate cement (CAC). Hydraulic Alumina Binders represent a new generation of hydraulic binders characterized by a very low content of calcium oxide (<0.1%) that made possible the design of calcium-free binding systems. In addition, these compositions have setting characteristics that are easier to adjust than for ULCC's.

The nature of the hydraulic binder (CAC or HAB) determines the evolution of the hydraulic setting process and the nature of hydraulic products that are formed. The setting process is also influenced by the amount of water in the system and by the effect of proprietary chemical admixtures which can have an accelerating or retarding action.

The challenge of designing a hydraulic binder system is to simultaneously control the rheology of the mix and the hydraulic setting process, and to obtain a ceramic texture with good mechanical strength at high temperatures. The obstacles of a successful design are generated by insufficient understanding of the complex interactions between the hydraulic binder, the flow and setting additives and their influence on the characteristics of ceramic obtained after firing.

2.1. Hydration

The thick slurry formed by the mixing of a hydraulic cement with water and aggregate is called a paste. Setting is the initial stiffening, usually occurring within several hours and hardening is the development of strength over a longer period of time. Setting and hardening occur due to chemical reactions, which are collectively described as hydration, despite the fact that these processes are more complicated than the formation of an insoluble hydrate from an anhydrous salt [15].

2.1.1. Hydration of hydraulic binders

The most common hydraulic binders of castable refractories are calcium aluminate cements with more than 70% alumina, having as mineral phases $C_{12}A_7$, CA, CA_2, and α-Al_2O_3 (where C=CaO, A=Al_2O_3) [15-16]. The major phase in these cements is the monocalcium aluminate (CA) which imparts high mechanical strength and refractoriness to the cement whereas rapid setting is associated with the presence of $C_{12}A_7$ which dissolves rapidly in water. The hydration of calcium aluminates in a refractory cement is a complex process, not yet fully understood [17]. The main crystalline products of hydration are CAH_{10}, C_2AH_8, C_3AH_6, and AH_3,

Table 2.1-1. Main hydration products of calcium aluminate cement pastes [19].

Temperature	Hydration Products
< 21°C	CAH_{10}, aluminous gel
21-35°C	C_2AH_8, aluminous gel + crystalline AH_3
>35°C	C_3AH_6 + crystalline AH_3

(where H=H_2O) their formation being dependent on ambient temperature [18]. Figure 2.1-1 shows schematically the formation of the main hydration products of cement pastes [19].

The most stable calcium aluminate hydrates are the cubic C_3AH_6 and AH_3, while the hexagonal CAH_{10} and C_2AH_8 are metastable and convert to the more stable cubic structures:

$$3\ CAH_{10} \rightarrow C_3AH_6 + 2AH_3 + 18H_2O \qquad (1)$$

$$3\ C_2AH_8 \rightarrow 2C_3AH_6 + AH_3 + 9H_2O \qquad (2)$$

$$C_2AH_8 + CAH_{10} \rightarrow C_3AH_6 + AH_3 + 9H_2O \qquad (3)$$

Figure 2.1-1. Hydration of calcium aluminate cement particles [19].

The proposed mechanism of hydration for calcium aluminate cement [20] starts with an induction period, when the hydration rate is extremely low. A tarnishing type of reaction takes place, in which a layer of amorphous hydrates is formed over the entire surface of the cement

particles. When the hydration layer grows to reach a critical thickness, the stress caused by intruding molecules of water ruptures the layer. As a consequence, the diffusion barrier is removed and the induction period ends. The reaction as a whole accelerates with the formation of crystalline nuclei of metastable hexagonal hydrates that grow by a dissolution-crystallization mechanism. Depending on the initial crystallinity of the calcium aluminate, CAH_{10} can be detected after 6 to 24 hours and C_2AH_8 after 24 hours [21]. The conversion of metastable hexagonal hydrates to stable cubic hydrates results in a volume reduction of 53% for CAH_{10} to C_3AH_6 transformation, and 16% for C_2AH_8 to C_3AH_6 transformation. This volume reduction is responsible for an increase in open porosity and a subsequent decrease in strength [17, 22].

A similar hydration mechanism takes place during the hydration of Hydraulic Alumina Binders (HAB). This new generation of hydraulic binders for advanced castables is based on the amorphous meso-phase of transition of alumina (ρ-alumina) which reacts with water to form a hydraulic bond. HAB can be produced either by dehydration of Gibbsite in vacuum at 600°C or by a brief contact with hot air blast at 600 to 900°C. A commercially available HAB contains about 60% ρ-alumina, a small content of χ-alumina and residual aluminum hydroxide (Gibbsite) and can be used as a direct replacement for calcium aluminate cement. ρ- Alumina reacts with water at room temperature by the following process [23] :

$$2 \; \rho\text{-}Al_2O_3 + (4+x) \; H_2O \rightarrow Al_2O_3 \cdot 3H_2O + Al_2O_3 \cdot (1+x) \; H_2O \qquad (x=0\ldots1) \qquad (4)$$

$$\text{Bayerite} \qquad \text{Bohemite gel}$$
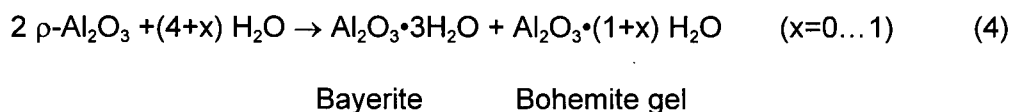
There are several commercially available HAB produced by Alcan Chemicals Limited (Actibond 101 and Actibond 102) and Alcoa Industrial Chemicals (Alphabond 100 and Alphabond 200). Alcan Chemicals has announced the release of HAB products (XAA series) having improved green strength whilst retaining other refractory properties [24]. One of the characteristics of hydration of HAB is that the amorphous phase of hydration (bohemite gel) is

8

not prone to transformation into a final crystalline product [23]. Table 2.1-2 shows typical

chemical and physical properties of HAB developed by Alcan Chemicals (Actibond and XAA

series) and Alcoa Chemicals (Alphabond). Although the hydration behavior of the hydraulic

binders (CAC and HAB) for castable refractories is not yet fully understood there are some

essential features that may be highlighted:

- The dormant period that follows the initial hydration is due to the development of amorphous

  phases and allows the self-flow behavior and the installation of the castable material.

- The setting occurs when the amorphous layer present on the surface of cement particle is

  transformed by a dissolution-crystallization mechanism.

Compared to calcium silicate cements, whose hydration has been thoroughly studied,

very little or contradictory results are found for high alumina compounds. The results of

research concerning the role of the degree of crystallinity of calcium aluminates are more

scattered [21]. In order to fulfill the need for a better understanding of the hydration process,

most of the research is directed to the analysis of hydration of synthetic high-purity calcium

aluminates with controlled properties [17,21,22]. The complexity of the hydration process and of

the subsequent transformations are the main obstacle in approaching the fundamental studies

on colloidal interactions occurring in the binding system of castable refractories, where besides

the hydraulic binder chemical additives and ultrafine reactive particles are also present.

Table 2.1-2. Typical chemical and physical properties of HAB [24,25].

HAB Products	XAA2004 XAA2005	Actibond 101 Actibond 102	Alphabond 100 Alphabond 200
Al_2O_3 (%)	86	>86	90
Na_2O (total) (%)	0.36	0.4	0.5
Na_2O (soluble) (%)	0.03	0.03	
Fe_2O_3 (%)	0.02	0.02	
SiO_2 (%)	0.02	0.02	0.2
CaO (%)	0.03	0.03	<0.1
L.O.I. (%)	~12	~12	~8
Specific surface area (m^2/g)	190-260	190-261	271

2.1.2. Setting

A characteristic phenomenon of the hydration of calcium aluminates is the anomalous setting behavior. As the temperature of hydration is increased, the setting time becomes longer until it reaches a maximum value at around 28°C. Above this temperature the setting time decreases rapidly with increasing temperature. This phenomenon has been proven for commercial grades of calcium aluminate cement as well as for pure monocalcium aluminate [26].

Studies of the effect of temperature on the hydration of commercial cements, and synthetic samples containing CA and CA-CA$_2$ mixtures concluded that the cause for the anomalous setting behavior is the difficult nucleation of calcium aluminate hydrates at around 28°C [27]. At much lower temperatures, formation of CAH$_{10}$ occurs readily. As the temperature increases, formation of this hydrate becomes less favorable on thermodynamic grounds. Additional amorphous products are probably formed and the setting time becomes longer [28]. At around 28°C, nucleation of CAH$_{10}$ becomes increasingly difficult, but the rate of formation of the second metastable phase (C$_2$AH$_8$) is still sluggish, perhaps because of the slow growth of the nuclei. The thermodynamically stable C$_3$AH$_6$ can be formed at this temperature only by conversion of the metastable hexagonal hydrates. Therefore, in the critical range from 25 to 30°C, precipitation of the hydrates takes much longer time than at other temperatures, because none of the crystalline hydrates associated with calcium aluminate cement forms readily [28]. This mechanism was also supported by the investigations on calcium aluminate hydration in the presence of admixtures of C$_2$AH$_8$ and CAH$_{10}$. It was determined that addition of crystalline hydrates as low as 10% eliminates the anomalous behavior [26].

Because of the peculiarities of the calcium aluminate cements hydration, and in order to favorably modify the properties of freshly mixed or hardened refractory castables (to control the

flow properties and the working and setting time), different chemical admixtures are generally used [29].

The effect of the setting additives can be followed by measurements on the hydraulic binder pastes (Vicat method, electrical conductivity or microcalorimetry) or, in an indirect way, by flow measurements of the whole castable in order to assess the influence of the admixture on the working time. Typically, a chemical admixture may modify more than one property, e.g. a specific additive may increase the working time as well as reduce the water requirement. In practice, the placement of the refractory castable may involve the use of two or more admixtures simultaneously, leading to complex interactions [30].

Setting retarders influence the kinetics of hydration by slowing down the dissolution of anhydrous cement particles. The mechanism proceeds by blocking the dissolution, by adsorption onto the cement grain and/or generating combinations with calcium ions. Typically, retarders are hydroxylated carboxylic acids (such as citric, gluconic or tartric acid) and their derivative alkaline (most commonly sodium) salts [31]. Some of the plasticizer admixtures can have a secondary effect, of retarding the setting time. A typical example is sodium hexa meta phosphate (SHMP), that may react with calcium ions in solution to form a complex salt :

$$2Ca^{2+} + (Na_4P_6O_{18})^{2-} \rightarrow 4Na^+ + (Ca_2P_6O_{18})^{2-} \qquad (5)$$
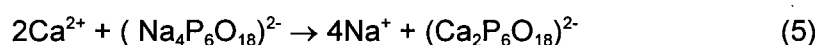
This activity will not only modify the ratio of calcium to aluminate ions in solution, but will also change the rate of dissolution of monocalcium aluminate [30]. The effect of a setting retarder depends on the temperature, the level of admixture and the composition of the castable (type of hydraulic binder, presence of other admixtures and presence of ultrafine powders).

The variation of setting time of CAC CA-14M Alcoa with the temperature for different levels of admixture of citric acid is shown in Figure 2.1-2. An increase in the amount of citric acid does not always bring a greater retardation. The setting time is usually lower in the

presence of 0.75% citric acid than in the presence of 0.5%. The results for 0.25%, which have been omitted in Figure 2.1-2 for clarity reasons, were very similar to 0.5%. Another interesting aspect is that addition of 1% citric acid resulted in maximum setting time at 28°C, as in the absence of any admixture, while additions in the range of 0.25-0.75% resulted in a maximum setting time at around 20°C [30].

Experimental results show, Figure 2.1-3 [16], that even though sodium gluconate is the most effective retardant (ten times more effective than boric acid and sodium citrate), the effect of each admixture depends on the nature of the calcium aluminate phase. The temperature has a very strong influence on the retardant effect of boric acid (compositions C1-C3 in Table 2.1-3). Also the data for the explosion test show that even at a high level of addition of boric acid, the temperature is the deciding factor in the structure of hydration products. By correlating the mechanical strengths after curing and drying with the curing time of castables (C1, C4, C5, and C6), it appears that even if the dissolution of aluminate cement is considered complete after 24 hours, the conversion reactions are not completed after 72 hours. It appears that by increasing the content of alumina cement (from 5% to maximum 15%), there is no significant decrease in setting time as a function of the content of alumina cement (C1, C7, C8 and C9). In this study [16] no direct correlation between the flow values and level of admixture and level of calcium aluminate cement has been observed.

In the case of ultra-low cement and no-cement castables, due to the low levels of hydraulic binder and high content of ultrafine powders (such as microsilica and reactive alumina), the hydration process is delayed and there is a need for the use of accelerator admixtures [22, 32]. It is believed that accelerators influence the dormant period of hydration by forming nuclei of crystallization which reduce the time necessary for homogeneous nucleation from the amorphous phase of calcium aluminate [32, 33].
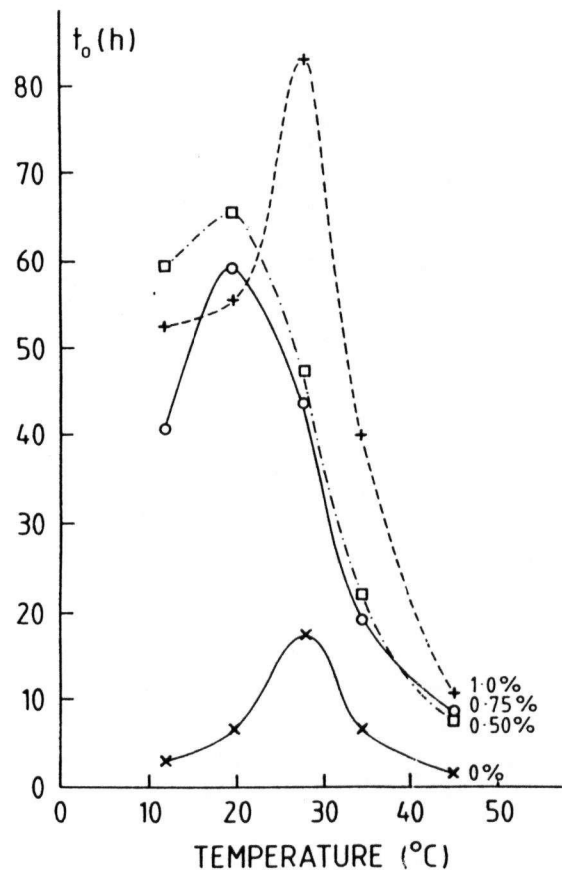
Figure 2.1-2. Variation of setting time of calcium aluminate cement CA-14M, with temperature for different levels of Citric Acid [30].
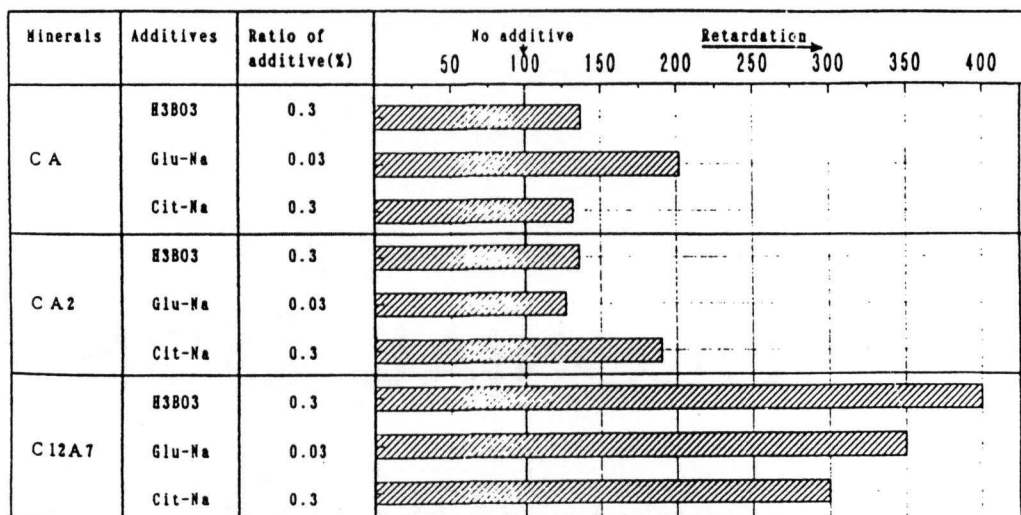
Figure 2.1-3. Effect of setting time retarders on different calcium aluminates [16].

Table 2.1-3. Properties and composition of experimental CAC based castables [16].

Number of Castables	C1	C2	C3	C4	C5	C6	C7	C8	C9
Alumina Cement(%)	5	5	5	5	5	5	2	10	15
Additives(%) Sodium Hexametaphosphate	0.05	0.05	0.05	0.05	0.05	0.05	0.05	0.05	0.05
Boric acid(%)	0.02	0.01	0.03	0.02	0.02	0.02	0.02	0.02	0.02
Curing temperature(°C)	20	5	35	20	20	20	20	20	20
Curing time(h)	24	24	24	11	16	72	24	24	24
Properties of Castable Flow value(mm)※1	202	180	197	—	—	—	183	202	158
Hardening Time(hr:min)※2	6:20	17:30	2:50	—	—	—	9:20	6:15	6:45
Modulus of rupture(MPa) after Curing	3.6	1.8	3.3	0.3	1.8	4.2	1.2	7.7	11.0
after Dring	6.6	4.1	7.1	5.2	4.2	7.6	3.0	17.8	23.3
Crushing strength(MPa) after Curing	13.8	13.6	11.7	1.8	7.0	17.8	4.5	34.5	62.1
after Dring	37.4	24.0	38.2	30.3	27.1	37.8	13.7	88.0	128.7
Explosion Test※3 600°C	OOO	OOO	OOO	OOO	OOO	OOO	OOO	OOO	OOO
700°C	OOO	OOO	OOO	OOO	OOO	OOO	xxx	OOO	OOO
800°C	OOO	OOx	OOO	OOx	OOx	OOO	xxx	OOx	Oxx
900°C	OOx	Oxx	OOO	xxx	xxx	OOO	xxx	OOx	Oxx
1000°C	xxx	xxx	OOO	xxx	xxx	OOO	xxx	xxx	xxx
1100°C	xxx	xxx	OOO	xxx	xxx	OOO	xxx	xxx	xxx
1200°C	xxx	xxx	OOx	xxx	xxx	xxx	xxx	xxx	xxx

※1 Vibration Flow(10sec)
※2 Heat evolution Time
※3 ×:Explosion,O:non

The most common and most effective accelerator for CAC is lithium carbonate. Other lithium containing chemicals, such as lithium hydroxide and lithium chloride, are more soluble, react more violently and are therefore more difficult to use [30, 33]. It is considered that, in solution, the lithium ions interact with the amorphous $Al(OH)_4^-$ groups to precipitate insoluble lithium aluminate thereby increasing the $Ca^{2+}/Al(OH)_4^-$ ratio [31,33]. This conclusion is also supported by studies of hydration of pure monocalcium aluminate and CAC Alcoa CA-25 in the presence of 0.7wt.%LiCl, which found the presence of C_2AH_8 at 12°C and C_4AH_{10} at 25°C. Neither of these hydrates are normal reaction products at low temperatures in the absence of lithium salts [30, 34].

All the alkaline salts have an acceleration effect on CAC, which decreases with the atomic number of the cation (Table 2.1-4). The influence of the anion component on the setting time is not yet understood [35]. As in the case of setting time retarders, the effect of the accelerators is specific to each of the calcium aluminate phases (Figure 2.1-4).

Table 2.1-4. Experimental values for setting time for CAC Ciment Fondu Lafarge with 0.01% alkali salts admixtures [35].

Anions	OH^-	Cl^-	$HCOO^-$	F^-	CH_3COO^-	PO_4^{3-}
Cations	Setting time (s) (16110 s for pure cement)					
Li^+	290	340	370	650	925	1260
Na^+	5060	9240	10680	1720	9560	9300
K^+	7120	9660	10950	4400	10560	10680
Rb^+	9010	10100	NA	5180	10830	10800
Cs^+	10940	11150	11520	5780	11030	10950

Minerals	Additives	Ratio of additive(%)	Acceleration ← → No additive Retardation
C A	Li2CO3	0.01	
	Ca(OH)2	0.3	
	Na2CO3	0.3	
C A2	Li2CO3	0.01	
	Ca(OH)2	0.3	
	Na2CO3	0.3	
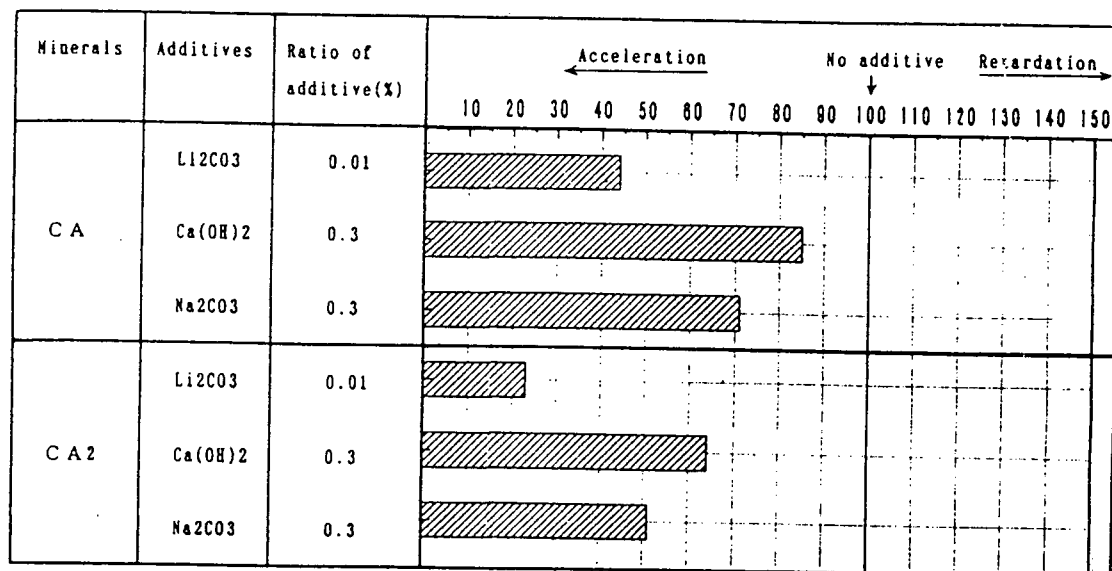
Figure 2.1-4. The relative individual effect on setting time of monocalcium aluminate (CA) and dicalcium aluminate (CA_2) phases [16].

The effect of combination of accelerators and retarders may be studied by measurements of electric conductivity on fresh cement pastes. The electric conductivity is proportional to the degree of hydration [36]. The combination of accelerators and retarders is possible, in the same castable mix, and is recommended because the effects do not necessary cancel each other out, but intervene at different stages of the hydration process (Figure 2.1-5). By using lithium carbonate as an accelerator for CAC (for example Ciment Fondu Lafarge), the setting time may be too short. Additional use of citric acid adjusts the setting without interfering strongly with the total setting time [33].
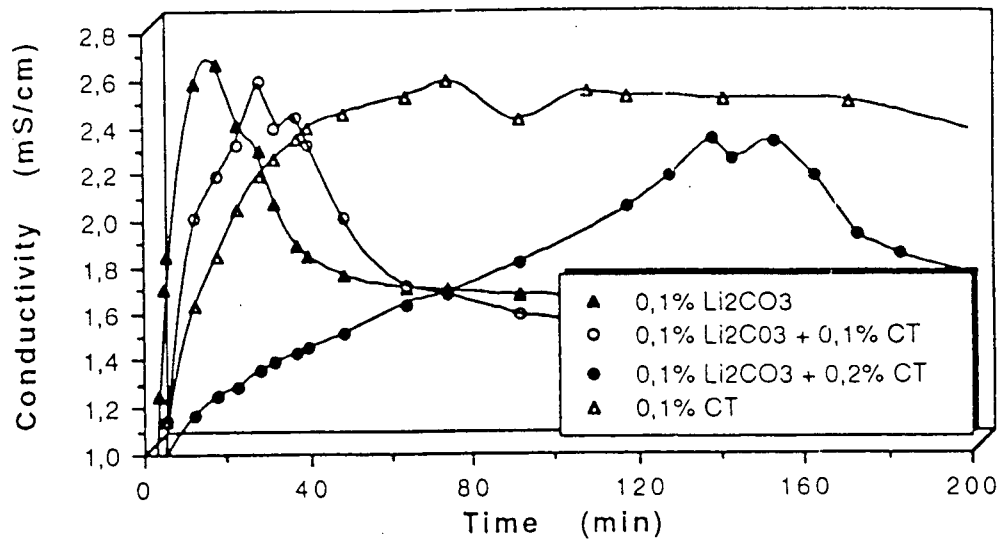
Figure 2.1-5. The effect of lithium carbonate and sodium citrate mixtures on electric conductivity of Ciment Fondu Lafarge pastes (CT= Sodium Citrate) [33].

Studies by Kondo et. al . [38] of the effect of six undisclosed setting additives on 50% and 60% alumina castables resulted in the description of the setting time of the castable by the following formula:

$$\ln(t_h) = A(10^3/T) - B + \theta X \qquad (1)$$

16

,where :

t_h - setting time (hours);

A, B - constants depending castable characteristics ;

θ -constant depending on the type of admixture;

X -concentration of accelerator (wt%)

T –temperature (K)

The setting process of HAB is similar to that of CAC in the sense that hydration of ρ-alumina markedly depends on curing temperature, being very slow at 5°C and rapid at 30°C. It also depends on the water/alumina ratio, the formation of Bayerite being reduced at smaller ratios [23,24]. It is possible to adjust the setting time of an ultra-low cement castable by accelerating the cement hydration with hydraulic alumina or vice versa [38].

In the case of ULCC with high content of silica fume (higher than 6 wt%), sodium tripolyphosphate (STPP) may have a dual role, acting both as a dispersing agent and as a setting accelerator. It is thought that the sodium from the dispersant would combine in solution with aluminate ions to form $Na^+Al(OH)_4^-$. This reaction would increase the $Al(OH)_4^-$ concentration, and thus (applying Le Chatellier's principle) would increase the rate of nucleation of calcium aluminate hydrates [39]. In fact, sodium aluminate is a strong setting accelerator, being very effective for ultra-low and no- cement castables [40].

At present, the mechanisms of hydraulic setting process are not fully understood. The setting behavior depends on: temperature, the nature and content of hydraulic binder, the presence of ultrafine powders, and the nature and content of admixtures. Because of the complexity of the processes, and the large number of variables, the selection of type and concentration of setting additive is made empirically by trial and error.

17

2.1.3. Interaction between hydraulic binder and reactive particles

In a colloidal system that contains a hydraulic binder, it can be usually assumed that the aggregate undergoes only surface reactions with the cement [15]. In the case of ARC, there is a high content of ultrafine reactive powders which, due to their high specific surface, do not act just as inert fillers but play a major role in the chemical and physical equilibria [13]. Materials typically used as ultrafine ingredients in low, ultra-low and no-cement castables include: reactive alumina, microsilica (silica fume), silicon carbide, chrome oxide and alumino-silicate minerals [40].

The name "microsilica" was introduced by Elkem A/S as a term for the silicon dioxide material obtained by the cleaning, classification, and homogenization of the silica fume produced by the smelting of silicon metal and ferrosilicon in an electric arc furnace [41]. Silica fume is composed of very fine (average diameter $\approx 0.1 \mu m$) spheres of amorphous silicon dioxide having a wide particle size distribution and specific surface values around 10-20 m^2/g [42-43].

It is well known that in an aqueous suspension with cement, following the chemisorption of Ca^{2+} ions on their surface, silica fume particles react at high pH with $Ca(OH)_2$ to form a hydrated layer of calcium silicate. The overall reaction may be expressed as:

$$SiO_2 + nCa(OH)_2 + mH_2O \rightarrow nCaO\bullet SiO_2\bullet(m+n)H_2O \qquad (6)$$

Adsorption of OH^- ions leads to an increase of the coordination number of silicon atoms on the surface of silica fume particles, which consequently weakens the oxygen bonds to the underlying silicon atoms and as a result silicon atoms go into solution as silicic acid [44]. The dissolution of silica fume depends on the OH^- concentration per unit surface, which is determined by specific surface, quantity of silica fume, and the pH of the solution [45]. It is possible that the formation of calcium silicate hydrates decreases the concentration of calcium

ions and decreases the ratio of calcium to aluminate ions in solution. This may explain the retardant effect of the silica fume particles on the hydration of CAC and HAB in castable refractories.

Studies carried out on the hydration of CAC Secar 51 and Secar 80 (Lafarge) showed that the main change in the hydration process is the formation of gehlenite hydrate (C_2ASH_8). In contrast to C_2AH_8 , the C_2ASH_8 phase is stable after very long curing times and is therefore expected to have a positive effect on the mechanical strength after curing. Although crystals of gehlenite hydrate may form at temperatures as low as 20°C, they are the main phase formed during hydration at 40-70°C according to the following reaction [46]:

$$C_2AH_8 + S \rightarrow C_2ASH_8 \qquad (7)$$

In the microsilica-blended cement pastes hydrated at 40°C and fired at 1000°C the gehlenite remains one of the major crystalline phases, together with cristoballite and anorthite that is formed by direct reaction between calcium aluminates and silica [41]. The interaction between silica fume and CAC is influenced by the presence of plasticizers such as sodium tripolyphosphate (STPP). The precipitation of insoluble calcium tripolyphosphate at low phosphate concentrations (up to 0.5wt%) gives a retardant effect while at high concentrations (from 0.75wt% up to 3%) there is an accelerating effect, increasing with the concentration of the admixture and specific surface area of silica fume [39]. The behavior of the silica fume-CAC -STPP system is further complicated by the fact that the reaction between silica fume and CAC can also lead to an amorphous precipitate, much like the C-S-H product in Portland Cement hydration [47].

In pastes of CAC (Secar 71 Lafarge) and silica fume hydrated at 20°C, C_2ASH_8 is the main crystalline phase (some $CASH_{10}$ occurring for high surface area silica fume) formed at low levels of STPP (0.2wt%). By increasing the level of STPP to 0.75 wt %, C_2AH_8 may also be observed [48].

At 25°C, the hydration behavior of silica fume/monocalcium aluminate mixes depends on the water/cement ratio. For binary mixes containing more than 25wt% silica fume, the precipitation of calcium aluminate hydrates is delayed for up to 3 days. In mixes containing 75wt% silica fume and 25wt% monocalcium aluminate, at a water/cement ratio of 0.8, the presence of C_2ASH_8 was detected after 1 to 3 days of hydration. However, at water/cement ratio of 2.0 the presence of C_2ASH_8 could not be detected [22].

Regarding the influence of alumina additions on hydration of calcium aluminate cement, it was found that the specific surface and the Na_2O content are determining factors. During early hydration of monocalcium aluminate in the presence of reactive alumina, a significant amount of Na^+ ions is released into solution, leading to high values of $Al(OH)_4^-$ concentration, low CaO/Al_2O_3 ratios (<0.1) in the liquid phases and, as a result, to an accelerated hydration [32]. These changes in the composition of the solution are due to reorganization reactions in the first reaction layer present on monocalcium aluminate and alumina particles [50].

The existence of an initial reaction layer, not only on the surface of CAC but also on the surface of the particles of alumina, is substantiated by the behavior of alumina suspensions in $Ca(OH)_2$ saturated solutions. The proportion of the $Ca(OH)_2$ adsorbed on this reaction layer varies from 8% to 72% of the total $Ca(OH)_2$ available in solution (20.9mmol/l) and increases with the specific surface of alumina particles. Further evidence is provided by the formation of C_2AH_8 on the surface of alumina grains in saturated solutions of $Ca(OH)_2$ [51].

At a constant content of Na_2O, the specific surface area seems to control the hydration process. By increasing the surface area of reactive alumina, the hydration is accelerated [32]. It is not clear if this effect of the high specific surface aluminas is produced only by an increase of $Al(OH)_4^-$ concentration. At higher specific surface area of reactive aluminas, there is also present a retarding effect probably generated by higher consumption (by superficial adsorption) of the available water for hydration and a consequent decrease in water/cement ratio [51]. The

increase in hydration speed of monocalcium aluminate in the presence of reactive alumina of different surface areas may be studied by microcalorimetry and is presented in Figure 2.1-6. [32].
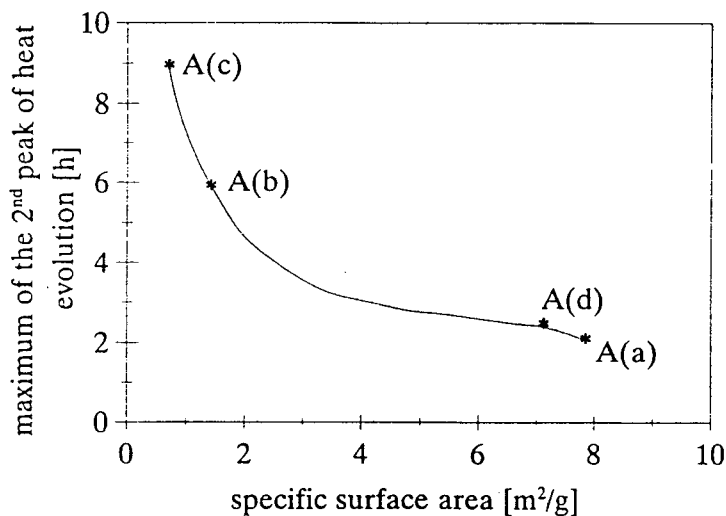
Figure 2.1-6. Evolution of heat of hydration in CA/alumina mixes with the specific surface area of four different types of alumina [32].

Investigations on the influence of reactive alumina on the setting time of CAC, based on conductivity measurements, showed that by increasing the specific surface the early precipitation of hexagonal hydrates is delayed [52]. This finding suggests that an increase in specific surface of alumina results in slowing of the hydration process. Neither the calorimetric results (sustaining an accelerating effect of reactive alumina), nor the conductivimetric results (sustaining a retarding effect) are confirmed by experimental studies on LCCs and ULCCs, which showed that the specific surface of alumina and its soda content have no measurable influence on the setting time [40]. This apparent contradiction is resolved if considered that in the presence of reactive alumina, even if the dissolution rate of the anhydrous CAC may be increased, the products of reaction contain large amounts of amorphous material, as confirmed by microstructural studies [32] .

2.2. Rheology

An important rheological feature of ARC is the self-flow property, i.e. flow taking place under the action of gravity without any external energy input such as vibration, pressure etc. It is generally desired to improve the flow properties with a simultaneous increase in refractoriness and hot strength. There are two basic criteria that have to be fulfilled in order to obtain a self-flowing refractory castable:

- the system has to be well dispersed without compromising the hydraulic setting characteristics,

- the "geometric" interaction or friction between particles has to be minimized [53].

The first criterion is necessary and may be accomplished by using good quality superfine powders and proper additives. The second criterion is satisfied by increasing the volume of the fluid phase to amounts exceeding the porosity of the coarse refractory aggregate structure, so that large particles are being forced apart and self-flow may occur. However, unless the liquid phase has a density and viscosity that prevents settling of coarse particles, self flow may be obstructed even at high amounts of viscous phase [54].

Rheological properties of cement and castables are generally studied by empirical methods and which are closely related to the application procedures [52]. Despite the research effort, a complete characterization of the rheological behavior of refractory castables has yet to be achieved. Inconsistencies exist in the data obtained by various investigators due to variances in structure, composition, and preparation of experimental materials as well as differences in test conditions and methods [55]. Refractory castables contain particles that are too coarse to allow measurement in laboratory viscometres under controlled shear rate, making it impossible to make true scientific measurements of the rheological characteristics of these materials. Moreover, the understanding of the phenomena involved in determining the cement paste rheology has not yet reached a sufficient level for analysis of the more complex "suspension" formed by fresh concrete [56]

2.2.1. Zeta potential

Measurements of zeta potential of pure clinker phases and technical cements generally provide additional information on the formation of calcium silicate and aluminate hydrates [56]. The formation of the double layer on cement particles may be illustrated by the Bokris-Devanatahan-Muler model [57]. According to this model, the cement particle surface, when contacted with water, begins to react and thereby generates surface charges and ions which, may be released into solution in considerable quantities. These ions, in the first step, stay near the charged surface and form an electric double layer. Both thermal movement and generation of new ions of the same charge, displace these ions from the surface in the second step, thus establishing a double layer which may be described with a common Stern-Graham model, though it is entirely different in its nature and the structure of its inner part. Hence, the composition of the electrical double layer on cement should be significantly affected by the hydration reaction. The zeta potential in this model represents the potential between the gel-layer developed on cement particles and the surrounding electrolyte [58]. It is not possible to measure zeta potential of cements during the first minutes of hydration, regardless of the method used. If the pH value is high (pH>12), it is possible to measure it as early as two minutes after the cement/electrolyte suspension has been prepared. Under these conditions, data obtained for Portland cement lead to the conclusion that a layer of $Ca(OH)_2$ is precipitated around the particles, and hence the measured zeta potential is that of calcium hydroxide [59].

The zero point of charge of cement in aqueous suspension depends on the type of cement and the ionic strength the of solution. Na^+ and K^+ are potential determining ions for cement particles and fine silica ultrafine powders [60].

The presence of surfactant agents produces a stabilization of the double layer by inducing a zeta potential on cement particles in the early stages of the hydration, and can also contribute to minimize the effect of flocculating agents such as $CaSO_4$ [61-62].

23

Superplasticizers and air entraining agents are responsible for a partial hydrophobization of cement particles which may explain their setting time retarding influence [63]. There are also reported correlations between zeta potential, fracture toughness, and flexural strength of hardened Portland cement paste, indicating the importance of colloidal properties on the structure of hardened concrete [64].

Studies on synthetic C_4AH_{13} and C_3AH_6 in lime water, ethanol, and dimethylsulfoxide suspensions, in the presence of sodium lignosulfonate, sodium naphtalene sulfonate formaldehyde condensate, and sodium melamine sulphonate condensate, showed that the evolution of the zeta potential of hydration products depends on the adsorption level of the admixture. C_4AH_{13} has a negative zeta potential in lime water (-9.1mV) and a weak positive potential in ethanol (+2.3mV). Minimal adsorption of admixtures causes a sharp potential decrease in both media. As the adsorption increases, the potential remains practically constant between -18 and -20 mV. C_3AH_6 has a similar zeta potential in lime water (-8.7mV) that can reach values of -12 to -18 mV in the presence of plasticizers [65].

For Portland cement pastes, Ca^{2+} determines not only the zeta potential of the cement particles, but also the potential of the amorphous hydration products (C-S-H phase) [66]. Although the fluidity of fresh cement paste containing admixtures correlates with the repulsive force of cement particles (Figure 2.2-1), there is no consistent relationship between the fluidity and zeta potential. This suggests that a force, other than electrostatic repulsion acts on the dispersion of cement particles [67].

There is currently no data on the zeta potential of hydrating CAC or HAB particles of colloidal systems with characteristics similar to ARC (i.e. low w/s, high content of ultrafines, presence of plasticizers)
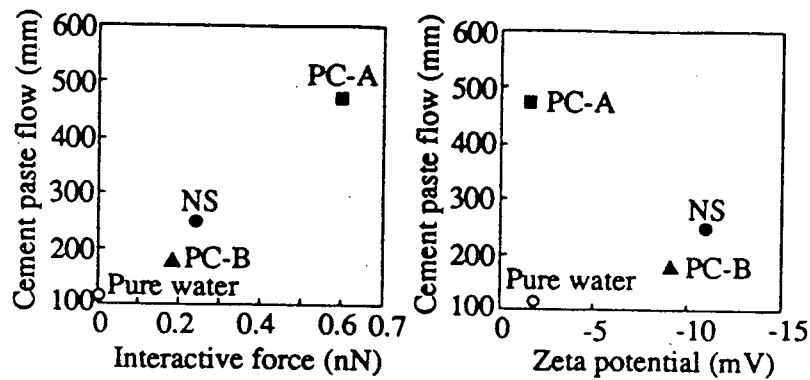
Figure 2.2-1. Variation of flow (measured according to JIS R 5201) with zeta potential of cement particles in the presence of: naphtalene condensate (NS), acrylic acid-ester copolymer (PC-A) and olefin-maleic acid copolymer [67].

2.2.2. Rheology of cement pastes

Most of the work on the rheology of fresh cement pastes has been done on Portland cement, with only a few studies being done on CAC pastes. Even for the well studied case of Portland cement, a thorough definition of the shear and time-dependent properties of this material is not yet possible. The reason for this is that the rheological behavior of fresh cement pastes depends on several factors [68] of different nature, such as:

- physical factors (the water/cement ratio, the cement grain size and shape, etc.);

- chemical and mineralogical factors (the cement composition and its structural modifications due to hydration processes);

- mixing conditions (type of mixer, mixing rate and time);

- measurement conditions (the characteristics of measuring instrument, experimental procedures, etc.).

Cement pastes are non-Newtonian dispersed systems and the most suitable instrument for determining their rheological properties is the rotational viscometer because it permits measurements in controlled flow conditions. Since cement pastes are dispersed systems, coaxial viscometers are preferred, as friction phenomena among particles are avoided and flow conditions are closer to the viscometric ones [69].

The use of coaxial viscometers is hindered by several factors. Particle settling during measurement may account for an anomalous shear thinning that may be misinterpreted to be a part of the structure buildup or breakdown. Also, if the gap of the measuring cell is too large, an uneven flow distribution across the annulus may be observed due to yield values inherent in the fluid system [70]. In order to avoid the problems encountered with rotational viscometers there are several guidelines that should be observed [71] :

- the minimum dimension of the annular gap width should be 10 to 100 times that of the particles;

- the gap should be as narrow as possible to allow for uniform flow condition within the annular space;

- apparent slippage should be avoided, if possible, through the use of grooved cylindrical surfaces.

During viscometric measurements of cement pastes, a hysteresis (thixotropic or antithixotropic) behavior is commonly observed. It is suggested that this effect may be the result of the development and breakdown of a "secondary structure". This structure is related to gel formation and is not to be confused with the floc structure of the paste existing before the application of a shear stress [72].

The shear strain rate versus shear stress curves obtained with viscometers depends strongly on the flow history, on the colloidal structure of the cement pastes, and also on the apparatus used [73].

According to Chappuis [74], in order to simulate the shearing conditions of the cement paste during concrete placing, rheological measurements in viscometers must be carried at very low speeds. Also, in order to avoid any possible interference of the measurements with the hydration process the measuring time has to be very short. These aspects are essential in order to obtain reliable data from viscometric measurements using concentric coaxial viscometers. Viscometric measurements were carried out, during the dormant period of two alumina cements (fast setting and a normal cement one) at different water to cement ratios in order to further investigate the rheological behavior of cement pastes. The results of these measurements are presented in Figures 2.2-2 and 2.2-3 [74], in logarithmic scale for shear stress. Several conclusions can be drawn from these figures:

- During the dormant period all pastes exhibit a continuous thickening with time;

- For each cement, when the scale of the shear stress is logarithmic, the experimental points seem to be on parallel straight lines, the slope of these lines being a measure of the relative thickening of the cement paste with the time;

- For a given cement, the relative thickening of the cement paste is independent of the water to cement ratio;

- For both cements, but more visible for cement N (normal cement), there is a certain ratio of water to cement above which no further important decrease in viscosity is recorded. This may be related to hydration characteristics of alumina cements; in particular, to the fact that, after the initial moments of mixing with water during the whole dormant period the quantity of hydrated cement is quasiconstant.
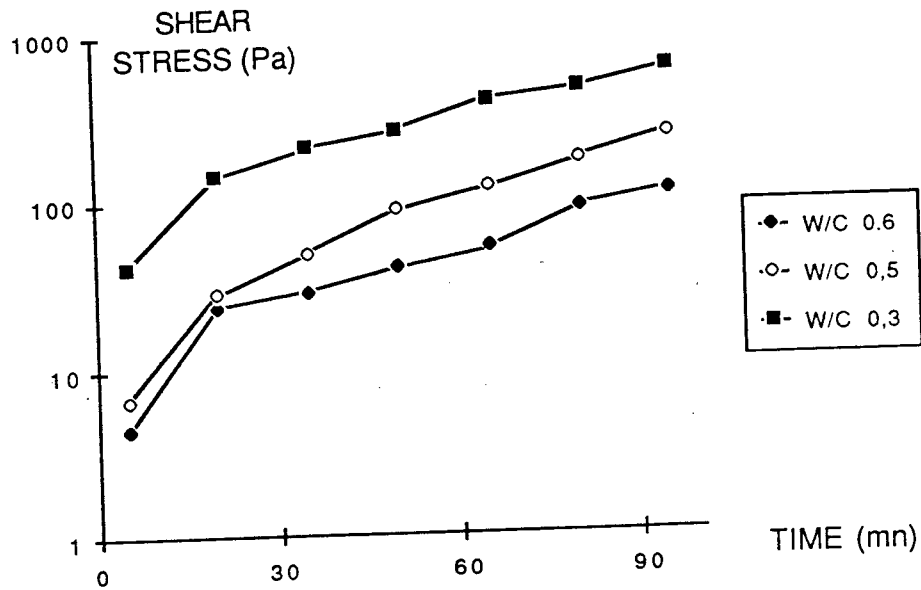
Figure 2.2-2. Variation of shear stress with time, at different water/cement ratios for a fast setting aluminous cement [74].
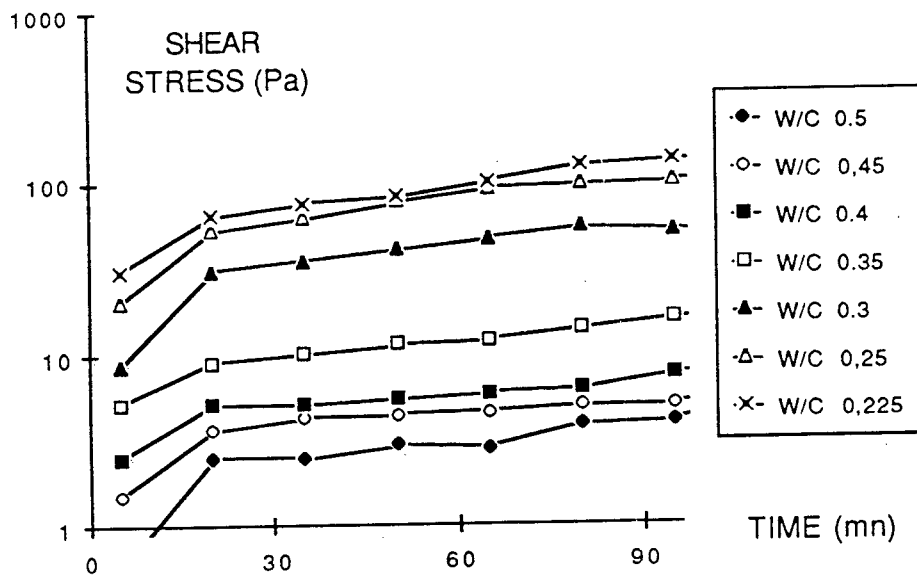
Figure 2.2-3. Variation of shear stress with time at different water/cement ratios for a normal aluminous cement [74].

In order to establish the influence of the initial mixing on rheological behavior of alumina cements, the same test procedure as above was applied for fast setting at a water/cement ratio of 0.5 for two different periods of initial mixing (3 minutes and 30 seconds). The results are shown in Figure 2.2-4. It can be seen that these two cement pastes have a completely different behavior, although they have been prepared at the same water to cement ratio and from the same cement.

The studies made by Chappuis are in agreement with the work done by A. Papo and B. Caufin [75], who studied the hydration of Portland cements by means of oscillatory rheological techniques and obtained a the following relation for the variation of viscosity with time:

$$\eta = \eta_0 + (\eta_R - \eta_0)(t/t_R)^N \qquad\qquad (2)$$
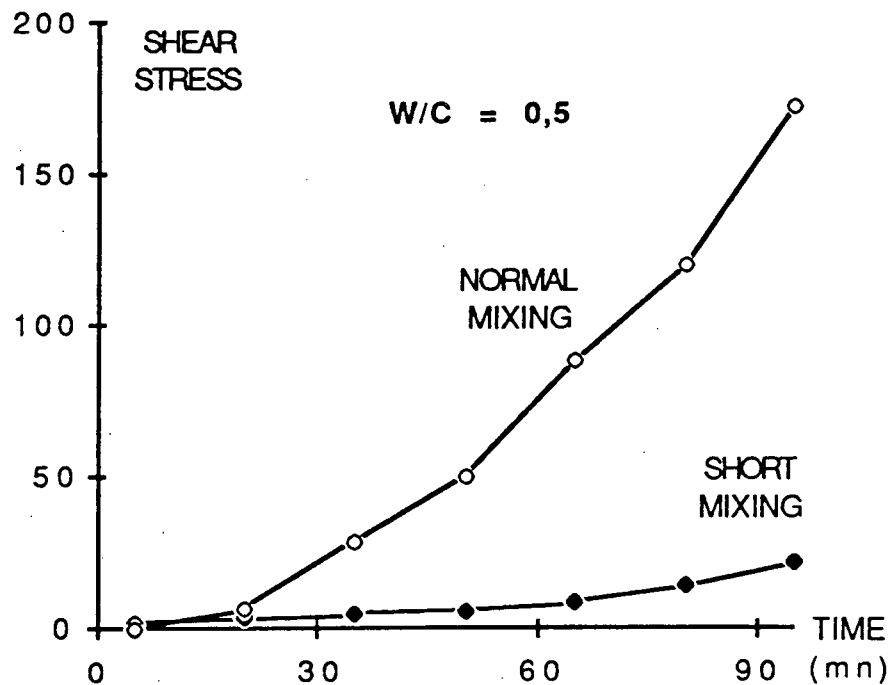
Figure 2.2-4. Variation of shear stress with time for a fast setting cement for different mixing time [74].

where: η-the viscosity of paste

η_0-initial value of viscosity

t-current time

t_R -the time at which the material has a very high characteristic viscosity (η_R)

N-parameter describing the kinetics of the cement hydration process

Therefore it was established that, even though the volume fraction of the binder in a compact castable mixture is only equal to 25-35%, the behavior of the molding system is determined by the binder [76].

Cement pastes in the presence of silica fume and plasticizers display all known types of flow, from typical Newton to pseudoplastic with a well defined yield stress value. The attempt to characterize the more complex systems such as binary mixes of silica fume and cement resulted in a great variety of flow curves presented by different researchers. These inconsistencies are believed to be the result of a specific effect of silica fume on the formation of the primary aggregate structure of such systems. A characteristic feature of this effect seems to be a well defined thixotropic behavior [77]. Even in the case of simple systems such as refractory mortars, an accurate correlation between rheological characteristics and flow could not be obtained [78]. The explanation for this lack of knowledge is due not only to the difficulty of setting up accurate and significant measurement techniques [71] or to the complex structure of fresh cement pastes, but also to the complex chemical and physical interactions that result in a continuously evolving microstructure [73].

Simultaneous viscosity and calorimetry measurements of fresh cement pastes containing reactive powders (Figure 2.2-5) showed that there are two exothermic effects occurring: a long term and a short term one. The long term effect corresponds to the massive precipitation of hydrates and its kinetic influences the kinetic of strength development and hardening of castables [79]. The nature of the short term effect is not known. The exothermic

30

reaction corresponding to the short term effect leads to the stiffening of the binder and it is associated with flow decay in castables [80].

Mineral system = CAC(25)RA(75)

Mineral system = CAC(25)SF(25)RA(50)
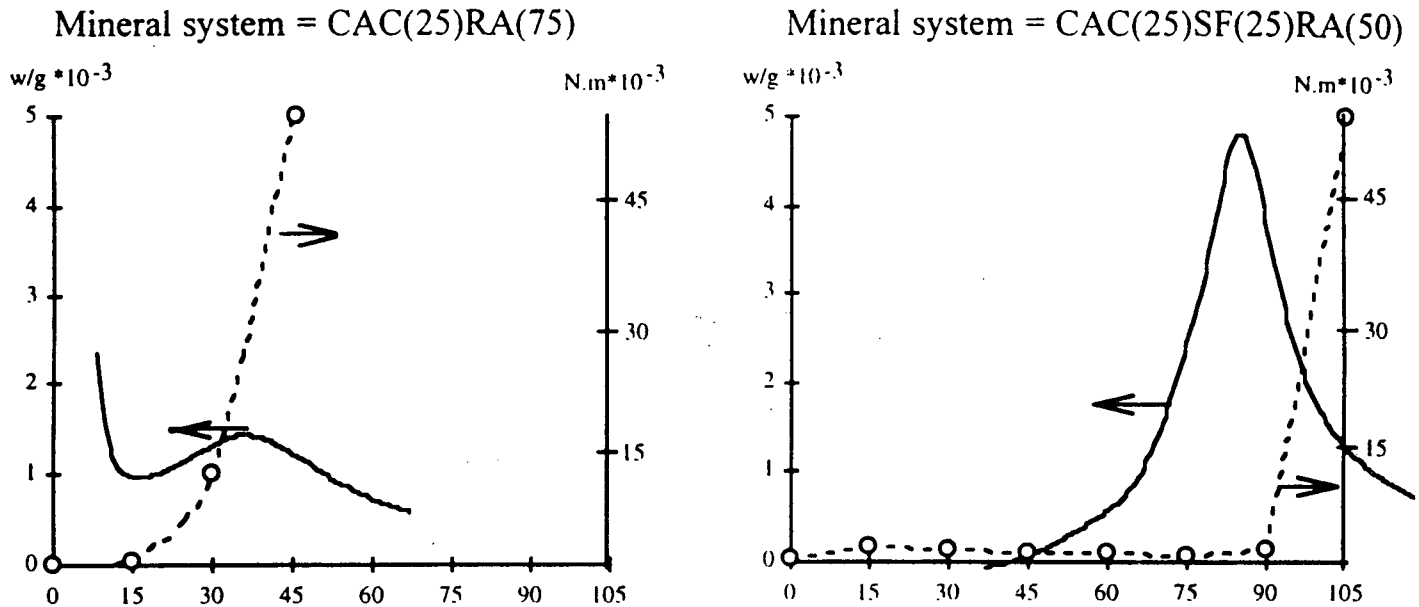
Figure 2.2-5. Variation of viscosity and short term exothermic effect, in time for pastes containing calcium aluminate cement (CAC), reactive alumina (RA) and silica fume (SF) [80].

At present, the study of the rheology of fresh cement pastes can offer qualitative information regarding the influence of reactive powders and admixtures on flow and setting behavior of ARC systems. Although significant progress has been made in recent years in refining of the experimental measurement methods, it is not yet possible to obtain precise information regarding the optimization of admixtures, or the influence of reactive powders.

Because it is impossible to correlate viscosity of simple suspensions of hydraulic binders components with flow of castable the study of rheology cement pastes is not a reliable tool in the design of ARC systems.

31

2.2.3. Flow

The determining factor in obtaining a self-flow ARC is the particle size distribution. While the addition of plasticizers and selection of hydraulic binder-setting admixture systems may bring substantial improvement, no self-flow behavior is possible without a proper particle size distribution (Figure 2.2-6) [81].
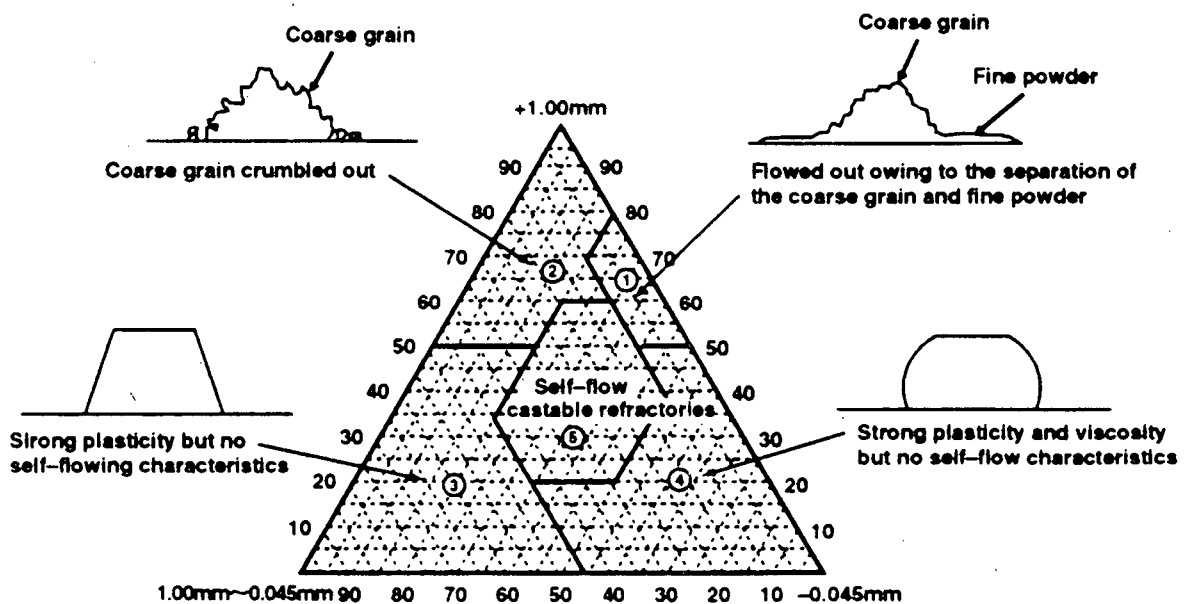
Figure 2.2-6. The influence of particle size composition in determining the flow characteristics of a castable [81]

It was demonstrated that a gap sized distribution gives poor workability and flow while a continuous one gives improved workability, low water requirement and good compactness resulting in low shrinkage and high strength [53].

Although a number of packing models for continuous distributions have developed over the last century, only Furnas and Andreassen distributions have been used in the design of castables [84]. Furnas type distributions for castable refractories are based on the assumption that the particle packing factor of narrow sized fraction of any material is constant at 50% voids.

32

The Furnas model is however cumbersome and difficult to use. The Andreassen model is much simpler but it has been criticized for its empirical nature. The Andreassen particle size distribution is expressed by the following equation:

$$CPFT=(d/D)^q \times 100 \qquad (3)$$

where,

CPFT - cumulative (volume) percent of particles finer than the current dimension *d* (%);

d - current particle size (μm);

D - maximum particle size in the system (μm);

q - Andreassen exponent that characterizes the distribution.

Computer simulations have shown an upper limit for the *q* value if a dense packing is desired. Values of *q* below 0.37 may give 100% density for infinite distributions, whereas *q* above 0.37 will give a packing with porosity no matter how wide the distribution [82].

The main objections raised against the Andreassen model are due to the fact that the equation assumes the existence of infinitely small particles and does not require any shape factor [83]. In spite of these imperfections the Andreassen model works better for refractory castables than the Furnas model [84]. Experimental results based on the behavior of fused alumina castables have shown that in order to get good flow for castables the *q*-value should not exceed 0.3 . For high *q*≈0.3, the castables are vibratables, and for lower *q*≤ 0.25 the self-flow behavior is dominant [85]. The experimental evaluation of self-flow behavior of refractory castables still lacks enough fundamental basis, which results in the absence of a universally accepted standard. Presently, the most used laboratory test for self flowing is the use of truncated conical mold [86]. In this method, the mold (described by ASTM C230) is filled with refractory castable then rapidly lifted and the castable is allowed to spread freely under its own weight. The relative increase in diameter of the castable is considered to be the flow value. The

cone itself was arbitrarily chosen, without any consideration neither to its relative dimensions, or to the volume that it generates [87].

This test is purely empirical but is the only type of test widely accepted, due to its simplicity and the fact that it can accurately describe the flow behavior of castables in the field applications. It is considered that the 50% self-flow is the minimum value needed for reasonable pumping/pouring consistency, and that the110% self-flow is the maximum value above which the segregation occurs [86].

Fine reactive powders are important in determining the self flow behavior because they represent the fine end of the Andreassen distribution and their amount is closely related to the Andreassen exponent value. Silica fume is the key component for the manufacturing of ARC because it has small particle size and a good dispersibility, features that combined bring a flow improvement for reduced water levels, Figure 2.2-7 [88]. The experimental observations revealed that the quality of silica fume is an important factor for a good self-flow behavior. Still there is controversy regarding the definition of a good quality silica fume. The following factors are most often cited in literature as characteristics of a good quality silica fume: high specific
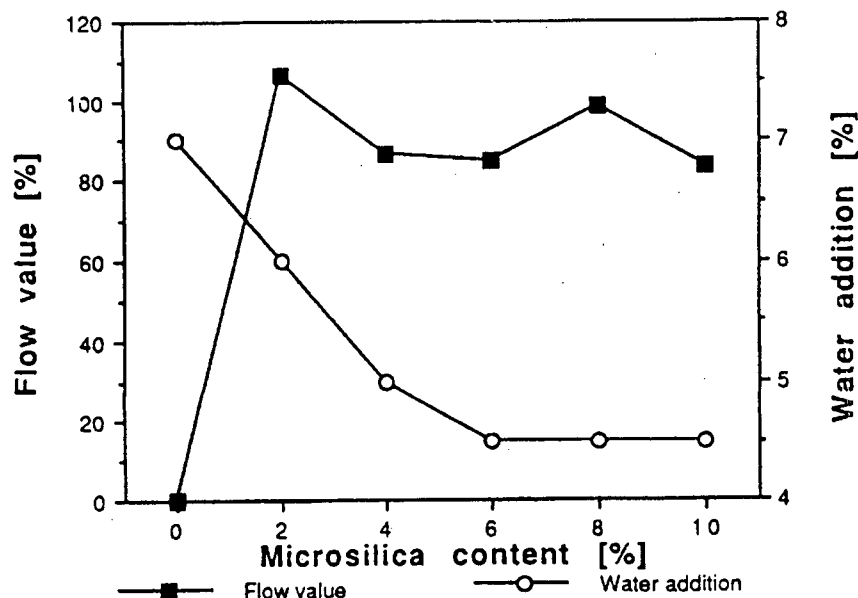
Figure 2.2-7. Influence of microsilica additions on flow and water levels of a ARC [88].

surface (usually above 20 m²/g measured by BET method) [47, 48], high chemical purity (over 98% SiO_2) [42, 84], and low level of soluble soda (less than 0.05%) [40]. Figure 2.2-8 shows a comparison between four different types of silica fume that have the chemical composition presented in Table 2.2-1 [84].

Comparing the flow behavior of castables prepared with silica fume type D, E, F, and G and taking into account their chemical composition, it may be considered that the most detrimental impurities are Na_2O and K_2O, but influence of the content of CaO, Fe_2O_3, MgO and Al_2O_3 is unknown and cannot be identified from the presented data.
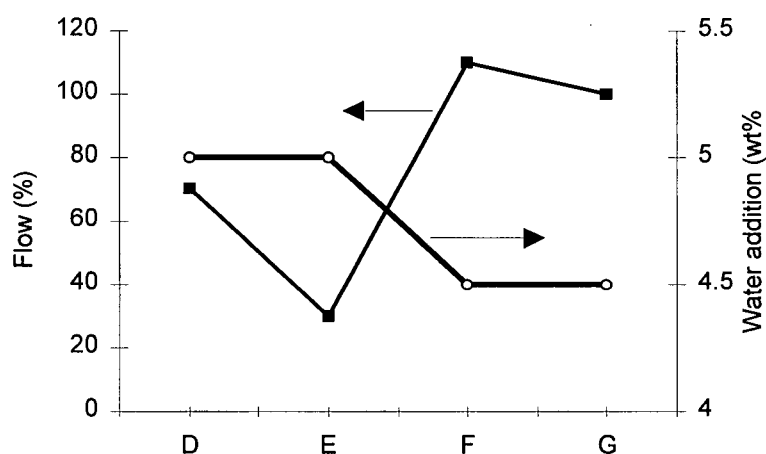
Figure 2.2-8. Comparison between different types of silica fume on flow behavior of a tabular alumina based castable composition [84].

Table 2.2-1. Chemical composition of the silica fume types used in flow measurements in Figures 2.2-3 and 2.2-4 [84].

Component	SiO₂	Al₂O₃	CaO	Fe₂O₃	MgO	Na₂O	K₂O
A	96	0.6	0.15	0.1	0.4	0.3	0.4
B	99	0.06	0.14	0.01	0.04	<0.01	0.11
C	97	0.4	0.15	0.1	0.3	0.1	0.2
D	95	0.4	0.2	0.08	0.2	0.05	0.5
E	95	0.3	0.3	0.08	0.2	0.09	0.5
F	98	0.4	0.2	0.05	0.1	0.02	0.2
G	98	0.3	0.2	0.07	0.1	0.02	0.3

Figure 2.2-9 shows the effect of variation of the CAC content on the flow behavior of tabular alumina based castables having 8% silica fume with compositions presented in Table 2.2-1 [84]. It is clear that the flow decreases sharply with increasing the CAC content. In order to maintain a similar flow level, an increase of 1.5% CAC requires an increase of 0.5% water. In all cases, the low purity silica fume type A gives low values of flow. The purity of silica fume is critical especially for castables having an ultra low cement content. It is not clear why the silica fume type C gives a better flow at 1.5% CAC even though it is less pure than silica fume type B.

The addition of HAB has a strong effect on the flow of the castable. Both the free-flow and the vibra-flow decrease significantly with the HAB content (as shown in Figure 2.2-10) [85]. If the pattern of variation of free-flow and flow under vibration are compared, it results that for a self-flowing castable ($q \sim 0.25$) having a high percent of silica fume, a large addition of HAB will not bring a dilatant behavior, due to the thixotropic effect of silica fume.
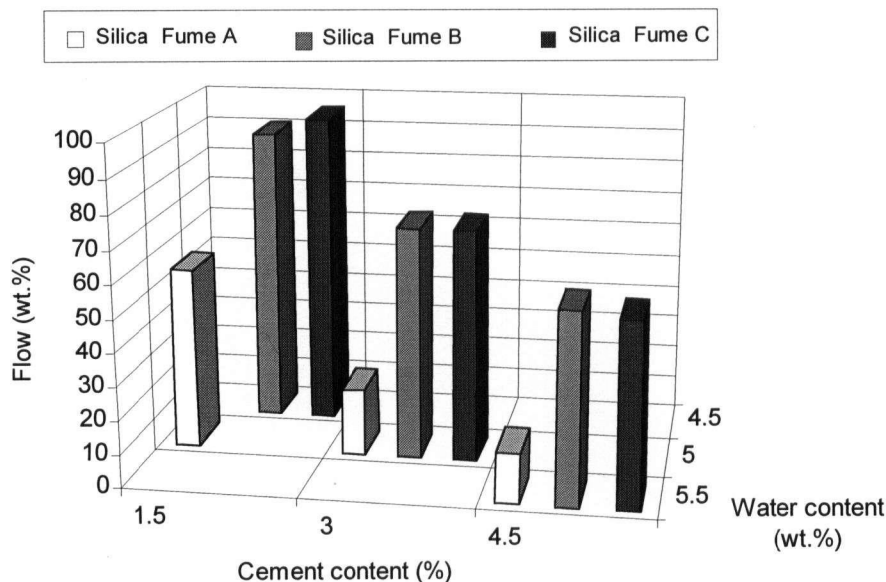
Figure 2.2-9. The effect of CAC content variation on the flow of tabular alumina based castables at 8% silica fume [84].
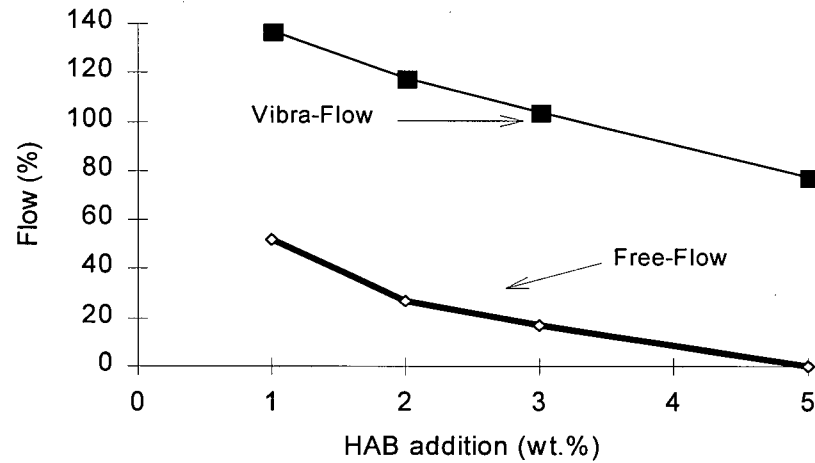
Figure 2.2-10. Variation of flow with HAB Alphabond 200 addition for a no cement fused alumina castable containing 8% silica fume (q=0.26) [85].
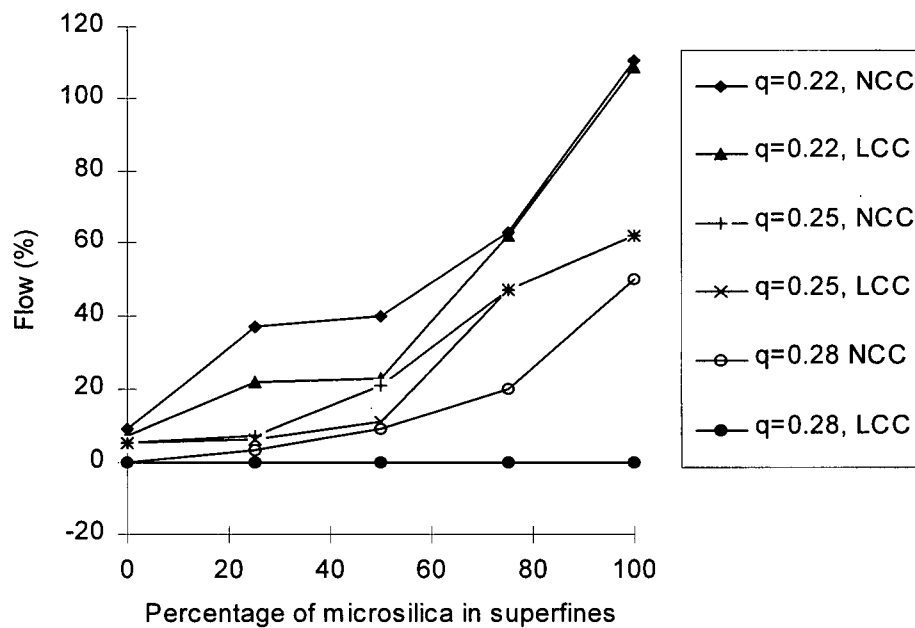
Figure 2.2-10. The effect of replacement of silica fume with calcined alumina in fused alumina based NCC and LCC for Andreassen exponent q=0.22-0.28 [89].

It is generally accepted that good quality silica fume has a much better effect on flow than a reactive alumina even when the particle size distribution of the two superfine powders are similar [88].

The effect of mixtures of silica fume and reactive alumina on flow have not yet been thoroughly investigated. Figure 2.2-10 shows the effect of replacement of silica fume type F (Table 2.2-1) with calcined alumina (CT 300SG) in fused alumina based NCC and LCC (6% CAC) for Andreassen exponent $q=0.22-0.28$ [89].

Several conclusions may be drawn from the data presented in Figure 2.2-10:

- for high cement content (6%) and high q-value (0.28) there is no self-flow for any silica fume/reactive alumina ratio;

- the flow decreases with the increase of the reactive alumina content for all self-flowing compositions, the decrease being stronger at low q-value;

- the content of CAC has no influence on flow at lower q-values (<0.25) and reactive alumina content in the ultrafine fraction less than 25%;

- the role of reactive alumina and silica fume on flow is intimately related to the hydration process.

Recently Alcoa Industrial Chemicals announced the release of a group of alumina based raw materials called Matrix Advantage System (MAS), intended to be used as a total replacement in self-flowing castables [90]. MAS consists in a set of reactive alumina powders having a bimodal particle size distribution with an average particle size of 1-1.7μm and a specific surface of 3.8-4.7 m^2/g (BET) and a set of dispersing powders that are obtained by premixing different chemical admixture of undisclosed composition with bimodal reactive alumina. MAS is claimed to give a self-flow behavior for castables at very low water levels (4-4.2%). According to the data presented, the self-flowing castable compositions seem to have a

gap sized distribution [91] and their flow behavior cannot be described by the Andreassen model.

The MAS is very important for the design of spinel or high alumina based self-flowing castables intended to work at high temperatures and in severe corrosion conditions (or reducing atmosphere), when the absence of silicon oxide from their compositions is a necessity.
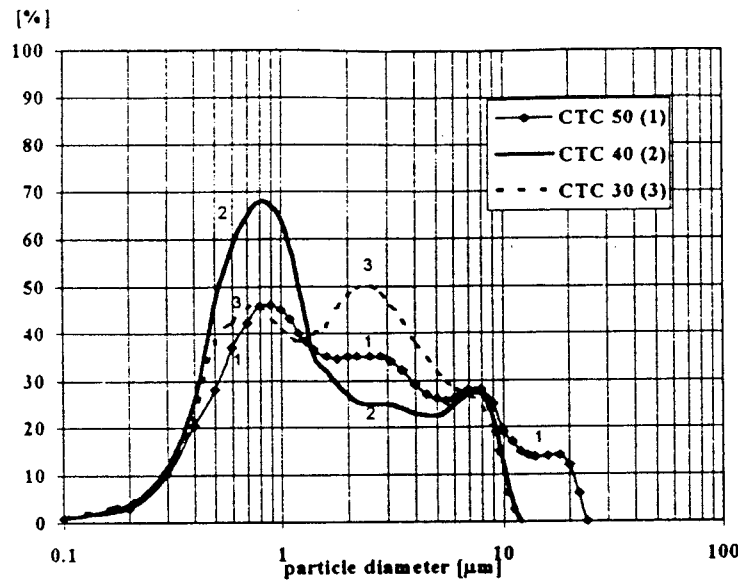
Figure 2.2-11. Particle size distribution for CTC reactive aluminas [90].

An other interesting aspect is that the self flow behavior is obtained by the additions of reactive alumina powders in a proportion of around 17% and 0.5-2% dispersing alumina powders, which are more than ten times coarser than silica fume. It seems that the bimodal (Figure 2.2-11) distribution is a key factor in obtaining the self-flow behavior in the case of MAS [90,91].

2.2.4. Plasticizers

Plasticizers allow a given degree of workability to be achieved at lower water levels. They act by adsorption at the solid liquid interface, in this respect resembling setting time retarders. There is a wide overlap between the two properties, many plasticizers acting as setting time retarders and vice versa.

Three principal types of plasticizers are in common use, consisting in salts of: Sulfonated Melamyneformaldehyde Polymers (PMS), Sulfonated Naphtaleneformaldehyde Polymers (PNS) and modified Ligno-Sulfonate materials (LS). Commercial formulations often contain other substances added to alter the setting behavior or for other reasons [92].

In the case of ARC, due to their low content in hydraulic binder and to their high content of fine reactive powders, the term is extended also to inorganic materials (usually phosphates) that act as dispersants for silica fume and reactive alumina. It seems that the inorganic (phosphate) plasticizers act by removing the hydrophobic impurities (residual carbon) from the surface of silica fume particles while organic macromolecular plasticizers act mainly by steric repulsion [53]. There are only a few studies concerning the effect of plasticizers on flow because their mechanism of action is not yet well understood and because the self-flow behavior is extremely sensitive to plasticizers admixture. At the present stage the levels of plasticizer admixture for self-flowing castables are established only by experimental means.

The difference in action between organic and inorganic plasticizers is reflected by the fact that even though the organic plasticizers have a lower effect on the zeta potential of reactive alumina and CAC, they may be more effective in enhancing the flow. The use of organic dispersant proves to be more effective as shown in Figure 2.2-12. Also the flow is more sensitive to changes of the organic dispersant concentration than for the inorganic [93].
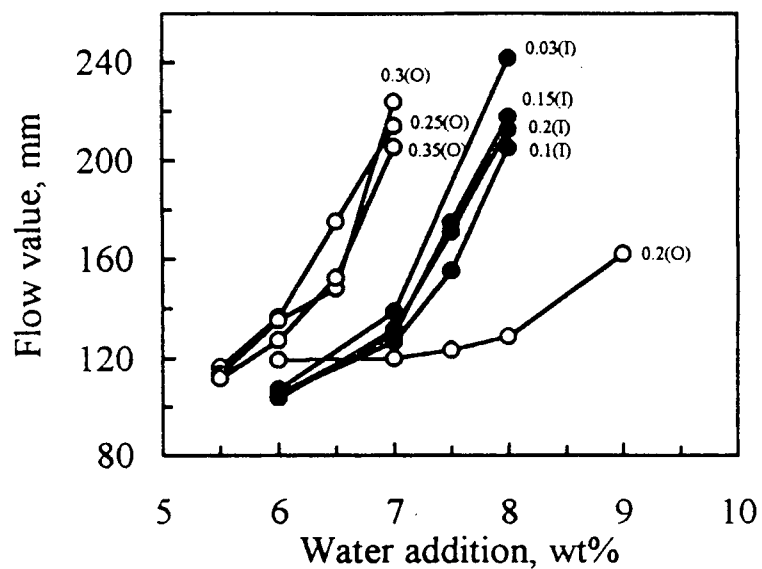
Figure 2.2-12. Variation of flow with water addition for different levels of melamine polymer plasticizer (O) and sodium hexametaphosphate (I) [93].
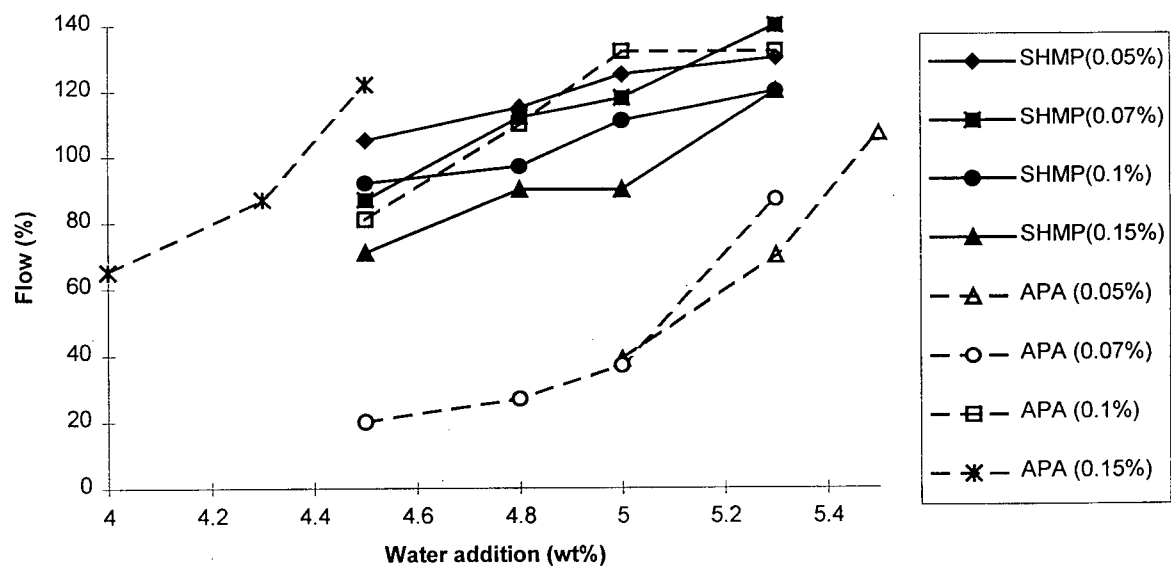
Figure 2.2-13. Flow of a fused alumina castable as a function of water content for different concentrations of sodium hexametaphosphate (SHMP) and an ammonium polyacrylate (APA) [94].

As shown in Figure 2.2-12 [94] an organic dispersant proves to give a better flow if used at the proper level. Minor changes in the concentration of the organic dispersant result in a dramatic change in flow. Also, the castables made with different concentrations of ammonium polyacrylate had to be analyzed in different ranges of water contents in order to characterize their self-flowing behavior. The flow is less sensitive to the addition of SHMP. It is shown that viscosity measurements on the suspension of the fine fractions could not be correlated with data resulted from flow measurements [94]. The effect of plasticizers on flow depends strongly on the castable composition and on the nature and content of hydraulic binder and reactive powders.

The interaction between plasticizers and the hydraulic binder should not be analyzed only from the flow enhancement or water reduction standpoint. Due to their influence on the setting process, plasticizers can also improve the castable workability, i.e. the time period in which the flow behavior is maintained. Figure 2.2-14 shows the decay of flow with time for three castable compositions having 10% reactive alumina 5% silica fume (Elkem 971) and 5% HAB (Actibond 101, Actibond 102 and XAA2005) with an admixture of sodium tripolyphosphate or sodium polyacrylate [95].

Even though all three types of HAB have the same chemical composition (Table 2.1-2 [24]), there are important differences in the effect of plasticizer admixtures with time. In all cases, it seems that sodium polyacrylate is more efficient than sodium tripolyphosphate with respect to the initial flow value and workability.

The castable that contains Actibond 101 and STPP has a similar flow behavior to the one containing Actibond 102 and SPA. Moreover, the action of plasticizers extends also after the hydraulic setting process.

For the type of castables presented in Figure 2.2-14, it is reported that while for compositions made with Actibond 101 there is no effect of plasticizers on green strength, for

compositions containing Actibond 102 and XAA2005 the green strength of specimen with STPP

addition was 20-25% higher than that of specimens prepared with SPA [95, 96].
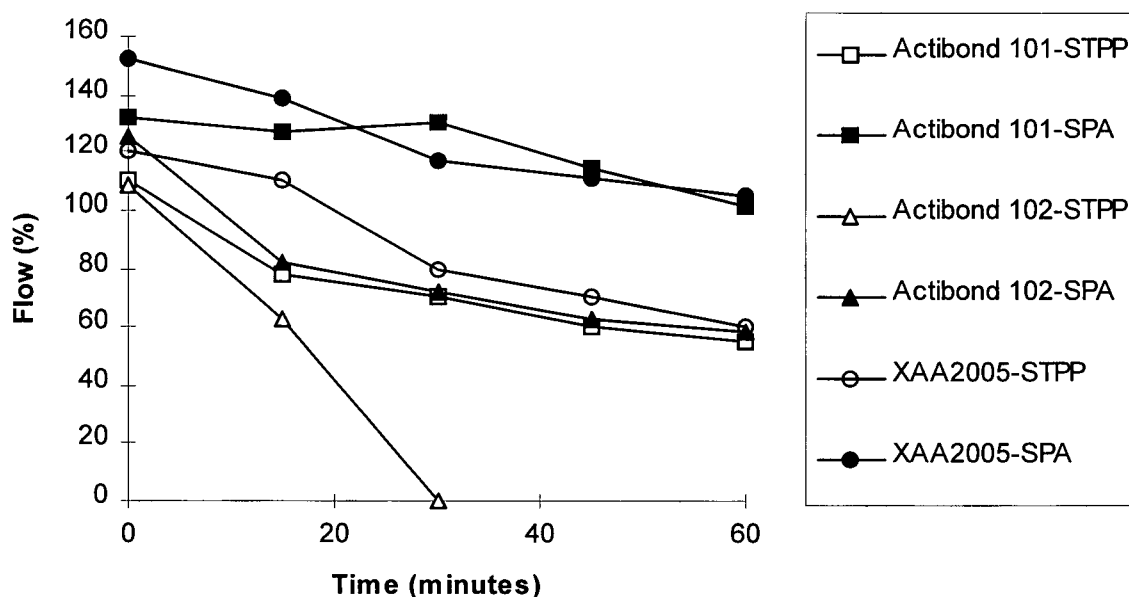
Figure 2.2-14. Variation of flow with time for NCC having different types of hydraulic binder and different plasticizer admixtures: sodium tripolyphosphate (STPP) and sodium polyacrylate (SPA) [95].

At the present stage, due to insufficient understanding of hydration mechanisms, of the

self-flow behavior fundamentals, and the action of plasticizers, there is not yet a scientific

approach to the study and optimization of plasticizer admixtures for ARC, all the current studies

being carried out by experimental means.

2.3. Non-crystalline hydration phases

Studies on cement pastes with microsilica [97], show that a certain fraction of the microsilica reacts with calcium aluminate cement and water to form the so called CASH phases in addition to the CAH and AH normally found in hydrated cement. The CASH phases are of zeolithic nature and the amount of these products of hydration depends on the quality (purity) of silica fume. In spite of the fact that, at temperatures higher than 40°C [46] or after long term hydration at room temperature and at low water/cement ratios [22], crystallized forms of CASH (C_2ASH_8) were detected in pastes containing calcium aluminate cements and silica fume, there is no evidence of any crystalline compound that may develop during the induction period of hydration at room temperature.

2.3.1. Structure and composition of CSH phase

The amorphous CASH phase is similar to the CSH phase developed during hydration of Portland cement, and may be regarded as a CSH phase with a high degree of Al^{3+} substitution [98]. CSH is believed to have layered structure. However, a precise structural determination has not been performed because of the lack of long range crystallinity [92]. The structure of CSH is nearly amorphous (i.e. gel-like), in which the degree of crystallinity is significantly reduced through the omission of bridging tetrahedra from silicate chains and disorder in the attachment of silicate anions of various sizes and hydroxyl anions to CaO sheets. Although structurally in a single phase form, the only XRD effects definitely attributable to CSH are a diffuse peak between d=0.27 and 0.31 nm, and a sharper peak near 0.182 nm [92]. The broad peak demonstrates the presence of wide distributions of d-spacing, suggesting a structure that could be highly variable locally. The periodicity in the diffuse peak relates to Ca-Ca distance in CaO

planes. The periodicity in the sharper peak near 0.182nm is found in any material containing silicate dreierketten but also may include contributions from CaO structure [99].

It is currently unknown whether the strong compositional fluctuations of the CSH gel phase are statistically random or there might be correlations in the Ca:Si occupancy over small distances (i.e. clustering). Attempts in obtaining Selected Area Electron Diffraction (SAED) patterns have generally failed. Part of the difficulty in the reliability of SAED investigations may relate to sample amorphization by the ion beam milling process and/or beam damage in the microscope [100]. It is supposed that the thermal damage during the preparation of specimens is more important than beam damage in the microscope [101].

Many models have been proposed to explain the crystalline and chemical observations that have been reported for CSH. The "solid solution model" considers CSH as a solid solution between tobermorite and calcium hydroxide. In this model, the CH phase is incorporated between tobermorite layers [102] or the whole CSH phase is considered to be a continuous sequence of defective tobermorite-like layers [103]. The "nanophasic model" considers CSH to be a mixture of tobermorite and jenite structural elements at the nanometer scale. Although subcrystalline regions may be present, according to this model, they are confined to small fragments of Ca-O layers with attached silicate fragments that are several nanometers long [104]. The "buckled-sheet" model is similar to the nanophasic model in that it assumes that CSH structure is a result of the hydration kinetics. CSH is supposed to form in narrow ribbon-like sheets, which can buckle and curve as a result of the local ionic concentration when they formed. These sheets are linked in localized nanocrystalline regions that represent nucleation sites for the new structures. This model can account for a very wide range of compositions as well as for the presence of an amorphous phase [105]. CSH layered type structures were observed also in the case of magnesite based ARC, where an MSH gel is formed in the binding

phase [106]. Crystalline MSH may form probably via dissolution-precipitation of an amorphous phase that becomes more crystalline during aging [107].

TEM studies revealed the presence of a mesoscale (1-10nm) structure in CSH gels, structure that consists of a multitude of nanocrystalline regions on the scale of <5nm, each with homogeneous composition, short range ordered regions on the scale of 1nm with a variable composition and structure, and an amorphous matrix with a strongly variable composition [100].

Much controversy exists related to the composition of CSH due to variances in experimental conditions, difficulty in acquiring reliable data, and due to its compositional variance. Generally it is considered that the Ca/Si ratio fluctuates between 0.6 and 2 [104]. Some researchers have shown however, that Ca/Si ratio can vary more widely, up to 2.8 [99]. EDX studies of CSH gel using a 1nm size spot showed the Ca/Si ratio to fluctuate between 0.5 and 5.9 [100].

Regarding the Al/Si ratio there is much dispute not only regarding the degree of substitution but also for the morphological characteristics of the substitution process. It has been reported [108] that Al^{3+} is not incorporated directly into the CSH phase but into other phases such as $(Ca_2(Al,Fe)(OH)_6) \cdot X \cdot xH_2O(AF_m)$. This type of substitution leads to maximum Al/Si ratios of 0.12-0.18 [98]. TEM analysis of CSH single phase [101] in mature cement phases showed that the Al/Ca ratio increased linearly with the Si/Ca ratio according to the equation:

$$Si/Ca = 0.444 + 2.25 \, Al/Ca \qquad (4)$$

This equation was also applied to the analyses of CSH in a range of slag cements pastes, with a wide range of Ca/Si ratios [109]. The behavior described by Equation 4 it is not consistent with the hypothesis that aluminum is present in substituted AF_m phase but is consistent with a fixed Al/Si ratio in a series of CSH particles of varying Si/Ca ratios. Additional information may be obtained if we analyze the solubility surfaces in the $CaO-SiO_2-Al_2O_3-H_2O$ system (Figure 2.3-

1). C_2ASH_8 (stratlingite) cannot coexist with calcium hydroxide but can coexist with calcium aluminate hydrates or with CSH having low calcium and high aluminum compositions [92]. These findings may explain the fact that during hydration of CAC in the presence of silica fume an initial amorphous phase is replaced after three days of hydration at room temperature, by C_2ASH_8 [22].
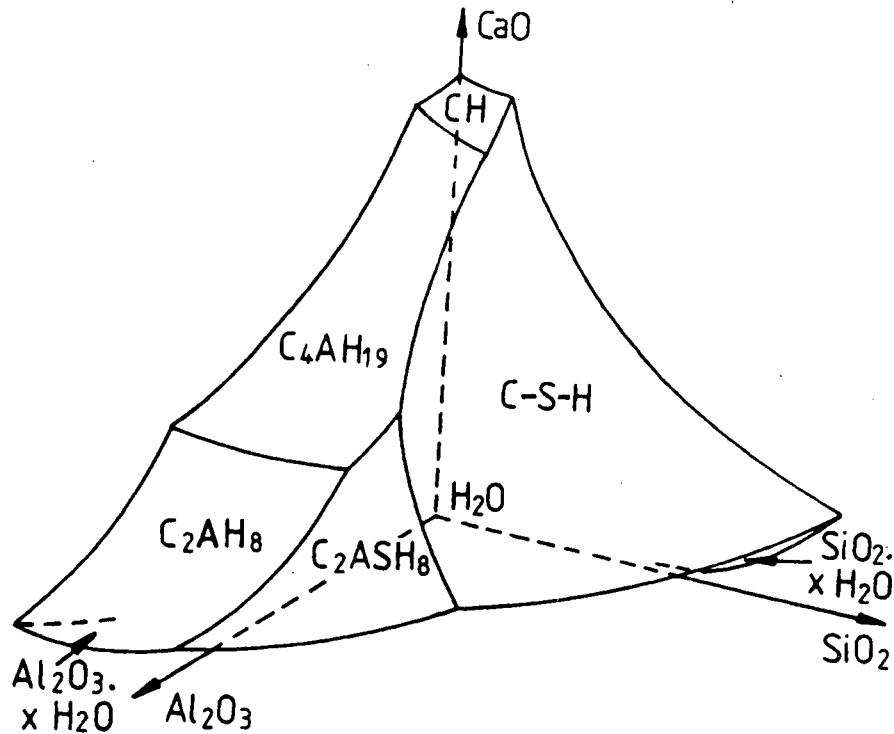
Figure 2.3-1. Metastable equilibria in the $CaO-SiO_2-Al_2O_3-H_2O$ system (solubility curves) [92].

In order to identify if there is a clear solubility limit of Al in CSH and if there is a solid solution of CSH and Al rich compatible phases, Magic Angle Spinning Nuclear Magnetic Resonance was employed to study the structure of stratlingite and CSH gels containing up to 13 mol% Al_2O_3 [111]. It resulted that as a function of Ca/Si ratio, two CSH phases can coexist, being separated from each other by a small invariant field in the vicinity of compositions having Ca/(Al + Si) =1. This ratio suggests that stratlingite is the coexistent phase. This is also sustained by finding C_2ASH_8 as a coexisting phase in high alumina content compositions [112].

Although most of the researchers consider that the maximum degree of aluminum substitution in CSH can not exceed Al/Si=0.2 there is reported experimental data of amorphous material having the composition $C_{(0.7-0.98)}A_{(0.37-0.42)}S_1H_x$ that was in equilibrium with stratlingite. The amorphous material maintained its composition after curing for 90 days at 20-55°C [113].

Unfortunately, no NMR studies were performed in order to determine the type of aluminum substitution in these amorphous compositions. However, for CSH gels with lower level of substitution, NMR studies have been shown that Al^{3+} substitutes for Si^{4+} in bridging tetrahedra and that other phases may occur with CSH in which Al^{3+} exists in octahedral coordination [111]. In addition it has been shown that the structure of Al containing CSH consists of dimers and short chains for Ca/Si >1 and long chains for Ca/Si <1 [112].

2.3.2. Formation of CASH phases

The mechanism of formation of CASH phases in ARC is not yet well understood. The only phase identified as crystalline CASH phase is Stratlingite. In mixes of 30-50% silica fume and 50-70% CAC, [46] crystalline C_2ASH_8 may be detected after 1 day at 40-70°C or after 1 week at 20-70°C. Because in these experiments the conversion of hexagonal to cubic hydrates was inhibited, it is assumed that starlingite was formed by direct interaction of silicic acid with C_2AH_8.

At room temperature C_2ASH_8 may form from mixes containing 75% silica fume and 25%CAC at low water/solid ratios, after 3 days of hydration. It is interesting that in this case, prior to crystallization of C_2ASH_8, the main hydration product is an amorphous phase. It is considered that in ARC the formation of Stratlingite is not induced by the process of conversion of metastable hydrates [22].

It is not known if the CASH phase in ARC is formed just by interaction between calcium aluminate hydrates and silicic acid dissolved from silica fume particles or whether a direct

interaction between the basic components of CaO-SiO_2-Al_2O_3-H_2O system is possible. Mixes of reactive alumina calcium oxide and silica fume were allowed to react in solution (water/solid ratio =15) for two years before poorly crystallized Stratlingite was observed. By hydrothermal treatment at 150°C, a very well crystallized and almost pure phase was obtained.

Mixtures of CAC Secar 71, metakaoline (AS_2), and lime as freshly calcined $CaCO_3$, after 3 days contained only traces of stratlingite the main crystalline phases being CH and C_2AH_8. The same mixtures if allowed to react in a 0.2N NaOH solution, contained a well crystallized strallingite after 3 days [111]. These experiments show that for compositions close to stratligite (Ca/Si=2 and Al/Si=1) the material formed by direct reaction is a stable amorphous gel. Crystallization occurs only by hydrothermal treatment or in the presence of alkaline ions.

Investigations of interactions between metakaoline and calcium hydroxide at temperatures of 20-55°C, for compositions in the range of C/AS_2=0.4-6 revealed that for C/AS_2<1, a characteristic product of reaction is an amorphous material. After 180 days of hydration at 20°C these mixes contained only stratlingite and an amorphous material.

After 90 days of hydration at 55°C (Figure 2.3-2), the hydration products of composition C (C/AS_2=1.5) are stratlingite, a hydrogarnet phase ($C_3AS_{0.5}H_5$), and an amorphous material having the composition $C_{(1-1.2)}SA_{(0.12-0.16)}H_x$ [113]. It is interesting that in this case the previous conclusions regarding stratlingite as a coexistent phase with CSH having maximum level of substitution Al/Si=0.2, are confirmed. The only products of hydration, for compositions D and E (having C/AS_2=0.75 and respectively 0.4), at 55°C were stratlingite an amorphous material having the same composition ($C_{(0.7-0.8)}S_1A_{(0.37-0.42)}H_x$) in both cases.
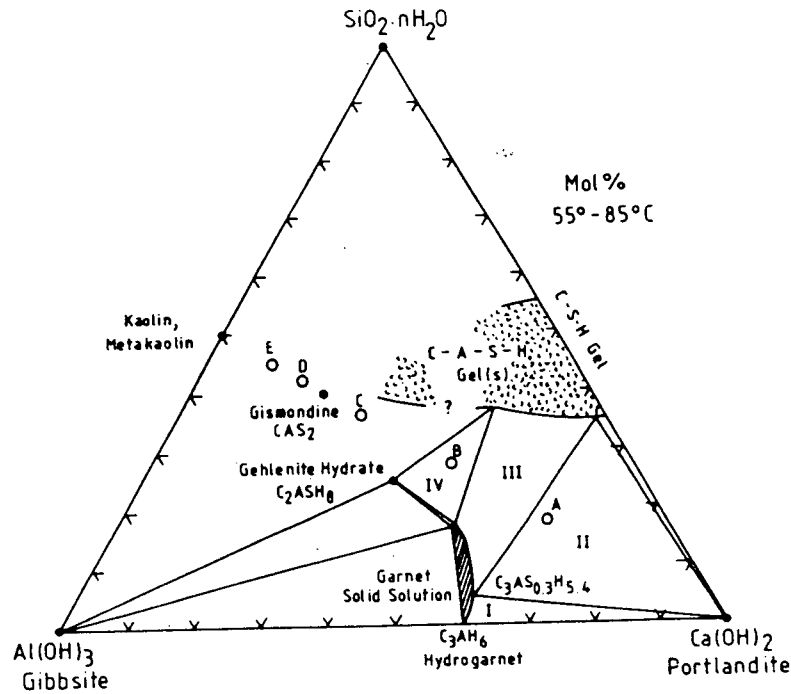
Figure 2.3-2. Phase equilibrium in CaO-SiO$_2$-Al$_2$O$_3$-H$_2$O system at 55°C [113].

For composition E, the amorphous material had the same composition for both temperatures of hydration (20 and 55°C). An other aspect that has to be mentioned is the presence of KOH in solution during hydration (the metakaolin used in these experiments contained 2% K$_2$O) [113]. The presence of K$^+$ ions may be responsible for the formation of stratlingite at these temperatures. It results that in the presence of alkali stratlingite may crystallize in equilibrium with an amorphous CASH phase having Ca/Si <1 and Al/Si=0.37-0.42. The amorphous material is very stable, a gel having the composition C$_{0.58}$S$_1$A$_{0.38}$H$_x$ being present even after 90 days of hydration at 85°C.

Although during hydration of pastes CAC and silica fume, stratlingite crystallized from an amorphous material could be identified, there is no data regarding the composition of the amorphous CASH material formed during hydration of ARC.

2.4. Formation of ceramic matrix

An advanced refractory castable may be considered as a mix of refractory aggregate which acts as an inert filler at temperatures below 1000°C, and a binding system which is a mix of reactive ceramic powders, hydraulic binder, chemical admixtures, and water.

After casting, the components of the binding system achieve a very intimate relationship, and the initial fluid suspension of binding system transforms into a rigid hydraulic matrix after setting, and finally into a ceramic matrix after firing. When fired the hydraulic bond is replaced by a ceramic bond as a result of solid state reactions, with or without the presence of a liquid phase [12].

2.4.1. Transition from hydraulic to a ceramic matrix

Each stage of processing of ARC (casting, setting and firing) is characterized by a succession of physical and chemical transformations and complex interactions between components. The physical and chemical interactions present in the initial stage after mixing with water include the following:

- The hydraulic binder enters an initial stage of hydration. The anhydrous calcium aluminate cement grains react with water and release Ca^{2+} and AlO_4^{5-} into solution until saturation. The initial hydration slows down, probably because of formation of a dense coating of $Al(OH)_3$ gel on the surface of the particles [20].

- Chemical admixtures dissolve in the binding system suspension, undertaking an active role in complex ionic equilibrium. Adsorption of plasticizers on the surface of cement and fine ceramic powders (reactive alumina and silica fume) modifies the zeta potential and the consequent fluidizing action is due to electric or electrosteric repulsion forces [65,115]. This repulsion effect is present even if, due to high ionic strength, the double layer is compressed

[60]. Accelerators influence the dormant period of hydration by forming crystallization nuclea, which reduces the time necessary for homogeneous nucleation from the dense gel coating around the cement particles, therefore, accelerating the hydration [33, 36, 67]. Retarders influence the kinetics of hydration by slowing down the dissolution of the anhydrous cement particles. The mechanism consists of blocking dissolution by adsorption on the cement grain and/or combination with calcium ions [17, 33, 36,115].

• Ceramic reactive fine particles (reactive alumina and silica etc.) have multiple roles in the suspension of the binder system. Due to their small particle size (0.1-1μm), they fill the voids between larger particles which would otherwise filled with water [13]. When used with appropriate plasticizers, they contribute towards an increase in the electrostatic repulsion between particles fluidizing the binding system [65,114]. Another aspect less studied is the chemical interaction of these particles with the hydraulic binder in suspension, although the long term, slow pozzolanic reactions in the hardened material are well documented. Within the first minutes of hydration the concentration of Ca^{2+}, Na^+, K^+, and OH^- increases, and, due to OH^- adsorption, silicon atoms diffuse into solution [114,116] according to the reaction:

$$SiO_2 + 2H_2O \rightarrow Si(OH)_4$$
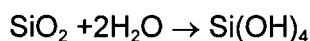
Further reactions of silicic acid with Ca^{2+} ions, which result in an $xCaO \cdot ySiO_2 \cdot mH_2O$ phase, are dependant on the water to cement ratio as well as on the cement to silica fume ratio [44,116]. There is no information available on the possible interactions between silicic acid, calcium ions and alumina gel on the surface of cement particles.

After hydraulic setting of the cement, the binding system transforms to a hydraulic matrix containing crystalline hydrates, unhydrated ceramic particles and amorphous phases of

hydration based on silica and alumina gel. The crystalline hydrated products have three main sources:

- Primary hydration of calcium aluminates results in a mixture of metastable hydrates, CAH_{10}, C_2AH_8, and C_3AH_x, developed in a pattern of hexagonal plates 0.25-2μm thick. Also, traces of C_3AH_6 in its characteristic morphology of icositetrahedron are present [19, 22].

- Interaction between the hydroxilated surface of reactive alumina grains and Ca^{2+} ions resulting in development of hexagonal C_2AH_8 crystals [51].

- Interaction between hydration phases generating crystalline gehlenite hydrate (C_2ASH_8) [22]. This hydrate is present at room temperature only in binding systems containing a high concentration of silica fume, and can be identified 1-3 days after casting. It is not clear if this crystalline product is formed by crystallization of amorphous CASH phases [100] or during conversion of metastable hexagonal hydrates in the presence of silica gel [46].

When heated up, the hydraulic matrix transforms to a ceramic matrix by a sequence of reactions with or without the presence of a liquid phase:

- Conversion and decomposition of hydration products. Conversion is complete at 54°C resulting in a mixture of stable, cubic hydrates. In ultra low cement ARC having high content of silica fume, the conversion may be completely inhibited due to formation of Stratlingite [46]. Amorphous CASH phase dehydrates at 100-220°C. At 750°C, decomposition of hydrated phases is complete resulting in solid reaction products: a mixture of calcium aluminates and transition alumina phases [117];

- Decomposition of natural alumino-silicate components (as Kyanite and Andalusite) starts at 1100°C, resulting in the formation of mullite and cristoballite:

$$3(Al_2O_3 \cdot SiO_2) \rightarrow 3\ Al_2O_3 \cdot 2\ SiO_2 + SiO_2$$

- Formation of low melting point feldspar phases and crystallization of mullite. Low temperature melting eutectic points (1300-1400°C) appear in the CaO rich part of the phase diagram of the system $CaO-SiO_2-Al_2O_3$ corresponding to anorthite and gehlenite. Depending on the amount of CaO present in system, this process will result in a mixture of low melting temperature glassy phase and mullite crystals [118].

The binding system starts to generate a ceramic matrix at about 800°C that is "physically" completed at about 1100°C, although the mullite formation process is at an incipient level. The further increase in temperature will bring the system closer to the equilibrium conditions, with a secondary mullite crystallized in this ceramic matrix [12].

2.4.2. Mechanical strength

Conversion of aluminous cement hydration products has a negative effect on mechanical strength of refractory castables. The first step which decreases the mechanical strength, after the setting of the calcium aluminate cement, occurs after the conversion of metastable hexagonal phases into cubic phases, which are stable at room temperature. It has been reported that some castable installations have started to dust and peel in the air due to this process [117].

The presence of aluminous cement is also detrimental to the mechanical properties of a refractory castable at high temperatures. Therefore, the most important issue is to lower the quantity of aluminous cement while maintaining the strength of the lining [115]. The mechanical strength of the green refractory castable may be increased by:

- reducing the content of alumina cement by partial replacement with reactive ceramic powders;

- decreasing the water to cement ratio that inhibits the formation of CAH_{10};

- obtaining a uniform distribution of the hydraulic binder in the castable matrix by use of

  deflocculants [119];

- elimination of flaws by optimization of flow.
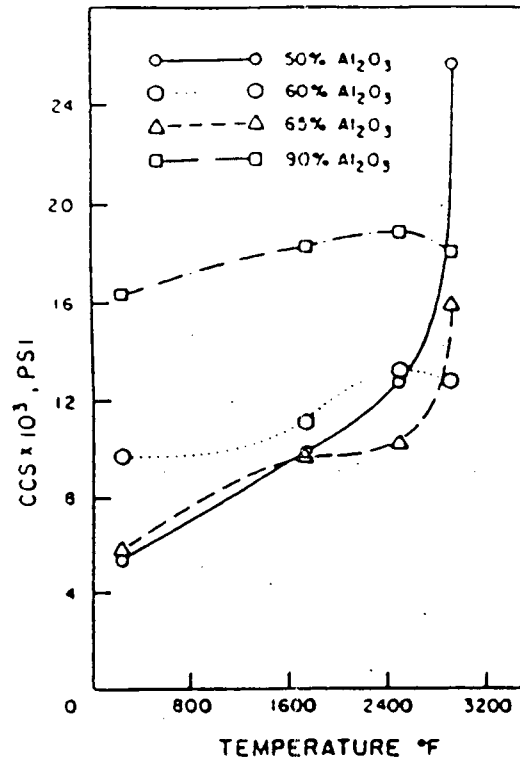
Figure 2.4-1. Variation of CCS of low-moisture castables with alumina content after firing [120].

The average chemical composition may be an important factor for improving the mechanical properties at room temperature, as shown in Figure 2.4-1, for Cold Compression Strength (CCS) and Figure 2.4-2, for Modulus of Rupture (MOR). It is interesting to mark that for both MOR and CCS at room temperature, the highest values are obtained for the 90% alumina castables while the lowest values are obtained for the 50% alumina one [120, 121].
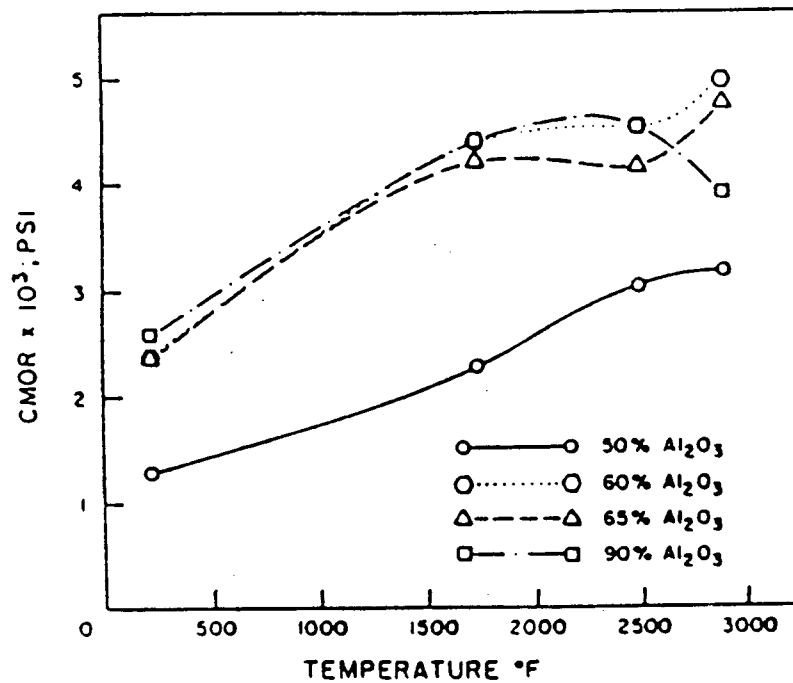
Figure 2.4-2. Variation of MOR of low-moisture castables after firing [120].

The amount of water used for casting has an important effect on mechanical properties (Figure 2.4-3). The effect of water reduction is more important for samples fired at high temperatures (1550°C). At these temperatures, there is a non linear behavior below 5.5% of casting water. A similar situation is indicated by MOR results, shown in Figure 2.4-4, but the nonlinearity for the case of high temperature curing is stronger.

If the water used for casting is further reduced, there is a maximum of CCS for samples containing 70% alumina, but for temperatures over 1375°C the highest CCS is obtained again by the sample having the highest content of alumina (90%), as shown in Figure 2.4-5, for ULCC in the firing temperature range 260-1375°C.
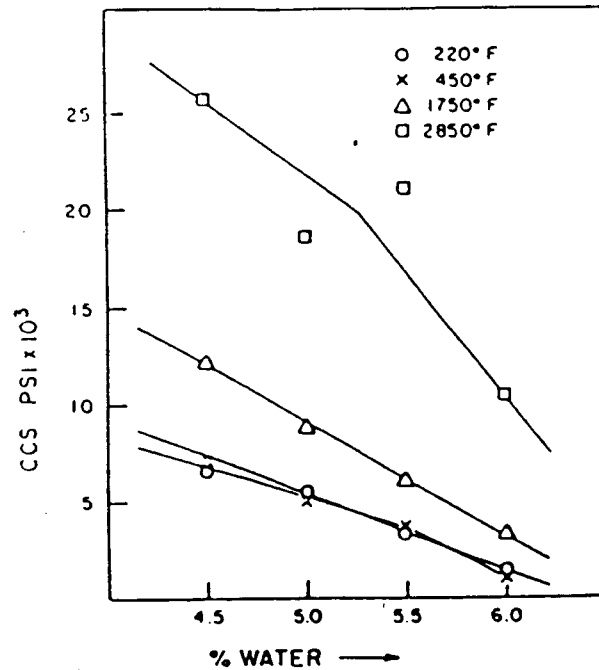
Figure 2.4-3. Variation of CCS with the water for casting for different firing temperatures [120].
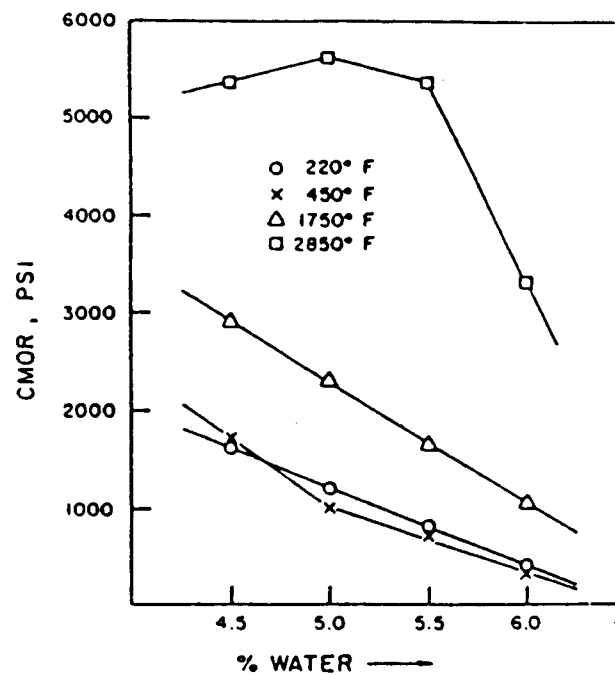
Figure 2.4-4. Variation of MOR with the water used for casting for different firing temperatures [120].

57
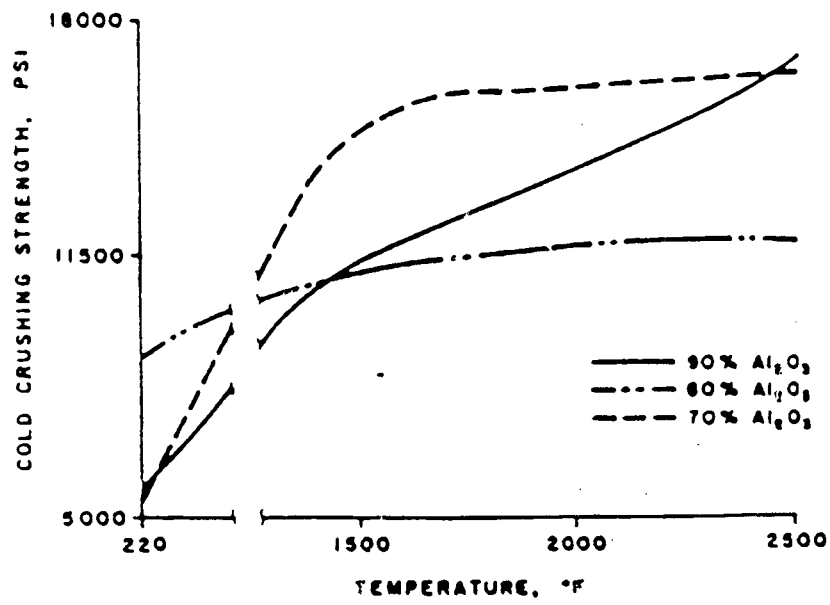
Figure 2.4-5. Variation of CCS with temperature for ULCC [121].
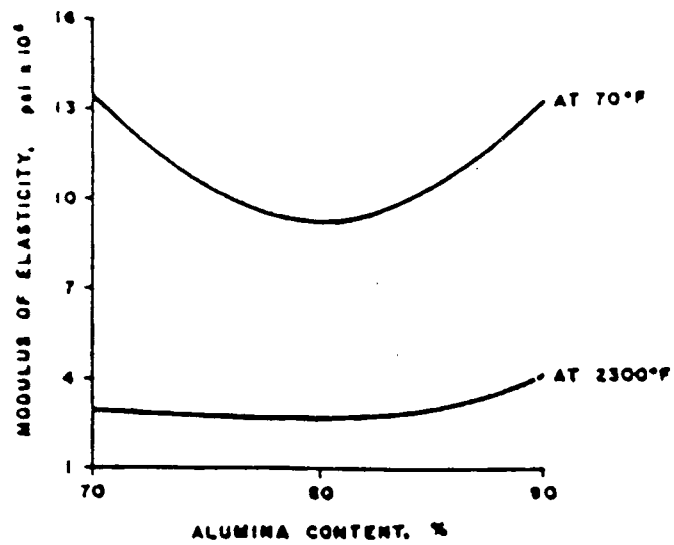
Figure 2.4-6. Variation of modulus of elasticity of a ULCC with alumina content [121].

58

This phenomenon may be related to a nonlinear variation of Young's modulus of ULCC with the alumina content (Figure 2.4-6). In the 1260°C temperature region, ULCC has a more plastic-like type behavior as small amounts of liquid phase begins to develop in the matrix of the castable. This liquid causes the marked reduction in the modulus of elasticity, but by increasing the alumina content, an increase of Young's modulus also occurs [121].

Figure 2.4-7 (a) shows the variation of CCS after drying, with the content of silica fume, for different levels of CAC in self-flowing tabular alumina castables. It is interesting to note that even if the strength after drying generally increases with cement content, this is only valid for compositions with a silica fume content of 6% or less. With 8-10% of silica fume there does not seem to be substantial differences in strength for the different cement contents. The reason is probably the combined effect of reduced water demand together with the reactivity of silica fume [122].

The reactivity of silica fume becomes pronounced after firing at 1000°C where there is a strong increase in strength with silica fume content up to about 4-6%. In this case, the higher strengths were obtained with the lowest cement content, as showed in Figure 2.4-7 (b).
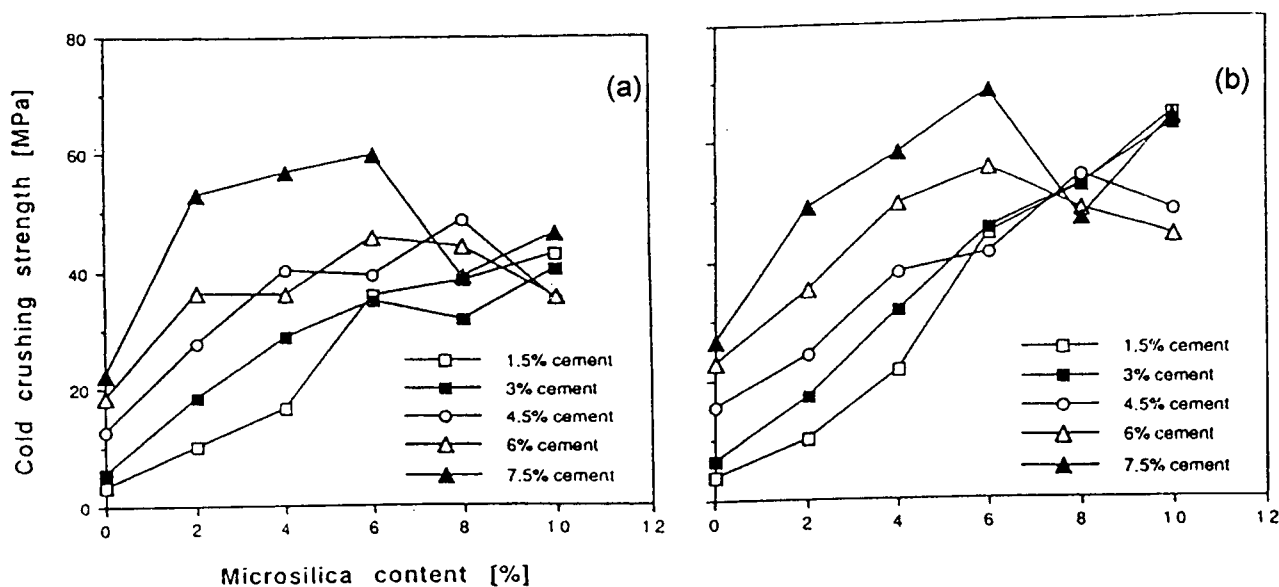
Figure 2.4-7 Variation of CCS with the content of silica fume after drying (a) and firing at 1000°C (b) for tabular alumina based castables with different content of CAC [122].

2.4.3. High temperature mechanical strength

The high temperature mechanical strength of refractory castables is a function of the equilibrium in the ceramic microstructure that is developed at firing or in service. The ceramic microstructure depends on the composition of the castable and on the service/firing temperature. The most common compositional domain for ARC is the CaO-SiO_2-Al_2O_3 system, Figure 2.4-8 [124]. Despite their low cement content, the low and ultra-low cement castables have a high crushing strength and a high modulus of rupture at high temperatures when mullite phase develops. On firing, the formation of low melting point phases is reduced, and increased refractoriness is observed [123]. The only reason for introducing calcium aluminate cement (and consequently CaO) is to obtain the setting and hardening of the castable.
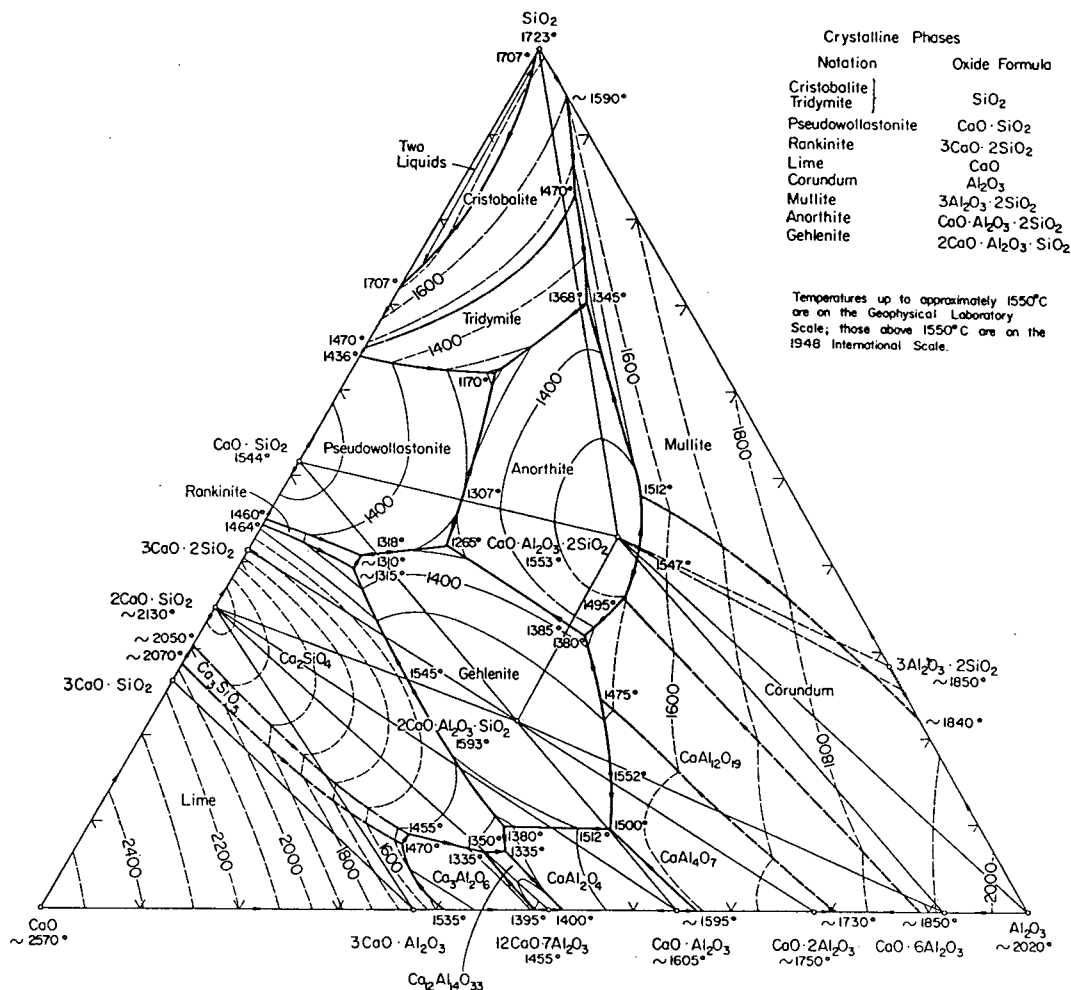
Figure 2.4-8. CaO-SiO_2-Al_2O_3 system [124].
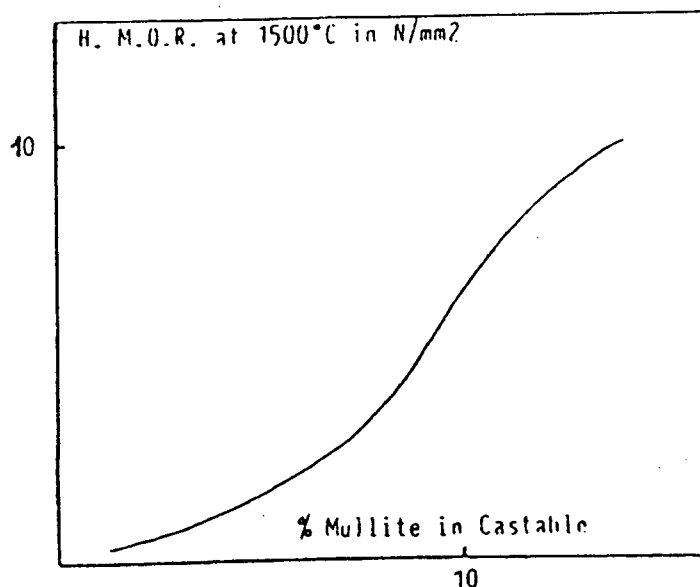
Figure 2.4-9. Evolution of HMOR of an ULCC, at 1500°C as a function of mullite content formed in the system [125].

The composition of the ceramic bond must be carefully selected from the Al_2O_3-SiO_2-CaO phase diagram in order to develop the maximum mullite content at high temperatures, while keeping good setting and hardening properties. Figure 2.4-9 shows the evolution of the Hot Modulus of Rupture (HMOR) of an ultralow cement castable at 1500°C with the proportion of mullite formed in the system [125].

The HMOR at 1370°C for different alumina-containing LCC is presented in Figure 2.4-10. It is interesting to note that HMOR of 75% alumina castable is higher than that of the 90% alumina composition. The 75% alumina castables had mullite both in grains and in the matrix. This provided a much better bonding than between the corundum aggregates and the matrix in the 90% alumina composition [126].

The high temperature strength of refractory castables can be improved by:

•reducing the CaO content by using low levels of CAC or by using HAB as a hydraulic binder;

•increasing the content of silica fume and reactive alumina in order to provide reactive ultrafine components for formation of mullite;

•addition of fine alumino-silicate powders.

61

A comparative study of the influence of alumino-silicate additions on the properties of bauxite based castables [127] shows that kyanite gives the highest strengths at 1200, 1300, and 1400°C. Andalusite also performs well at 1200 and 1300°C but produces a decrease in strength at 1400°C. Mullite addition has the least effect in strength, giving the lowest strength at 1400°C. All castables tested had a low strength below 1200°C which increased significantly when heated to 1300°C.
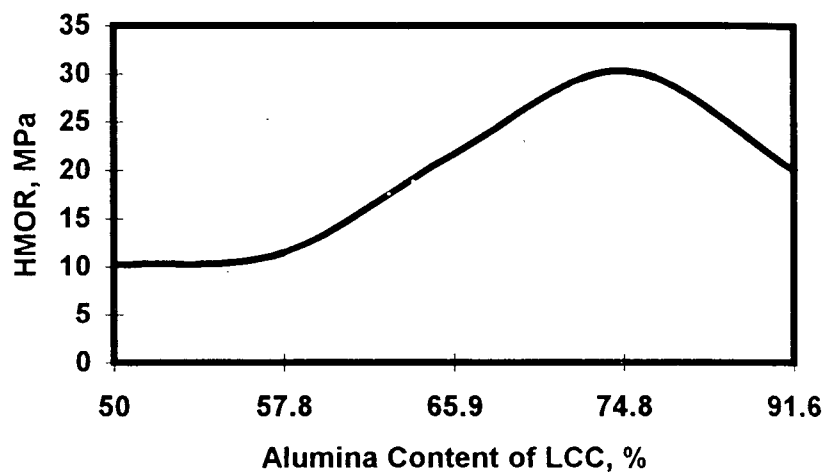
Figure 2.4-10. Variation of HMOR at 1370°C for different alumina content of LCC [126].

Both andalusite and kyanite transform to mullite and SiO_2 when fired at approximately 1300°C. The transformation is accompanied by a volume increase of 3-6% and 15%, respectively. The increase in strength due to addition of the alumino-silicates may be caused by a combination of two mechanisms. Firstly the decomposition of alumino-silicates which, under influence of impurities may well start below 1300°C, creates the mullite nuclea for further mullite formation. Secondly, the volume increase of kyanite and andalusite which, when transformed may cause the movement of liquid phase and as a result, more pores of the castable may

62

become filled with a liquid and the volume fraction in which mullite can develop increases. With mullite as dopant, the reaction formed mullite tends to grow as needle-like shape particles instead of rounded shaped particles. The formation of mullite in the castable matrix and the compositional particularities of the refractory aggregate are factors that determine high temperature strengths of refractory castables [128].
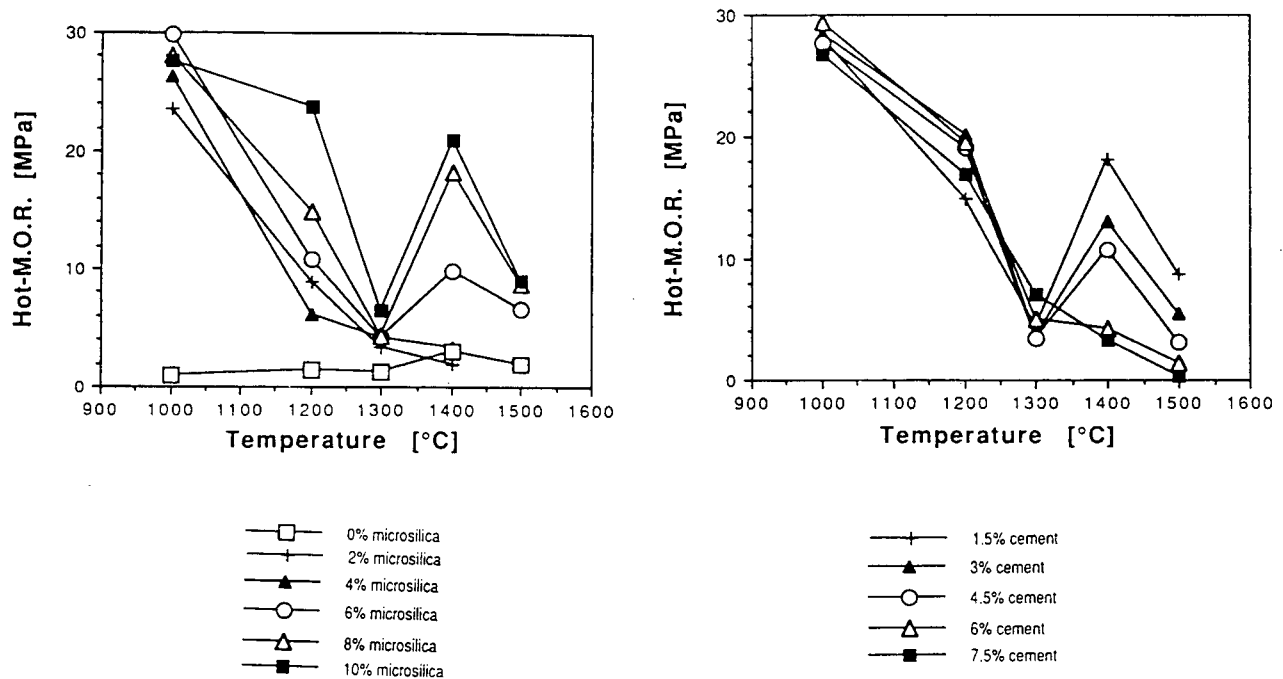
Figure 2.4-11. Variation of HMOR of tabular alumina based castables having: (a) constant content of CAC (1.5%) and different content of silica fume and (b) constant content of silica fume (8%) and different content of CAC [129].

Figure 2.4-11 shows the variation of HMOR of tabular alumina based castables for compositions having different content of silica fume (a) and different content of CAC (b). According to experimental results [129], an increase in microsilica content has a very strong influence on strength at temperatures above 1300°C. For a castable with 1.5% cement content, an increase in microsilica content from 4 to 6% more than doubles the HMOR at 1400°C and

63

has even a stronger effect at 1500°C. Furthermore, increasing the microsilica content from 6% to 8% results in almost doubling of strength at 1400°C. However at 1500°C the effect is less pronounced. Up to 1300°C there is no important difference in HMOR of samples with different microsilica content.

The increase in HMOR at 1400°C is caused by the growth of mullite from a liquid phase of a composition in the triangle anorthite-mullite-silica. During the first heat-up to 1400°C, the bond phase of the castable reacts and produces a viscous liquid consisting mainly of cement and microsilica. Within a few hours, alumina is dissolved with a subsequent mullite precipitation that strengthens the castable. The composition of the liquid is thereby changed as the silica content is reduced, and the total volume of the liquid is simultaneously reduced. This liquid phase containing silica explains the observed need for a minimum amount of microsilica in order to get mullite formation [129, 130].

There is a strong correlation between the content of CAC, silica fume, temperature and the amount of mullite formed in a castable, Figure 2.4-12. The apparently linear dependence
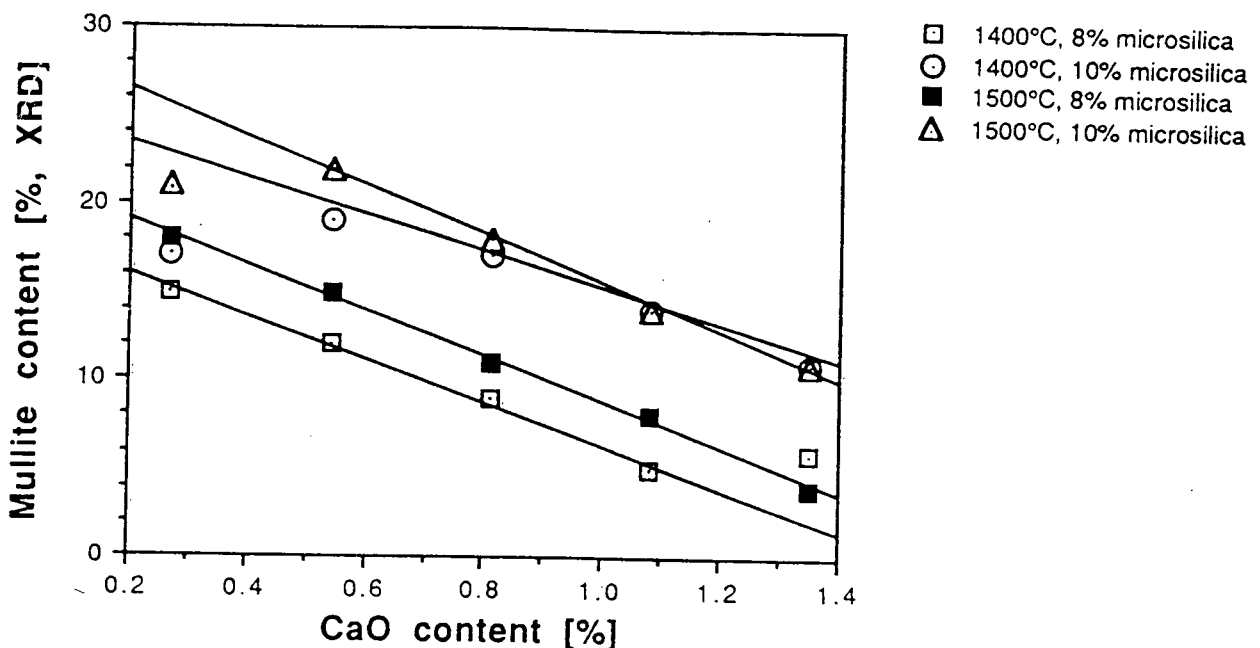
Figure 2.4-12. Variation of mullite content with CaO content for tabular alumina castables [129].

could indicate the existence of a liquid/glassy composition with fixed Ca/Si ratio [129].

At temperatures above 1400°C, the HMOR of refractory castables having HAB as a hydraulic binder, is about four times higher than that of the conventional LCC, as it is shown in Figure 2.4-13. However the HMOR of NCC castables below 1400°C is usually inferior or slightly lower than that of LCC. The effect of silica fume addition on strength of NCC is more important for temperatures below 1400°C
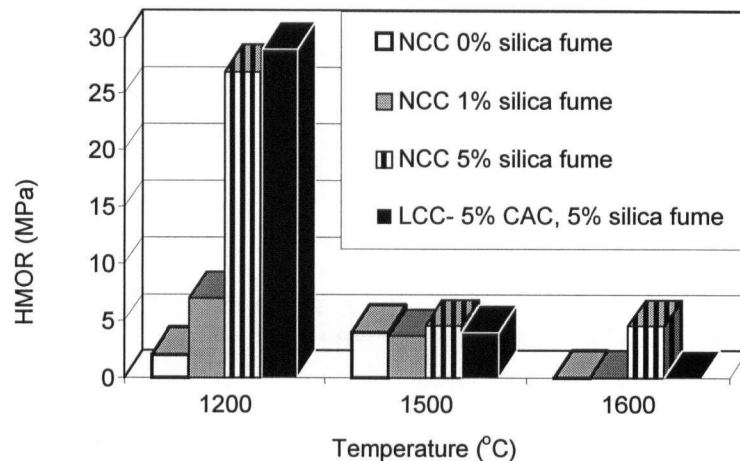
Figure 2.4-13. Variation of HMOR of NCC with temperature for different amounts of microsilica [25].

In samples consisting of only hydraulic alumina and silica fume, which were exposed to humidity, traces of mullite have been detected from 1085°C. However similar powder mixtures require higher temperatures for the initial mullite formation. This indicates a reaction between hydraulic alumina and silica during setting of a castable. Even though mullite is formed at low temperatures, probably due to diffusional hindrance, significant amounts are rarely found below 1300-1400°C.

In NCC samples, after firing at 1500°C, the fracture surface reveals a network of interlocked and elongated crystals (Figure 2.4-14). EDX analyses confirmed that the elongated crystals have a composition close to mullite. Between the crystals there is a liquid or

amorphous phase bonding the crystals together. Efforts were made to analyze these phase but only mullite and alumina were detected [38].
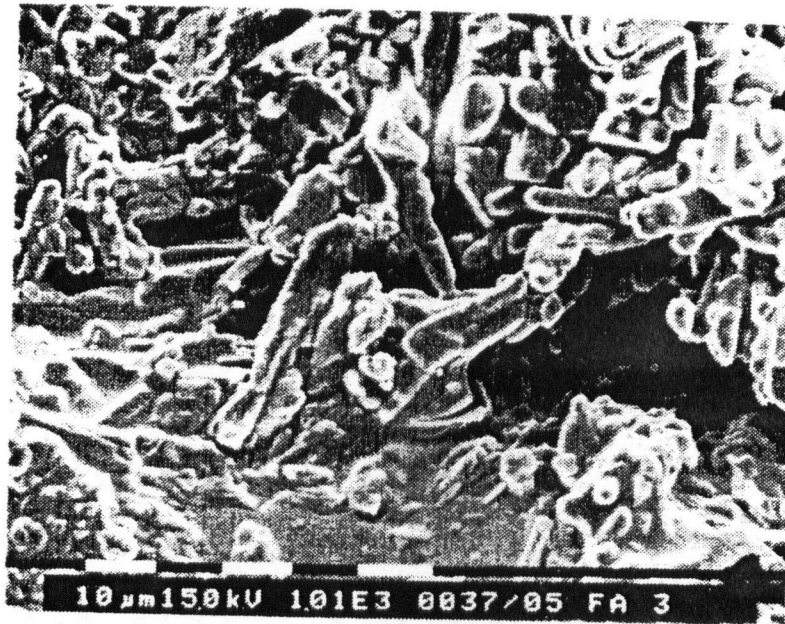
Figure 2.4-14. SEM of the fracture surface of a fused alumina NCC after firing 24 h at 1500°C [38]

The high mechanical strength of ARC at temperatures above 1300°C can be explained by the formation of mullite in the ceramic matrix. Even if traces of mullite can be detected at temperatures above 1100°C, there is not yet any satisfactory explanation of the fact that ARC can exhibit a continuous increase in strength at temperatures below 1000°C. This behavior is not characteristic only to ULCC and NCC. Also, LCC may show no strength degradation up to 1000°C. It is possible that in the presence of silica fume, the formation of metastable hexagonal hydrates is inhibited. Therefore, the conversion process, and its negative effect on mechanical strength, is limited.

Figure 2.4-15 shows the development of crystalline structure in an LCC with and without silica fume. It is seen that in the presence of silica fume the hydration process is inhibited (resulting in higher content of unhydrated CA and CA_2), the amount of crystalline hydrates is reduced, and Strallingite is formed in quantities comparable to C_3AH_6 [126].
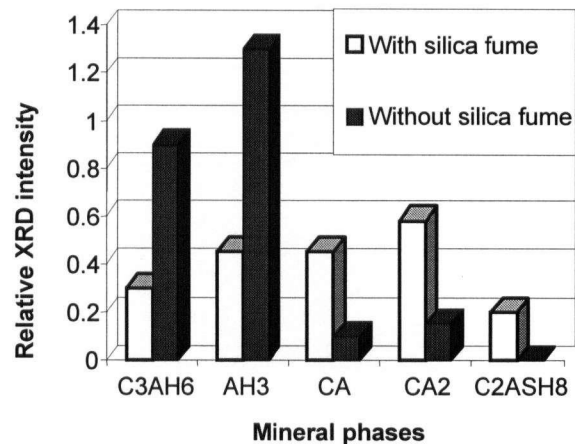
Figure 2.4-15. Content of crystalline structures in a hydrated LCC with and without silica fume addition [126].

For high temperature applications (>1500°C), or for the design of self-flowing magnesia spinel based castables, the presence of silicon dioxide in the castable is detrimental. Therefore, it is not possible to use silica fume as a flow enhancer and a reactive powder. For these applications, the only fine reactive component that generates flow and promotes the formation of ceramic matrix is reactive alumina or reactive magnesia spinel. These self-flowing castables are known as Silica Fume Free (SFF) castables.

The HMOR at 1500°C of tabular alumina SFF LCC (5% CAC Alcoa CA-270) based on reactive alumina (CTC 50) can reach 20MPa. For the same composition, if reactive alumina is replaced with reactive spinel (CTC 55), the HMOR can increase to 23MPa [90,91]. For tabular alumina based castables, the HMOR of Silica Fume Free LCC at 1500°C are similar to those of NCC with high amounts (8-10%) of silica fume. In the case of magnesia spinel based castables, any addition of silicon oxide results in total decay of high temperature properties. There is no available data discussing the evolution of hot strength with temperature for SFF castables.

2.5. Spray gunning

Refractory castables can be installed by vibrating, casting, gunning, and spray gunning. Spray gunning, Figure 2.5-1, is quickly becoming the preferred method of installing monolithics, due to developments in materials, equipment technology, and cost benefits.

The advantages of gunned installation of refractory castables are as follows [130]:

- easy, efficient, and fast installation;

- formless installation, i.e. no forms for casting/vibrating are necessary;

- material and man labor saving process;

- can easily meet emergency needs.

Spray gunning has all the above advantages, plus virtually no dusting, low rebound, giving better properties to the installed material. The water content of the spray gunned castable is precisely controlled during premixing, and the whole process of installation is also easier to control by the nozzle operators [131].
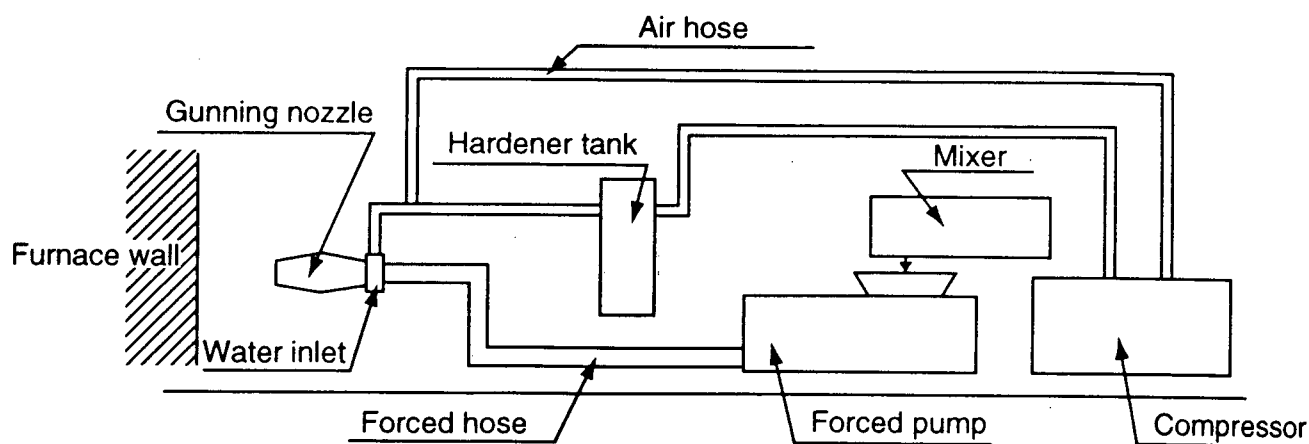
Figure 2.5-1. Spray gunning equipment.

In the spray gunning process, refractory castable is premixed with water in order to achieve a pumpable consistency, and then poured into the hopper of a concrete pump. The wet castable is transported under pressure through a hose, and ejected through a nozzle onto the wall or area of operation. At (or before) the nozzle, a setting accelerator admixture is injected into the wet castable. In the short time of traveling between the nozzle and the spraying target, due to the action of the setting accelerator agent, the castable changes from a pumpable mix to a plastic consistency. Because of the need for rapid stiffening, and the ability to be uniformly injected at the nozzle, a liquid accelerator system with a soluble accelerator is normally used.

The physical properties of the refractory material installed by spray gunning have slightly lower values than when similar materials are vibrated or cast, but superior to the properties obtained by conventional dry gunning. Figure 2.5.-2 shows a comparison of properties of gunned, spray gunned and vibratable mixes.

(a)   (b)   (c)
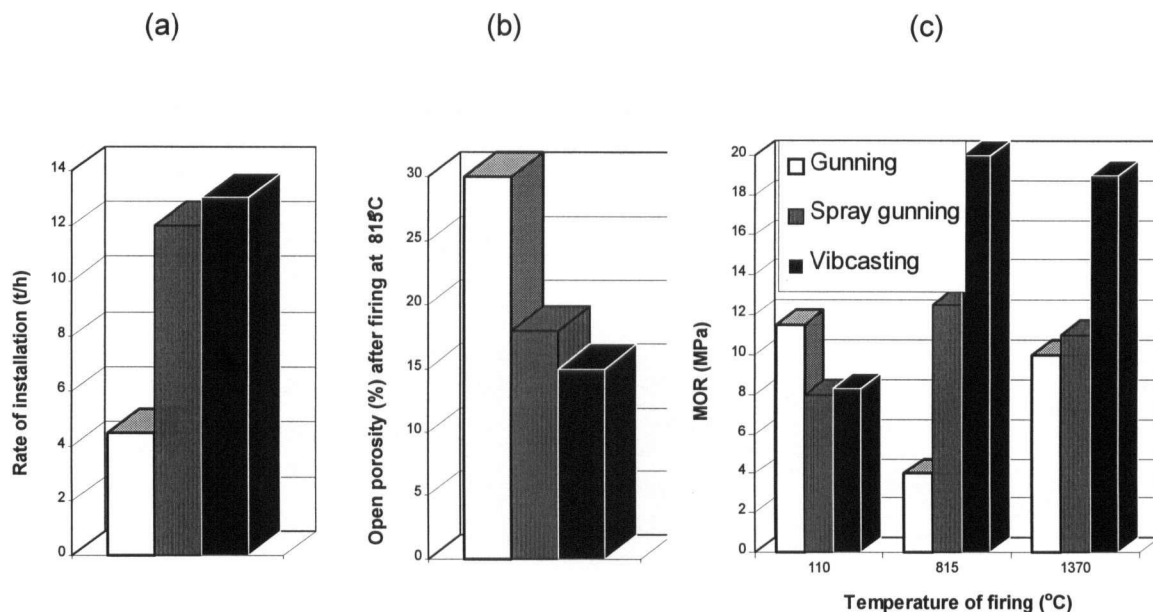
Figure 2.5-2. Comparison between dry gunning, spray gunning and vibcasting for LCC [132].

Spray gunning, as compared to dry gunning, offers a more efficient solution for installation of the castables. The porosity of the castable is reduced to half and the cold bending strength at relatively low temperatures of spray gunned LCC is almost three times higher than that of dry gunned mixes [132].

The main criterion that has to be fulfilled to obtain a successful spray gunning mix is a self-flowing and pumpable refractory castable. Besides self-flowing behavior, a castable should have a minimum dilatancy, high cohesivness and a low tendency to segregation [133].

Ideally the castable after acceleration should remain in a thickened but plastic state for a reasonable length of time. This facilitates troweling, finishing and checking for proper installation. For safety reasons, particularly for overhead installations, the material needs to stiffen quickly. Accelerators that cause rapid setting of stiffening or the castable are not acceptable as they cause laminations and nozzle clogging. It is important to minimize the amount of accelerator regardless of its type. Excessive acceleration leads to lower strength linings, due to extra water applied. Also, because many accelerators contain alkaline or alkaline earth cations, the refractoriness of the lining suffers with excessive amounts of the accelerator [134].

It is believed that the effect of an accelerator depends on the composition of a castable (CAC, silica fume and reactive alumina content, level of water for casting, and dispersant system). The mechanism of acceleration of self-flowing castables for spray gunning applications is not yet well understood, and at the present stage the selection of accelerator admixtures is made only on trial and error basis.

Figure 2.5-3 (a) shows the effect of different accelerator admixtures on the green strength of a fused alumina based LCC (4% CAC Secar 71) containing 2.5% silica fume Elkem 971 and 10% reactive alumina MA95 at 7% water addition. The experiments were done using STPP and PMS as dispersants. Figure 2.5-3 (b) shows the efficiency of accelerator admixtures

for the same compositions. The efficiency was determined indirectly by measuring the residual slump after adding accelerator admixture. A lower slump is considered to correspond to a high effectiveness.
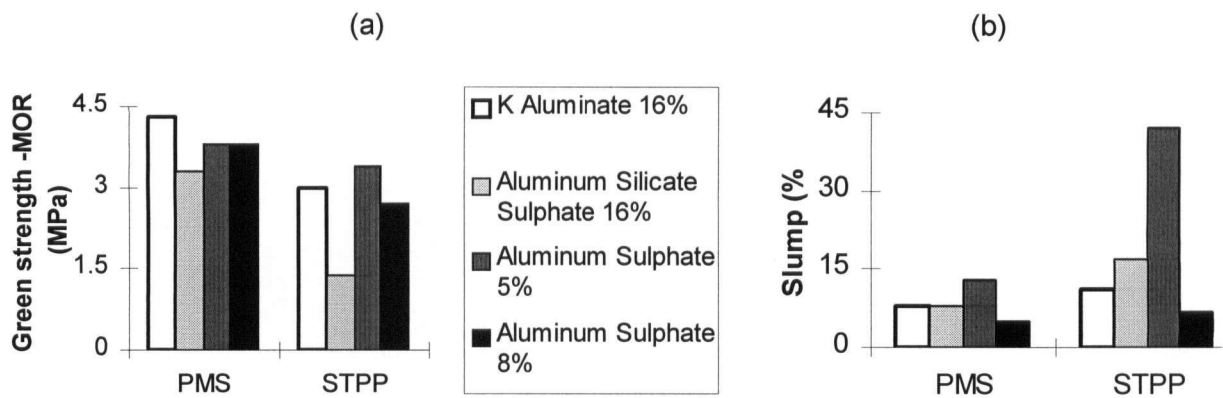
Figure 2.5-3. Green strength (a) and accelerator effectiveness (b) for tabular alumina based LCC for spray gunning dispersed with organic (PMS) and inorganic (STPP) [135].

It is shown that in the system presented above, the organic plasticizer (PMS) gives better results (green strength and effectiveness) than the inorganic one (STPP). The authors of this study also concluded that for the chemical admixture system that was studied the silica fume content should be maintained at levels below 4% in order to obtain a castable suitable for spray gunning.

Other chemicals considered to be efficient admixtures for spray gunning of refractory castables are: sodium silicate [133], alkaline earth carbonates and nitrates [134], sodium aluminate, and various phosphate agents.

3. Scope and objectives

Although, in recent years, a number of studies concerning the many complex variables that determine the rheologic, hydraulic and ceramic properties of Advanced Refractory Castables (ARC) have been performed, the fundamentals of free-flow and of transition from hydraulic bond to ceramic matrix are still only poorly understood. Most of the technical information regarding ARC is fragmentary, empirical and sometimes contradictory. This is mainly due to the following three factors:

- ARC are the most complex refractory formulations, involving hydraulic, colloidal and solid state interactions that are closely interrelated.

- There is a lack of methods for the precise characterization of the hydraulic and rheological properties of these materials.

- It is not possible to make a separate analysis of the rheological, hydraulic and ceramic properties of ARC because, most often, a single component may have multiple roles (e.g. microsilica has effects on hydraulic setting, flow and on the formation of ceramic matrix).

The primary scope of this work is to bring a better understanding of the phenomena involved in ARC processing by performing an integrated analysis of their hydraulic, rheological and solid sate (ceramic) properties, with a focus on the free flow behavior and on the role of hydraulic bond on the ceramic matrix formation. The results of this investigation are utilized for developing novel concepts for ARC processing, with a focus on spray-gunning, which is the newest, most demanding and most efficient application technique.

In view of the scope of the present work, the proposed investigation path includes the following objectives:

1. To develop an accurate viscometric method for determining the rheological properties of the suspension of fine fraction of the binding system of ARC. The currently used flow measurement methods are empirical and unable to obtain accurate information on the effects of the binding system components on the rheological properties of ARC.

2. To perform a thorough rheological investigation on ARC with the particular focus on:
   - effect of plasticizers and setting time admixtures on the rheology and hydraulic setting process;
   - effect of water content on the viscometric properties of binding systems
   - correlation between the viscometric properties of the binding system and the flow behavior of ARC;
   - role of particle size distribution on flow.

3. To investigate the effects of hydraulic binders and the rheological properties of ARC on the development of the ceramic matrix, including:
   - study of the effect of hydraulic binders and rheology on the evolution of mechanical properties with heat treatment temperature;
   - microstructural study of the transition from a hydraulic bond to a ceramic matrix in ARC.

4. To use the knowledge generated during the laboratory investigation to improve the spray-gunning technology of ARC and to validate the laboratory results on a pilot plant scale. The goals of this part of the work are as follows:
   - a significant improvement in plasticity and suppression of the premature setting of the freshly spray-gunned ARC material;
   - enhancement of the mechanical properties of the spray-gunned ARC installations by optimizing the nature and content of spray-gunning additives.

4. Experimental results and discussions

4.1. Experimental procedures and apparatae

The aim of the present research was to study the correlation between the parameters of colloidal processing and the properties of the ceramic matrix of ARC. For this purpose, in the first step of research, different test formulations of self-flowing ARC were designed. In order to establish a correlation between the rheology of the binding system and flow, a new method of measuring the viscosity of the binding system was developed. The setup of the method included the design of the concentric-cylinder measuring cell and the novel measurement procedure (i.e. sample preparation, shear stress levels, and measurement timing).

Additional characterization of the experimental ARC compositions was done by strength measurements (CCS, CMOR and HMOR), microstructural analysis by XRD, SEM, EDX and open porosity measurements.

4.1.1. Experimental compositions

For the experimental ARC compositions the following raw materials were used:

1. Refractory aggregate (45-4750μm):

- Mullite based calcines containing 60 and 70% Al_2O_3 (Mulcoa 60 and Mulcoa 70, CE Minerals Ltd.), fraction: -4+8 mesh (2360-4750 μm), -8+20 mesh (850-2360 μm) , -35 mesh (<425 μm) , and -100 mesh (<150μm);

- Calcined bauxite Alphastar, CE Minerals Ltd., -100 mesh (<150μm);

- Mulcoa 90 (90% Al_2O_3), CE Minerals Ltd., -100 mesh (<150μm);

- Tabular alumina, La Roche Chemicals Ltd. (99% Al_2O_3) fractions: -4+14 mesh (1180-4750μm), -14+28 mesh (600-1180 μm), -28+40 mesh (425-600μm), -50 mesh (<300μm), -100 mesh (<150μm), -325 mesh (<45μm).

2. Fine fraction:

- Calcined alumina RGA -325 mesh (<45μm);

- Calcined Kyanite -325 mesh (<45μm), Virginia Kyanite Mining Corporation

- Calcined alumina AC34B5, Pechiney, Aluchem

- Reactive alumina: A-3000, Alcoa and C90, C94, Alcan Chemicals Ltd.

- Hydraulic binders:

    - Calcium Aluminate Cement: Secar 71, Lafarge;

    - High Alumina Binder: Alphabond 100, 200 and 300, Alcoa.

- Silica fume:- Elkem 971U, Elkem Norway (SF1);

    - Globe Metallurgical, Globe (SF2);

    - Duralum AB, Washington Mills Ltd (SF3).

3. Plasticizers:

- phosphate plasticizers: sodium hexametaphosphate (SHMP), sodium tripolyphosphate (STPP)

- organic plasticizers: sodium naphtalenesulfonate formaldehyde polycondensate Daxad 19 (NSFC), sodium polmetayacrilate Daxad 30 (SPMA), sodium polyacrilate Darvan 811 (SPA).

4. Setting time regulators: citric acid, lithium carbonate and sodium aluminate

The experimental compositions were designed in order to obtain very good self-flow properties at low water levels (i.e. 100% flow for water contents lower than 6wt.%). Low and ultra- low cement castable formulations were made based on mullite refractory aggregate

(Mulcoa 60 and Mulcoa 70) having the medium fraction (-100 mesh) based on Mulcoa 90 or calcined bauxite Alphastar. The ceramic components of the binding system of low and ultra-low cement castable formulations included: calcined alumina, calcined kyanite, silica fume and calcium aluminate cement Secar 71 (4% for low cement and 2% for ultra-low cement compositions). No cement self-flowing castables were made based on tabular alumina refractory aggregate. The ceramic components of the binding system include: HAB (Alphabond 100, 200 and 300), calcined alumina, reactive alumina and silica fume see (Table 6).

Table 4.1-1. Characteristics of the experimental castable compositions.

Type	LCC	ULCC	NCC
Aggregate	Mullite based calcines Mulcoa 60, Mulcoa 70	Mullite based calcines Mulcoa 60, Mulcoa 70	Tabular Alumina
Binding System	CAC Secar 71 (4%) Silica Fume Raw Kyanite Calcined Alumina	CAC Secar 71 (2%) Silica Fume Raw Kyanite Calcined Alumina	HAB Alphabond 200 (1.75%) Silica Fume Tabular Alumina (-325 mesh) Calcined Alumina

4.1.2. Viscosity measurements

Refractory castables contain particles that are too coarse to allow viscosity measurements in laboratory viscometers under controlled shear rate. It is thus impossible to make true scientific measurements on the rheological characteristics of these materials. Moreover, the understanding of the phenomena involved in establishing the cement paste rheology has not yet reached a sufficient level to allow the characterization of the more complex "suspension" formed by fresh concrete [56].

Assuming that the coarse refractory aggregate has an inert behavior in the fresh castable suspension, and ignoring the effects of small quantities of water absorbed in the open pores it may be hypothesized that it has no direct contribution to the dispersion process.

Therefore, it is assumed that the rheology of the castable refractories may be described by the rheology of a suspension that:

- includes all the fine powders of the binding system (i.e. hydraulic binder and fine reactive powders) fine particles of aggregate and chemical admixtures;

- is prepared in conditions similar to those existing during mixing of the castables (i.e. high shear rate generated between particles of refractory aggregate);

- has water content similar to that of the corresponding castable;

- is subjected to viscosity measurements at shear rates similar to those existing during the installation of self-flowing castables (i.e. low shear rates).

Accordingly, the composition of mixes subjected to viscosity measurements consisted in binding systems (i.e. hydraulic binder, ceramic reactive powders and chemical admixtures), refractory aggregate fraction -100 mesh (<150μm) and water.

The fine fraction of refractory aggregate -100 mesh was included in the mixes for viscosity measurement due to the high water absorption capacity of this fraction and the shear rates that are provided during mixing and measuring the viscosity of the binding system. The refractory aggregate fraction -35 mesh was not considered because, although it has a high porosity and a continuous particle size distribution, the largest particle size in the system is 425 μm. Because the gap of the coaxial cylinder measuring cell has to be 10 to 100 times that of the largest particle in suspension and because of the irregular shape of the -35 mesh particles, the use of this fraction requires measuring gaps well above 5 mm. According to literature data, [70,71] large measuring gaps do not allow for uniform flow conditions within the annular space of the measuring cell and thus the use of the refractory aggregate fraction -35 mesh was not considered for viscometric measurements.

It is well known that castable refractories require an intensive mixing process in order to acquire self-flowing behavior, but at the present stage there is no data or method for

assessment of the levels of shear stress developed during mixing. It is not possible to use the mixer that is typically used for castables (i.e. planetary mixer) for mixing the samples for viscosity measurements, because the absence of coarse aggregate particles results in significantly lower shear rate levels applied during mixing.

When mixing a self-flowing castable refractory with water the material remains dry for a certain period of time (usually more than 20 seconds, depending on the castable composition, water content, weight of the castable, mixing speed and mixer type). The mixing of the sample was intended to reproduce as accurate as possible the mixing conditions of self-flowing castable refractories. The wetting time was used as a factor indicating the intensity of the mixing process. In order to simulate the high shear rate levels at which the binding system of an ARC is subjected when mixed in the presence of coarse aggregate particles, the samples were placed in plastic cylindrical containers having 11 cm diameter and 15 cm height with 1kg of 1.25 cm diameter ceramic balls. After adding the right amount of water the containers were homogenized for 10 minutes at 60 rpm. Figure 4.1-1 shows experimental data comparing the wetting time for two ARC compositions mixed in a Hobart mixer and the wetting time for the correspondent viscosity samples mixed at different weight ratios of ceramic balls to sample.

Although the mixing time for castable refractories in a planetary mixer was 5 minutes, the samples for viscosity measurements were mixed for 10 minutes in order to assure homogeneity. It was found that there is no difference between the viscosity of homogeneous samples mixed for 5 or 10 minutes.

A Brookfield DV-II viscometer was used for measurements of the viscosity of binder systems. The measurements were taken with a set of spindles with concentric-cylinder geometry, having a measurement gap of 4.5 mm. The custom-made spindle system had the characteristic apparatus setting constants SRC=0.391 and SMC=4.51. The viscosity data was collected using DVGATHER data acquisition software. The measurements were performed at

three slow speeds: 0.5 rpm (0.1905 s^{-1} shear rate), 1 rpm (0.391 s^{-1} shear rate), and 2.5 rpm (0.9775 s^{-1} shear rate), within 10 minutes from the end of the mixing time in order to avoid an interference from the hydration process in the case of fast setting samples.
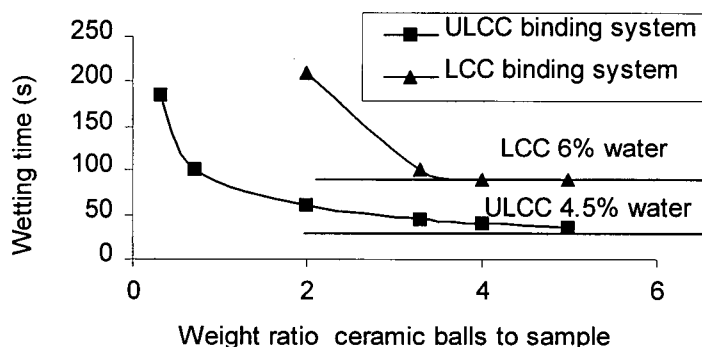
Figure 4.1-1. Wetting time for two ARC compositions and as a function of the weight ratio ceramic balls to sample, for experimental binding systems.

4.1.3. Flow measurements

For flow measurements the ASTM C230 standard, modified for self-flowing was used. Samples of a 1 kg castable mix were mixed with water for 5 minutes in a Hobart mixer and the resulting material was poured into the truncated cone and leveled. The cone was immediately pulled straight up and off the material, allowing it to flow across a smooth surface. After 2 minutes the final diameter of the castable was measured at four different locations and the values obtained were averaged. The self-flow value was determined as a percentage of increase in diameter as follows:

Self-Flow (%) = (Average Final Diameter - Initial Diameter) x100 /Initial Diameter (5)

4.1.4. pH measurements

The pH measurements were taken at room temperature (20°C) using a Corning 130 pH-meter with a VWR Scientific 34105-023 pH probe. It is not possible to directly measure pH of

the concentrated suspension of the binding system due to high diffusion gradients and potential damage of the probe. The first approach was therefore to extract, by vacuum filtration of the concentrated suspension of the binding system, enough interstitial solution in order to perform a pH measurement. The process of filtration is however difficult and in order to obtain enough sample for a measurement in the first 10 minutes after mixing, large quantities of material are required (i.e. about 1kg of binding system).

A simplified approach was to dilute a small portion of the binding system (1-2g of paste) at a 1/50 ratio and to stir it using a magnetic stirrer. For all the samples, during the first 5 minutes after mixing, pH had decreased by 0.3- 0.5 pH units. It is therefore, not possible to obtain any measurement in the first 1 to 3 minutes after diluting a binder suspension due to a continuous decrease of pH values in this interval. At about 4-5 minutes after dilution the pH becomes more stable but it still has a constantly declining slope of about 0.003 pH units/minute. The results of the dilution technique were compared with those of extraction technique. A constant difference of about 0.510 between the pH of the solution extracted from concentrated binder and the pH diluted suspension measured at 10 minutes after dilution was observed. The pH of the samples prepared at 1/100 dilution, compared with the liquid filtered under vacuum direct from concentrated suspensions of binding systems, was about 1.1-1.3 units lower. It was considered that this pH variation was not allowing a precise measurement. At dilution levels of 1/10 and 1/25 there were difficulties in cleaning and calibrating the pH probe after each measurement.

4.1.5. Particle size distribution and specific surface

The particle size distribution of binder system components was measured using a Horiba Particle Size Distribution Analyzer CAPA 700. In order to obtain information on very fine,

high surface active particles (such as silica fume and reactive alumina) nitrogen absorption method in a BET QUANTA SORB apparatus was used.

4.1.6. Setting time measurements

There is no standard method for measuring the setting time of refractory castables. The measurements of the setting time of binding system were made using the Vicat apparatus (described in ASTM C191-82). The setting time is considered to be the time interval between casting and the moment in which the Vicat needle attached to the Vicat apparatus does not leave any imprint on the surface of the cement.

4.1.7. Curing

After mixing and pouring in molds castable specimens and binding system samples were cured using the following procedure:

- 24 hours in the molds, covered by a plastic sheet at room temperature;
- after demolding 24 hours at room temperature in air;
- 24 hours at 230^0C;
- firing at specified temperature with a 200°C/hour heating rate and a 5 hours soaking time.

4.1.8. Cold crushing strength (CCS) and modulus of rupture (MOR)

Mechanical properties after drying and firing of the experimental castable compositions were studied by measuring Cold Compression Strength, and Modulus of Rupture using an Universal Testing Instrument INSTRON TTC. MOR was measured by three point bending test on 17.5×2.5×2.5 cm bars at a 12.5 cm lower span using a crosshead speed of 0.125

cm/minute. In a good-quality refractory lining the castable material should be free of macro-defects and therefore, the fracture surface of each specimen that was subjected to mechanical measurements was visually examined in order to identify if any macro-defect (such as large pores or aggregate segregation) was present. In some cases, due to improper preparation of the specimens, such macro-defects resulted in much lower MOR values and the results were discarded for both MOR and CCS measurements. Each data point presented was reported as an average of 3-5 defect free specimens for each test. This procedure of selection was applied in order to avoid a large scattering of data due to human error in processing of the experimental specimens or the use of a large number of large (non-standard) size specimens. By using only data resulted from sets of specimens that were free of macro-defects the standard error for all experimental data points was below ±10%. CCS was measured on 2.5×2.5×2.5 cm cubes out of half bars resulted from MOR test, using a crosshead speed of 0.125 cm /minute.

4.1.9. Hot modulus of rupture (HMOR)

As a part of the research program, a Hot Modulus of Rupture Testing Apparatus was constructed in the Ceramics Laboratory of Metals and Materials Engineering Department of the University of British Columbia. The apparatus was designed to comply to the requirements of ASTM C 583 for testing of HMOR of refractory castables, to utilize as much as possible the resources already existent in the department, and to allow an easy and efficient operation.

The apparatus consists of an electric furnace placed inside the frame of an Instron Universal Testing Machine. The main characteristics of operation are:

- maximum testing temperature: 1500°C.

- maximum heating rate: 400°C/h.

- maximum number of specimens (15x2.5x2.5 cm) loaded in a single run: 12.

- maximum force load: 15 kN.

- cross head speed 0.25 -0.0025 cm/min.

The Hot Modulus of Rupture Testing Apparatus is described in detail in the Appendix.

4.1.10. Microstructural analysis

Experimental castable refractories and binding systems are analyzed after different thermal treatments in order to identify the microstructural changes.

The fracture surface of castable samples or binding systems, were analyzed by SEM using a Hitachi S570 SEM microscope having a Kevex EDX detector. SEM with its high resolution and depth of field at high magnifications was used to investigate ceramic structure development. The specimens of castable refractory and binding system samples were carbon coated and EDX elemental analysis was performed.

Individual components of the binding system (i.e. reactive ceramic powders and hydraulic binders) were dispersed in iso-propanol and deposited in a thin layer on carbon stubs. In order to obtain high-resolution SEM images, some of the silica fume samples were gold coated and analyzed at low accelerating voltage (5kV).

The density of the castable specimens and binding system samples was measured by hydrostatic method. Water infiltration was done by boiling the specimens in deionized water for 4 hours, under vacuum at room temperature.

Binding system samples of low, ultra low, and no cement castables was studied by X-ray diffraction (using a Philips PW 1011 X-Ray diffractometer) in order to identify the crystalline phases formed by reaction in the matrix of castable refractories.

4.2. Rheology

The study of rheology of self-flowing ARC was focused on the following subjects:

- the effect of dispersant admixtures;

- influence of plasticizers on pH of binding systems (BS) and the possible correlation between the pH and viscosity;

- effect of particle size distribution on self-flowing behavior;

- the correlation between the viscometric characteristics of the BS and the self-flow behavior.

This approach was undertaken because of the lack of knowledge on the self-flowing behavior of ARC and the specific effect of plasticizer admixtures to the flowing characteristics. The aim of this research was to establish for the first time a direct correlation between the rheological properties (such as viscosity, shear rate-shear stress characteristics) and flow, and also to provide a tool for optimization and design of self-flowing ARC compositions.

4.2.1. Rheology of binding systems

4.2.1.1. Rheology of binding systems for LCC

These experiments were conducted in correlation with the study of flow behavior of castable refractories. The initial experiments established the basic rheological characteristics (viscosity levels, non-Newtonian behavior and thixotropy) of concentrated suspensions of BS. The first compositions included BS of LCC containing silica fume, calcined alumina and calcium aluminate cement in equal proportions.

Figure 4.2-1 shows the rheological behavior of compositions of the binding system as a function of the water/solid ratio (w/s) and the hydration time. The principal factor controlling the viscosity of the BS is the w/s ratio. The w/s ratio also determines the variation of viscosity with time, especially for high w/s ratios. In order to obtain accurate data, it was therefore necessary to insure a proper timing of the measurements. In order to minimize the effect of hydration, the measurements were taken at the shortest possible time after mixing, which was 5 minutes.
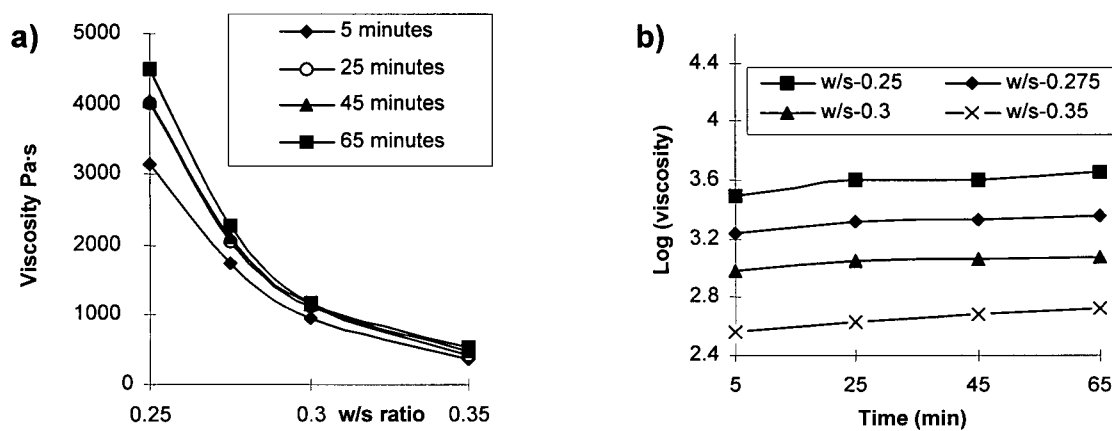
Figure 4.2-1. Rheological characteristics of a mix containing equal quantities of Secar 71 CAC, SF1, and Pechiney AC 34 B5 calcined alumina, with an admixture of 0.133% SHMP, at 0.1905 s^{-1} shear rate: a) viscosity as a function of w/s ratio for different times after mixing, b) semi logarithmic dependence of viscosity versus time after mixing for different w/s ratio.

Another important aspect resulting from Figure 4.2-1b is that the BS suspensions have a similar rheological behavior as concentrated suspensions of CAC. These results are in good agreement with the data presented by Chappuis [74] related to the rheological characteristics of CAC, i.e.:

• during the dormant period all pastes exhibit a continuous thickening with time;

• for each cement, when the scale of the shear stress is logarithmic the experimental points seem to be on parallel straight lines and the slope of variation is a measure of the relative thickening of the cement paste with time;

- for a given cement type, the relative thickening of the cement paste is independent of the water/cement ratio.

These results are also in agreement with Papo and Caufin [75], who studied the hydration of Portland cements using oscillatory rheological techniques and obtained the following relation for the variation of viscosity with time:

$$\eta = \eta_0 + (\eta_R - \eta_0)(t/t_R)^N \qquad (2)$$

where: η - the paste viscosity

η_0 - initial value of the viscosity

t - current time

t_R - the time at which the material has a very high viscosity (η_R)

N - parameter describing the kinetics of the cement hydration process

Similar characteristics were observed at three different shear rates (0.391 s^{-1}, 0.9775 s^{-1} and 1.955 s^{-1}), for different concentration of plasticizer admixture and for different type of plasticizer: STPP and/or SHMP.

For the BS presented above, by analyzing the dependence between the shear rate and the shear stress using a 10 second step-wise cycling measurements, a hysteresis (thixotropic) behavior was observed. This behavior demonstrates that the formation of the gel as a product of hydration is also a determining factor for the rheology of BS for ARC. According to the studies of the rheology of the hydraulic systems that is the result of the development and breakdown of a "secondary structure" related to gel formation during initial hydration and is not to be confused with the flocculated structure of the preexisting paste [72].
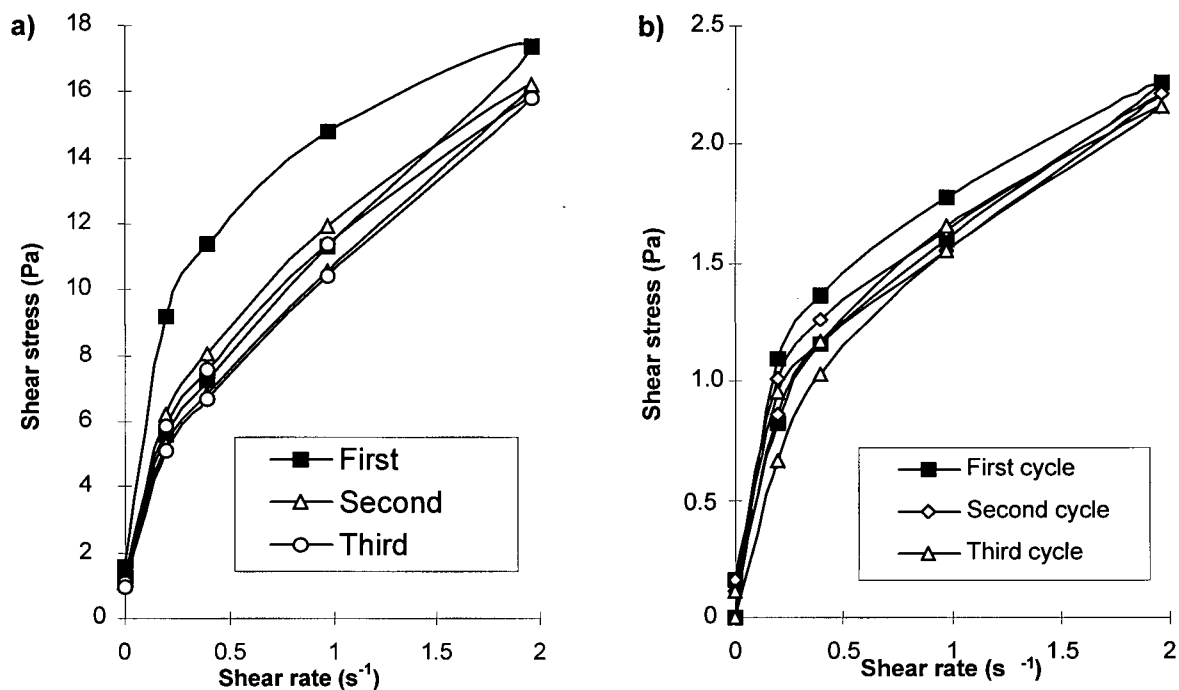
Figure 4.2-2. Hysteresis thixotropic behavior of BS containing equal quantities of Secar 71 CAC, SF2 and Pechiney AC 34 B5 calcined alumina, with an admixture of 0.133% SHMP, for a) 0.25 w/s ratio and b) 0.35 w/s ratio.

The data for BS of LCC are presented in Figure 4.2-2 for two different w/s ratios. By increasing the w/s ratio, there is also a decrease in the hysteresis amplitude, indicating a lower thixotropy besides the normal decrease of the shear stress levels.

The results on this preliminary set of experiments lead to the following conclusions:

- the ULCC BS suspensions showed a rheological behavior similar to the hydraulic cement suspensions, during dormant period;

- the hydration rate, during dormant period, was not affected by the water/solid and water/cement ratios;

- it was not possible to identify a well defined yield stress of BS suspensions containing calcined alumina and silica fume;

- the thixotropic behavior is dependent on the solid/water ratio.

Based on the above data it was decided that in order to study the rheological behavior of BS for ARC it is necessary to maintain the following parameters of viscometric measurements:

- the lowest possible shear rate levels;

- the shortest possible time after mixing with water;

- measuring times at low shear rate of minimum 30 seconds in order to avoid any possible misleading results due to insufficient torque strain at low angular velocity of the spindle.
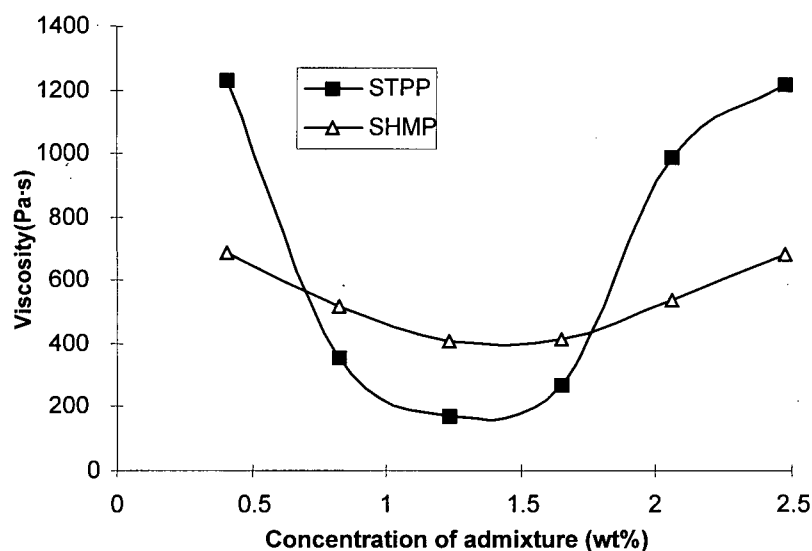
Figure 4.2-3. Variation of viscosity with the level of admixture of plasticizers (STPP and SHMP) for a binding system containing equal quantities of Secar 71 CAC, SF2 and Pechiney AC 34 B5 calcined alumina, at 0.275 w/s and 0.1905 s^{-1} shear rate.

During this stage of the research, the initial measurements of the effects of dispersant admixtures on the viscosity of BS for LCC were completed. STPP and SHMP were used as dispersant admixtures. The measurements were taken at 0.1905s^{-1} shear rate for a w/s=0.275 at 5, minutes after mixing with water. One example of such measurements is presented in Figure 4.2-3.

Because in the experimental compositions of BS for LCC both CAC and calcined alumina have the specific surface lower than 1 m^2/g, while silica fume (SF2) has a specific surface of 12.4 m^2/g, the concentration of dispersant admixture was expressed in Figure 4.2-3 as weight percentage of the silica fume content. Both dispersants proved to be effective in dispersing the LCC binding system. STPP has produced the lowest viscosity (170-200 Pa·s) in a narrow range around 1.25 wt%. SHMP produced the lowest viscosity of 400 Pa·s but the variation of viscosity with concentration was less important. Although STPP gives lower viscosity the use of SHMP is easier to control, i.e. it is more tolerant to errors of admixture.

Literature data indicate that organic plasticizers act differently than phosphate (inorganic) plasticizers [93,94]. However there is no information regarding the possible interaction effect between organic and inorganic plasticizers. The next stage of our research study was conducted therefore to establish the interaction of organic and inorganic plasticizers on the rheology of BS of self-flowing ARC.

4.2.1.2. Rheology of binding systems for ULCC

Experimental compositions (Table 4.2-1) of BS were designed to correspond to self-flowing ULCC's based on Mulcoa 60 refractory aggregate and having an Andreassen exponent $q=0.22$. Although kyanite -325 mesh has a different particle size distribution compared to -100 mesh Mulcoa 90, the latter was used to replace kyanite in the 3 component binding system in order to study its influence as a suspension stabilizer.

Table 4.2-1. Experimental compositions of BS for ULCC.

Component	3 ceramic components binding system	4 ceramic components binding system
silica fume (wt%)	23.8	23.8
kyanite -325 mesh (wt%)	-	19.04
calcined alumina AC 34 B5 (wt%)	9.52	9.52
CAC Secar 71 (wt%)	4.76	4.76
Mulcoa 90 -100 mesh (wt%)	61.89	42.85

The effect of dispersant additives on the rheology of BS was studied using designed experiments and response surfaces of two factor groups (Table 4.2-2). The type of silica fume factor was included as a supplementary qualitative factor (4 ceramic component BS were prepared using silica fume Elkem 971-SF1 and silica fume Globe Metallurgical-SF2).

Table 4.2-2. The experimental design actual factor levels for plasticizer admixtures.

Plasticizer	Low level (wt%), -1	High Level (wt%), +1
STPP	0.05	0.15
SHMP	0.1	0.3
SNFC -(Daxad 19)	0.04	0.06
SPMA (Daxad 30)	0.04	0.06

The measurements were performed at three levels of shear rate: 0.1905 s^{-1}, 0.391 s^{-1}, and 0.9775 s^{-1}. A two level factorial central composite rotatable ($\alpha=1.41$) design was chosen. The experimental design and the statistical analysis of the rheology data were performed using Design-Expert 5.0.7 software produced by Stat-Ease Inc. In order to establish correlation with the castable flow the concentrations of plasticizer and the levels of water were expressed in values corresponding to the whole self-flowing castable compositions.

For organic plasticizers the levels of admixture were arbitrarily chosen based on values employed in literature data, while in the case of STPP and SHMP the values were chosen based on the viscometric measurements performed during the study of rheology of BS for LCC.

Figure 4.2-4 represents the experimental design layout in coded values (i.e. −1=low level, 0=mid level and +1=high level). Combinations of phosphate-organic plasticizer (STPP-SNFC and SHMP-SPMA) were used as factors of the design. The resulting response surfaces were obtained through least square fit to experimental data. The design, fit and plotting routines are parts of the Design Expert program.
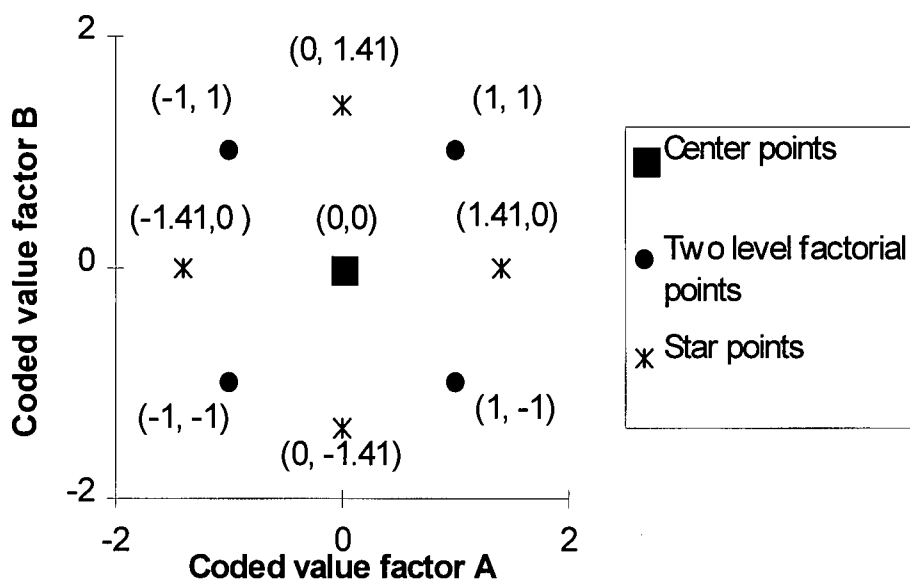
Figure 4.2-4. Experimental factorial design layup represented in coded values.
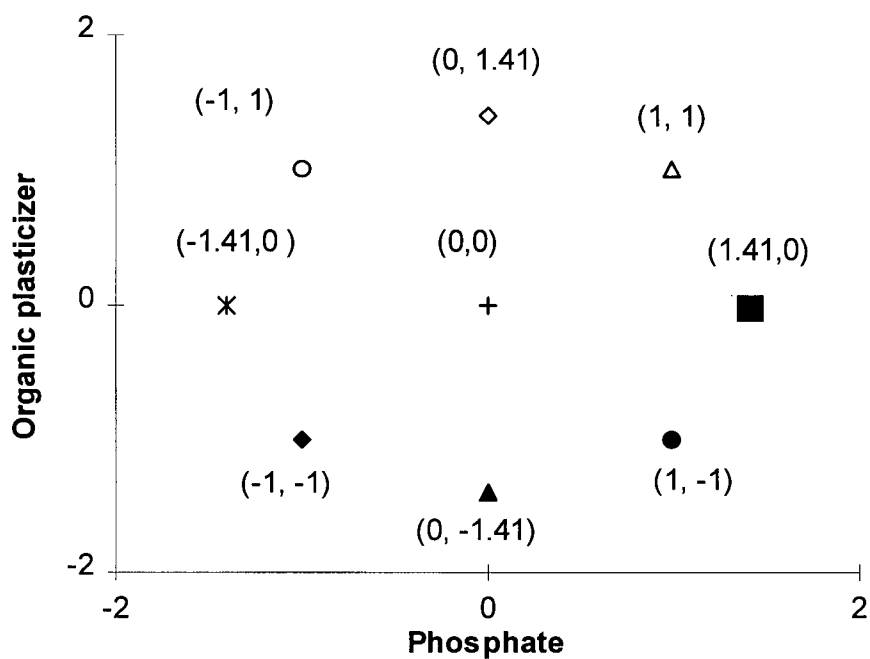
Figure 4.2-5. Individual notation of experimental data points of the central composite design.

The notation of individual design points, in terms of concentration of organic and inorganic dispersants, in the shear stress-shear rate graphs that are presented in this chapter is shown in Figure 4.2-5. The coded values correspond to the concentration levels presented in Table 4.2-2.

In parallel to the viscometric measurements the binding system compositions were also subjected to pH measurements at 1/50 level of dilution.
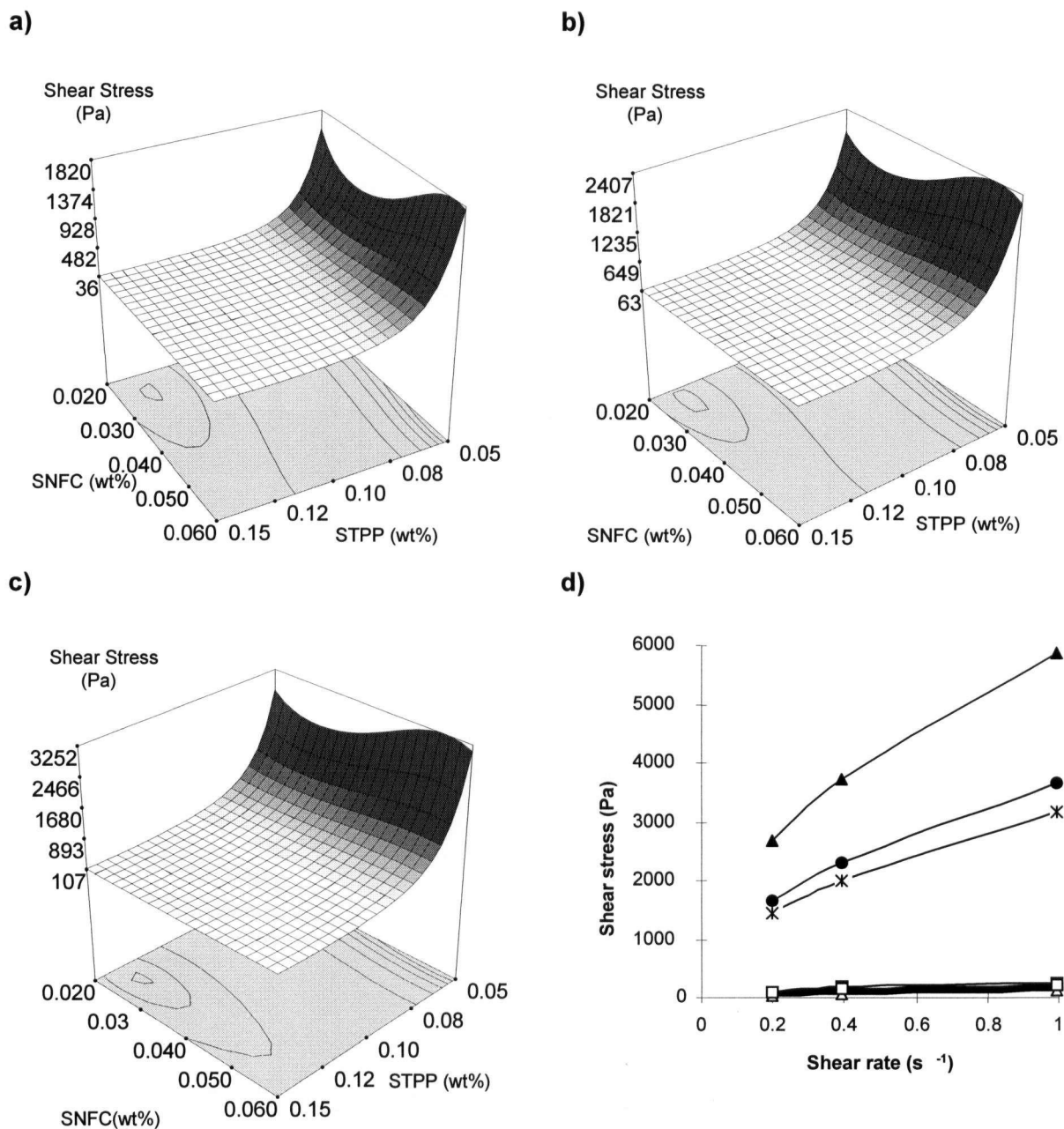
Figure 4.2-6. The effect of STPP-SNFC plasticizer admixture on rheological behavior of 4 component BS for ULCC containing SF2 at: a) 0.1905 s^{-1}, b) 0.391s^{-1}, and c) 0.9775 s^{-1} shear rate. d) Shear stress-shear rate dependence for experimental data points indicated in Figure 4.2-5.

As shown in Figure 4.2-6, for a four component BS containing SF2, for all three shear rates employed the profile of variation of shear stress with shear rate is similar indicating that the amount of plasticizer has no direct effect on the thixotropic behavior.

For STPP if employed in concentrations higher than 0.08% low levels of viscosity are obtained. The optimum level of STPP admixtures is around 0.14% although there is no important variation of its effect in the range of 0.09-0.15%. The model predicts also an increase in the viscosity for STPP concentrations higher than 0.185%. Although the presence of SNFC brings a certain positive contribution to the dispersion of the BS, its effect is more visible at low concentration of STPP.

Figure 4.2-7. Variation of shear stress with concentration of STPP- SNFC admixture for a 4 ceramic component BS containing SF2, at 0.1905s^{-1} shear rate.

Point prediction algorithm (Figure 4.2-7), indicated that the optimum concentration of dispersant admixture is 0.137% STPP and 0.026% SNFC resulting in shear stress levels between 36.2 and 41.3 Pa at 95% confidence interval. The actual value of shear stress at 0.1905s^{-1} for the optimum level of admixture determined experimentally was 40.8 Pa.
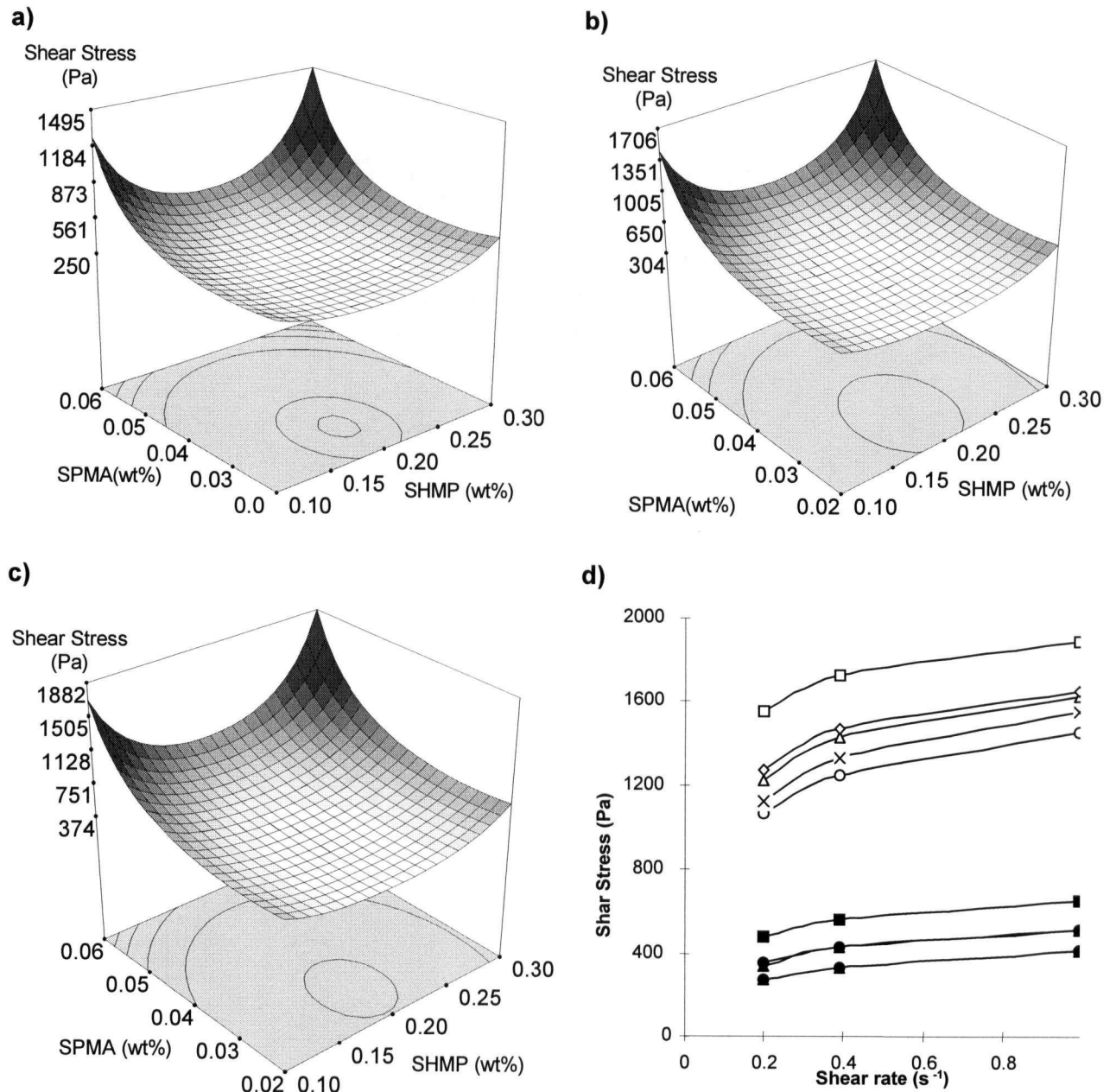
Figure 4.2-8. The effect of SHMP-SPMA plasticizer admixture on rheological behavior of 4 component BS for ULCC containing SF2 at: a) 0.1905 s⁻¹, b) 0.391s⁻¹ and c) 0.9775 s⁻¹ shear rate. d) Shear stress-shear rate dependence for experimental data points.

As shown in Figure 4.2-8 the effect of SHMP-SPMA admixture on viscosity of the 4 component BS for ULCC containing SF2 has similar characteristics to that of STPP-NSFC

(Figure 4.2-6). For all the shear rate levels employed, the variation of shear stress indicates that both SHMP and SPMA have no specific determining effect on thixotropy of the mix. Compared to STPP the use of SHMP leads to higher shear stress and viscosity of the BS. The variation of the shear stress with concentration of SHMP is weaker as compared to STPP. The optimum level of plasticizer admixture is of about 0.2% SHMP and 0.028% SPMA.
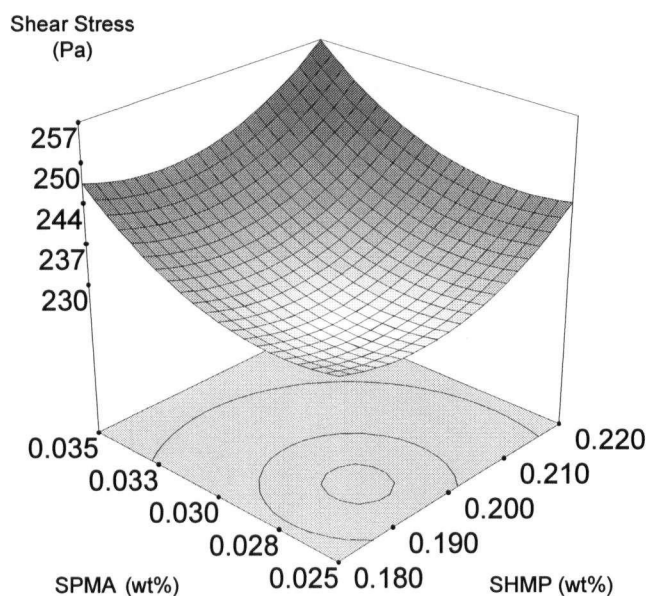
Figure 4.2-9. Variation of shear stress with concentration of SHMP-SPMA admixture for a 4 ceramic component BS containing SF2, at $0.1905s^{-1}$ shear rate.

Point prediction algorithm (Figure 4.2-9) showed that, for the optimum concentration of plasticizer admixture the shear stress level obtained for a $0.1905s^{-1}$ shear rate is 250 Pa. This value is 7 times higher than that obtained in the case of STPP-SNFC admixture. The actual value of shear stress at $0.1905s^{-1}$ for the optimum level of admixture determined experimentally was 258 Pa.

The important effect, on shear stress values, is shown by the phosphate additive (SHMP). SPMA has no significant effect in reducing viscosity, if used in concentrations below 0.04%
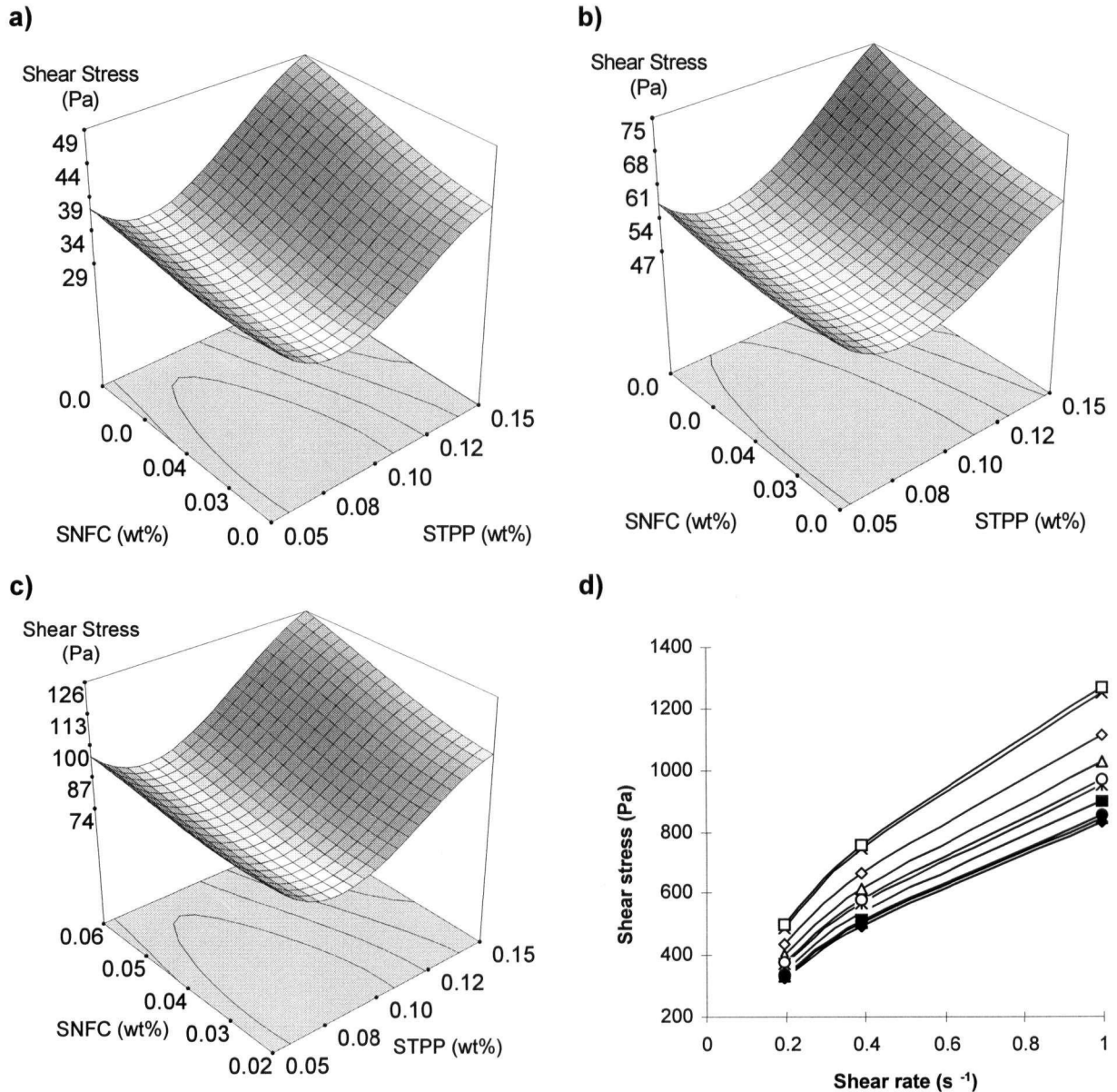
Figure 4.2-10. The effect of STPP-SNFC plasticizer admixture on rheological behavior of 4 component BS for ULCC containing SF1 at: a) 0.1905 s^{-1}, b) 0.391s^{-1}, and c) 0.9775 s^{-1} shear rate. d) Shear stress-shear rate dependence for experimental data points.

The data presented in Figure 4.2-10 suggest that, by using SF1, very low levels of shear rate (and viscosity) are obtained. Compared to the BS containing SF2, for the same fluidity levels, the use of SF1 allows for a reduction in the water for mixing of castable of about 25%

(the equivalent water content was 5% for BS based on SF1, and 6% for BS based on SF2). For a low water content (5%) and low concentration of STPP, the shear stress values are below 150 Pa. This suggest that in the case of SF1 it is possible to obtain a self-flowing castable even without plasticizer admixtures by increasing the water content to 6%.

From the data presented in Figure 4.2-10 is apparent that STPP has the most important effect on the rheology of 4 component BS containing SF1, while SNFC has just a minor positive influence. The shear stress levels increase at higher concentration of STPP (0.15%) and higher concentration of SNFC (0.06%)

The optimum concentrations of plasticizer admixture, for all shear rate levels employed are at 0.078% STPP and 0.024% SNFC. The fact that, in the case of SF1, the optimum levels of STPP are slightly lower than in the case of silica fume SF2, while there is no important change in the concentration of SNFC, confirms the literature data [53, 93] regarding the following hypothesis of BS-plasticizer interactions:

- organic and phosphate plasticizers have different mechanisms of action: while organic plasticizers act by steric repulsion and adsorption on cement particles, phosphate plasticizers act by adsorption on high specific surface particles (in this case silica fume) resulting in an increased electrostatic repulsion.

- the surface characteristics of silica fume particles (specific surface, level of impurities), are determining factors for the self flow behavior of refractory castables and also determine the optimum concentrations of plasticizer admixture.

Figure 4.2-11 shows the variation of shear stress with concentration of STPP-SNFC admixture, at $0.1905s^{-1}$ shear rate, for the 4 component BS for ULCC containing SF1, around the optimum concentration of admixture. Similar optimum ranges for the concentration of plasticizer admixture were found for shear rates of $0.391 \ s^{-1}$ and $0.9775s^{-1}$.

As in the case of STPP-SNFC admixture, by using the SHMP-SPMA mix *in the* BS based on SF1 (Figure 4.2-12) several aspects can be outlined by comparison with the rheological behavior of the BS containing SF2 for ULCC:
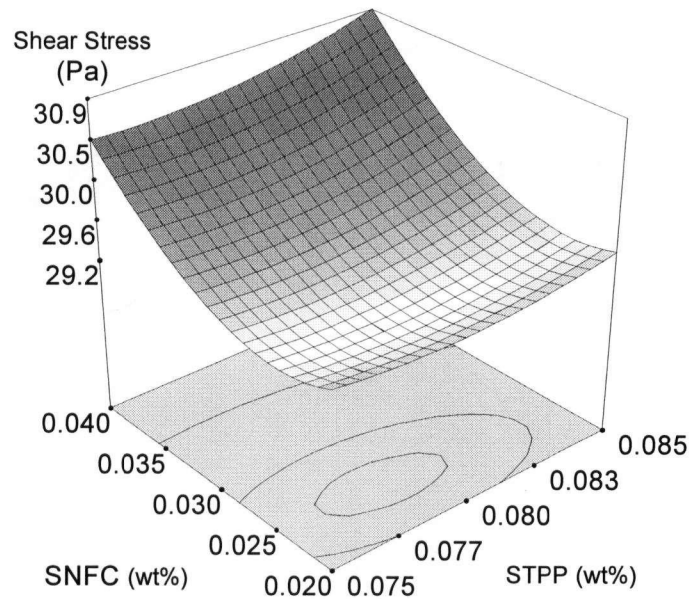
Figure 4.2-11. Variation of shear stress with concentration of STPP-SNFC admixture for a 4 ceramic component BS containing SF1, at $0.1905s^{-1}$ shear rate.

- the profile of variation of shear stress, for all shear rates employed, indicates maximum values for low levels of plasticizer admixtures;

- there is a positive interaction between the organic and phosphate plasticizer;

- the organic and phosphate plasticizers have comparable effects both showing a relative decrease in the shear stress of the BS;

- the use of the high purity silica fume (SF1) brings a decrease in the optimum concentration of phosphate plasticizer while the optimum concentration of organic plasticizer remains practically unchanged.
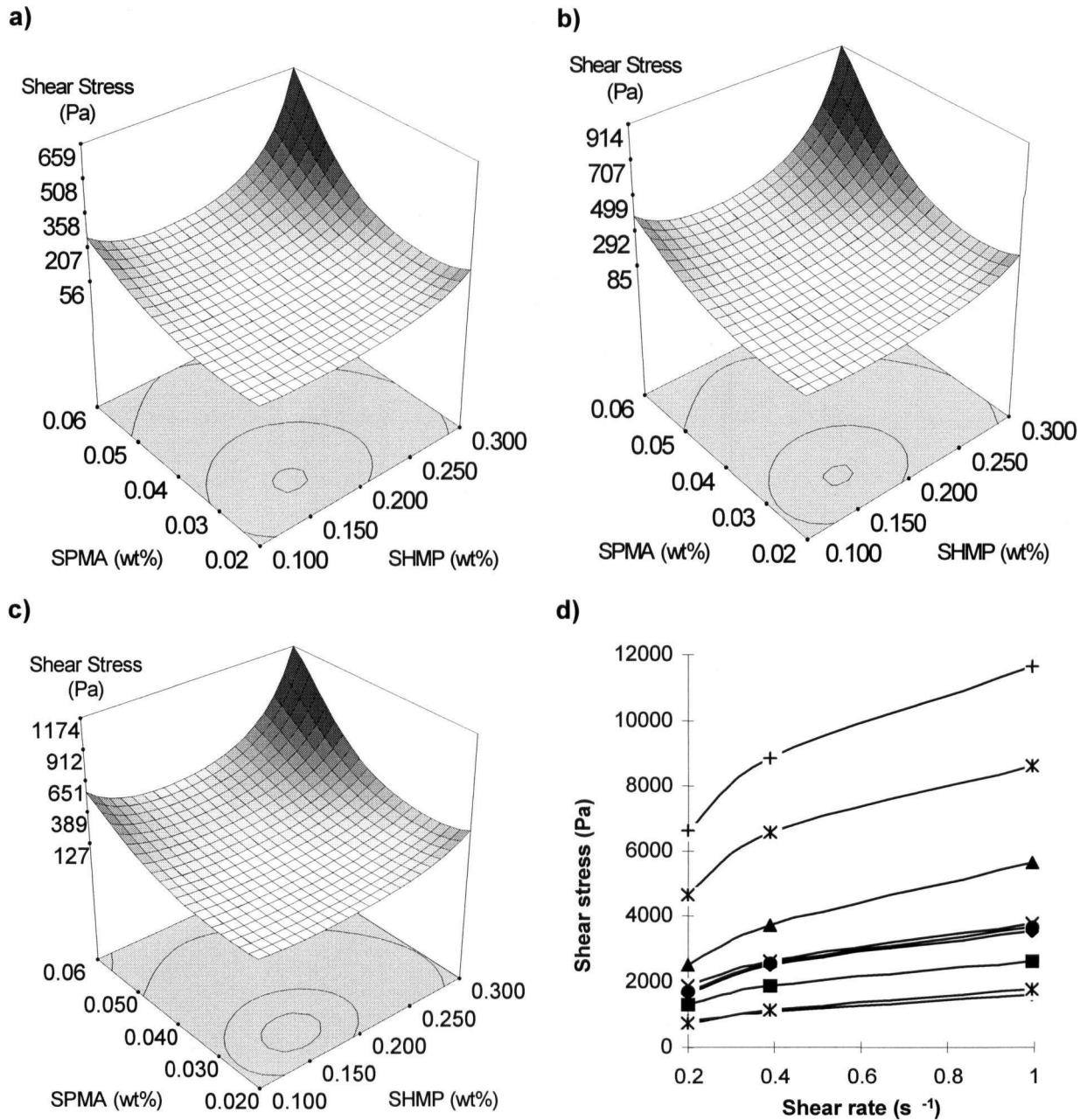
Figure 4.2-12. The effect of SHMP-SPMA plasticizer admixture on rheological behavior of 4 component BS for ULCC containing SF1 at: a) 0.1905 s⁻¹, b) 0.391s⁻¹ and c) 0.9775 s⁻¹ shear rate. d) Shear stress-shear rate dependence for experimental data points.

Comparing the rheological behavior of the 4 component BS containing SF1 dispersed with SHMP-SPMA and STPP-SNFC the following observations could be made;

- SHMP-SPMA is less effective in dispersing the BS for ULCC than STPP-SNFC, the minimum values of shear stress experienced for all three shear rates being almost twice;

- it is not possible to identify a well defined yield stress so it is not possible to describe the rheological behavior of the BS as a typical Bingham fluid;

- the shear stress-shear rate variation for all levels of admixture shows that these BS exhibit a thixotropic behavior, and the thixotropy is not determined directly by the concentration of plasticizer admixture but is clearly influenced by the relative level of shear stress.

For the 4 ceramic component BS for ULCC containing SF1, the optimum concentration of SHMP-SPMA plasticizer admixture was found to be at 0.016% SHMP and 0.028% SPMA, for all the three shear rates employed.

The variation of shear stress with concentration of SHMP and SPMA at 0.1905 s^{-1} shear rate, detailed near the optimum level of admixture is presented in Figure 4.2-13.
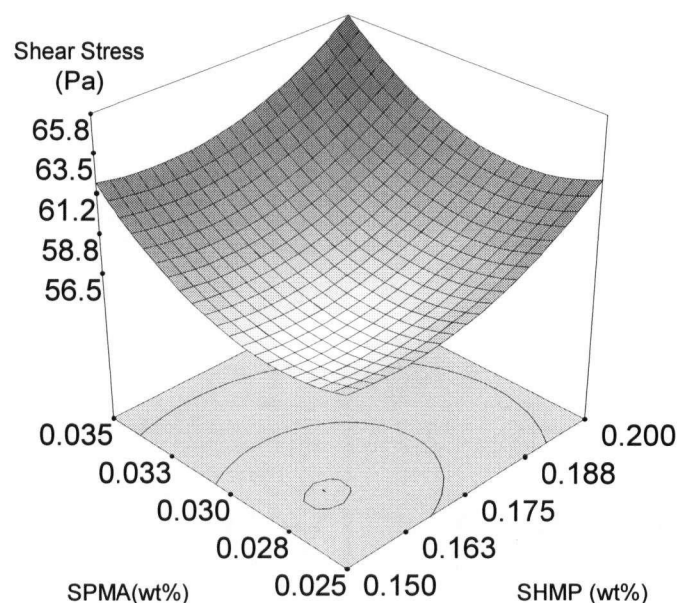
Figure 4.2-13. Variation of shear stress with concentration of SHMP-SPMA admixture for a 4 ceramic component BS containing SF1, at 0.1905s^{-1} shear rate.

At the present stage there is no clear understanding of the effect of fine reactive powders of natural aluminosilicates on the behavior of the BS of ARC. While it is generally agreed that that aluminosilicate minerals such as kyanite have a positive contribution to the mullitization process [127], there is doubt over their influence on the rheology.

a)

b)

c)

d)
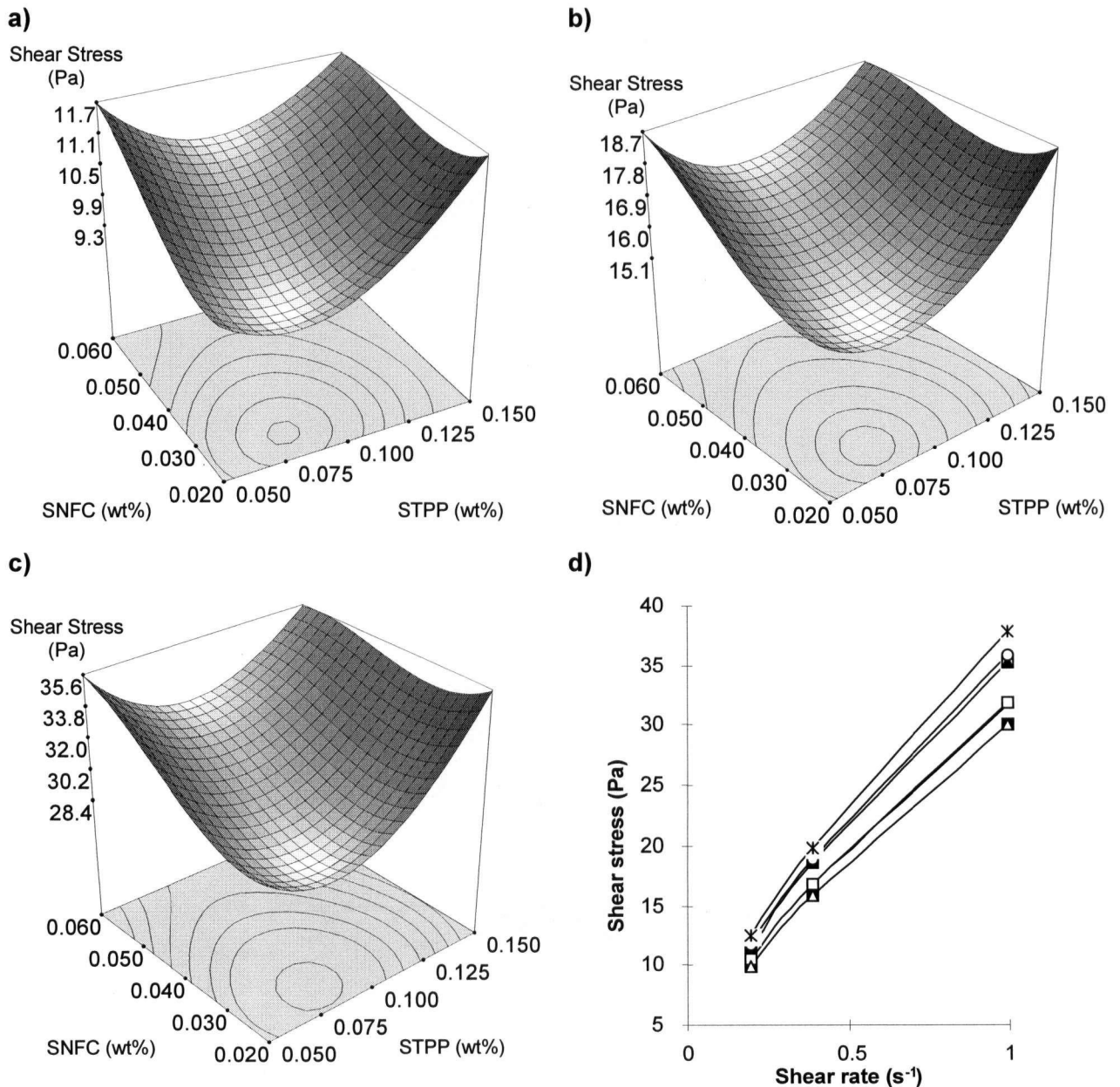
Figure 4.2-14. The effect of STPP-SNFC plasticizer admixture on rheological behavior of 3 component BS for ULCC containing SF2 at: a) 0.1905 s^{-1}, b) 0.391s^{-1}, and c) 0.9775 s^{-1} shear rate. Shear stress-shear rate dependence for experimental data points d).

In order to asses the influence of natural aluminosilicates on the rheology of BS, experimental mixes in which the kyanite content was replaced by -100 mesh Mulcoa 90 were prepared. Preliminary experiments showed that if kyanite is replaced with Mulcoa 90 an important decrease in viscosity is experienced. For this reason it was decided that, even if these compositions were made with SF2, the water level had to be lowered to 5% .The composition of 3 ceramic components BS ULCC is presented in Table 8. The data presented in Figure 4.2-14 suggests that by replacing kyanite with -100 mesh Mulcoa 90 several effects occur:

- the viscosity of the BS sharply decreases (i.e. the shear stress levels are three times lower than those of the 4 components BS, for a equivalent water content reduced from 6 to 5 %);

- the region of optimum level of admixture is reduced, the graphs indicating a region of low viscosity at high concentration of SNFC, but this region falls outside the limits of the experimental layout (concentration of SNFC higher than 0.068%);

- the optimum range of plasticizer admixtures (Figure 4.2-15) is found to be at low level of STPP (0.08 %) while for SNFC there is no important change (0.027%).
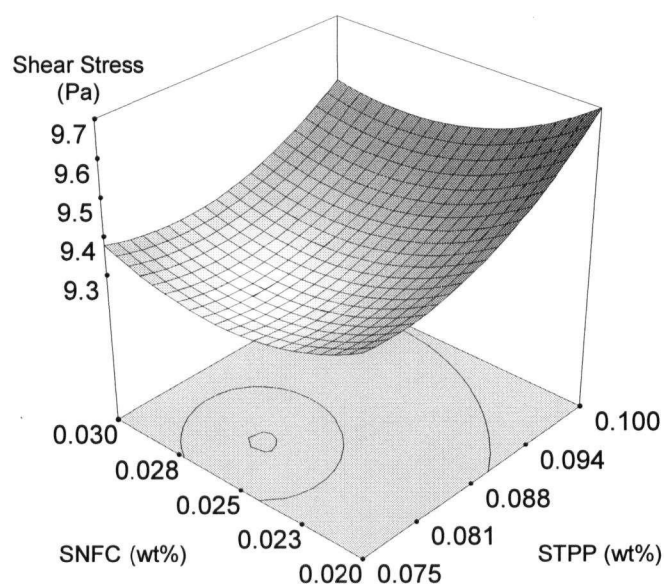
Figure 4.2-15. Variation of shear stress with concentration of STPP-SNFC admixture for a 3 component BS, at $0.1905s^{-1}$ shear rate.
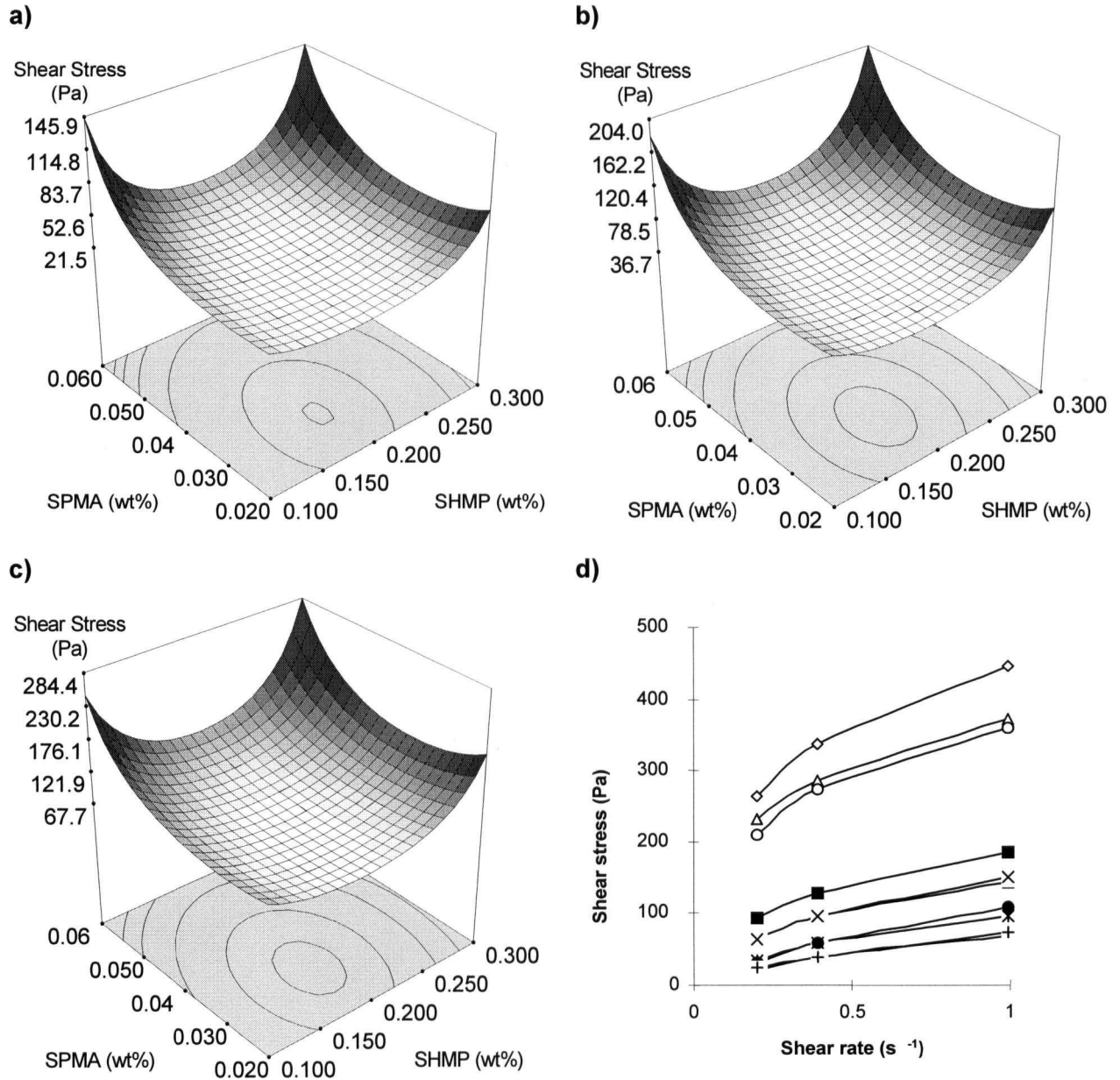
Figure 4.2-16. The effect of SHMP-SPMA plasticizer admixture on rheological behavior of 3 component BS for ULCC containing SF2 at: a) 0.1905 s^{-1}, b) 0.391s^{-1} and c) 0.9775 s^{-1} shear rate. Shear stress-shear rate dependence for experimental data points d).

The variation profile of the shear stress with the composition of plasticizer admixture, for the 3 component BS is very similar with that of 4 component BS, for the shear rates employed (Figure 4.2-14 a), b), c) and Figure 4.2-16 a), b), c)). Despite the different level of shear stress

the effect of SHMP-SPMA admixture is similar even with respect to the composition of the optimum level of admixture in order to obtain a minimum viscosity. Contrary to the case of STPP-SNFC admixture there is no indication of the existence of a low viscosity compositional field at high concentration of organic plasticizer. As presented in Figure 4.2-17 the lowest shear stress levels (and consequently lower viscosity) are obtained for a concentration of plasticizer admixture of 0.185% SHMP and 0.035% SPMA. At 0.1905 s^{-1} shear rate, the minimum shear stress is 20.4 Pa, which is more than double than the minimum that can be obtained with STPP-SNFC.
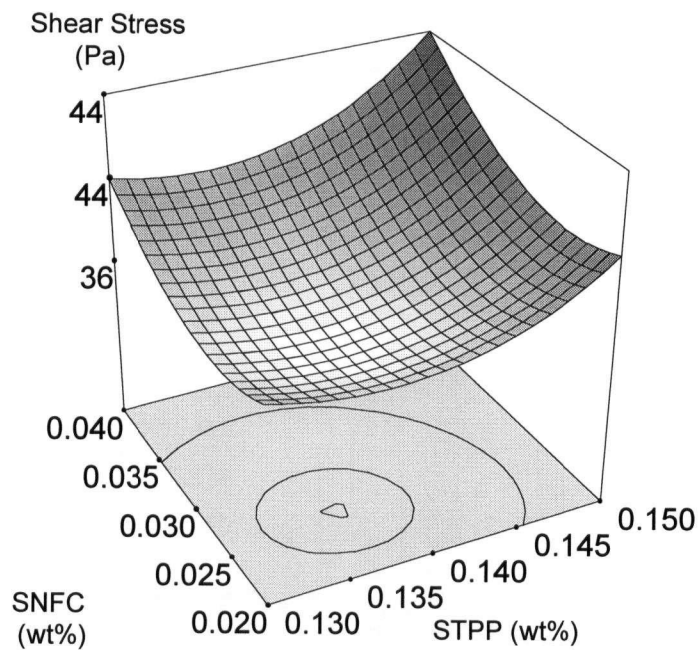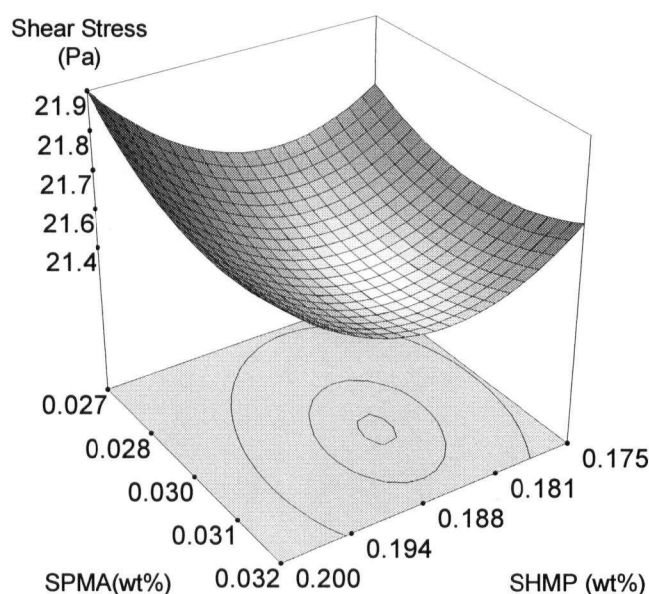

Figure 4.2-17. Variation of shear stress with concentration of SHMP-SPMA admixture for a 3 ceramic component BS containing SF1, at 0.1905s^{-1} shear rate.

By analyzing the rheological behavior of BS for ULCC several conclusions can be drawn with regard to of these mixes and to the role of plasticizer admixtures:

- In order to obtain the lowest shear stress (i.e. higher fluidity), the optimum concentration of plasticizer admixture was similar for different shear rates of all experimental compositions.

- For all the binding systems, the STPP-SNFC admixture is more effective than SHMP-SPMA. The most important effect in reducing the viscosity of BS was shown by the phosphate

105

plasticizers. Although the organic plasticizers have a positive influence on concentrated suspensions of BS, they are not as effective as phosphates.

- Comparing the phosphate additives, STPP proves to be more effective than SHMP for all studied BS. For the same shear rate and composition of BS, at optimum concentration, the use of STPP leads to shear stress levels less than half of those obtained by using optimum concentration of SHMP. The biggest difference was shown in the case of the four component BS with for which the minimum shear stress levels given by SHMP-SPMA combination was more than seven times higher than that given by STPP-SNFC.

- Although STPP was more effective than SHMP in providing low viscosity BS, its effect was more sensitive to concentration variations, composition of the BS and quality of silica fume. A good dispersing effect can be obtained for STPP only for a precise and narrow range of concentration and that may explain the fact that SHMP is preferred by some researchers.

- The quality of silica fume (i.e. its purity and specific surface) is an important not only for obtaining a low viscosity BS, but also in determining the requirement of the phosphate plasticizer. If compared to the high purity SF1, the low quality SF2 not only requires larger water contents, in order to achieve similar shear stress levels, but also requires higher concentration of the phosphate plasticizer.

- There is no influence of the quality of silica fume on the optimum requirement of organic plasticizer admixture. This confirms the theory that the organic plasticizers act by adsorption on the surface of CAC particles and by steric repulsion.

- Kyanite has a strong effect on the rheology of BS by significantly increasing the viscosity. Due to this effect it was impossible to measure the shear stress variation with concentration of plasticizer admixture of three- and four-component BS, at the same water level. By replacing the kyanite with an inert fraction of Mulcoa 90 the optimum requirement of STPP

was decreased from 0.137% to 0.080%, while in the case of SHMP there was no noticeable influence (0.187% respectively 0.193%).

- Kyanite has no visible influence on the requirement of organic plasticizer. The pattern of variation of shear stress with concentration of STPP-SNFC admixture indicates that a field of low viscosity may exist at high concentration of SNFC. This effect may be due to the fact that the SNFC is also a very effective dispersant for alumina slurries. Because the three component binding systems have a high concentration of high alumina particles (i.e. 61.89% Mulcoa 90) a higher concentration of SNFC can result in a better dispersion of Mulcoa 90 particles.

- Similar to BS for LCC (Figure 4.2-2) all ULCC mixes show a shear thinning behavior (Figures 4.2-6d, 8d, 10d, 12d, 14d and 16d). In the range of shear rate employed in our experiments (0.1905-0.9775 s^{-1}) the shear thinning is independent of the concentration of plasticizer admixture, but there is a clear pattern of variation with the shear stress. While the plasticizers have no specific effect on establishing the non-Newtonian behavior of the BS, by providing a better dispersion of the concentrated suspension, they can modify the variation of the shear stress with shear rate.

- None of these suspensions can be described as a typical Bingham fluid, being impossible to identify a well defined yield stress. While in some cases (Figures 4.2-10d and 4.2-12d) it may be considered that there is a convergence to a common value of the yield stress, for the majority of binding system compositions (Figures 4.2-6d, 8d, 14d and 16d) the shear thinning behavior seems to depend on the overall level of shear stress at a given shear rate.

In order to study the effect of SNFC on the viscosity of three component BS at high concentration of organic plasticizers, measurements at 0.9775 s^{-1} shear rate were performed on the mixes containing an equivalent concentration of STPP of 0.1% and 5% water.

As shown in Figure 4.2-18, the field of low viscosity at high concentration of organic plasticizer, (as predicted by the response surface model), exists in the range of 0.2-0.4% SNFC. Above 1.2% SNFC there is an important increase in viscosity. That means that the rheological behavior of BS although, governed by complex interactions, that can be successfully studied by adequate viscometric techniques supported Design of Experiment models. The minimum viscosity in the range of concentrations of 0.8-0.1% SNFC is 45.3 Pa, while the minimum viscosity in the range of 0.012-0.068% SNFC (that was employed in the response surface model) was 31 Pa. These variations are significant as the standard error of measurement is ± 1.2 Pa. Because the viscosity levels at high concentration of organic plasticizer are higher than those existing in the compositional field studied by response surfaces, further investigation of this domain was not considered.
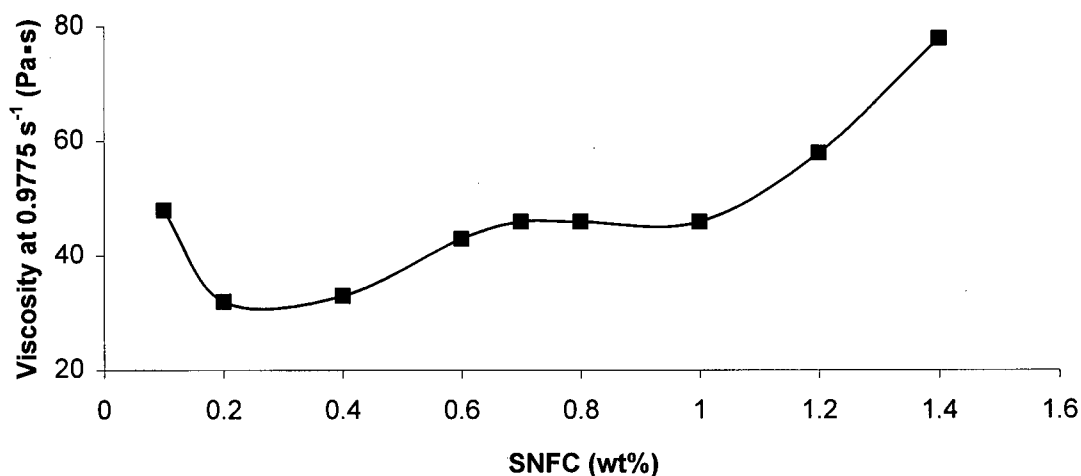
Figure 4.2-18. Variation of viscosity with concentration of SNFC for a three component binding system containing SF2, at 5% water and 0.1% STPP.

4.2.1.3. The influence of water content

The next step of research was directed towards establishing the influence of water content on the rheological behavior of BS suspensions. Preliminary experiments on the viscosity of BS for LCC, in the presence of phosphate plasticizers admixture showed that there is a good correlation between the viscosity, at a given shear rate, and the water/solid ratio, as shown in Figure 4.2-19.
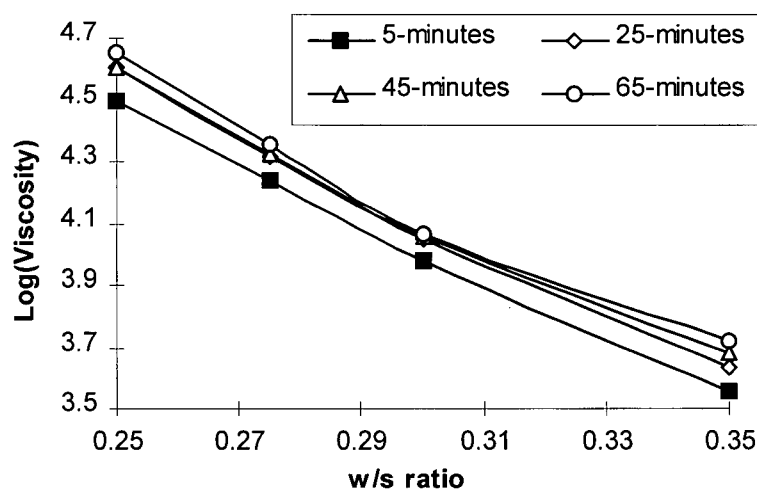
Figure 4.2-19. Semi-logarithmic variation of viscosity with w/s ratio for a BS for LCC containing equal quantities of CAC, SF2, and calcined alumina, with an admixture of 0.133% SHMP, at 0.1905 s⁻¹ shear rate and at different times after adding water.

The data shown in Figure 4.2-19, can be correlated with the experimental results of the rheology study of BS for ULCC, It is thus possible to describe the rheology of a given BS of a castable refractory as a function of water level and shear rate employed. It was necessary to obtain evidence if this type of dependence exists also in the case of more complex BS of ULCC, in the presence of organic-inorganic plasticizer admixture. The data presented in Figure 4.2-20 show a clear pattern of variation of shear stress with the water content. The shear stress may be defined by an empirical equation of the following type:

$$\sigma = A \times w^B \tag{6}$$

, where

A, B - constants

σ- shear stress,

w- water content

▲ shear rate 0.1995 s^{-1} $\sigma = 3.41E{+}05w^{-5.79}$ $R^2 = 0.986$
X shear rate 0.3910 s^{-1} $\sigma = 3.80E{+}05w^{-5.57}$ $R^2 = 0.992$
● shear rate 0.9775 s^{-1} $\sigma = 5.13E{+}05w^{-5.42}$ $R^2 = 0.981$
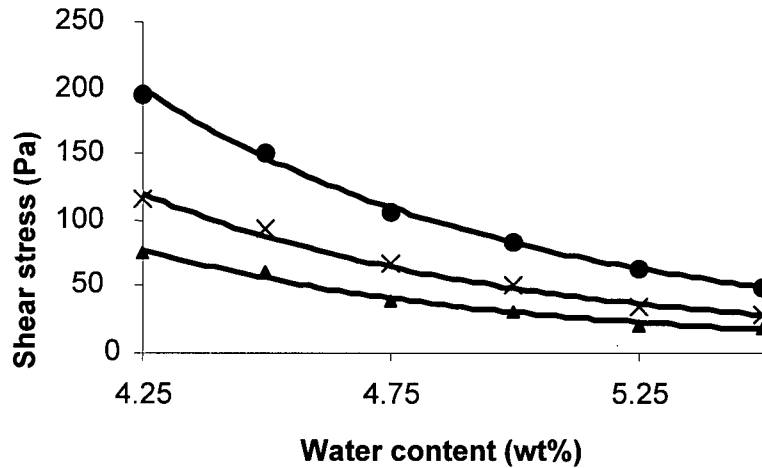
Figure 4.2-20. Variation of shear stress with water content, at different shear rates, for a 4 component BS for ULCC using SF1 and a plasticizer admixture with 0.1% STPP and 0.012% SNFC.

The parameters A and B could be considered as functions of the shear rate (γ). For example Figure 4.2-21 shows a good linear correlation of the parameters A and B with the shear rate, for the binding system presented in Figure 4.2-20. The parameters A and B can be therefore expressed as a function of the shear rate as follows:

$$A = (m+n\gamma) \tag{7}$$

$$B = w^{-(p/(\gamma+r))} \tag{8}$$

where m, n, p and r are constant parameters.

From Eq.(7) and (8) it results that at high shear rates ($\gamma >> p$), $B \to 1$ and the variation of shear stress with shear rate is described by the Bingham model. Therefore, the terms mw and nw may be considered as the apparent yield stress and the apparent Bingham plastic viscosity constant:

$$\sigma = mw + \gamma nw \tag{9}$$

When $\gamma = 0$ the yield stress σ_y, of the binding system can be also derived from Eq.(7-9) :

$$\sigma_y = mw^{p/r} \tag{10}$$

a)
$A = 2.25\text{E}+06\gamma + 2.87\text{E}+06 \quad R^2 = 0.982$

b)
$1/B = -0.0145\gamma - 0.1705 \quad R^2 = 0.971$
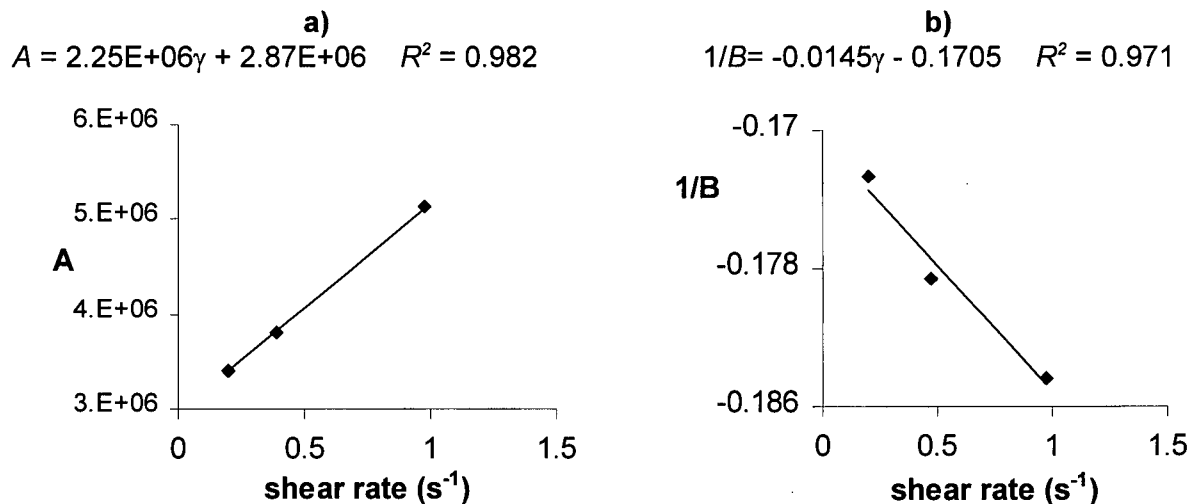
Figure 4.2-21. Correlation of the parameters A and B with shear rate, for a 4 component BS for ULCC using SF1 and a plasticizer admixture with 0.1% STPP and 0.012% SNFC.

For the binding system presented in Figure 4.2-20, based on Eq. (6), (7) and (8), the variation of the shear stress with the shear rate and the water content may therefore be expressed by the following empirical formula:

$$\sigma = (m+n\gamma)\, w^{-(p/(\gamma+r))} \qquad\qquad (11)$$

A similar correlation was found for a ULCC binding based on SF1 containing 0.15% STPP and 0.04% SNFC (Figure 4.2-22).

▲ shear rate 0.1995 s^{-1} σ=5.62E+05$w^{-5.79}$ R^2 = 0.986
X shear rate 0.3910 s^{-1} σ=6.68E+05$w^{-5.57}$ R^2 = 0.992
● shear rate 0.9775 s^{-1} σ=8.59E+05$w^{-5.42}$ R^2 = 0.981
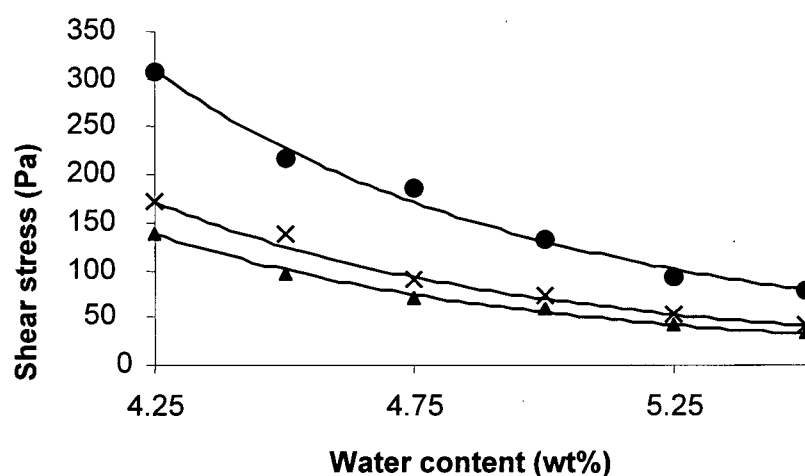
Figure 4.2-22. Variation of shear stress with water content, at different shear rates, for a 4 component BS for ULCC using SF1 and a plasticizer admixture with 0.15% STPP and 0.04% SNFC.

Figure 4.2-23 shows a good linear correlation of the parameters A and B with the shear rate, for the binding system presented in Figure 4.2-22. The binding systems presented in Figure 4.2-20 and 4.2-22 differ just by the concentration of the plasticizer admixture. The main difference induced by changing the concentration of plasicizer admixture is a proportional increase (i.e. 69% change) of parameters m and n (see Figures 4.2-21 and 4.2-23).

$A = 3.82E+05\gamma + 4.86E+05 \quad R^2 = 0.998$

$1/B = -0.0145\gamma - 0.1721 \quad R^2 = 0.977$
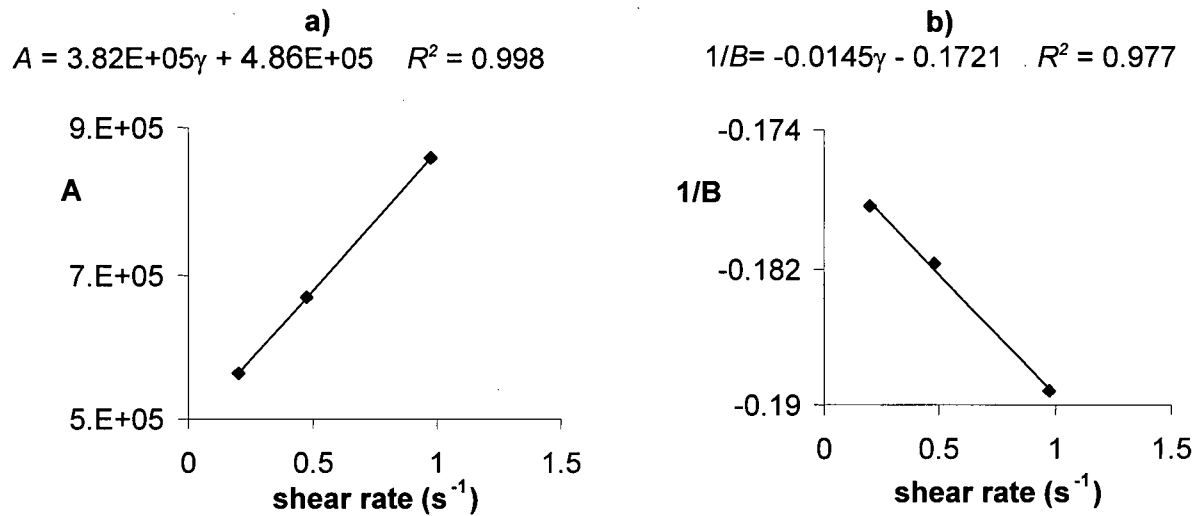
Figure 4.2-23. Correlation of the parameters A and B with shear rate, for a 4 component BS for ULCC using SF1 and a plasticizer admixture with 0.15% STPP and 0.04% SNFC.

▲ shear rate 0.1995 s^{-1} $\quad \sigma = 5.16E+06w^{0.181} \quad R^2 = 0.981$
X shear rate 0.3910 s^{-1} $\quad \sigma = 5.27E+06w^{0.183} \quad R^2 = 0.972$
● shear rate 0.9775 s^{-1} $\quad \sigma = 5.46E+06w^{0.186} \quad R^2 = 0.961$
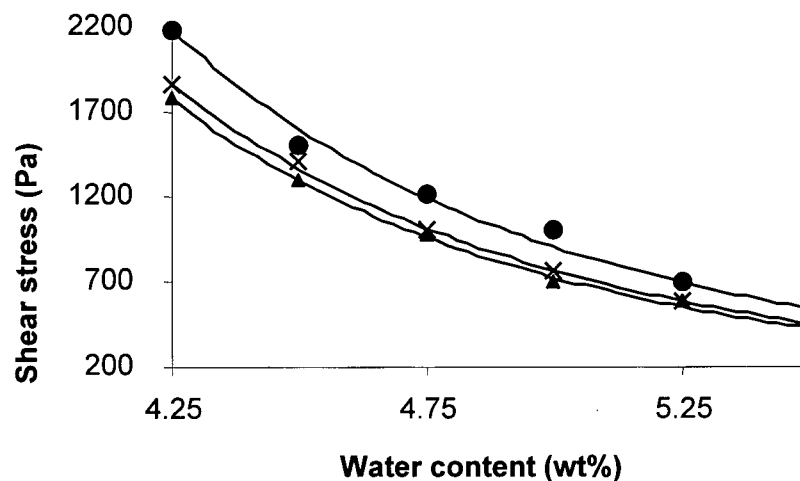
Figure 4.2-24. Variation of shear stress with water content, at different shear rates, for a 4 component BS for ULCC containing SF1 and a plasticizer admixture with 0.15% SHMP and 0.06% SPMA.

113

The ULCC binding system based on SF1 (Figure 4.2-24) is dispersed with 0.15% SHMP and 0.06% SPMA. The use of SHMP-SPMA admixture results in significantly increased shear stress levels. Due to a good correlation of the parameters A and B with the shear rate (Figure 4.2-25), the rheological behavior of this binding system can be also described by the Eq. (11).

a)

$A = 5.08E+06\gamma + 3.82E+05 \quad R^2 = 0.991$

b)

$1/B = -0.0045\gamma - 0.1805 \quad R^2 = 0.952$
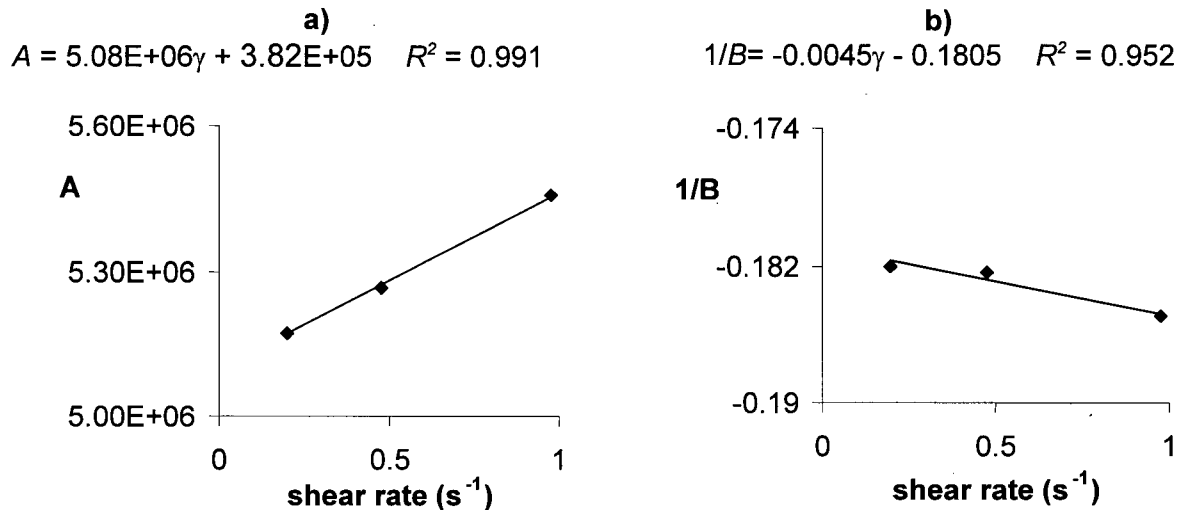
Figure 4.2-25. Correlation of the parameters A and B with shear rate, for a 4 component BS for ULCC containing SF1 and a plasticizer admixture with 0.15% SHMP and 0.06% SPMA.

Much lower shear rates were obtained for a ULCC binding system based on SF1, with a plasticizer admixture consisting of 0.15% SHMP and 0.06% SPMA (Figure 4.2-26). However there is still a good correlation of the parameters A and B with the shear rate (Figure 4.2-27). By comparing the rheology of the ULLC binding system dispersed with SHMP-SPMA admixture it results that the variation of the shear rate is induced mainly by a proportional change (92.4%) of parameters m and n (Figures 4.2-25 and 4.2-27). This finding is consistent with the observation, made in previous experiments, that the plasticizers have no specific effect on establishing the non-Newtonian behavior of binding systems.

▲ shear rate 0.1995 s^{-1} σ=1.21E+06$w^{0.182}$ R^2 = 0.981
X shear rate 0.3910 s^{-1} σ=1.22E+06$w^{0.183}$ R^2 = 0.972
● shear rate 0.9775 s^{-1} σ=1.27E+06$w^{0.186}$ R^2 = 0.961
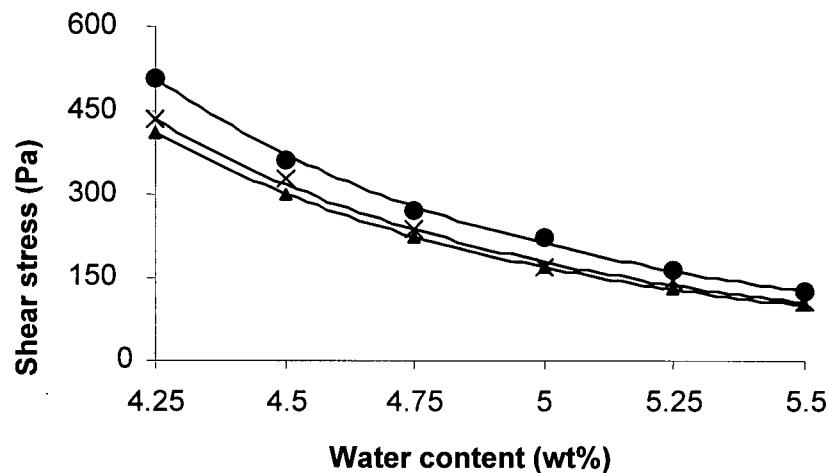
Figure 4.2-26. Variation of shear stress with water content, at different shear rates, for a 4 component BS for ULCC containing SF1 and a plasticizer admixture with 0.1% SHMP and 0.02% SPMA.

a)
A = 1.19E+06γ + 8.91E+04 R^2 = 0.960

b)
$1/B$= -0.0045γ - 0.1808 R^2 = 0.973
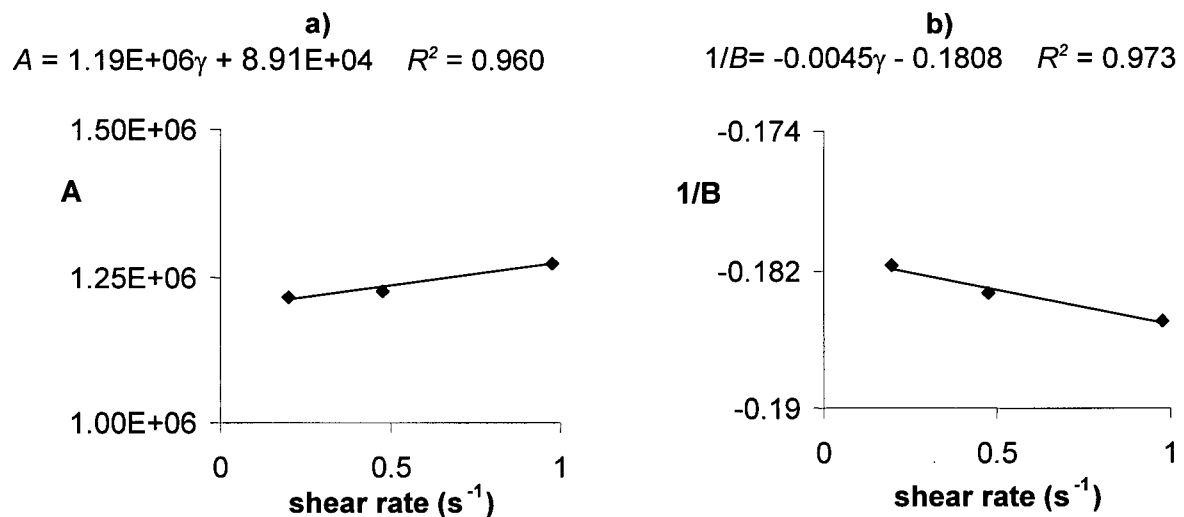
Figure 4.2-27. Correlation of the parameters A and B with shear rate, for a 4 component BS for ULCC containing SF1 and a plasticizer admixture with 0.1% SHMP and 0.02% SPMA.

The ULCC binding systems containing SF2 showed a pattern of variation of the shear stress with the water content similar to the binding systems containing SF1 (Figure 4.2-28).

a)

▲ shear rate 0.1995 s^{-1} $\sigma = 1.48E+06 w^{-0.174}$ $R^2 = 0.967$
X shear rate 0.3910 s^{-1} $\sigma = 1.61E+06 w^{-0.180}$ $R^2 = 0.968$
● shear rate 0.9775 s^{-1} $\sigma = 1.84E+06 w^{-0.192}$ $R^2 = 0.988$

b)

$A = 1.39E+06\gamma + 4.64E+05$ $R^2 = 0.979$

c)

$1/B = -0.0023\gamma - 0.1694$ $R^2 = 0.982$
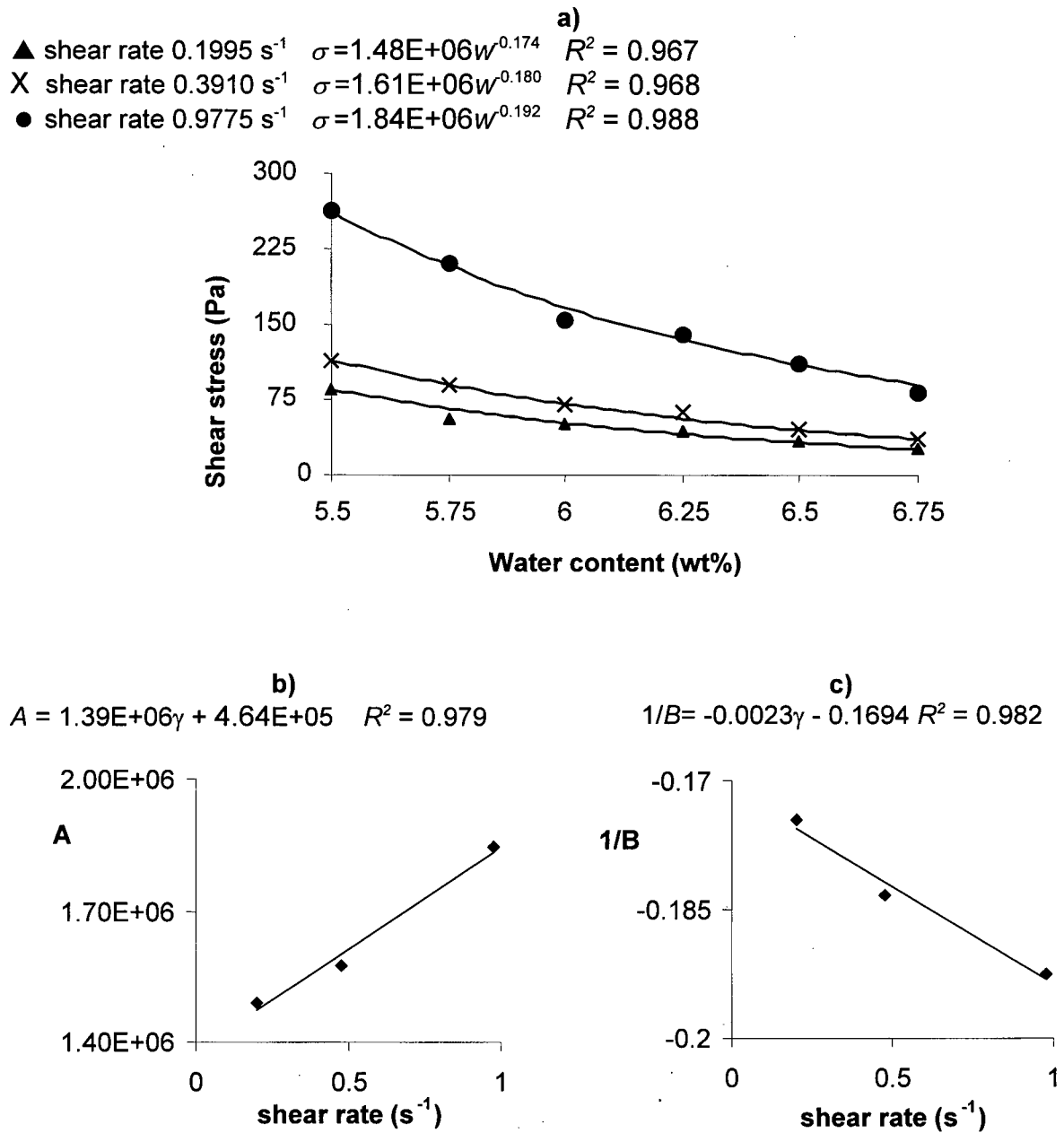
Figure 4.2-28. Variation of shear stress with water content, at different shear rates, for a 4 component BS for ULCC containing SF2 and a plasticizer admixture with 0.1% SHMP and 0.04% SPMA and correlation of the parameters A and B with shear rate.

It is appropriate to comment at this point on the general concept of yield stress in viscous suspensions. Strong but contradictory views about the nature of the yield stress have been held

116

in the past, partly because the importance of the characteristics of the measuring instrument were not fully appreciated. The use of relatively new controlled stress rheometers, which allow for the application of a constant small stress to a sample for an indefinite time, has resulted in understanding of the subject. Barnes and Walters [137] studied a PVA latex adhesive and an aqueous solution of "Carbool", a thickening agent. In tests with a controlled strain rate instrument, using an 8:1 range of strain rates, they obtained graphs that suggested the existence of a well defined yield stress. However, a similar test with a much lower mean strain rate produces a graph of similar shape but with a much smaller intercept. In measurements at very low strain rates, using a controlled-stress rheometer these materials were found to behave as Newtonian fluids, The "apparent yield stress" found earlier was considered as a result of extremely high Newtonian viscosities at the low shear rates that were employed. This facts determined Barnes and Walters to conclude that the concept of a yield stress is a myth. However other researches disagree. Cheng [138] found that there are some materials for which, as the shear rate is reduced progressively from a high level, the stress falls initially, but at very low shear rates, the stress goes through a minimum and begins to raise.

At the present time there are no theoretical models for describing the non-Newtonian behavior of such complex systems as the concentrated suspensions of binding systems. The difficulties in analyzing these rheological systems are related to the high volume fraction of solid particles (>0.8) and to their wide particle size distribution (0.1-300μ). The empirical model derived in this work from the analysis of experimental data, offers a new perspective for studies of a transitional feature between the Bingham flow and non-Newtonian shear thinning behavior in refractory binding systems, with no discontinuity with regard to shear rate or water concentrations.

4.2.2. Setting

Another important benefit of the study of the rheology of binding systems is related to the hydraulic setting. As previously mentioned, plasticizers have an influence on the hydration process, the most well known case being that of SHMP, which, depending on its concentration, may act as a setting retardant or accelerator of the calcium aluminate cement.

In the present study, the rheology study of BS for ULCC focused on the shear stress-shear rate dependence at different concentration of plasticizer admixture. Setting time experiments were performed in order to verify the influence of the inorganic and organic salts on the reaction of hydration.

a)

b)
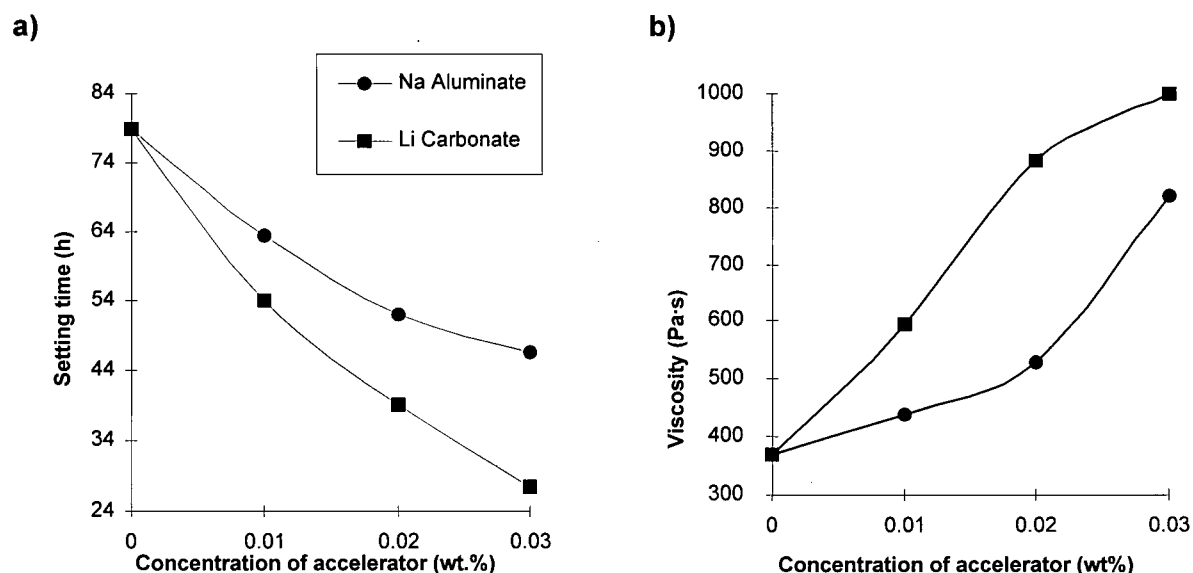
Figure 4.2-28. Variation of the setting time a) and viscosity b) at $0.1955\ s^{-1}$ as a function of the setting accelerator content for the 4 component BS based on SF2 at 0.1% STPP and 0.04% SNFC.

Since all initial experimental binding systems had setting times longer than 24 hours, the use of accelerators such as lithium carbonate and sodium aluminate was necessary. As presented in Figure 4.2-28 a) for a four components BS with 0.1%STPP, 0.05% SNFC and SF2, the most effective accelerator was lithium carbonate, which increased the viscosity. Sodium

aluminate was less effective as a setting accelerator and had only a small negative effect on the viscosity.

Because neither accelerator produced a required short setting time (i.e. less than 24 hours) and both had a negative effect on viscosity, it was considered that the BS presented in Figure 4.2-28 was not suitable for a self-flowing ULCC. In order to study the effectiveness of accelerators on the setting time, more experiments were performed with different concentrations of plasticizer admixture. The study was focused on the mix of STPP and SNFC, due to the low viscosity level induced by this admixture.
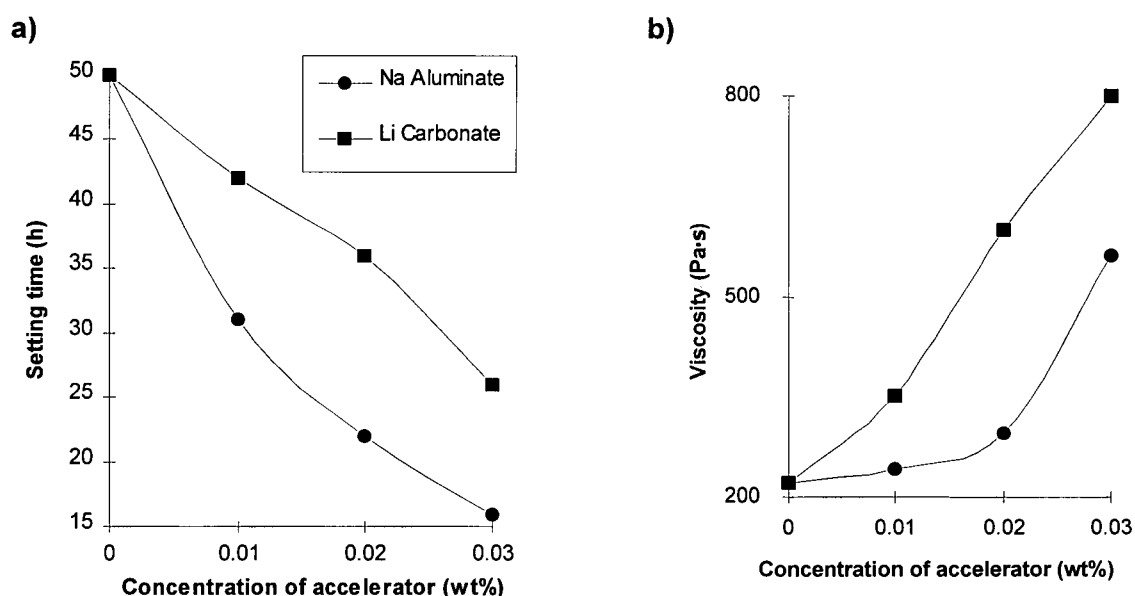
Figure 4.2-29. Variation of setting time a), and viscosity at 0.1955 s^{-1} b), as a function of setting time accelerator concentration for a 4 ceramic components BS based on SF2 at 0.1% STPP and 0.02% SNFC.

For the BS based on SF2 the experimental compositions of plasticizer admixture were based on the low viscosity fields presented in Figure 4.2-6. Comparing the data presented in Figures 4.2-28 and 4.2-29 it resulted that a low concentration of SNFC (below 0.02%) is an important factor in achieving a good setting time. Further examination of the variation of setting time and viscosity with the level of accelerator (Figure 4.2-30) showed that both accelerators were more effective while having a limited effect on the viscosity, at lower concentration of

SNFC (0.012%). More importantly, for low concentrations of sodium aluminate and concentrations of SNFC of 0.012%, it was possible to obtain a simultaneous effect of reducing the setting time and the viscosity. This result confirms a dual role of SNFC as a plasticizer and setting retarder. For low concentration of SNFC, sodium aluminate may act as a dispersant, further enhancing the fluidity of the BS, while lithium carbonate has no dispersant effect.
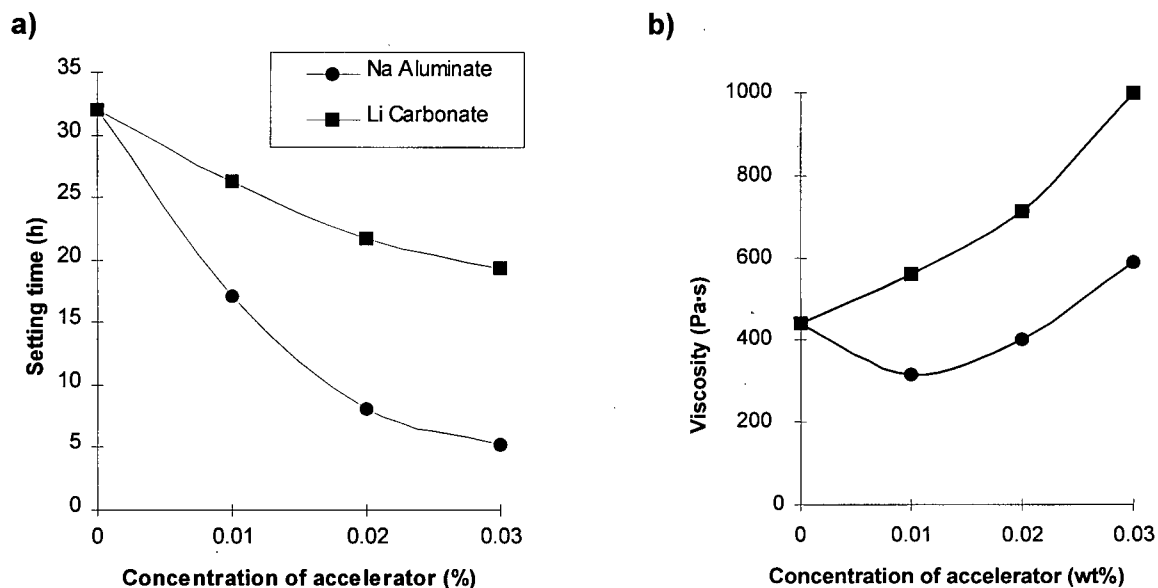
Figure 4.2-30. Setting time a) and viscosity at 0.1955 s^{-1} b), versus concentration of accelerator for a 4 ceramic component BS based on SF2 at 0.1% STPP and 0.012% SNFC.

It was also found that SNFC forms a viscous precipitate in water, in a solution of sodium aluminate. This may account for the increase in viscosity caused by the sodium aluminate in BS containing high concentrations of SNFC, but does not explain the similar effect obtained by the addition of lithium carbonate. This behavior can be considered a result of complex chemical and physical interactions within the binding system suspension. Therefore, it may be incorrect to define certain chemical additives as being only plasticizers or setting agents. It would be more correct to define a system of chemicals as a plasticizer-setting time admixture. The analysis of

the system is further complicated by the fact that the same plasticizer (as in the case of SHMP) may exhibit both a retarding or accelerating effect, depending on its concentration.
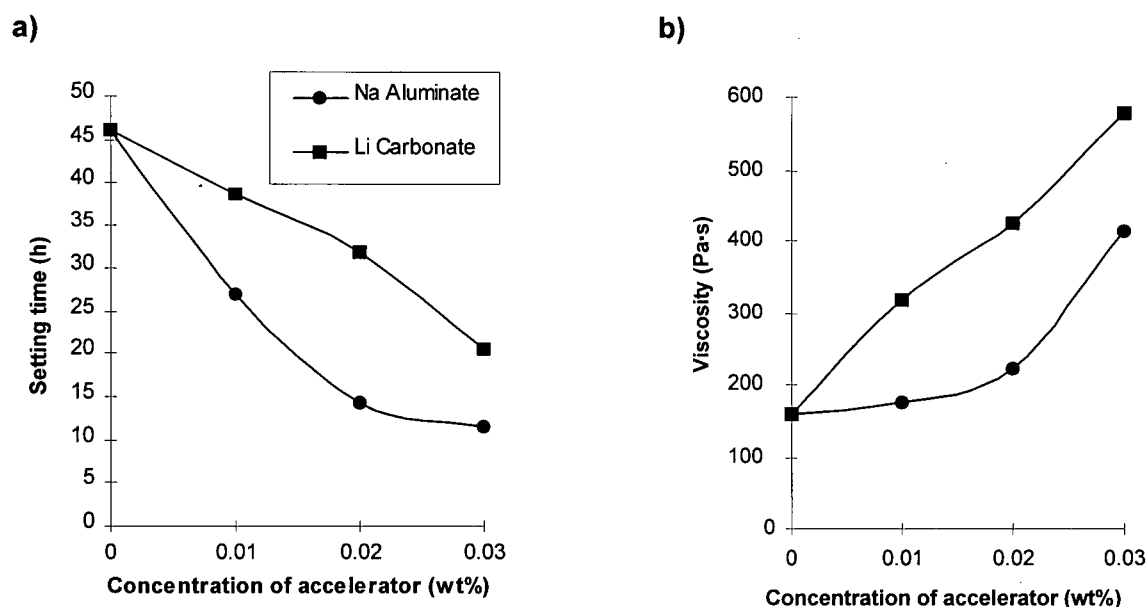
Figure 4.2-31. Setting time a) and viscosity at 0.1955 s^{-1} b) versus concentration of accelerator for the 4 component BS based on SF1 at 0.1% STPP and 0.012% SNFC.

According to the data presented in Figure 4.2-29 and 4.2-30, sodium aluminate can be used in order to simultaneously obtain a low viscosity and an acceptable setting time of a BS for ULCC, if the concentration of SNFC is below 0.02%. Similar results were obtained for BS based on SF1. In this case the effect of the accelerators was more significant, while the negative effect of increasing the viscosity was less significant (Figure 4.2-31).

Experiments on BS based on SF1 at relatively high concentration of STPP (0.15%) showed (Figure 4.2-32) that higher concentrations of STPP minimize the negative effect produced by SNFC on the setting time, also increasing the viscosity, especially with the addition of lithium carbonate. This was probably due to a weak accelerating effect of STPP in the 0.1-0.15% range of concentrations.
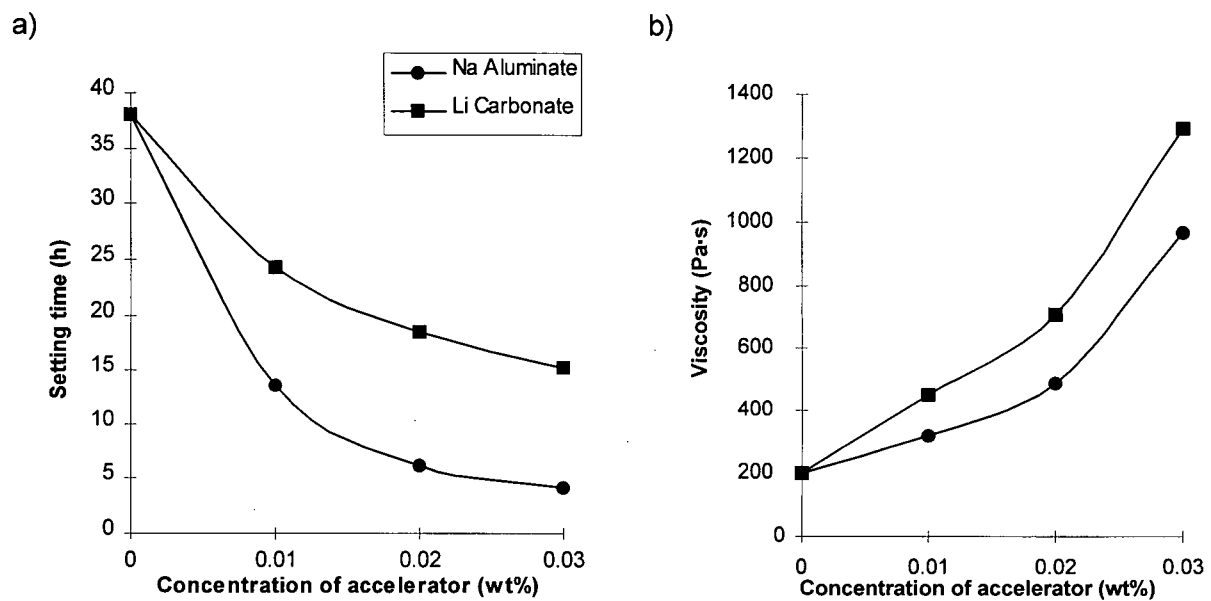
Figure 4.2-32. Setting time a) and viscosity at 0.1955 s⁻¹ b) versus setting concentration of accelerator for the 4 component BS based on SF1 at 0.15% STPP and 0.012% SNFC.

By correlating the setting time results with the rheology of binding systems, several conclusions can be made:

- the properties of silica fume (i.e. specific surface and impurities) have an important role in the rheology of the BS and their hydraulic setting behavior;

- the difficult hydraulic setting of BS of ULCC can be avoided by using a proper accelerator-plasticizer admixture;

- the organic plasticizers (such as SNFC and SPA) may have an important set retardant effect at high concentrations, that makes their use impracticable;

- STPP proved to have a weak accelerating effect in the range of 0.1-0.2 % and although high concentrations of STPP are beneficial for obtaining a good setting time, a significant increase in viscosity occurred for concentrations above 0.15%;

- there is a clear interaction between the accelerators and plasticizers, the viscosity of the BS being the result of the setting-plasticizer admixture.

As shown above, the most efficient plasticizer admixture is not necessarily suitable for a hydraulic setting process, while a high level of accelerator can completely compromise the flow

characteristics of the binding system. As different grades of silica fume have different requirements of plasticizer, it is necessary to choose a standard plasticizer admixture, which simultaneously achieves a low viscosity level and allows for a proper hydraulic setting. In our experiments, the standard plasticizer admixture was established thorough numerical optimization, selecting as a design criterion the minimum viscosity (for BS with both SF1 and SF2) and the minimum increase of viscosity (for concentrations of sodium aluminate up to 0.02%), as shown in Figure 4.2-33. The concentration of SNFC, which should be below 0.02%, was considered an absolute criterion. Lithium carbonate was not considered for further investigation due to its detrimental effect on the fluidity and a difficult to control effect on the setting time. The desirability function provided by the optimization routine of Design Expert software indicated that the optimum plasticizer admixture was at 0.10201% STPP and 0.01185% SNFC. For simplicity, 0.1% STPP and 0.012% SNFC values were adopted as standard content of plasticizer admixture for BS of ULCC.
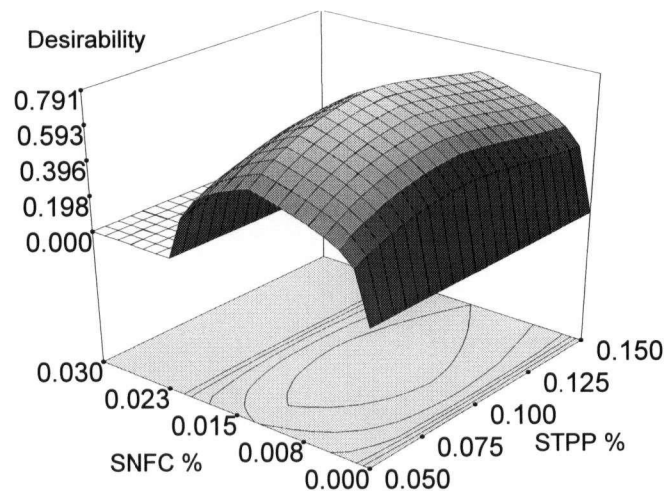
Figure 4.2-33. The optimum content of STPP-SNFC plasticizer admixture for the BS of ULCC.

4.2.3. pH of binding systems

The pH of binding systems was analyzed simultaneously with the viscosity measurements in order to establish a correlation between the chemical and physical interactions induced by the dispersants. In the case of 4 components BS based on SF2, both STPP-SNFC and SHMP-SPMA admixture systems have a noticeable effect on pH (Figure 4.2-34).
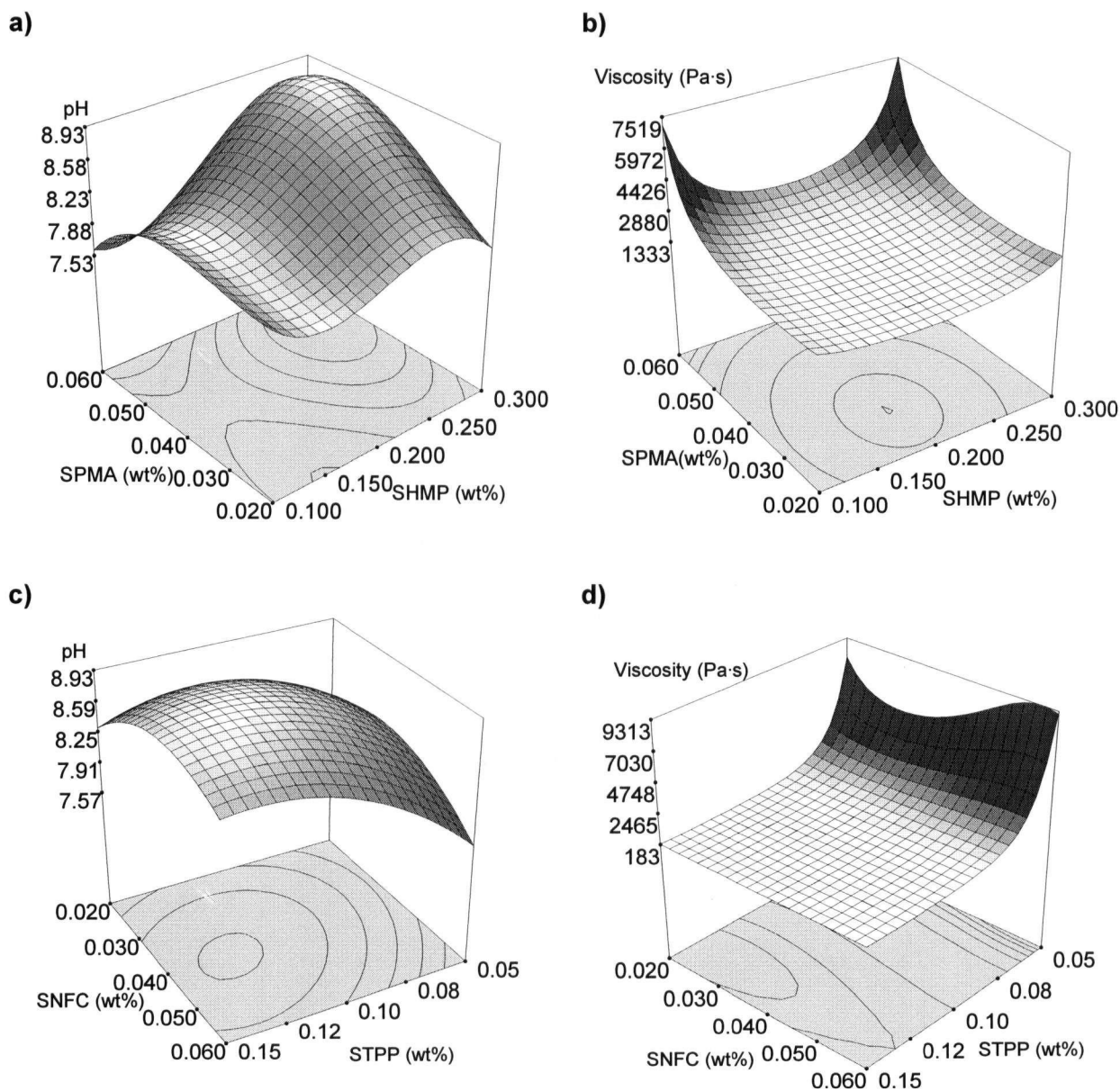
Figure 4.2-34. Variation of pH and viscosity (at 0.1955 s^{-1} shear rate) with concentration of admixture for a 4 component BS based on SF2: a) , c) pH, and b), d) viscosity for SHMP-SPMA (a and b) and STPP-SNFC (c and d).

In both cases the maximum of pH was at high concentrations of phosphate plasticizer and no apparent correlation existed between viscosity and pH. For SHMP-SPMA admixture there is a maximum of pH in a region of high viscosity, which may be attributed to a higher degree of hydration. For the STPP-SNFC admixture the maximum pH levels correspond to a region of
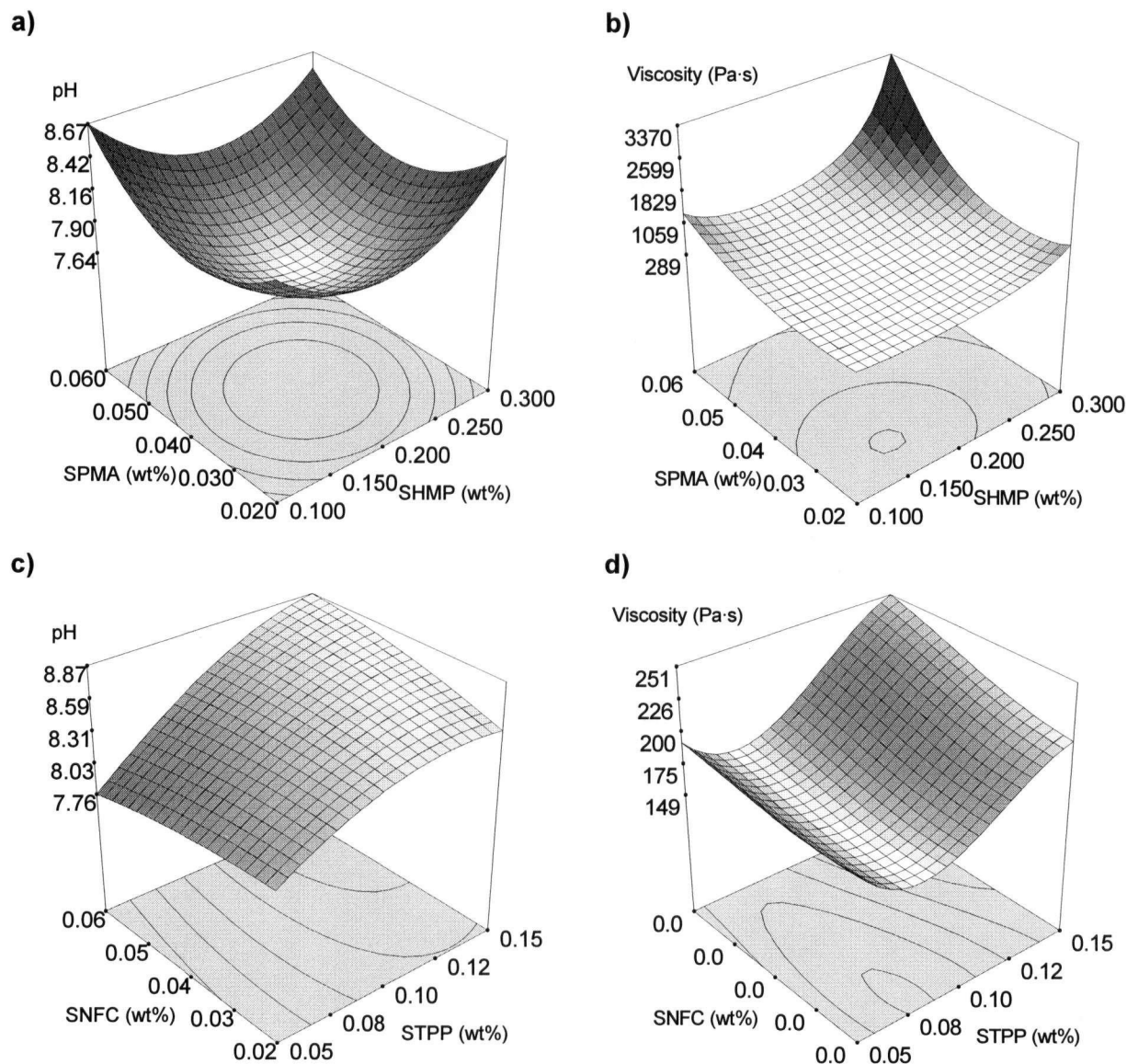
Figure 4.2-35. Variation of pH and viscosity (at 0.1955 s^{-1} shear rate) with concentration of admixture for a 4 component BS based on SF1: a) , c) pH, and b), d) viscosity for SHMP-SPMA (a and b) and STPP-SNFC (c and d).

modest increase in viscosity. This behavior suggests that for a low concentration of dispersant, there is no important influence of the reaction of hydration on the variation of viscosity, the dispersion of the concentrated suspension being just a result of adsorption equilibria. This finding is consistent with the results of setting time experiments with respect to the difficult hydration at low levels of phosphate additive, but does not explain the presence of a pH maximum for relatively high concentrations of organic plasticizer. It may be considered that during the initial contact with the water and chemical admixtures, the CAC particles participate in a high rate adsorption-ion exchange process with the organic plasticizers and the initial (first 10 minutes after contact with water) hydro-electrolytic effect is not determinant for the length of the dormant period.

In the case of 4 component BS based on SF1 with SHMP-SPMA admixture, there is a minimum of pH in a region of low viscosity, which is clearly due to a low degree of initial hydration (Figure 4.2-35). For both pH and viscosity, the STPP-SNFC effect seems to be determined mainly by the concentration of STPP, but high viscosity and pH levels can be correlated only at high concentrations of STPP.

For the three component binding system based on SF2, the study of variation of pH and viscosity with the concentration of plasticizer admixture shows similar patterns to those of four components BS, but there are some noticeable differences (Figure 4.2-36):

- the low levels of pH are higher than for the four component BS, due to the absence of kyanite, which has a weak acid reaction in solution;

- the SHMP does not affect the pH and viscosity at the level SPMA does;

- the organic dispersant has a more important influence in establishing the pH level.

It may be hypothesized that for low concentrations of dispersant, the pH is a result of the equilibrium pH of ceramic components. At higher concentration of dispersants, a higher degree of initial hydration may be responsible for the increase of both pH and viscosity. However, this initial hydration could not be directly related to the length of the dormant period or to the final hydraulic setting.
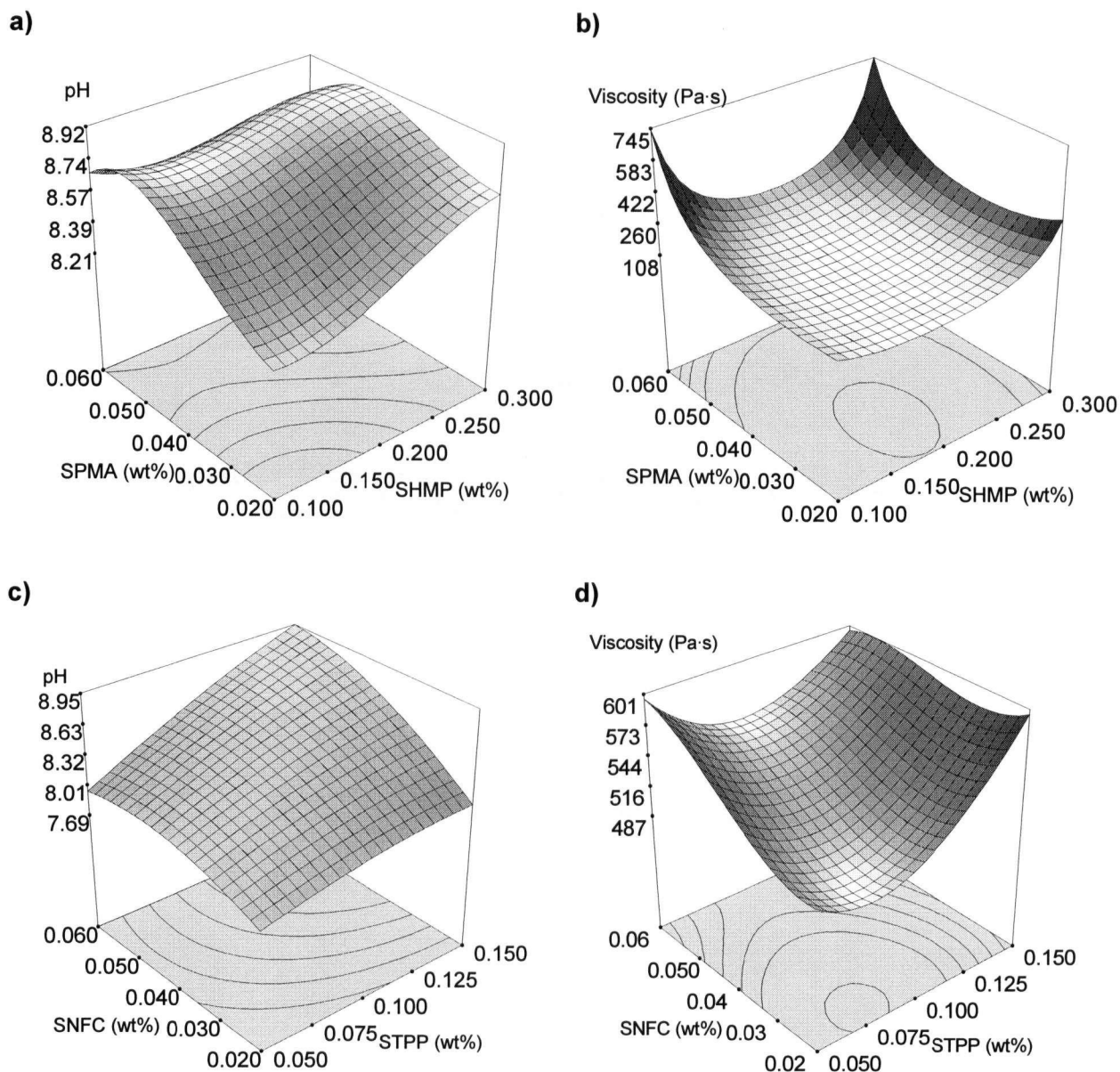
Figure 4.2-36. Variation of pH and viscosity (at 0.1955 s⁻¹ shear rate) with concentration of admixture for a 4 component BS based on SF2: a) , c) pH, and b), d) viscosity for SHMP-SPMA (a and b) and STPP-SNFC (c and d).

4.2.4. Flow

The self-flowing of refractory castables is a phenomenon not yet well understood. The experimental methods for evaluating the self-flow behavior still lack fundamentals, which results in the absence of an accepted standard method of testing. In our experimental work the truncated cone method (ASTM C230 adapted for self-flow measurements) was used. It basically consist of a modified slump test for measuring the yield stress.

Although there have been studies regarding the measurement of self-flow of castables using the truncated cone method, most of the literature data is focused on the flow behavior of different castable compositions and only a few analyze the method itself. The truncated flow cone method measures only the relative increase in diameter of the castable under its own weight without any regard to the flow pattern. During the present experimental work it was considered that if only the relative increase in diameter is considered, the result of the measurements can be misleading. Therefore for clarity reasons, it was necessary to make some considerations regarding the flow pattern of the castables.

A uniform plastic and stable flow pattern is characterized by a uniform and circular spread of the castable on the flow table, considered to be the behavior of a true self-flowing castable (Figure 4.2-37)

Figure 4.2-37. Uniform plastic and stable flow pattern.

If the particle size distribution contains too much of the coarse fraction (0.2-10 mm) and medium fraction (0.045-0.2 mm), an increased flow and the segregation of the coarse particles occurs, due to a more fluid suspension of the fine fraction. Even though strong segregation is

easily identifiable, slight segregation may be identified only by an asymmetric and non circular flow pattern (Figure 4.2-38).
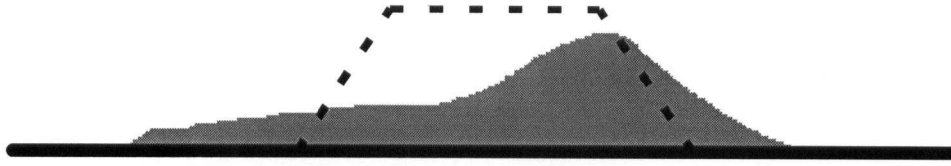
Figure 4.2-38. Segregation, asymmetric flow pattern.

An excess of medium fraction (although it will produce initially an increase in flow), translates to an increase in the mechanical interaction between the refractory aggregate particles. A low viscosity suspension and the mechanical interlocking between the aggregate particles can produce pump and hose clogging during castable pumping. The first sign of aggregate particle interaction is the persistence of a ring shape trace on the upper surface of the castable, originated by the circular upper edge of the truncated cone (Figure 4.2-40).
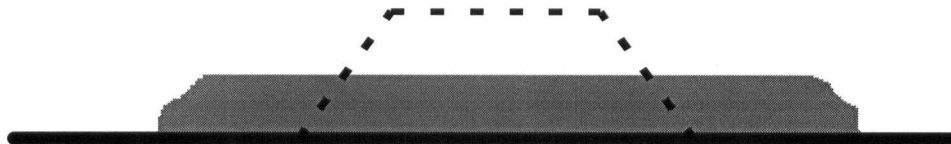
Figure 4.2-40. Particle interaction flow pattern.

If the coarse aggregate fraction (4-8 mm) is in excess, even if the binder phase is more fluid there is not enough material to fill all the voids between the coarse particles and an increase in the flow results, with the largest aggregate particles expelled to the surface of the castable (Figure 4.2-41). This unwanted flow pattern is difficult to distinguish. It is particularly difficult to identify for low flow values, when the binder is viscous and the air entrapped during mixing may account for some of the intergranular volume. Coarse particle separation can usually be identified for flow values of 90-110%. In the present work, if not explicitly stated, all

the self-flow measurements should be assumed to be performed for a stable, plastic and regular flow.
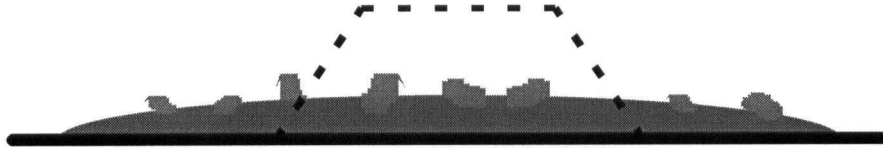
Figure 4.2-41. Coarse particle separation, flow pattern

The self-flow phenomenon is considered to be due to a fluid binder and a carefully designed particle size distribution of the refractory aggregate. Regarding the particle size of the refractory aggregate, as mentioned in Chapter 2.2.3 there are two main theories related to the packing characteristics of the castables. A flow model [81] considers that in order to obtain the self flow it is necessary to achieve an equal proportion between the coarse (+1mm), medium (0.045-1mm), and fine (-0.045mm) fractions. No clear indication on the particle size distribution is given. Another model [82-85] states that in order to obtain self-flow behavior, the particle size distribution of the castable has to be a continuous one and it is suggested that the empirical Andreassen distribution gives the best results for the q exponent in the range of 0.20-0.30. There is no scientific background for choosing a certain value for the Andreassen exponent, all the conclusions being based on experimental observations. There is also no information regarding the influence of the deviations from the Andreassen distribution on self-flow behavior.

None of the above mentioned models take into account the influence of the surface characteristics and porosity of individual particle size fractions on the flow. In the present study the influence of the factors mentioned above was also studied.

4.2.4.1. LCC and ULCC

In the initial experiments, a Mulcoa type of aggregate (consisting of mullitic and bauxitic calcines) was used. The experimental castable compositions conformed to the Andreassen model using q=0.22. The cumulative particle size distributions of the individual components are presented in Figure 4.2-41.
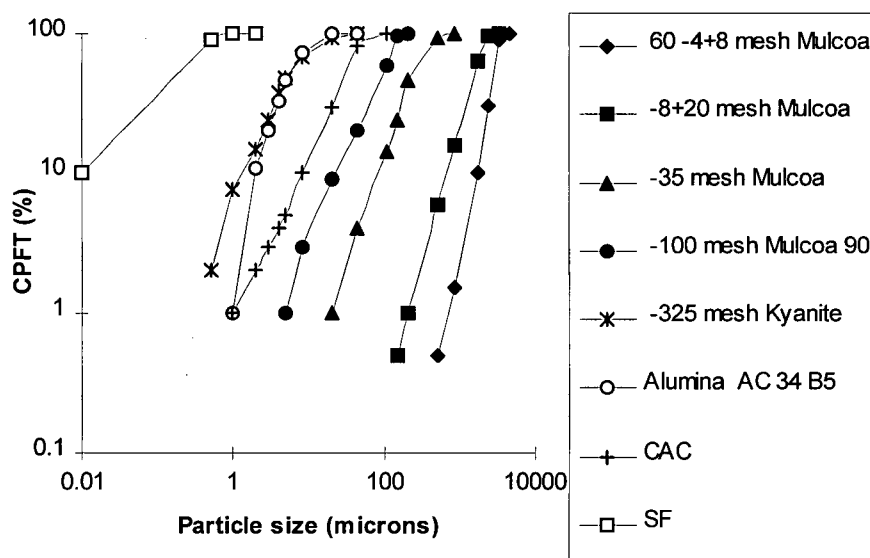
Figure 4.2-41. Particle size distribution of individual components of the refractory castables.

The best fit to an Andreassen distribution, showing 5% flow at 6.5% water content ,is presented in Table 4.2-4. Attention must be given to the composition of the medium fraction (Mulcoa 60 -35 mesh and Mulcoa 90 -100 mesh). The two components forming this fraction are different not only in their particle size distribution but also in their porosity, 7.9% and 2.9% respectively. If the water for casting can be divided into water for the dispersion of the binder and water absorbed in the porosity of refractory aggregate, the use of a refractory aggregate with lower porosity would result in more water available for the binder and consequently a more fluid binder and higher flow.

131

Table 4.2-4. Experimental self-flowing ULCC composition (q=0.24).

Component	Composition (wt%)
Mulcoa 60 -4+8 mesh	18
Mulcoa 60 -8+20 mesh	25
Mulcoa 60 -35 mesh	19
Mulcoa 90 -100 mesh	14
Kyanite - 325 mesh	8
CAC Secar 71	2
Calcined alumina AC 34 B5	4
SF2	10

In order to increase the flow of the castable by increasing the fluidity of the fine fraction the replacement of the -35 mesh Mulcoa 60 fraction with corresponding amounts of the lower porosity -100 mesh Mulcoa 90 fraction was therefore necessary. The increase in flow is significant while the deviation from an Andreassen distribution is almost negligible (Figure 4.2-42 a, b).
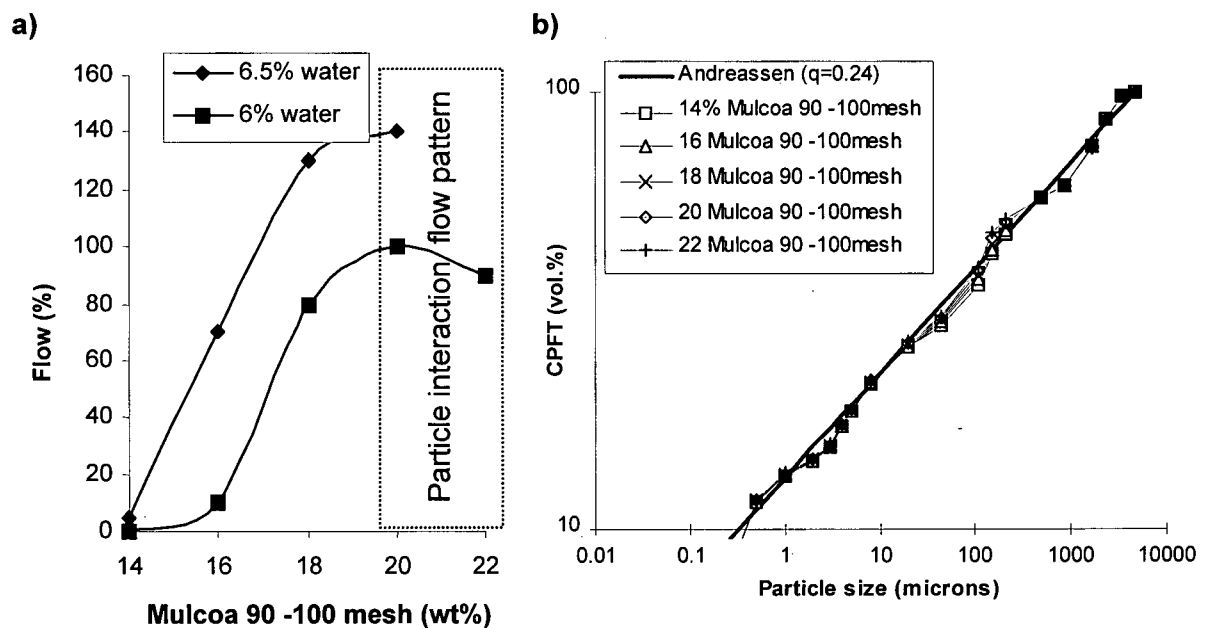
Figure 4.2-42. Variation of flow with the content of -100 mesh Mulcoa 90 fraction for 6 and 6.5% water a), and particle size distribution for ULCC compositions with different content of -100 mesh Mulcoa 90 b).

Another interesting aspect shown in Figure 4.2-42a, is the fact that a particle interaction flow pattern (Figure 4.2-40) may also occur at a constant content of medium fraction. The inclusion of 35 mesh Mulcoa 60 - in the medium fraction was not entirely correct, because while its fine grains belong to the medium fraction, its coarse grains could be considered to belong to the coarse fraction of the castable. The fact that, for almost the same Andreassen distribution, there is a large variation of the flow values and a change of the flow pattern demonstrates that the Andreassen model is not very reliable if applied to real polydisperse systems. One possibility is that the porosity and the shape factors can have a major influence on flow. Nevertheless the Andreassen distribution is a useful tool in establishing the starting point for the design of a self-flowing castable.

The influence of the Andreassen exponent on flow is not very clear. For a system composed of ideal particles (i.e. spherical with no porosity and no active surfaces) by decreasing the q value for any given particle size distribution, the ratio between the volume of particles finer than the given size and the free volume of the particles larger than the given size is increased. That reduces the interaction between particles of similar size and consequently increases the probability of displacement of a particle for a given value of stress. For real systems, besides the influence of the porosity, there exists another effect due to different surface activity (I.e. capability for adsorption of additives) of the individual components. Coarse and medium fractions of refractory aggregate can be regarded as inert particles due to their low specific surface (below 0.1 m^2/g). The fine fraction of the castable (silica fume and fine ceramic powders) is responsible for more than 95% of the specific surface of the total (silica fume grades used for castables have a specific surface of 13-24m^2/g)

The study of the rheology of BS showed that there is a power law dependency between the viscosity (and consequently of the yield stress) and the amount of water in the suspension. For a given level of water in the castable, if the value of the Andreassen exponent decreases,

the mechanical interaction between aggregate particles decreases. At the same time when the proportion of fine components in the BS increases, the ratio between the available water and the solid load in the BS decreases, the viscosity of the BS increases, and therefore the flow decreases.

For a set of castable components the Andreassen exponent that insures the maximum free flow is the result of two opposite effects: the decrease of mechanical interaction between particles, which is favored by a low q value, and the decrease of the viscosity of the binder suspension, which is favored by a high q value. While the mechanical interaction between the coarse particles of the refractory aggregate is just a result of the volumetric particle size distribution, the variation of the viscosity of the BS depends on the nature and content of the fine reactive ceramic components. Therefore it is not possible to define a unique Andreassen exponent for any self-flowing castable, because its value strongly depends on the nature (specific surface, composition and porosity) and the content of the BS. This may explain the relatively large dispersion (0.21-0.26) of the values of the Andreassen exponent considered optimum by different authors, or the concept of using different Andreassen exponents for the particle size distributions for the fine and coarse fractions of the castable [137].

In order to study the influence of the Andreassen exponent on the flow, it was necessary to minimize the effect of the individual components. Therefore, the particle size distributions of the experimental compositions were designed by keeping the composition of the BS (including silica fume, CAC, kyanite and alumina) constant and by maintaining the same ratio between the -35 and -100 mesh fractions of the refractory aggregate. The experiments were performed for ULCC compositions based on SF1 and SF2 for different water levels. The basic castable composition contained 18% of the-100 mesh fraction (refer to Figure 4.2-42 a). According to the data in Figure 4.2-42 b the deviations from the ideal Andreassen distribution produced by this procedure of design are negligible.

All compositions with the Andreassen exponent in the range q=0.19-0.26 (Figure 4.2-43) showed a self flow behavior, the best results being for the castables based on SF1.
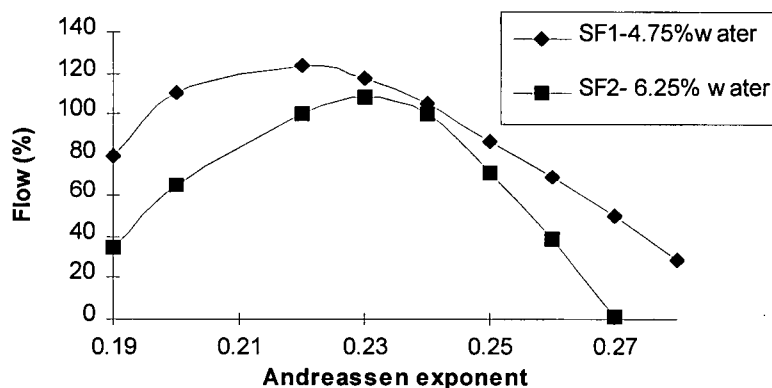
Figure 4.2-43. Variation of flow with Andreassen exponent for castables based on SF1 and SF2.

For both castable compositions the highest flow was obtained for q <0.24 (q=0.22 for SF1 and q=0.23 for SF2). For the castable made with SF2 not only was the water requirement higher, but the material was also more sensitive to the viscosity variations and less able to withstand a higher degree of particle interactions than the castable based on SF1 (particle interaction flow pattern was present for q>0.24). The results demonstrate that the rheological parameters of the BS are determining factors in establishing the optimum particle size distribution for self-flowing castables.

It is to be mentioned that in all experimental castables, the composition of the binding system was maintained constant, resulting in constant ratios between CAC and other ceramic components. It is known that during the hydraulic setting, the initial hydration of CAC decreases the fluidity of the BS. In order to establish the influence of CAC content, a set of castables compositions based on SF1 having constant contents of silica fume and variable contents of CAC (at the expense of calcined alumina and kyanite, which were maintained at a constant relative ratio) was designed. Two castables having different particle size distributions and the same concentration of plasticizer admixture (STPP-SNFC) were used.

As shown in Figure 4.2-44a, the increase of CAC has a negative effect on the flow values and this effect is stronger at higher q values. Considering that by increasing the CAC content and simultaneously decreasing kyanite and alumina content the particle size distribution remains practically unchanged, it results that the flow decrease can be attributed exclusively to a viscosity increase. If the flow is represented versus CAC/SF ratio (SF1=12.7% for q=0.22 and SF1=8.5% for q=0.26), the similar behavior of two compositions is obvious (Figure 4.2-44b). The almost identical flow levels for similar CAC/SF ratio show that for a given particle size distribution, the flow depends only on the rheology of the binding system.

The water level was chosen so that the flow for the samples containing 1% CAC was 130% for both series of compositions. As a result the water/BS ratio was different (0.163 for q=0.22, and 0.262 for q=0.26), which translates to an important difference in the viscosity, but the relative variation of viscosity of the BS was practically independent on the water content. This fact was in accordance with the data resulted from the rheology study on the binding systems (Chapter 4.2.1).

a)   b)
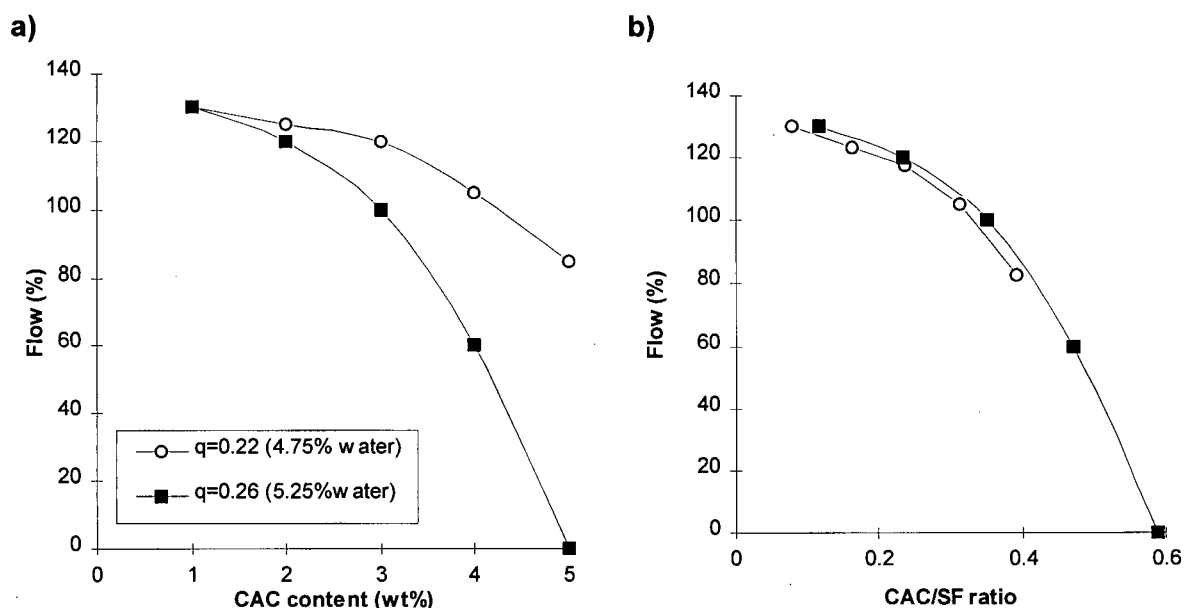
Figure 4.2-44. Variation of flow with a) CAC content, b) CAC/SF ratio.

The above data demonstrate that the use of the Andreassen model allows for adjustment of the medium fraction in order to minimize the effect of porosity. Also, a proper plasticizer-setting additive admixture makes it possible to design a series of castable compositions with optimized flow properties. The data presented in Figure 4.2-44 represent in fact a family of self-flowing low and ultra-low cement castables.

4.2.2.2. NCC

The preliminary studies demonstrated that concentrations of silica fume above 10 wt% can have a negative effect on the thermomechanical properties of the castables, and high SF/CAC ratios result in a difficult hydraulic setting. Owing to that, subsequent experiments were limited to compositions with a silica fume content in the range of 8-10%. In the design of self-flowing NCC compositions, several considerations were taken into account:

- As NCC are materials intended for special, demanding applications (high temperature and high corrosion resistance), tabular alumina was chosen as an aggregate;

- In order to minimize the thermal expansion mismatch between the aggregate and the binding system, kyanite was replaced with the corresponding particle size fraction of tabular alumina;

- CAC was replaced with HAB in order to maintain the CaO content below 0.1%;

- Low purity SF2 was considered improper, due to its high water requirement and high level of impurities.

Compared to CAC, the HAB manifests two important differences for its use as a hydraulic binder: it has a lower hydraulic activity (consequently a slower setting and low mechanical strength) and it induces a strong increase of viscosity. Also at HAB/SF ratio above 0.4 a dilatant behavior of the castable occurs.
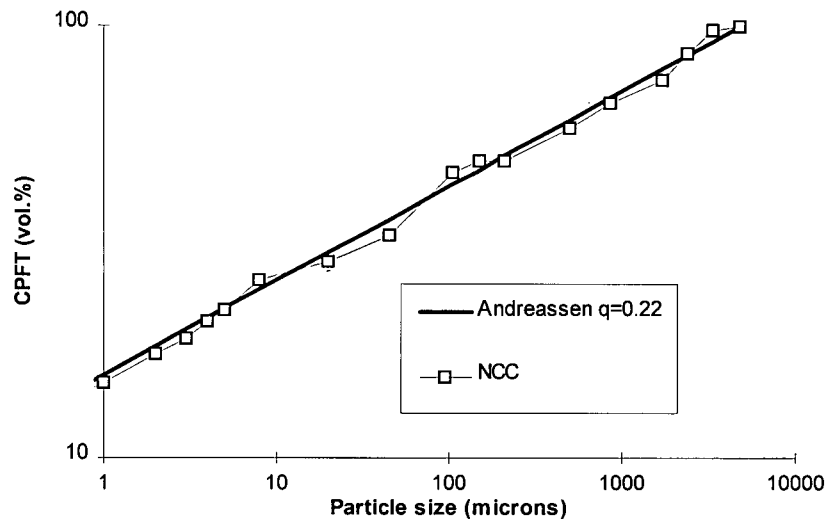
Figure 4.2-45. Particle size distribution of experimental NCC compositions.

Due to the high density of tabular alumina aggregate (3.5 g/cm^3) and to the fact that Andreassen distribution is volumetric, a 10% by mass silica fume corresponds to an Andreassen exponent of 0.22 (Figure 4.2-45). Also because of the low porosity of tabular alumina aggregate no adjustment of the medium fraction was necessary.

Based on the previous experimental results on the rheology of binding systems, the composition of the dispersant-setting additive admixture contained 0.1% STPP, 0.012% NFSC
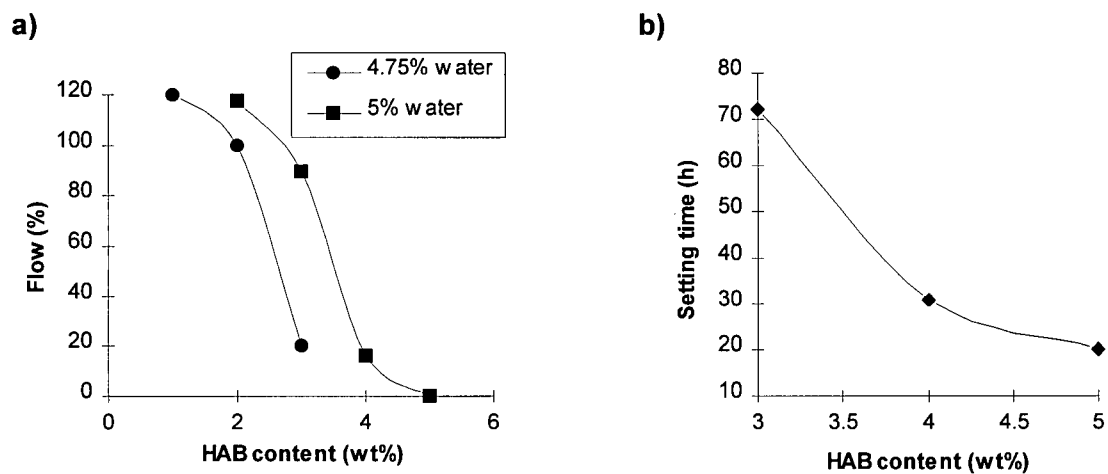
Figure 4.2-46. Variation of a) flow, and b) setting time with HAB content of NCC having $q=$ 0.22 and 10wt% SF1.

138

and 0.02% sodium aluminate. As shown in Figure 4.2-46, it was impossible to obtain a self flowing NCC at low water levels (below 5%) because the hydraulic setting was longer than 24h. By increasing the concentration of sodium aluminate above 0.04% the flow is totally compromised, with no significant effect on the setting time (Figure 4.2-47). It appears that the sodium aluminate is not an effective accelerator below 0.04%, the hydraulic setting being determined by the HAB/SF ratio
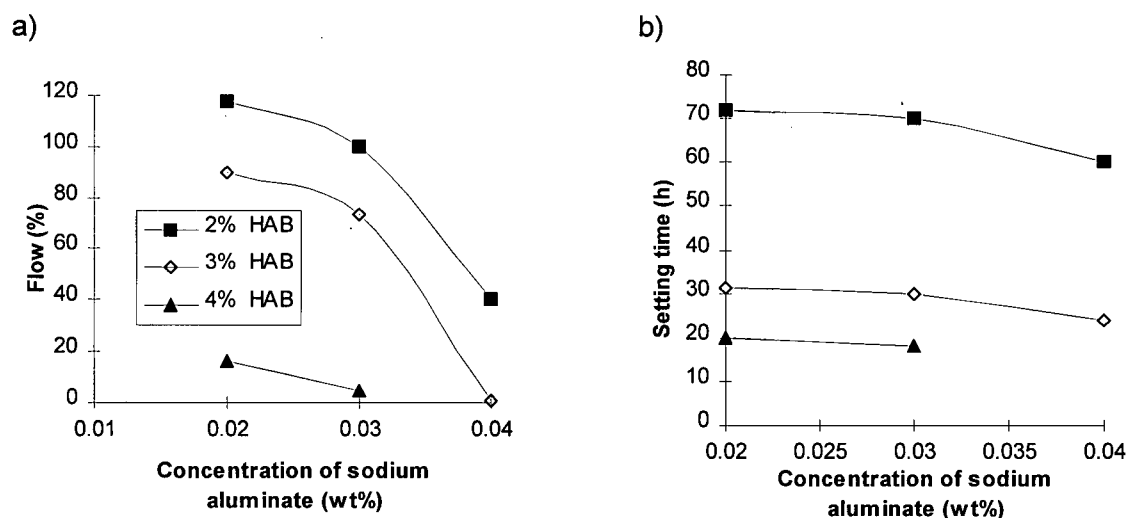
Figure 4.2-47. Variation of a) flow, and b) setting time concentration of accelerator for different HAB content NCC.

It is well known that CAC is an effective hydration accelerator for Portland cement and vice versa, and when mixed together many hydraulic binders have a reciprocal interaction during hydration. In order to explore the possible setting acceleration of HAB by CAC, experimental compositions of NCC were prepared at low content of HAB and low substitution ratios of CAC. These mixes also contained 0.02% sodium aluminate.

CAC has shown to be a very effective accelerator for HAB. If used in small concentrations (CAC/HAB < 0.33) it had almost no effect on flow, while the setting time was maintained below 24 hours. As shown in Figure 4.2-48, the CAC/HAB ratio has an effect more important even than (CAC+HAB)/SF ratio, for low concentration of hydraulic binder (<3wt%).
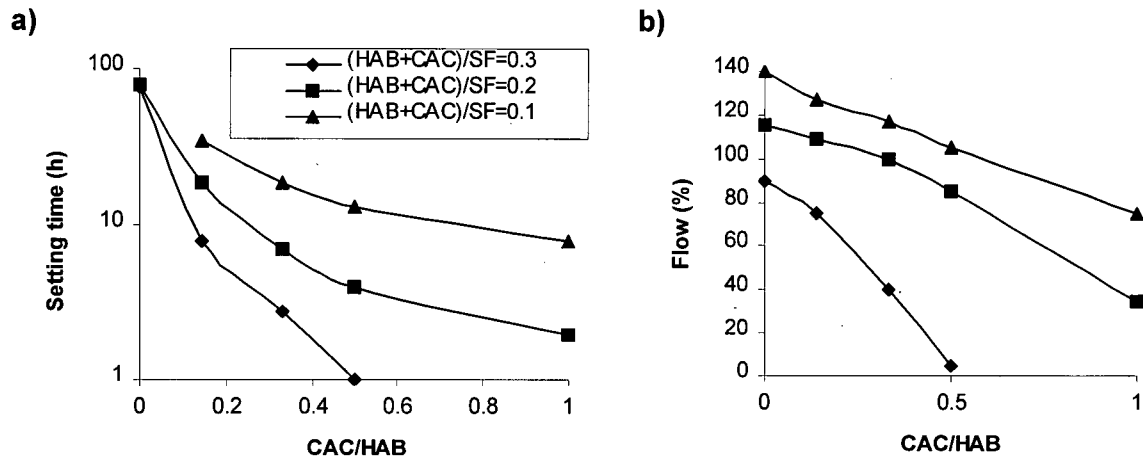
Figure 4.2-48. Variation of a) setting time and b) flow with CAC/HAB for NCC mixes with different (HAB+CAC)/SF ratio, at 5% water.

As it is shown in Figure 4.2-48 there is no unique solution to obtaining a good setting time and good self flow values. However, the properties of the system can be tailored in order to satisfy different design requirements as a function of the CAC/HAB and (CAC+HAB)/SF ratios. For further experiments it was considered that a ratio CAC/HAB=0.15 and a ratio (CAC+HAB)/SF=0.2 would provide simultaneously:

- good flow values (i.e. at least 100% at 5% water);

- setting time of maximum 15 h;

- low content of CaO brought by hydraulic binder (0.075%);

- acceptable green strengths.

All castables presented above have silica fume in their compositions. It is known that silica fume is the key component in achieving self flow behavior due to its small particle size (d_{av}=0.1μm), spherical shape of the particles, and high specific surface area (up to 24 m²/g). Although silica fume represents the ideal choice for self-flowing alumino-silicate castables, its presence in high alumina or in magnesia spinel castables has a detrimental effect on the

corrosion resistance and mechanical properties at high temperature. The replacement of silica fume with reactive alumina is a key factor in designing self flowing castables with high corrosion resistance to basic slags, but the currently available reactive aluminas are not suitable for providing self flow behavior comparable to silica fume [89]. There are several reasons behind the inferior flow properties due to reactive alumina replacement of silica fume:

- concentrated suspension of fine alumina particles exhibit a shear thickening as opposed to concentrated suspensions of silica fume, which showed shear thinning in our experiments;

- fine alumina particles are most often non spherical, i.e. have a hexagonal platelet shape with high aspect ratio, as opposed to the perfect spherical particles of silica fume, and this results in an increased particle interaction;

- the porosity of fine alumina particles depends strongly on the amount of alkalis and while for silica fume a content up to 2% can be considered negligible, for low porosity reactive aluminas it has to be maintained below 0.05%;

- fine alumina powders, with particle size comparable to that of silica fume (0.1μm) have a high water demand in order to produce low viscosity suspensions.

It is thus not possible to make self flowing castables at low water content by a total replacement of silica fume with fine alumina, using the Andreassen particle size distribution. For example Figure 4.2-49 shows the effect of alumina substitution for SF1 in a mullite-type calcines based ULCC (q=0.24) on the flow, for different average particle sizes of alumina.

Alumina type	Average diameter (μm)
PGA	0.06
A1000	0.9
C90LSB	1
A3000	3
AC 34 B5	5
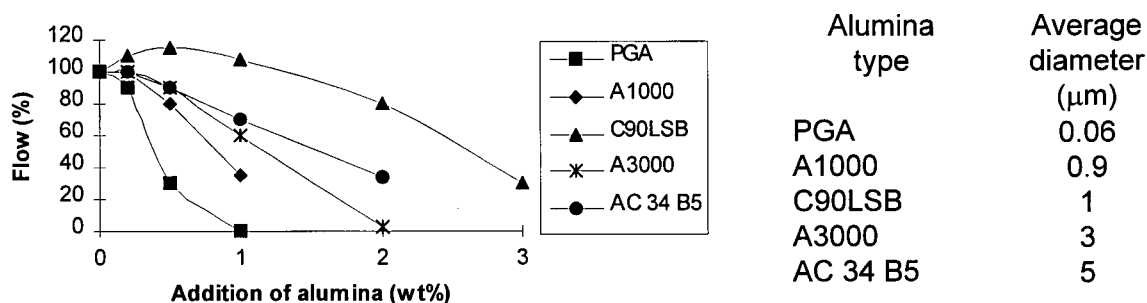
Figure 4.2-49 . Variation of flow with the content of various aluminas (of different particle size) that substitute SF1 in a binding system for ULCC (q=0.24).

With the exception of the samples prepared using the C90LSB alumina it may be said that the flow decreased with for a small particle size alumina, due to a higher water demand of the finer particles. The difference between CA2 and all the other aluminas presented in Figure 4.2-49 is that it has a bimodal particle size distribution (where $d_1 = 1\mu m$ and $d_2 = 4\mu m$). Based on the data presented above it was hypothesized that it may be possible to obtain a castable with self flow behavior without particle size distribution of self flowing silica fume free (SFF) NCC if:

- the medium and coarse fractions have an self-flowing Andreassen distribution, i.e. minimum particle interaction (low q);

- silica fume is replaced by a fraction of alumina with small amount of particles smaller than $1\mu m$ (and a high value of the Andreassen exponent) in order to lower the water demand;

- the amount of HAB is minimized in order to decrease the viscosity of the binder.

Particular attention was paid to the design of the fine fraction of the castable, in order to assemble the desired particle size distribution. Because special reactive alumina products with narrow particle size distribution for the whole range of 1-5μm are not available, the equivalent effect was obtained by blending a reactive alumina with bimodal distribution, a narrow particle size distribution alumina and a relatively wide particle size distribution alumina with a very low content of particles below 1μm (Figure 4.2-50). Considering that alumina powders having particle size over 10μm are not essential for the formation of the BS suspension, the SFF-NCC
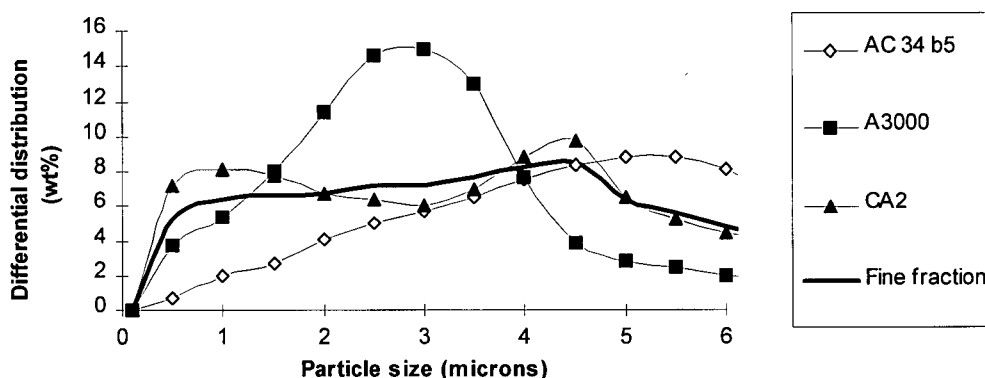
Figure 4.2-50. Differential particle size distribution for components and fine fraction of SFF NCC.

particle size distribution was designed for an Andreassen exponent q=0.22 for particles larger than 10µm and q=0.56 for particles smaller than 10 µm (Figure 4.2-51).
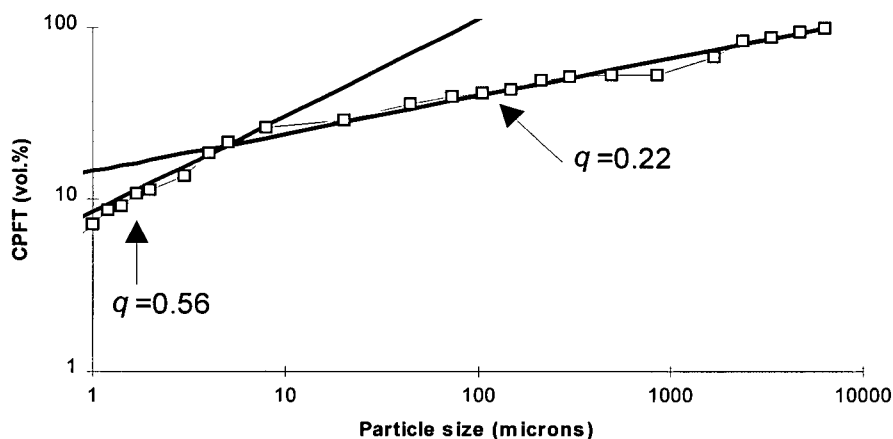
Figure 4.2-51. Particle size distribution of tabular alumina based SFF NCC.

The resulting SFF-NCC have a difficult hydraulic setting. Compared to the NCC containing silica fume, the process of hydrolysis is more difficult to be obtained simultaneously with the self flow behavior at low water levels, due to some additional impending factors, i.e.:

• phosphate dispersants have a negative effect on flow , the only effective dispersants being the organic acrylates (Figure 4.2-52) at relatively high range of admixture (0.6% for SMA), this resulting in a general retarding effect of the plasticizer agent;

• the increase of the content of HAB has a strong negative effect on the flow (Fig. 4.2-53 a);
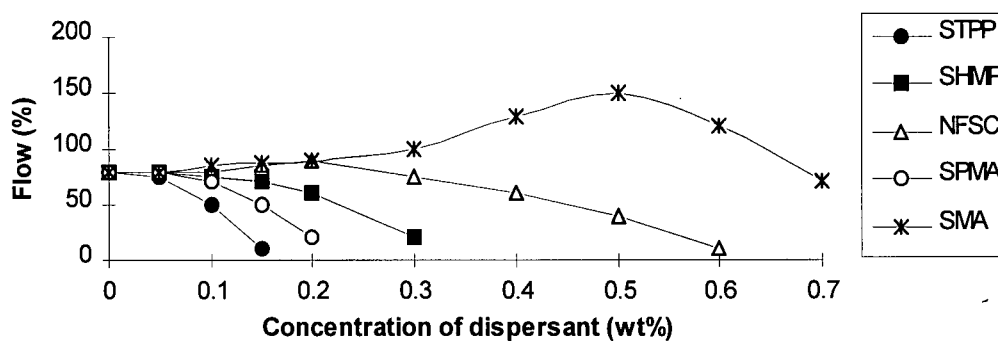
Figure 4.2-52. Variation of flow with concentration of dispersant for a SFF-NCC (1% HAB, 5.5% water).

- sodium aluminate has no dispersant effect on the fine fraction of reactive alumina, and a limited effect on the setting time at concentrations that insure self-flowing behavior (Figure 4.2-53 b);

- the use of CAC as an accelerator for HAB severely reduces the flow at any effective range of the admixture (Figure 4.2-53 c).

A setting time below 24 hours and a self-flowing behavior can be simultaneously achieved for SFF-NCC, by using a proper combination of plasticizer accelerator admixture. For
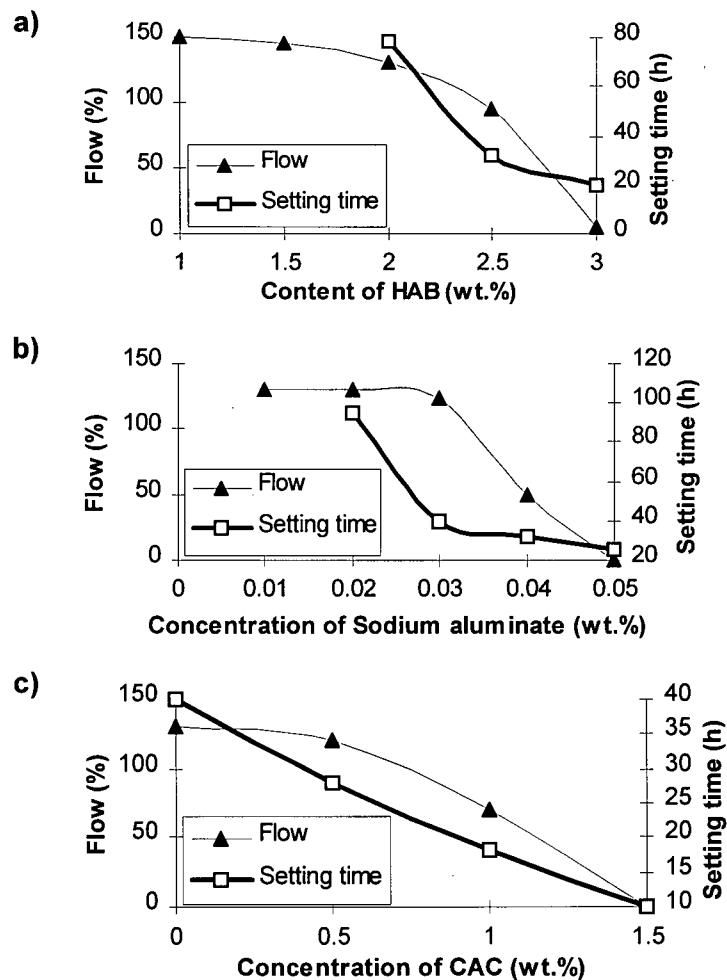
Figure 4.2-53. Variation of flow and setting time of a SFF-NCC at 5.5% water with: a) content of HAB , b)concentration of sodium aluminate, and concentration of CAC c).

example, a solution giving 18 h setting time and 70% flow at 5.5% water, was found for 0.5% SMA, 2% HAB, 1% CAC, and 0.03% sodium aluminate. The green strength of these castable was however found to be low (MOR≈ 2MPa), because of the low hydraulic activity and high water demand of the HAB, and the high porosity of the fine fraction of these castables (q=0.56). It is concluded that further improvement of SFF-NCC technology depends on the development of enhanced hydraulic activity HAB with low water demand, and the development of precision designed particle size distribution reactive alumina powders.

4.2.4.3. Correlation of viscosity and flow

If considered that for a given particle size distribution of the refractory aggregate (i.e. q=const.) the level of mechanical or geometrical interaction between refractory aggregate particles is constant ,the flow may be expressed as a function of the rheological characteristics of the BS. It means that the flow of a castable depends on the water level, the nature and content of fine reactive ceramic components and hydraulic binder, and the nature and concentration of dispersant admixture. The compositions presented in Figure 4.2-54 differ just by different type of silica fume. In both cases there is a good correlation between flow and viscosity of BS. For a given castable and a given shear rate the flow of a castable can be described as a function of the viscosity of the binding system.

For the data presented in Figure 4.2-54 the variation of flow of the castable and viscosity of the binding system was obtained by changing the water content. While for compositions based on SF1 the self-flowing behavior was obtained in the range of 4.25-5.5% water, for compositions based on SF2 the self-flowing behavior was obtained in the range of 5.5-6.75% water.

a)
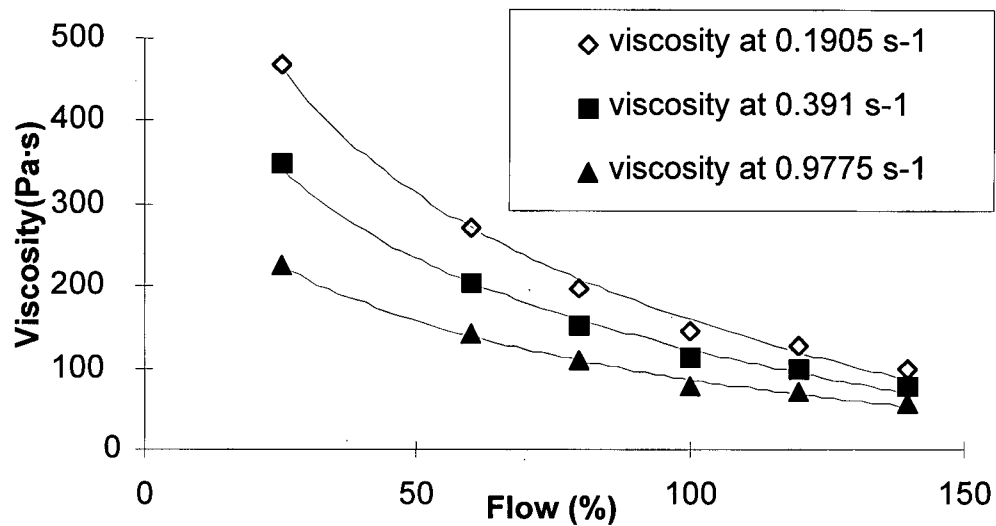
b)
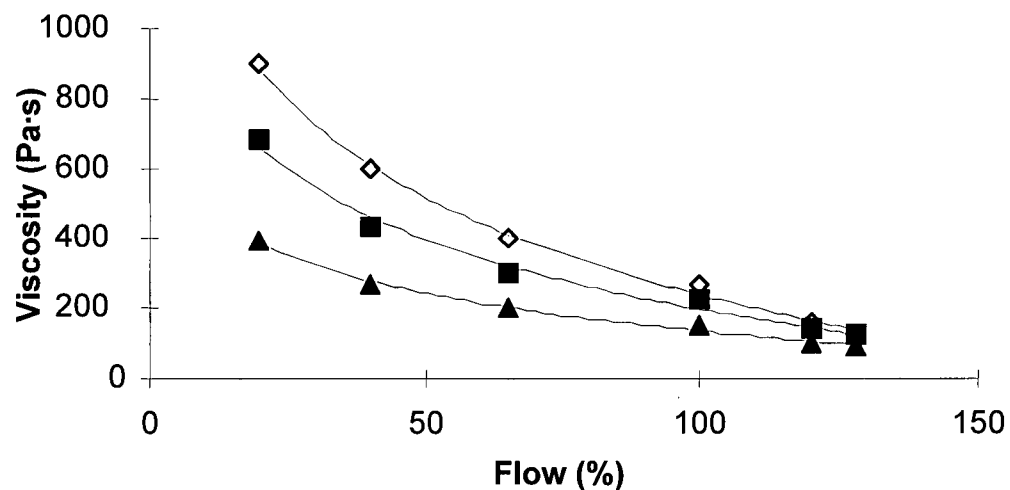
Figure 4.2-54. Correlation between the flow of ULCC (q=0.24) and the viscosity of BS for compositions based on: a) SF1 and b) SF2 at three different shear rates.

The pattern of correlation between flow and viscosity of BS differs for the two compositions. Even though the compositions based on SF2 have a significantly larger content of water their viscosities are almost double those of the compositions based on SF1 for a similar flow level. This behavior suggests a more complex correlation between flow of the castables and the rheology of its binding system. Due to the strong variation of viscosity with

the concentration of dispersants most of the experimental compositions based on SF2 had no self flow behavior, but for compositions based on SF1 flow measurements were performed for different concentration of plasticizer admixture.
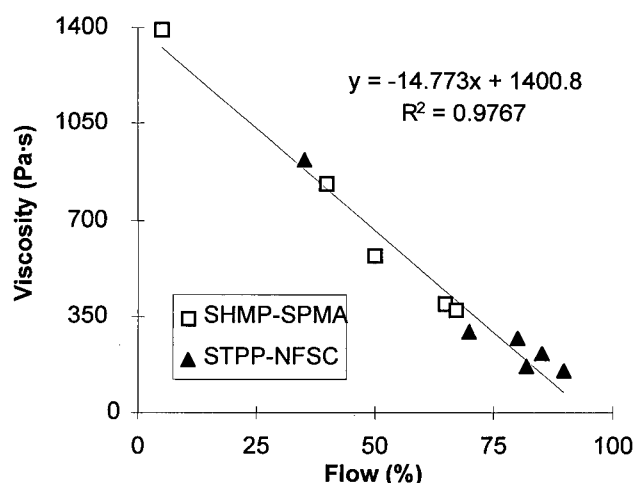
Figure 4.2-55. Correlation between the flow of ULCC and the viscosity (at shear rate of 0.1955 s^{-1}) of BS based on SF1 and dispersed with SHMP-SPMA and STPP-NSFC admixtures at 4.5% water

It was found that the flow correlates well with viscosity of the BS, regardless of the differences in the composition of dispersant admixture (Figure 4.2-55.). This type of correlation suggests that both viscosity of the BS and flow of the castable are controlled by the same factor that is embedded in the shear rate-shear stress dependence of these systems. The effect of water on the flow cannot be directly determined by measurements of viscosity of binding systems, as the variation of viscosity (and yield stress) with water content is nonlinear.

For data presented in Figure 4.2-55 the admixture systems that result in a viscosity higher than 1400 Pa·s cannot be evaluated by flow measurements. Viscosity measurements, with a proper apparatus setting, can be done well beyond that limit (in this case of up to 12000 Pa·s). This is why the study of viscosity of binding systems may prove useful. However, measurements of viscosity of BS cannot be a substitute of flow measurements due to the

complexity of involved factors (i.e. maximum particle size, particle size distribution, porosity and water absorption of different aggregate fractions). Viscosity data for BS constitute a complementary instrument for the design and optimization of self-flowing castables.

4.2.2.4. Self-flowing compositions for industrial applications

From the experiments performed during this stage of research it is concluded that the flow behavior is determined by a complex system of interacting parameters. Due to the multiple variables involved it was not possible to define a clear optimum for the design, but rather a group of castable compositions that can satisfy a certain range of design criteria. Additional

Table 4.2-5. ULCC compositions for q=0.24.

Component (wt%)	Mulcoa 47 aggregate	Mulcoa 60 aggregate	Mulcoa 70 aggregate	Mulcoa 90 aggregate
-4+8 mesh	18	18	18	19
-8+20 mesh	24	25	25	26
-35 mesh	15	15	15	16
Mulcoa 90 -100mesh	18	18	18	16
Kyanite -325 mesh	8	8	7	7
Calcined alumina (d_{av} =5μm)	4	4	5	5
CAC (70% Al_2O_3)	2	2	2	2
SF	11	10	10	9
STPP	0.11	0.1	0.1	0.09
NFSC	0.0132	0.012	0.012	0.0108
NAI	0.02	0.02	0.02	0.02

Table 4.2-6. ULCC composition for q=0.26.

Component (wt%)	Mulcoa 47 aggregate	Mulcoa 60 aggregate	Mulcoa 70 aggregate	Mulcoa 90 aggregate
-4+8 mesh	19	19	20	20
-8+20 mesh	25	26	26	28
-35 mesh	14.5	15	15	16
Mulcoa 90 -100mesh	17.5	17	16.5	15
Kyanite -325 mesh	9	8.5	8	7
Calcined alumina (d_{av} =5μm)	5	4.5	4.5	5
CAC (70% Al_2O_3)	2	2	2	2
SF	8	8	8	7
STPP	0.08	0.08	0.08	0.07
NFSC	0.0096	0.0096	0.0096	0.0084
NAI	0.02	0.02	0.02	0.02

148

constraints related to the desired thermomechanical behavior, ceramic structure, and compositional characteristics necessary to achieve corrosion resistance properties are also imposed, not considering the constraints related to the cost of different components. Therefore, in order to design a set of optimum castable compositions, it is rather important to define the dependencies in the system, that would allow for optimum results in any given set of requirements.

Based on the knowledge accumulated during this stage of research, a set of self-flowing castable compositions are recommended (Tables 4.2-5 - 4.2-8).

Table 4.2-7. LCC compositions for q=0.26.

Component (wt%)	Mulcoa 47 aggregate	Mulcoa 60 aggregate	Mulcoa 70 aggregate	Mulcoa 90 aggregate
-4+8 mesh	15	16	16.5	17
-8+20 mesh	23	24	24	26
-35 mesh	15	15	15	16
Mulcoa 90 -100mesh	18.5	18	17.5	15
Kyanite -325 mesh	8.5	8	7	6
Calcined alumina (d_{av} =5μm)	8	8	9	9
CAC (70% Al_2O_2)	4	4	4	4
SF	8	8	8	7
STPP	0.08	0.08	0.08	0.07
NFSC	0.04	0.0096	0.0096	0.0084

Table 4.2-8. NCC compositions for q=0.22.

Component (wt%)	Tabular alumina	Calcined bauxite	SiC
-1/4+8mesh	16	16	16
-8+14 mesh	20	19.5	19
-14+28 mesh	7	7	7
-28 mesh	15	14.5	14.5
Tabular alumina -100mesh	18	18.5	19
Tabular alumina -325mesh	8	8.5	8.5
Calcined alumina (d_{av} =5μm)	4	4	4
HAB (Alphabond 200)	1.75	1.75	1.75
CAC (Secar 71)	0.25	0.25	0.25
SF	10	10	10
STPP	0.1	0.1	0.1
NSFC	0.012	0.012	0.012
NAI	0.02	0.02	0.02

4.3. Mechanical properties

The formation of the ceramic matrix in self-flowing castables was studied by measurements of mechanical properties on specimens fired at relatively low temperatures (110-1370°C) when the hydraulic matrix is destroyed by the dehydration reactions, and the components of the stable ceramic matrix are not yet formed [12].

According to the phase diagram in the $CaO-SiO_2-Al_2O_3$ system for compositions containing less than 10% CaO, the lowest invariant point is the peritectic at 1345°C, which is surrounded by crystallization fields of mullite, anorthite, and tridymite (Figure 2.4-8). While the hydraulic matrix disappears at temperatures above 750°C (when decomposition of hydrated phases of CAC is complete [117]), the new crystalline ceramic structures do not form up to 1345°C.

The experiments presented in this section were focused on studying the transition from a hydraulic to a ceramic matrix for the self-flowing castables in the $CaO-SiO_2-Al_2O_3$ system.

The specimens subjected to mechanical testing were prepared in the self-flow range (50-140% flow) and molded by casting. Only SF1 and SF3 silica fume were used in our experiments, the SF2 being eliminated due to quality inconsistency. The experimental castable compositions were the ULCC based on Mulcoa 60 refractory aggregate (Table 4.2-5) and NCC based on tabular alumina aggregate (Table 4.2-8).

4.3.1. CCS and MOR

As shown in Figure 4.3-1, the CCS after drying and up to 540°C has no important variation with temperature. There is a small variation of CCS with water content, which can be

attributed to a small increase in porosity and to the negative effect of the water increase on the mechanical strength of the hydraulic matrix. After firing at 816°C, at water contents below 4.75%, there is an increase in CCS. In fact, for both compositions, a small increase in CCS can be detected even after firing at 540°C, for water contents below 4.75%. After firing at 1093°C, there is an important increase in strength for both compositions that results in CCS values of 53-67 MPa. The strength increase in the range of 816-1093°C depends on the water content,

a)   b)
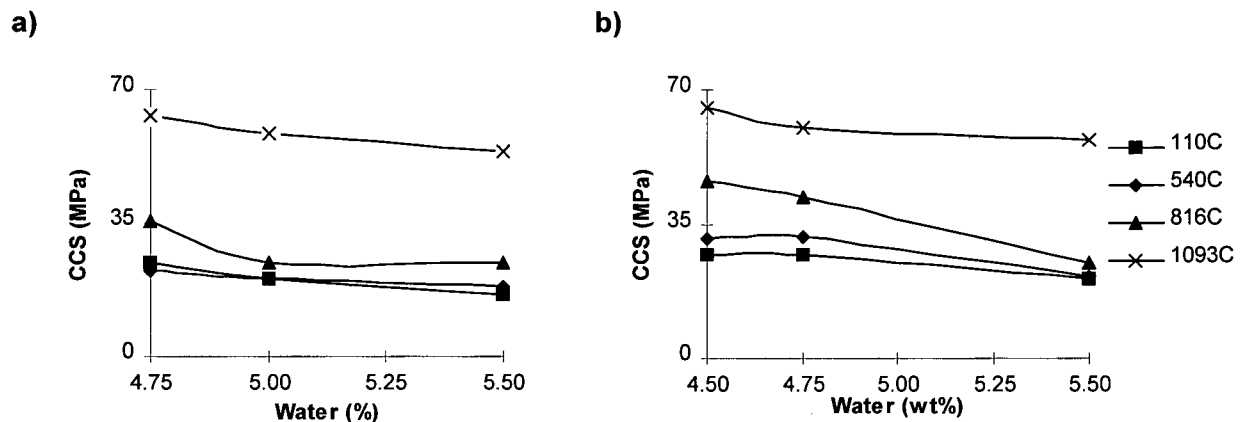
Figure 4.3-1. Variation of CCS with water content for ULCC based on: a) SF3 and b) SF1, after drying and firing at different temperatures.

being more significant at low water content.

Taking into account that the hydraulic matrix of ULCC undergoes a thermal decomposition at temperatures up to 750°C, the CCS increase, that can be detected for firing temperatures as low as 540°C, can be attributed only to an early development of the ceramic matrix. Moreover the influence of water content on the strength increase cannot be explained by the differences in homogeneity of the specimens, because both compositions were molded at similar flow values (compare with Figure 4.3-2).

If the flow is considered a measure of the amount of physical water existent in the binding system, the linear decrease of CCS obtained after firing at 1093°C can be considered a result of the increased interparticle distances. The CCS increase in the temperature range of 540-816°C cannot be explained by the effect of the smaller interparticle distances, because in this temperature range the two ULCC compositions have a different pattern of variation of CCS with the flow.
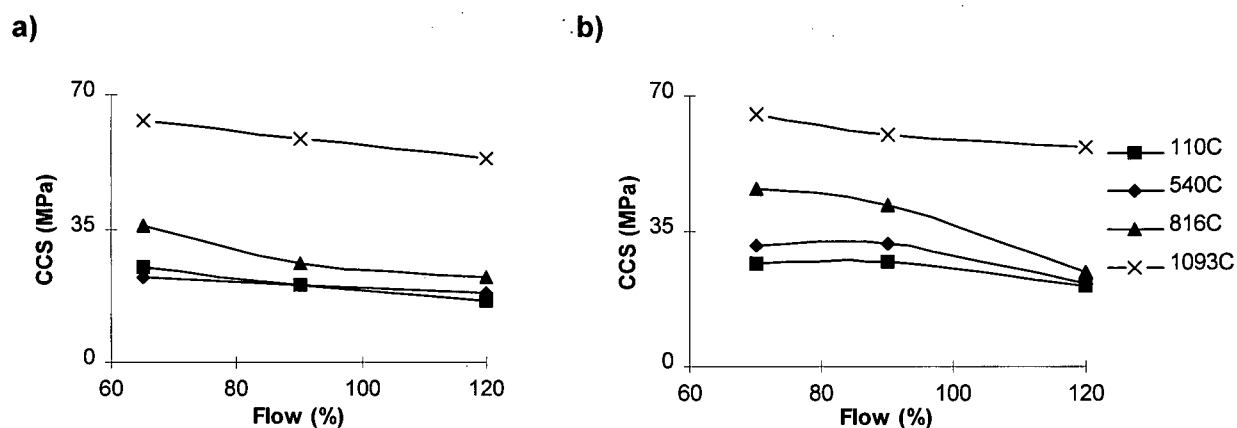
Figure 4.3-2. Variation of CCS with flow for ULCC based on: a) SF3 and b) SF1, after drying and firing at different temperatures.

In the case of NCC compositions the main hydraulic phase is HAB and the product of hydration consists of a mixture of bayerite and bohemite gel. The presence of aluminum hydroxide phases in NCC results in lower mechanical strength of the hydraulic matrix if compared to ULCC. Also, due to the fact that the hydraulic matrix generated by HAB is completely decomposed at 550°C, above this temperature the mechanical strength may be attributed only to the formation of a new bond of ceramic nature.

As it results from Figure 4.3-3 the CCS of specimens fired at 540°C is lower than that of dried samples where the mechanical strength is provided by the hydraulic bond. An exception is

presented by NCC compositions based on SF1 prepared at 4.25% water where the CCS after firing at 540°C equals the CCS after drying.

For NCC based on SF3 only after firing at 816°C the CCS equals that of the dried samples. For both compositions, the fastest CCS (by almost six times) increase is found in the range of 816-1093°C, for any water level that was employed. This strength increase represents evidence that the formation of the ceramic matrix in NCC starts at temperatures below 1093°C. For NCC based on SF1, at low water levels (<4.5%) the formation of the ceramic matrix starts below 816°C. It is difficult to sustain this hypothesis by other techniques (SEM, XRD) as any new phases are still amorphous.
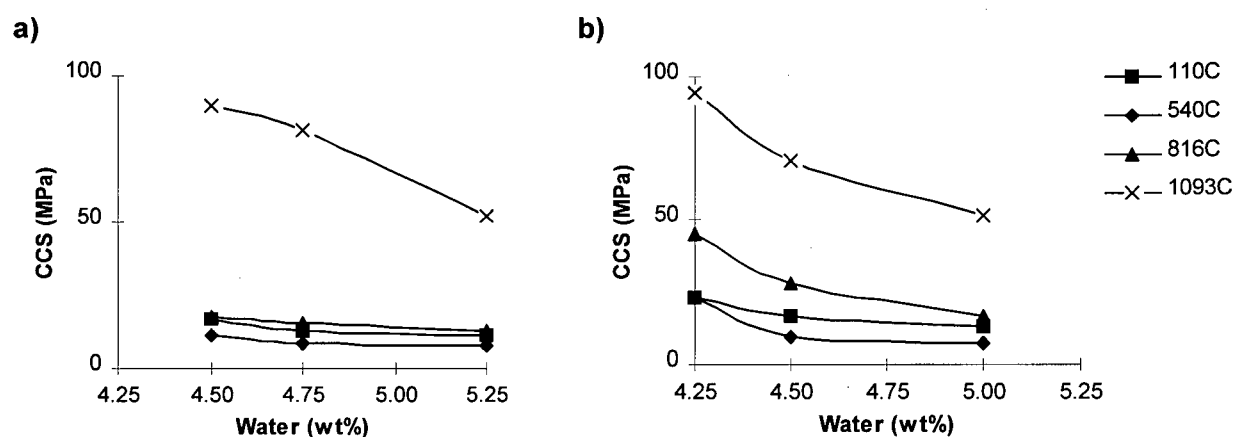
Figure 4.3-3. Variation of CCS with water content for NCC based on: a) SF3 and b) SF1, after drying and firing at different temperatures.

If the CCS is analyzed as a function of flow (Figure 4.3-4), for NCC compositions based on SF1, there is a linear correlation between flow and CCS after firing at 816°C and 1093°C. For compositions based on SF3 the linear correlation exists only at 1093°C.
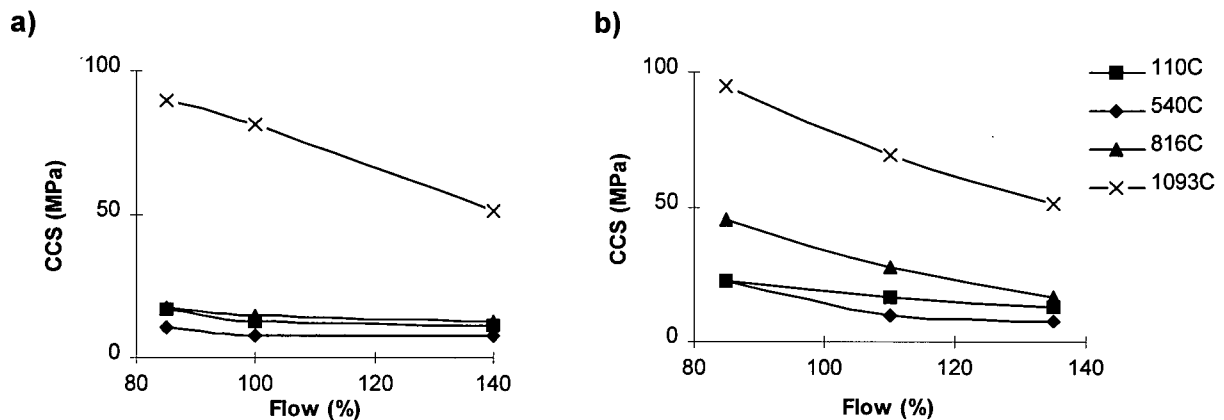
Figure 4.3-4. Variation of CCS with flow for a NCC based on: a) SF3 and b) SF1after drying
and firing at different temperatures.

From the above data experimental observations may be outlined:

- for all experimental compositions fired at 1093°C there is a linear decrease of CCS with flow;

- no direct correlation can be established between CCS and water content after drying or firing at temperatures up to 540°C;

- the quality of silica fume is not only essential in obtaining high CCS after firing at high temperatures, but also is a key factor in determining early development of the ceramic bond;

- low water contents have a positive influence on CCS of NCC and ULCC by promoting an early development of the new ceramic bond and by minimizing the decrease in strength produced by the decomposition of hydrated phases.

It may be further concluded that, for firing temperatures up to 1093°C, the CCS of self flowing castables is determined by two superimposing opposite trends:

154

- a strength decrease generated by the thermal decomposition of the hydraulic matrix;

- a strength increase generated by the early development of the ceramic matrix.
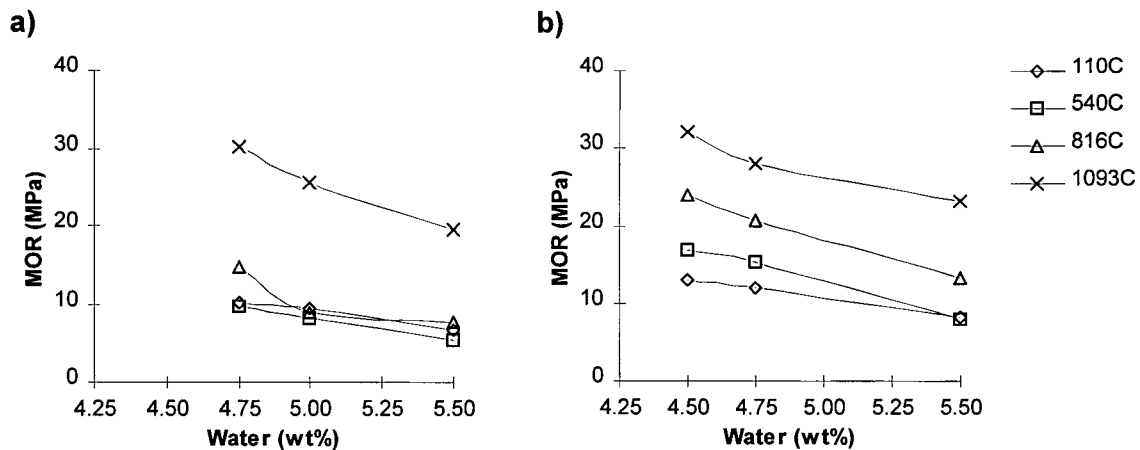
Figure 4.3-5. Variation of MOR with water content for ULCC based on: a) SF3 and b) SF1, after drying and firing at different temperatures.

The variation of MOR of ULCC with water content (Figure 4.3-5) demonstrates that after firing at 816°C, the ULCC compositions based on SF3 at water levels below 4.75%, show a significant increase in MOR. For ULCC compositions based on SF1 the MOR increase is clearly detectable already after firing at 540°. After firing at 816°C all ULCC based on SF1 have almost double increase in MOR, compared to the level obtained after drying.

For ULCC based on SF3, fired at 540°C, a decrease in MOR takes place for all water levels employed, if compared to the MOR of dried specimens. This decrease in MOR is attributed to the decomposition of CAC hydration products.
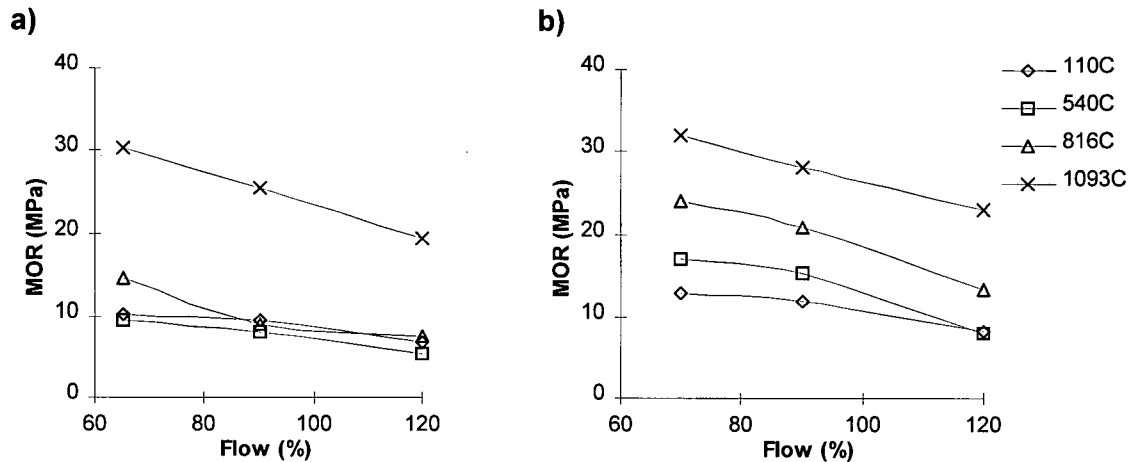
Figure 4.3-6. Variation of MOR with water content for ULCC based on: a) SF3 and b) SF1, after drying and firing at different temperatures.

For ULCC compositions after firing at 1093°C, there is a linear correlation between flow and MOR (Figure 4.3-6). This behavior is consistent to the fact that the strength of the ceramic bond depends on the interparticle distances. For ULCC based on SF1, the linear correlation exists also after firing at 816°C indicating that.

Analysis of the variation of MOR with temperature for the experimental self-flowing ULCC compositions (Figure 4.3-7) reveals that the purity of silica fume is the determining factor the early development of ceramic bond. Low water levels are also necessary for strength development below 540°C. Although both ULCC compositions, fired at 1093°C, show an increase of MOR from 6-12 MPa to 30-32 MPa, for specimens containing SF1, there is a constant increase in strength above 540°C. For the specimens containing SF3, the high values of MOR are achieved only at temperatures above 816°C, and initially decrease in strength is observed (especially for high flow).
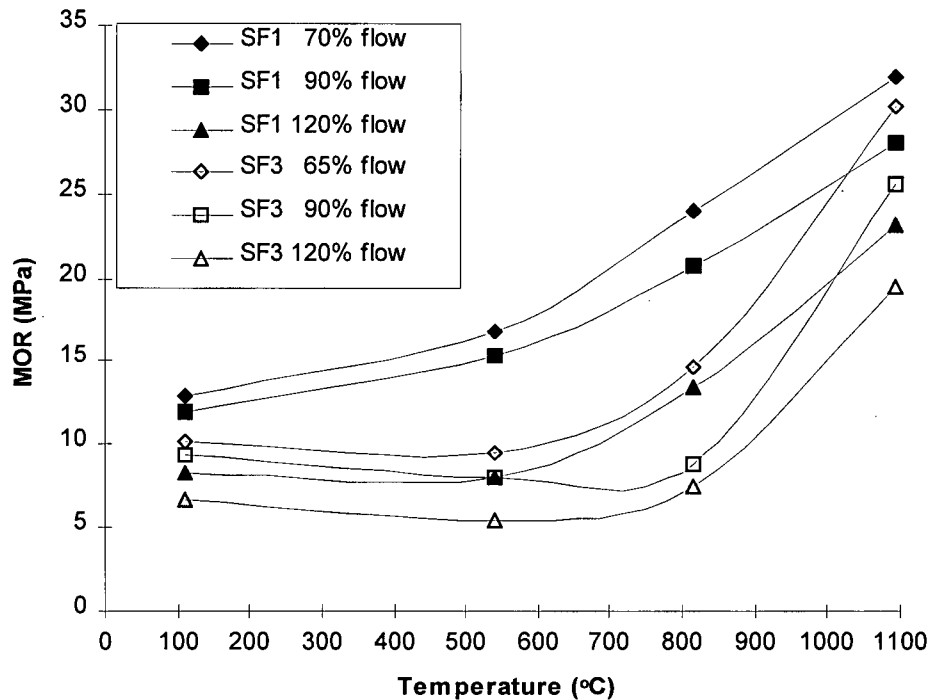
Figure 4.3-7. Variation of MOR with temperature, for self-flowing ULCC for different flow and different type of silica fume.

For NCC compositions, the variation of MOR with water and flow (Figures 4.3-9 and 4.3-10) shows a pattern consistent with the CCS data, characterized by the following:

• low MOR (6-8MPa) after drying, due to a weak hydraulic bond;

• a decrease in strength after firing at 540°C, due to decomposition of aluminum hydroxide phases;

• a significant increase in strength in the range of 816-1093°C that leads to MOR values up to 38MPa.

157
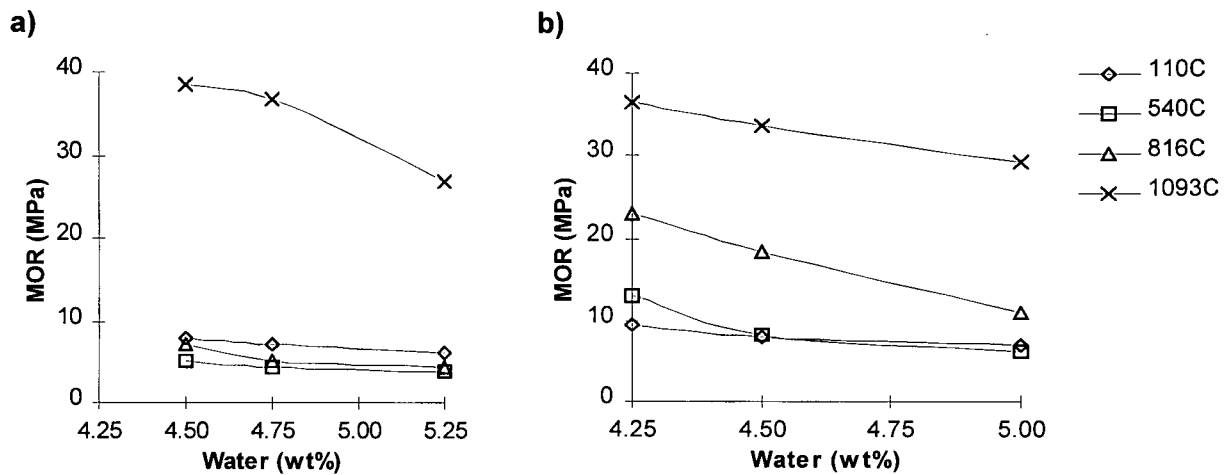
Figure 4.3-8. Variation of MOR with water content for NCC based on: a) SF3 and b) SF1, after drying and firing at different temperatures.
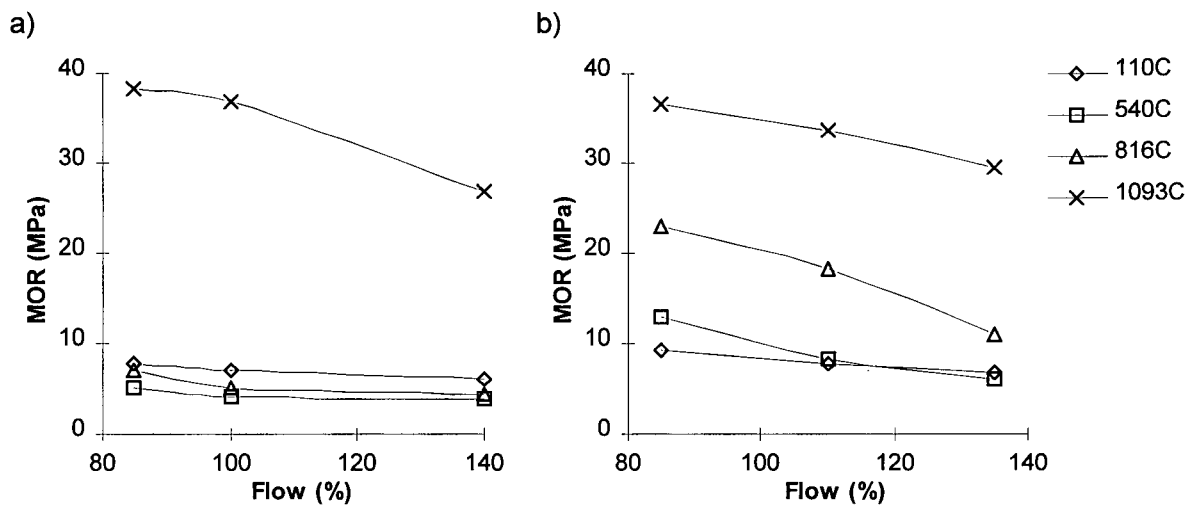

Figure 4.3-9. Variation of MOR with flow content for NCC based on: a) SF3 and b) SF1, after drying and firing at different temperatures

For both NCC compositions, there is a linear correlation between MOR and flow after firing at 1093°C. For NCC based on SF1 the linear correlation also exists after firing at 816°C.

Analysis of the variation of MOR with temperature for the experimental self-flowing NCC compositions (Figure 4.3-10), demonstrates that all the compositions based on SF3 experience a loss of MOR in the temperature range of 110-800°C. For firing temperatures around 700°C, there is a minimum of MOR regardless the flow value. Above 800°C there is a sudden increase in MOR which at 1093°C may be even higher than that of NCC based on SF1 at similar flow. However all the NCC based on SF1 have a continuous increase in MOR in the range of 540-1093°C and the effect of the high water contents in delaying the strength development plays a secondary role.
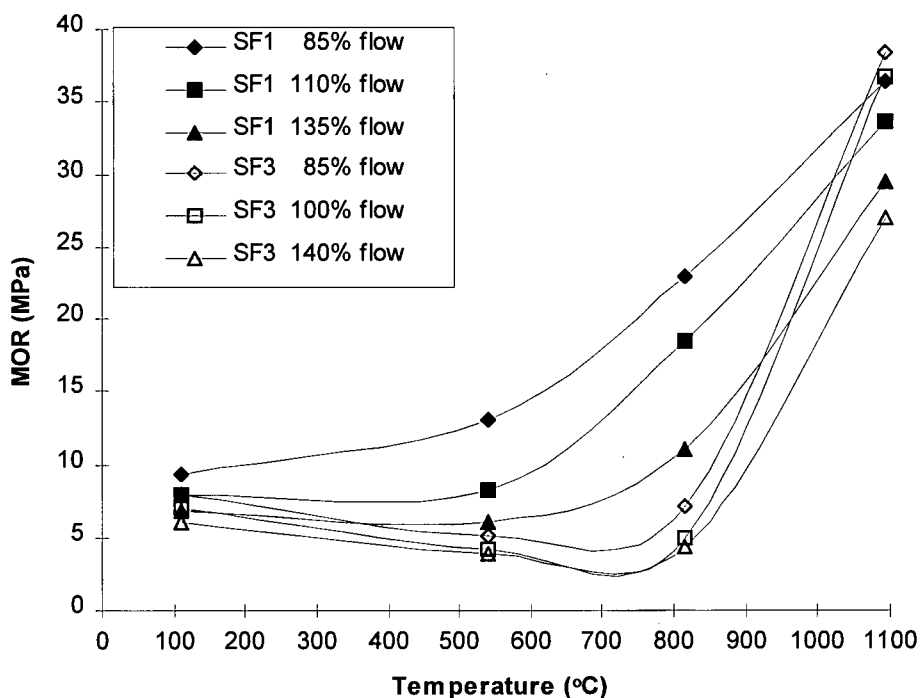
Figure 4.3-10. Variation of MOR with temperature, for self-flowing NCC for different flow and types of silica fume.

4.3.2. Correlation of MOR with open porosity

While the decomposition of hydraulic phases (including calcium aluminate hydrates, calcium alumino-silicate hydrates and aluminum hydroxide) implies an increase in open porosity, the possible formation of a liquid phase during sintering implies a decrease in open porosity. For ULCC based on SF3 the variation of MOR with open porosity (Figure 4.3-11 a) shows that, after firing at 540°C, the decrease in MOR is due to an increase in open porosity, as a result of decomposition of the hydraulic bond. At 816°C, for specimens with low water content, there is a noticeable increase in MOR, which cannot be justified by the decrease in open porosity. For firing temperatures above 540°C, the decrease in porosity of ULCC based on SF1 (4.3-11 b) takes place simultaneously with an increase in MOR, but no direct correlation may be established between the two properties. It may be concluded that for both ULCC compositions, the variation of MOR with the firing temperature is not determined by variations of the open porosity.

a)   b)
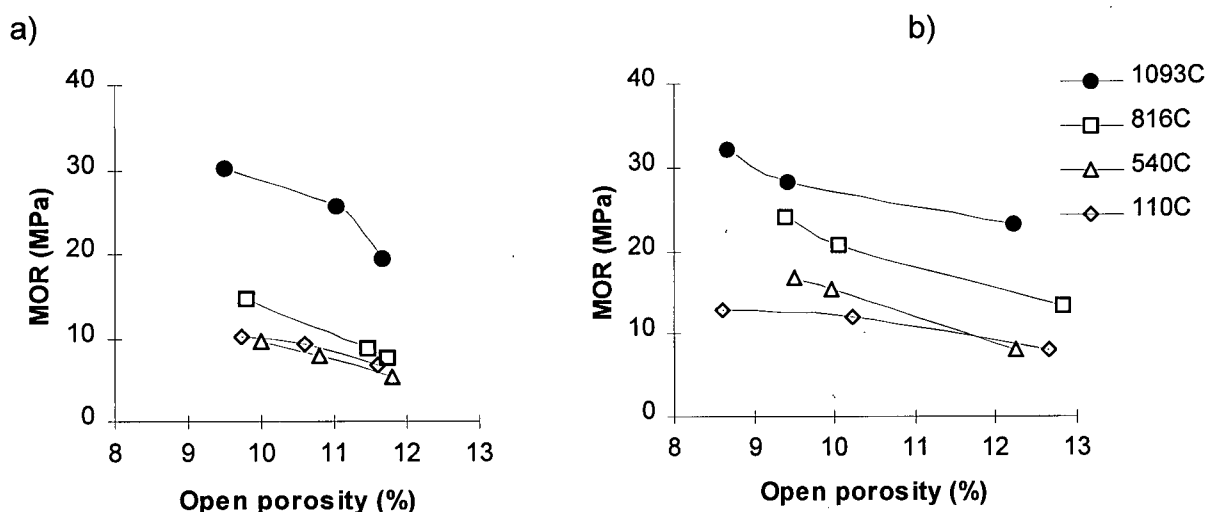
Figure 4.3-11. Variation of MOR with open porosity for a ULCC based on: a) SF3 and b) SF1 for different firing temperatures.
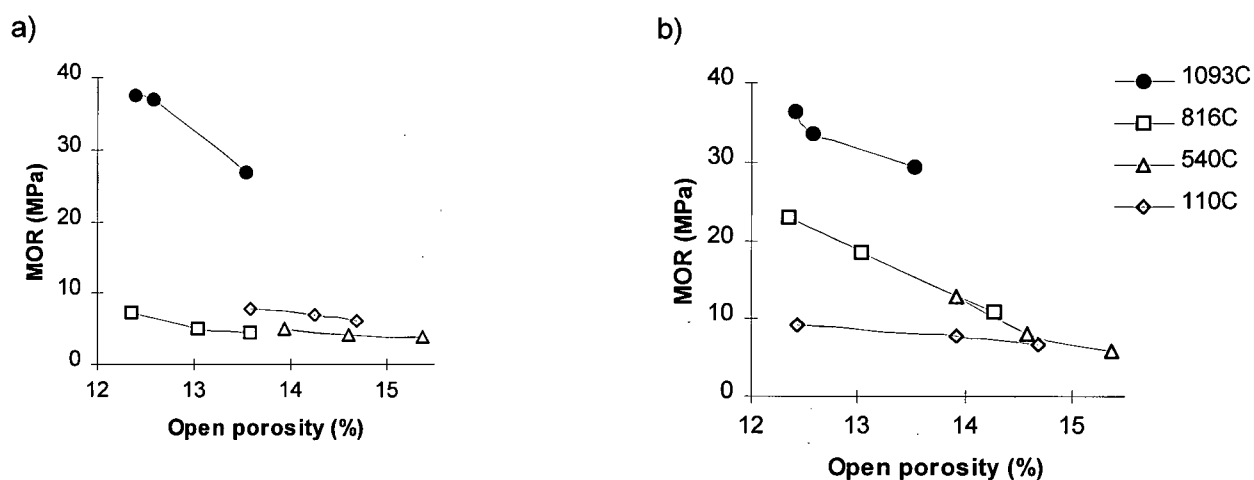
Figure 4.3-12. Correlation MOR-open porosity for a NCC based on: a) SF3 and b) SF1 for different firing temperatures.

The pattern of variation of MOR with open porosity for NCC (Figure 4.3-12) is similar to that of ULCC, but the effects induced by the purity of silica fume are more significant. For NCC based on SF3 the decrease or increase in open porosity in the 110-816°C range takes place without significant changes in MOR, while the increase in MOR above 816°C takes place with no significant change in open porosity. For NCC based on SF1 a direct correlation between MOR and open porosity may be assumed only in the 540-816°C range.

The study of the variation of MOR and open porosity of ULCC and NCC, at different temperatures, showed that the early development of the ceramic matrix in self-flowing castables is determined primarily by the purity of silica fume and secondary by the water contents and the type of the hydraulic binder. Also, as resulted from the experimental data, it is unlikely that the formation of the ceramic matrix, at temperatures below 1093°C, is triggered by the formation of a liquid phase. The following reasons should be considered:

- the decrease in porosity occurs especially at temperatures below 816°C when the formation of a liquid phase in $CaO-Al_2O_3-SiO_2$ system is not expected;

- the important increase of MOR in the 816-1093°C temperature range takes place without a significant decrease in open porosity.

4.3.3. HMOR

The HMOR of a refractory castable is a measure of the development of ceramic microstructure at equilibrium. For castables in the $CaO-SiO_2-Al_2O_3$ system this equilibrium is reached at temperatures above 1345°C through liquid assisted diffusion processes [129-130]. The low HMOR, combined with a "soft fracture", that is often observed in the first heat-up of castables in $CaO-SiO_2-Al_2O_3$ system at temperatures around 1300°C, has not been yet satisfactorily explained and it has been attributed to a "metastable liquid formation" [138].
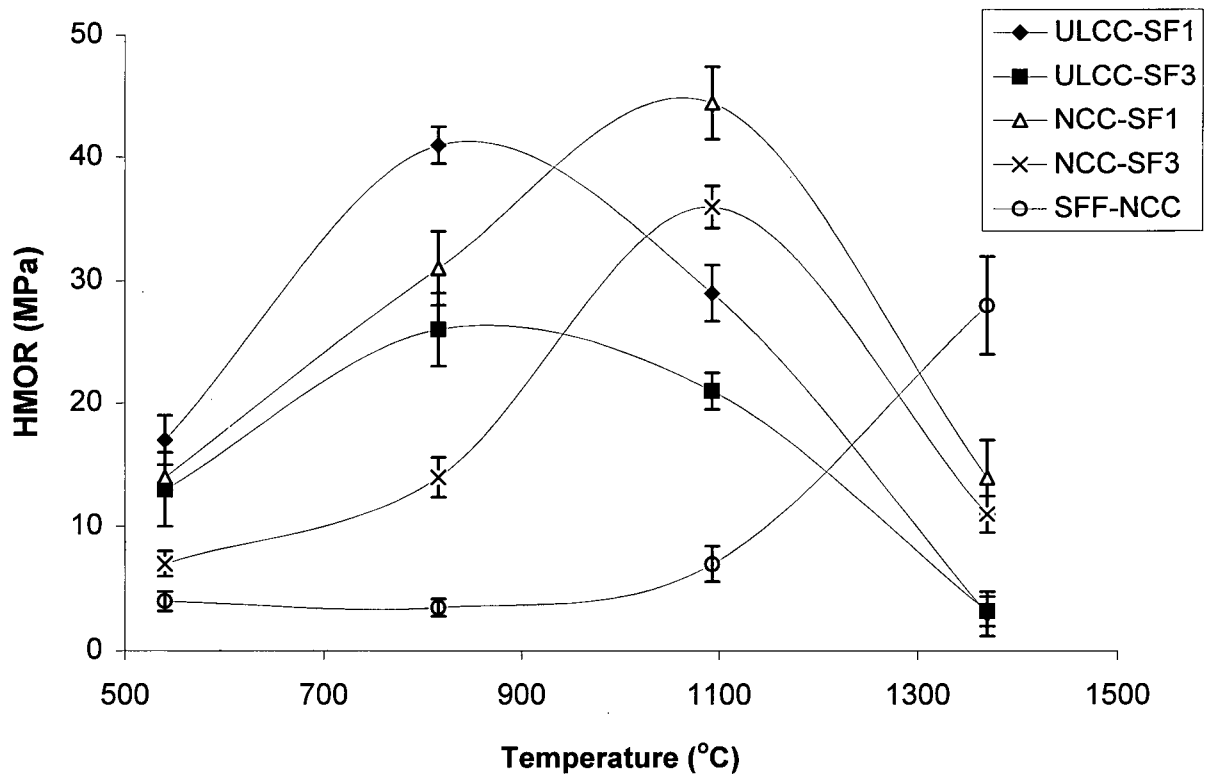
Figure 4.3-13. Variation of HMOR with temperature for LCC ULCC compositions based on SF1 and SF3, and for silica fume free NCC (SFF-NCC) at 80% flow.

As presented in Figure 4.3-13, the HMOR values at 540°C, for all experimental compositions, are in accordance with the corresponding MOR values. For both ULCC and

NCC, the HMOR at 1370°C does not depend on the type of silica fume and it is a result of the chemical composition of the castable. This demonstrates that at 1370°C, in both ULCC and NCC compositions, the amount of liquid phase is determined by their position in the CaO-SiO$_2$-Al$_2$O$_3$ system. The most important feature is given by the evolution of HMOR in the range of 540-1370°C. The HMOR values for specimens prepared with high purity silica fume SF1 are, at any temperature, higher than those containing SF3.

Regardless of the type of silica fume, the ULCC compositions have a maximum HMOR around 850°C (20-30MPa). At 1093°C a decrease in HMOR by 24-33% occurs, and at 1370°C HMOR further decreases to 2.2-2.6 MPa. As previously shown, for low flow and water levels, the transformation of the bond starts below 816°C and, according to HMOR data, the presence of the liquid phases at those temperatures is highly improbable. It is difficult to believe that the level of water for casting may influence the formation of any "metastable liquid" at temperatures above 800°C.

For self-flowing NCC, regardless of the type of silica fume, there is a continuous increase of HMOR in the range of 540-1093°C. It is not possible to attribute the strength increase of the NCC compositions based on SF1 to the formation of low melting point, rich in calcia liquids, at temperatures below 816°C. Even for NCC compositions based on a low purity silica fume (SF3), the sudden transformation of the matrix in the range of 850-1100°C may not be attributed to the formation of large amounts of a "metastable liquid" in the binding system.

For silica fume free no cement castable (SFF-NCC) compositions there is no significant strength development up to 816°C. Due to their high purity (99 % Al$_2$O$_3$), there is no liquid phase formation at temperatures below 1500°C and this is reflected in the increase in HMOR only above 1093°C. Although NCC and SFF-NCC have the same type of refractory aggregate and the same type of hydraulic binder (HAB), their behavior with regard the early strength

development is completely different. It results that the early strength development in any self-flowing castable is a direct consequence of the presence of silica fume.

These results lead to the following conclusions:

- a ceramic bond forms in the binding system of castables containing silica fume, at temperatures below the formation of liquid phases;

- the formation of the ceramic bond in the binding systems of self flowing castables depends also on the nature of the hydraulic binder and water contents;

- in favorable conditions (high reactivity silica fume, and low water contents) the ceramic bond may be formed well before the total decomposition of the hydraulic bond takes place;

- the early formation of the new ceramic bond is not triggered by the formation of a liquid phase.

The fact that the ceramic bond may be formed at temperatures below 540°C, before the complete thermal decomposition of the hydraulic bond, and well below the formation of liquid phases (1170°C, in CaO-SiO_2-Al_2O_3 system), raises questions on the exact nature of this ceramic bond and the characteristics of the sintering process occurring in the binding system of a self-flowing castable. It was therefore necessary to study the evolution of the microstructure of the binding system and to obtain additional information on the process of formation of this non-equilibrium ceramic bond.

4.4. Microstructure

For a better understanding of the initial stages of formation of the ceramic bond in self-flowing castable refractories, it is necessary to correlate the evolution of the thermomechanical properties of the castables with the microstructural evolution of the binding system.

The binding system of self-flowing castables contains fine ceramic reactive components that interact during the hydraulic setting and the first firing. Due to insufficient and sometimes contradictory literature data regarding the microstructural changes occurring at temperatures below 1345°C it was necessary to investigate the microstructural changes of individual components of the binding system. The fracture surfaces of castable specimens subjected to HMOR testing at different temperatures were analyzed by SEM and the chemical composition of specific fields was determined by EDS.

4.4.1. Microstructure of binding system components

The most important component of the binding system of self-flowing castable refractories is silica fume. SEM analysis shows that SF1 is composed of spherical particles having a diameter in the range of 0.05-1μm with no impurity inclusions (Figure 4.4-1 a) with a chemical composition, determined by EDS of more than 98% SiO_2. X-ray diffraction shows that SF1 is completely amorphous.

SF2 is composed of spherical particles of 0.1-0.5μm diameter (Figure 4.4-1 b). The average chemical composition is 94-95% SiO_2 2-2.5% Na_2O, 1-1.5% K_2O 1.2-1.8% CaO, 0.8-1,6% FeO. A characteristic of SF2 is that filamentary impurities are present. Also there are present agglomerates of particles formed by coalescence of fine (0.5-1μm) particles around larger particles (Figure 4.4-2).
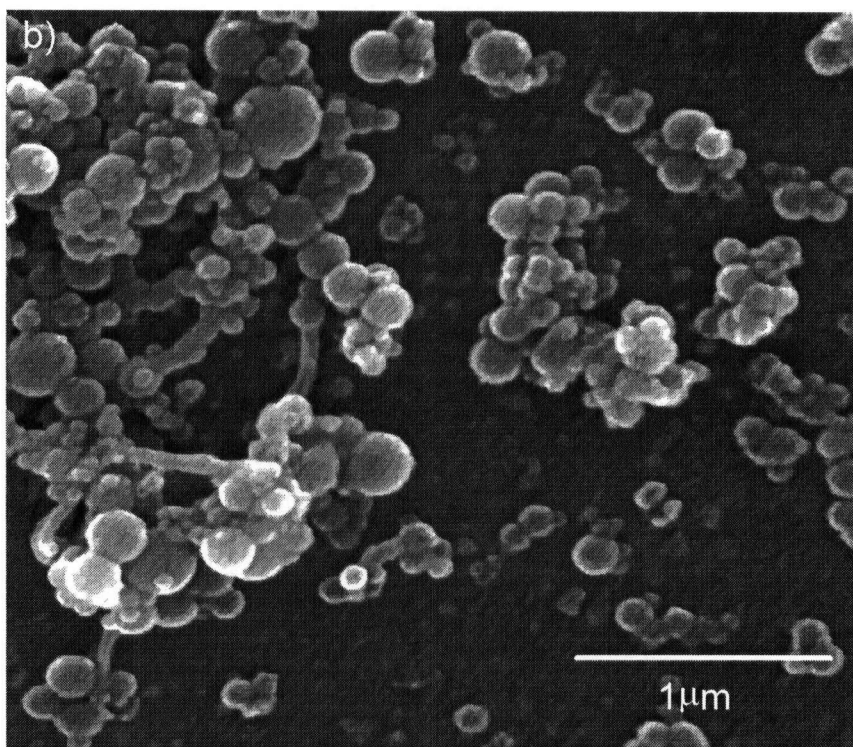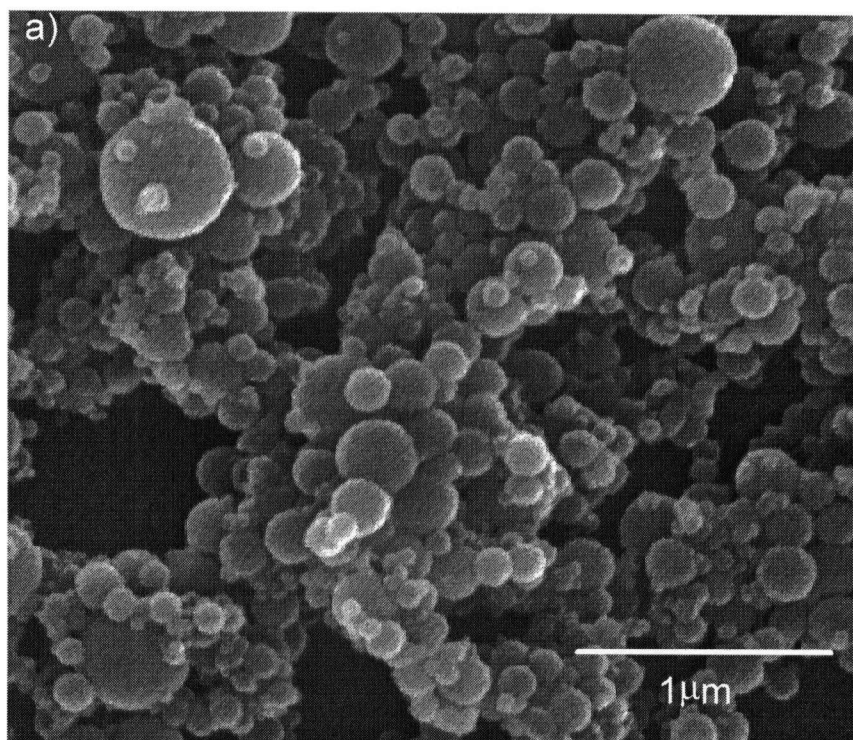
Figure 4.4-1. SEM of: a) SF1 and b) SF2.
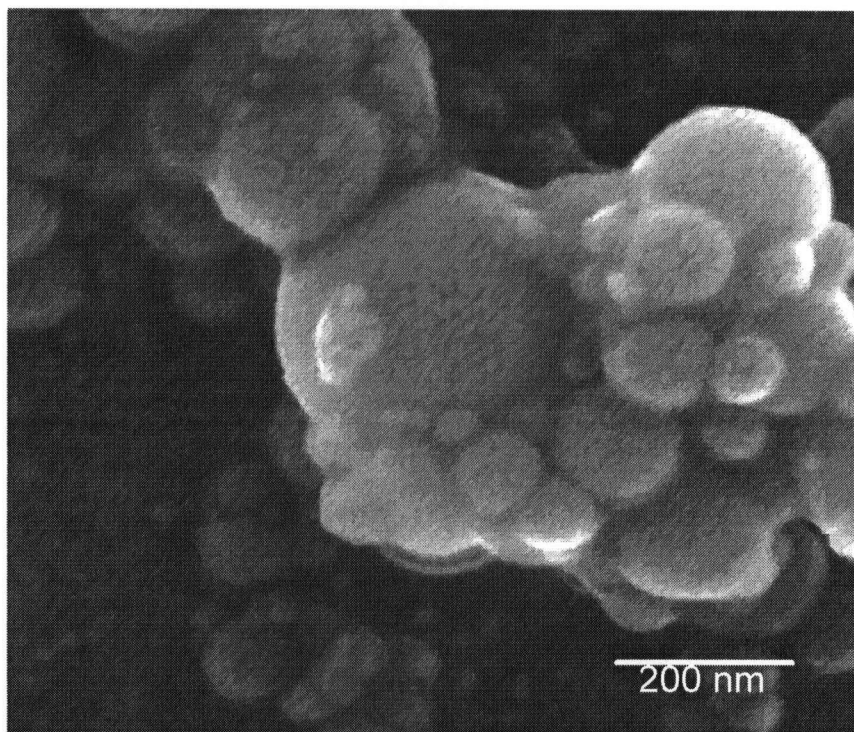
Figure 4.4-2. Agglomeration of SF2 particles.

The filamentary regions and coalescent regions have a low concentration of SiO_2 (84-89%) and high concentration of impurities, especially iron and alkali (8-10% Na_2O+K_2O and 4-6% FeO). The X-ray diffraction of SF2 shows that traces of quartz are present.

Silica fume SF3 consist of a mixture of high purity (99.5%) amorphous SiO_2 spheres having the diameter in the range of 0.1-0.005μm and some large diameter (5-40μm) spheres containing 20-40% ZrO_2 5-12 Al_2O_3 and 50-65% SiO_2. Even in the case of the large impure spheres of SF3 the cumulative content of alkali and iron oxide is below 1%. Silica fume SF3 does not contain any filamentary impurities or agglomerations.

The two components of SF3 were separated by sedimentation and by X-ray diffraction analysis it was found that the fine spheres of SF3 are completely amorphous, while the large spheres contain only traces of quartz and no other crystalline compound in the system SiO_2-Al_2O_3-ZrO_2.

With the exception of HAB (Alphabond) all the other components (CAC, calcined alumina and kyanite) of the experimental binding systems have a homogeneous chemical composition and are well crystallized. Calcined alumina AC 34 B4 is composed of 1-20μm corundum platelets with an average diameter of 5μm. CAC Secar 71 consist in particles of monocalcium aluminate (with traces of dicalcium aluminate) having the average diameter of 5μm. Raw kyanite consists of prismatic particles having particle sizes in the range of 5-50μm. Alphabond consists of completely amorphous non-spherical particles having a particle size below 1μm.

4.4.2. Microstructure of binding systems

Specimens were prepared by casting concentrated pastes of binding system with chemical admixtures and water levels similar to those of the corresponding castables. After drying the specimens were fired at temperatures up to 1100°C. The fracture surface of the specimens fractured at room temperatures was then analyzed by SEM.

The microstructure of the fracture surfaces of ULCC and NCC binding systems fired at 540°C, is represented only by silica fume agglomerate as shown in Figure 4.4-3 for an ULCC BS based on SF1. At this temperature regardless of the grade of silica fume and the nature of hydraulic binder that is used, the weakest bond in the system is in between the silica fume particles.
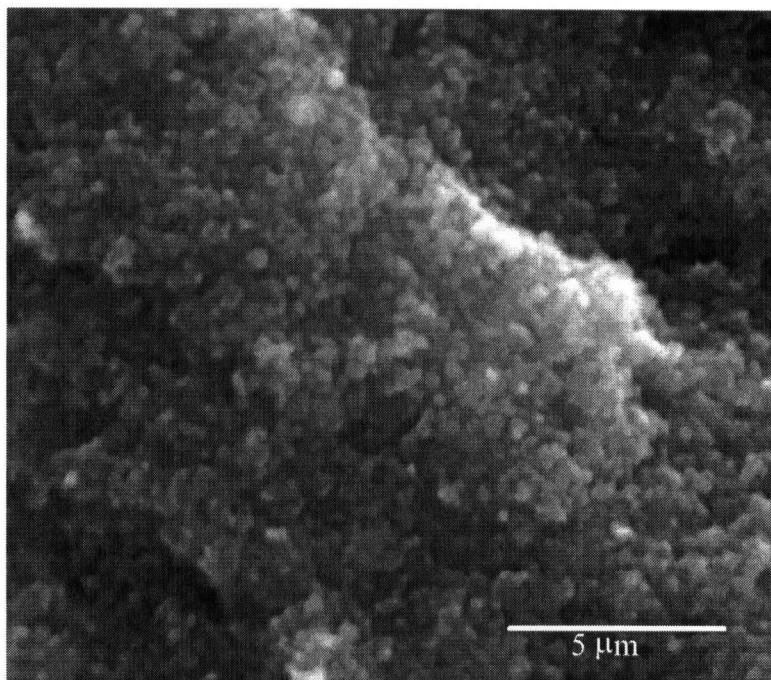
Figure 4.4-3. Microstructure of the fracture surface of a ULCC BS based on SF1.

The microstructure of BS specimens of ULCC based on SF3 after firing at 816°C shows that the fracture evolves through the silica fume matrix. There are also present interfaces between the silica fume matrix and the kyanite grains (Figure 4.4-4). The fracture at the interface of kyanite with silica fume particles is considered to be the result of the thermal expansion mismatch combined with a weak adhesion at the interface.

The presence of the interface between silica fume matrix and kyanite at the fracture surface of BS of ULCC based on SF1 after firing at 816°C is less visible than for the specimens based on SF3. A characteristic of the microstructure is the presence of zones with a molten or glassy appearance having a porous structure (Figure 4.4-5), and a chemical composition determined by EDS in the range of 20-35% SiO_2, 1.2-2.3% Na_2O, 2.1-3.6% P_2O_5, 17- 23% CaO, 39-54% Al_2O_3. Even if the composition of these molten zones is not constant, their ratio $CaO:Al_2O_3$ is in the range of 0.38-0.4 which corresponds to the $CaO:Al_2O_3$ ratio existing in CAC.
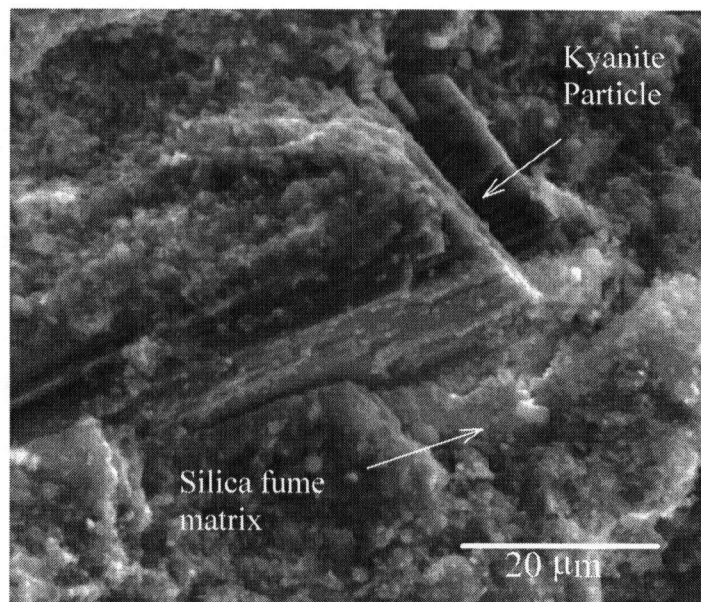
Figure 4.4-4. Fracture surface of a ULCC BS based on SF3 after firing at 816°C.
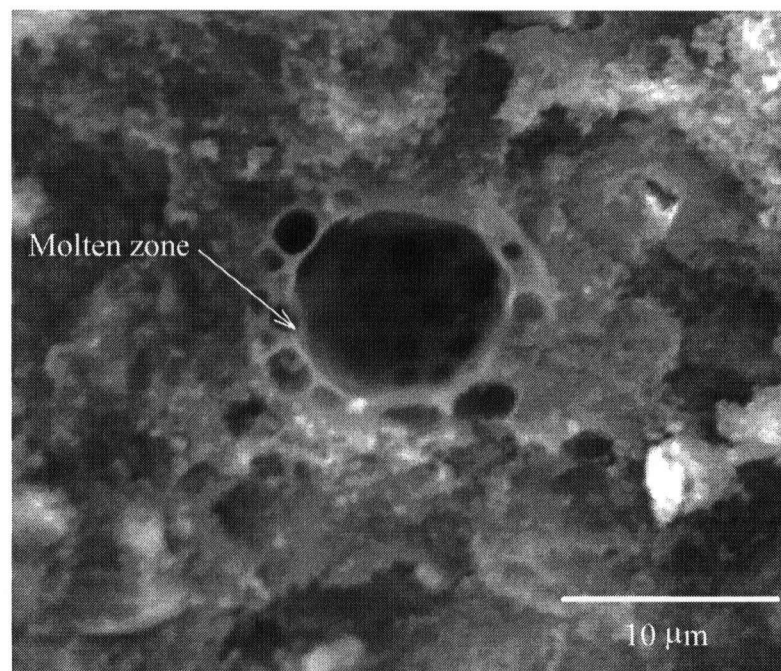
Figure 4.4-5. Fracture surface of a ULCC BS based on SF1 after firing at 816°C.

Taking into account that during initial hydration of the high silica fume:CAC ratio mixes only 25-30% of CAC reacts with water, and that the molten zones contain numerous pores, the following mechanism of formation of these zones is proposed:

- during the final stage of hydration, the initially unhydrated CAC particles react with the silicic acid dissolved from silica fume particles forming localized zones of calcium aluminum silicate hydrate phases. The presence of dispersant admixtures in the interstitial solution of the binding system paste brings a high concentration of alkali and phosphate ions that induce the formation of low melting point liquid;

- the melting temperature of these phases is below the temperature of decomposition of hydrated phases (750°C) and the closed pores formed are a result of the final stages of dehydration in the presence of liquid phases;

Even if small amounts of nonequilibrium liquid phases may be formed before the total decomposition of the hydraulic bond, they are confined to the space previously occupied by initially unhydrated CAC particles. Because the ULCC compositions under study contains only 2% CAC, and the molten zones have an isolated topology, the metastable liquids formed below 816°C are not determinant for the formation of ceramic bond or strength development.

The fracture surface of BS of NCC, regardless of the type of silica fume that is used, is covered by the silica fume matrix. Isolated zones of fracture at the interface of the silica fume matrix and tabular alumina -325 mesh grains are present. There are no zones with glassy appearance (Figure 4.4-6).

The SEM of the fracture surface of BS of ULCC based on SF3 after firing at 1093°C shows the presence of isolated zones with molten or glassy appearance, but the fracture propagates mainly through the silica fume matrix. Interfaces between silica fume matrix and calcined alumina and kyanite grains are visible. The presence of delaminations at the interface of kyanite with the silica fume matrix demonstrates that at this temperature the process of thermal decomposition of kyanite had already started (Figure 4.4-7).
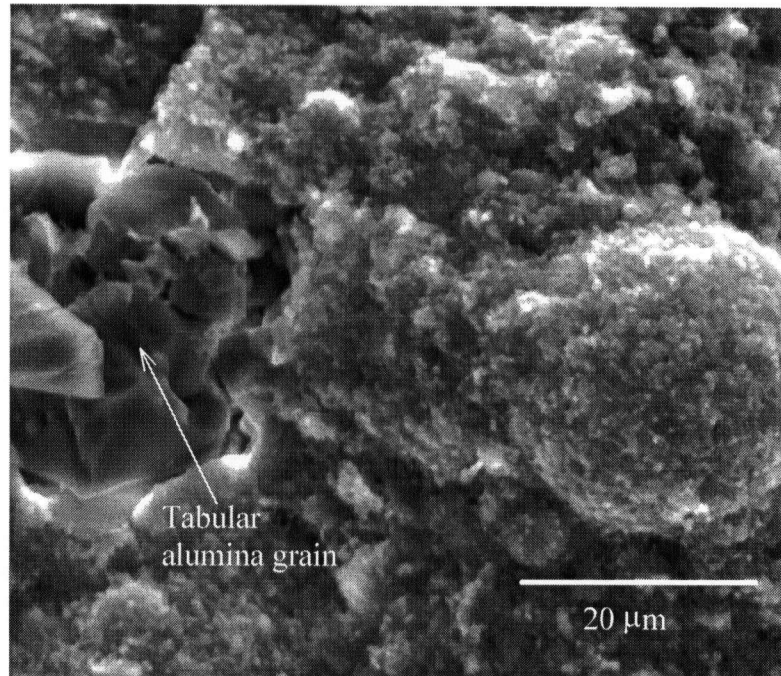
Figure 4.4-6. Fracture surface in a BS of an NCC based on SF3 after firing at 816°C.
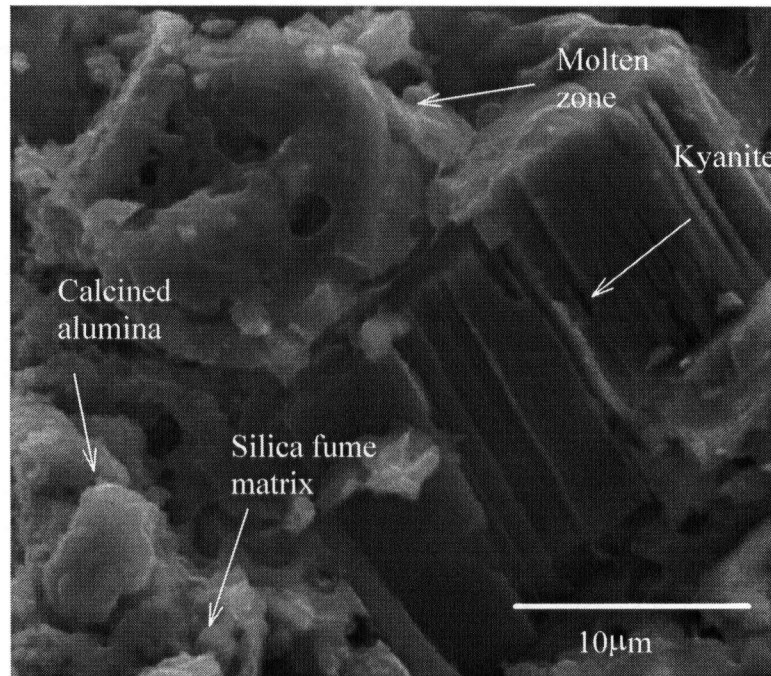
Figure 4.4-7. Fracture surface of a ULCC BS based on SF3 after firing at 1093°C.
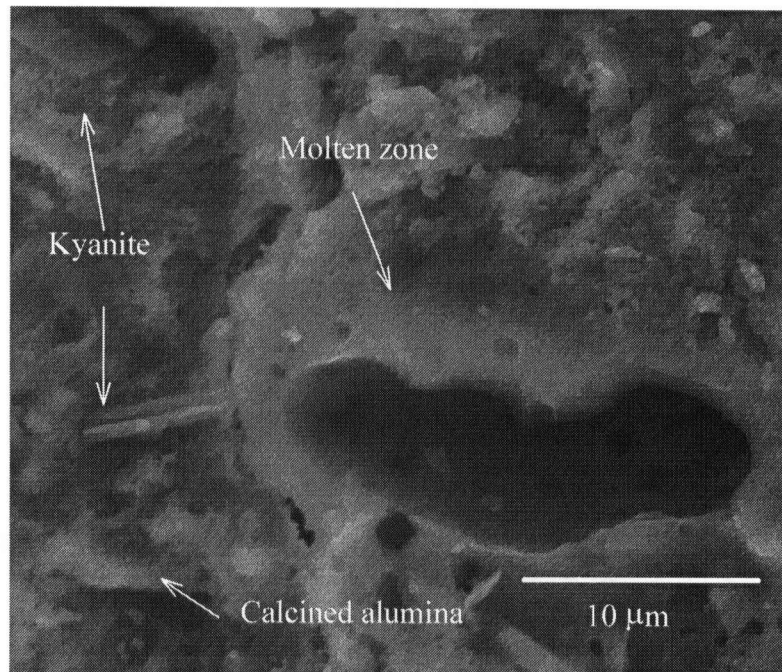
Figure 4.4-8. Fracture surface of a ULCC BS based on SF1 after firing at 1093°C.

The SEM of the fracture surface of BS of ULCC based on SF3 after firing at 1093°C is somehow similar to that of the specimens based on SF1(Figure 4.4-8).The zones with molten or glassy appearance, and interfaces between the silica fume matrix and the kyanite grains are visible. The most important difference is the presence of the silica fume matrix. It is not possible to identify individual particles of silica fume in the fracture surface of the SF1 matrix after firing at 1093°C, but at the same time the fracture surface cannot be described as having a molten material appearance. Similar differences in silica fume matrix were found for NCC specimens.

In order to clarify this issue, experiments were performed to establish the influence of heat treatment on the microstructure of silica fume particles. SEM specimens of silica fume were prepared by casting from concentrated pastes prepared with additives, followed by drying and firing.
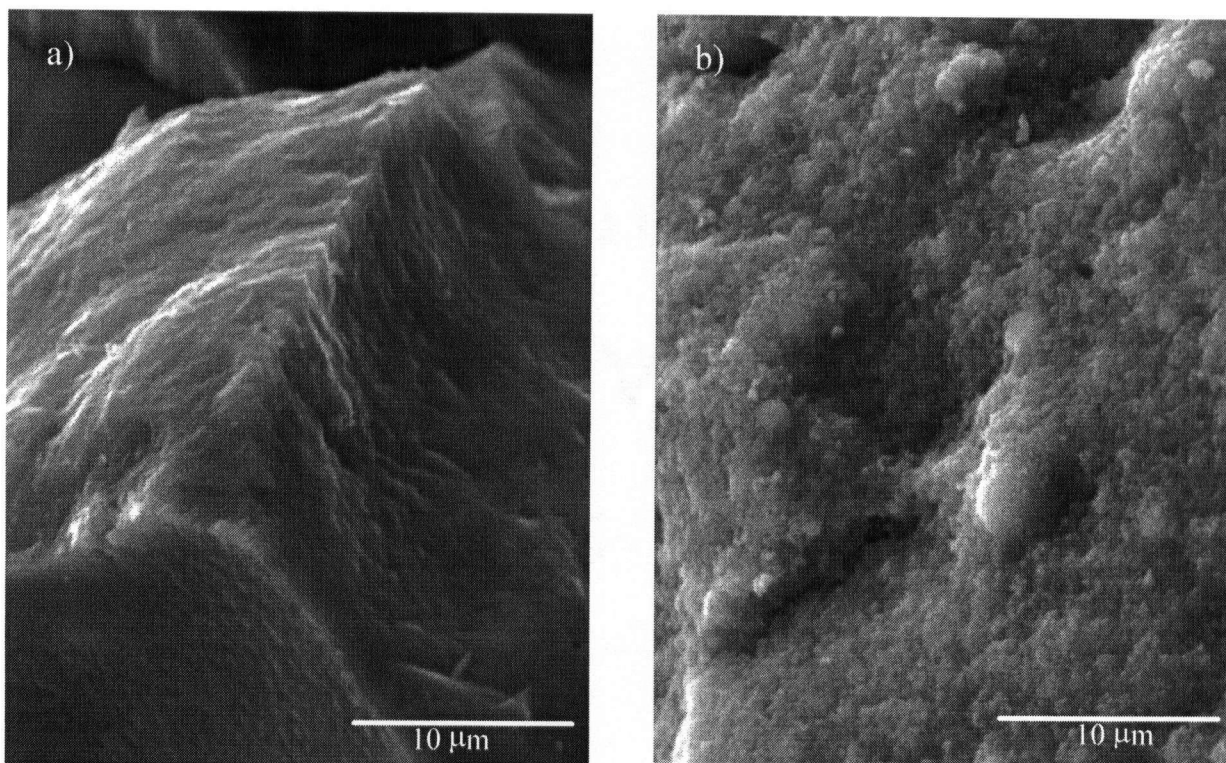
Figure 4.4-9. Microstructure of fracture surface of: a) SF1 and b) SF3 after firing at 1093°C.

After firing at 816°C the microstructure of the fracture surface of SF1 and SF3 specimens was very similar to that of the silica fume matrix present in the corresponding BS at the same temperature. An important difference occurred however after firing at 1093°C (Figure4.4-9). While for SF3 (Figure 4.4-9 b) the microstructure at 1093°C is virtually unchanged if compared to 816°C, for SF1 the spherical particle aggregate is transformed to a monolithic body. The roughness of the fracture surface suggests that the transformation takes place by the coalescence of the outer layer of SF1 particles (Figure 4.4-9 a). At 1371°C the SEM of SF1 shows a completely fused material (Figure 4.4-10 a), while for lower grade impure SF3 a porous matrix is obtained by superficial coalescence of fine silica fume particles (Figure 4.4-10 b).
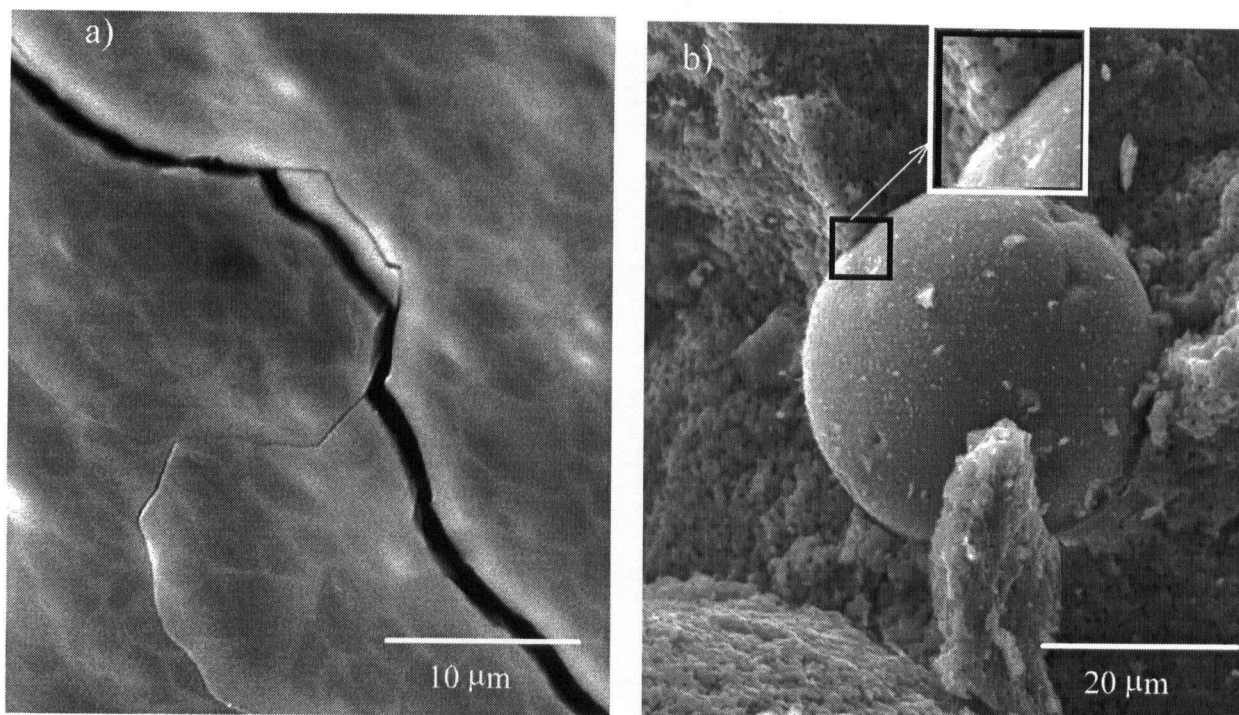
Figure 4.4-10. Microstructure of fracture surface of: a) SF1 and b) SF3 after firing at 1371°C.

If the fusion of silica fume particles was due to the presence of impurities, which may form low melting point eutectics, the first to transform should have been the low purity SF3. Although most of the impurities of SF3 are concentrated in the large size particles (5-30μm) after firing at 1371°C the large impure particles of SF3 are not transformed, and do not have a good adhesion with the aggregate of fine particles (Figure 4.4-10 b).

After firing at 1371°C the fracture surface of ULCC BS is composed, for both SF1 and SF3, of a silica fume matrix with glassy appearance. X-ray diffraction showed that mullite is already formed at this temperature, a fact that is confirmed by the presence of needle-shape structures with aluminosilicate composition (Figure 4.4-11 a). It is not possible to accurately determine the chemical composition of these structures because of the background interference given by the film that covers them.
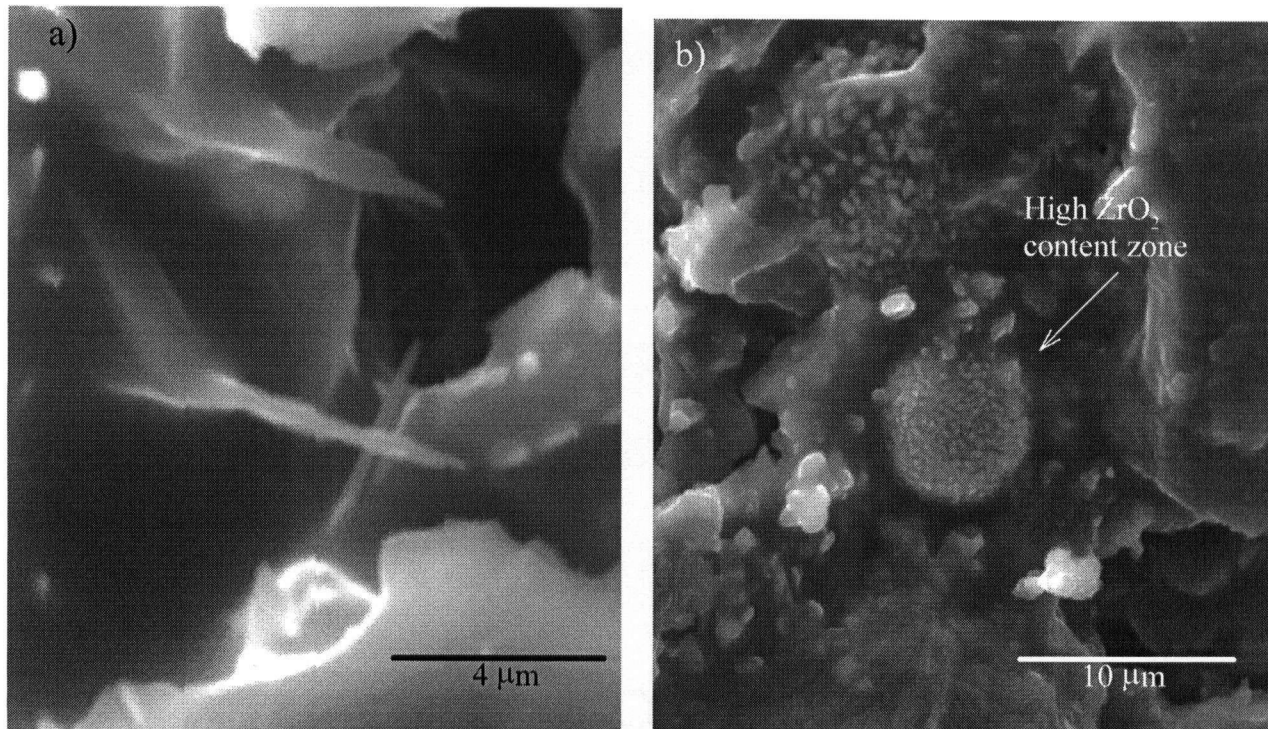
Figure 4.4-11. SEM of fracture surface of ULCC BS based on :a) SF1 and b) SF3, after firing at 1370°C.

The fracture surface binding systems of ULCC based on SF3 had some spherical structures having a rough surface and a 10-30μm diameter (Figure 4.4-11 b). EDS analysis showed that their chemical composition contains more than 50% ZrO_2 and 10-15% Al_2O_3, 20-40% SiO_2 and 2-7% CaO. X-ray diffraction showed the presence of traces of monoclinic zirconia. Based on their aspect and content of ZrO_2 it is concluded that these structures represent the large impure particles of SF3 that reacted with the surrounding matrix.

After firing at 1370°C the fracture surface of the BS of NCC based on SF1 shows the presence of a glassy matrix covering all the particles of the BS. Although the presence of mullite has been detected by X-ray diffraction, no mullite could be identified on the fracture surface of the BS (Figure 4.4-12 a)

The microstructure of the fracture surface of the ULCC BS based on SF3, after firing at 1370°C, consists of large particles of SF3 surrounded by a porous matrix (Figure 4.4-12 b). The fracture at the interface of large impure SF3 particles with the surrounding porous matrix is clearly visible. No interaction or attack of the BS matrix on these large particles, as in the ULCC specimens, was detected.
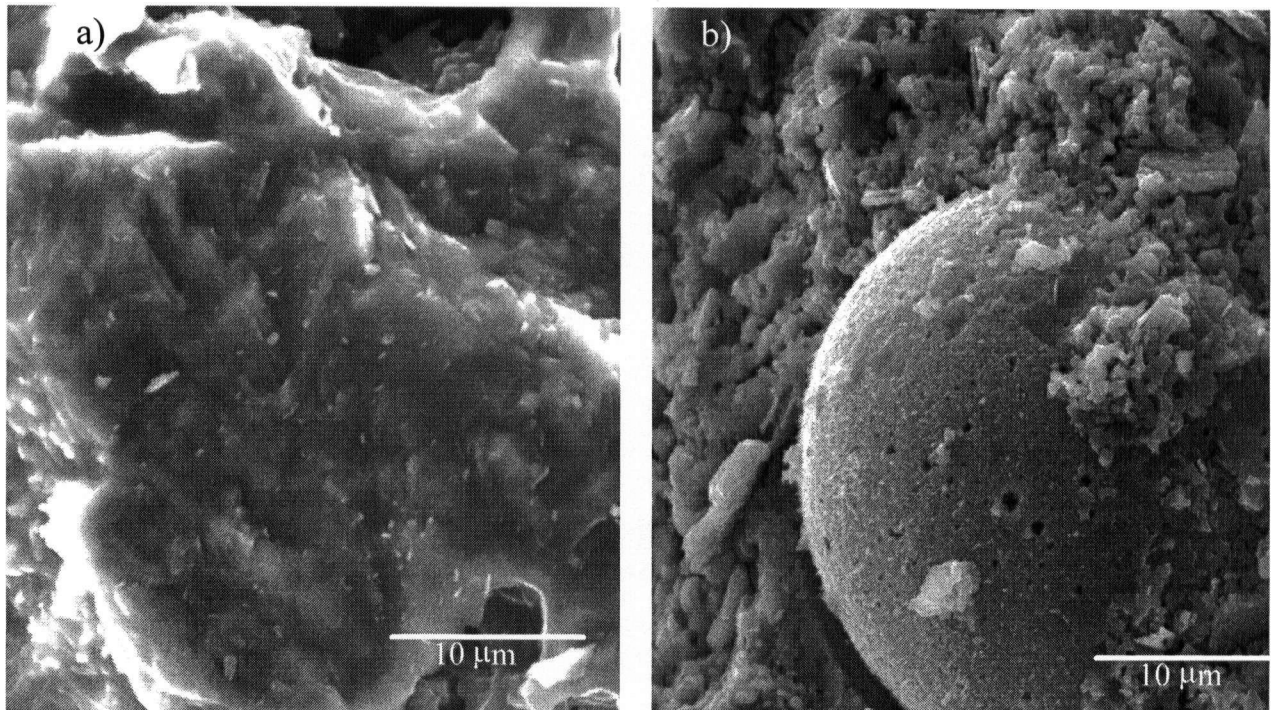
Figure 4.4-12. SEM of fracture surface of NCC BS based on :a) SF1 and b) SF3, after firing at 1370°C.

4.4.2. Microstructure of experimental castable compositions

HMOR of experimental castable compositions was measured according to ASTM C 583, using an apparatus designed and constructed in UBC that has a strain control capability. By interrupting the crosshead advance immediately after the measurement, but before the breaking of the specimen, it was possible to obtain fracture specimens with minimum damage due to subsequent handling. After cooling to room temperatures the fracture surface obtained during the HMOR measurements was analyzed by SEM.

The microstructure of both, ULCC and NCC specimens subjected to HMOR testing at 540°C is represented only by silica fume agglomerate. At this temperature, regardless of the grade of silica fume, the weakest bond in the system is between the silica fume particles. The fracture surface of experimental compositions is very similar to that of the corresponding BS fractured after firing at 540°C

At 816°C the fracture surfaces are significantly different for all self flowing castable compositions (Figure 4.4-13). For the ULCC with SF3 the fracture propagates through the silica fume matrix, and refractory aggregate grains. Based on chemical composition, determined by EDS analysis of individual components of the binding systems and of the fracture surface the following phases were identified:

- silica fume matrix;
- calcined alumina-silica fume matrix interface;
- kyanite-silica fume matrix interface.

As in the case of the fracture surfaces of the BS, there are also present isolated zones of glassy material with the approximate composition of 22-36% SiO_2, 1.3-2.5% Na_2O, 2.1-3.6% P_2O_5, 17- 23% CaO, 39-54% Al_2O_3 .

While the fracture at the interface of the silica fume matrix with calcined alumina was to be expected (due to the high strength of alumina and a low interaction with the silica fume matrix at 816°C), the fracture at the interface of the silica fume matrix with kyanite (Figure 4.4-13 b) can be explained only as a result of thermal expansion tensions.
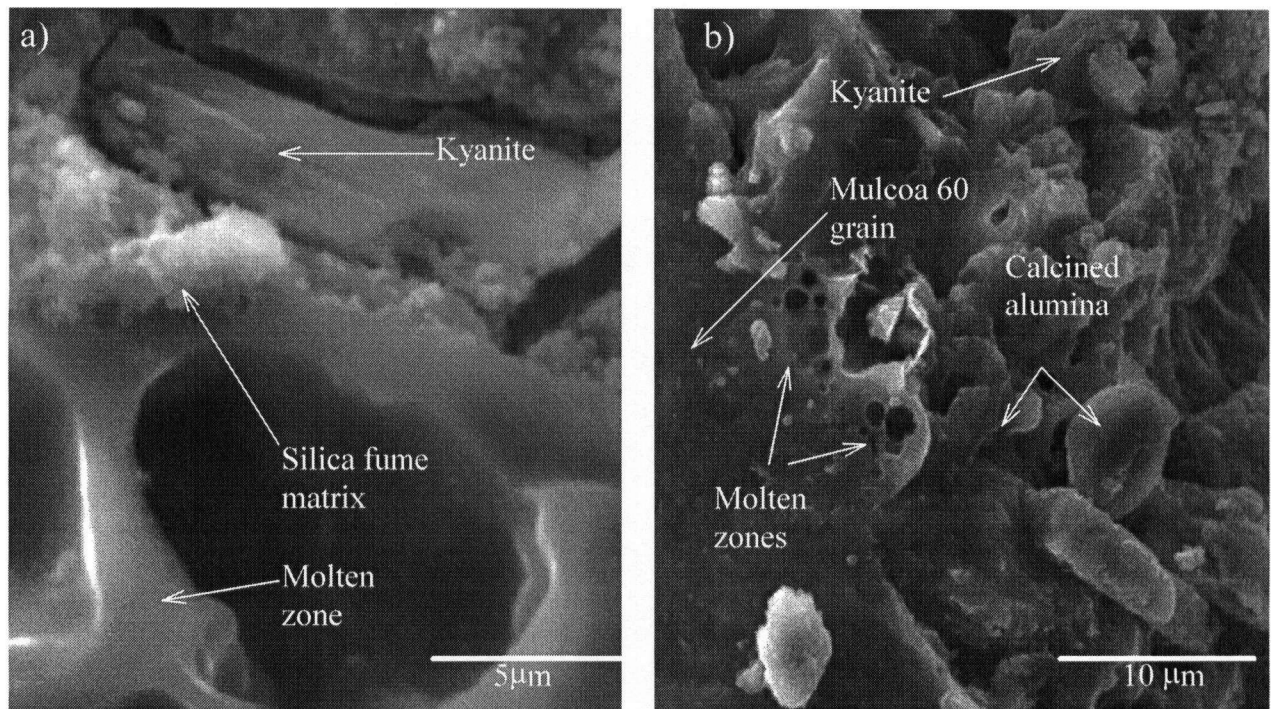
Figure 4.4-13. SEM of ULCC specimens based on: a) SF1, and b) SF3, fractured at 816°C.

The fracture of self flowing ULCC based on SF1 at 816°C has similar characteristics as described above, but the fracture at the interface with kyanite particles is more definite, and there is also a clear delineation between the silica fume matrix and the molten zones (Figure mic4.4-13 a).

The chemical composition of molten zones is characterized by a SiO_2 concentration of 28-39%, that is higher than for mixes based on SF3. This may be explained by a higher reactivity of SF1, and consequently a higher concentration of silicic acid in the interstitial solution of the binding system.

For both ULCC compositions, the evolution of the fracture through the refractory aggregate grains, although it is not a characteristic feature, indicates a significant strength development of the binding system.

The SEM study on NCC fractured at 816°C shows that the fracture is present at the boundary between silica fume particles. In NCC with SF3, there are also present isolated zones of fracture at the interface of the silica fume matrix with the tabular alumina aggregate (as in NCC binding system specimens) (Figure 4.4-14 b). In NCC based on SF1 the fracture is exclusively at the interface of silica fume particles (Figure 4.4-14 b).
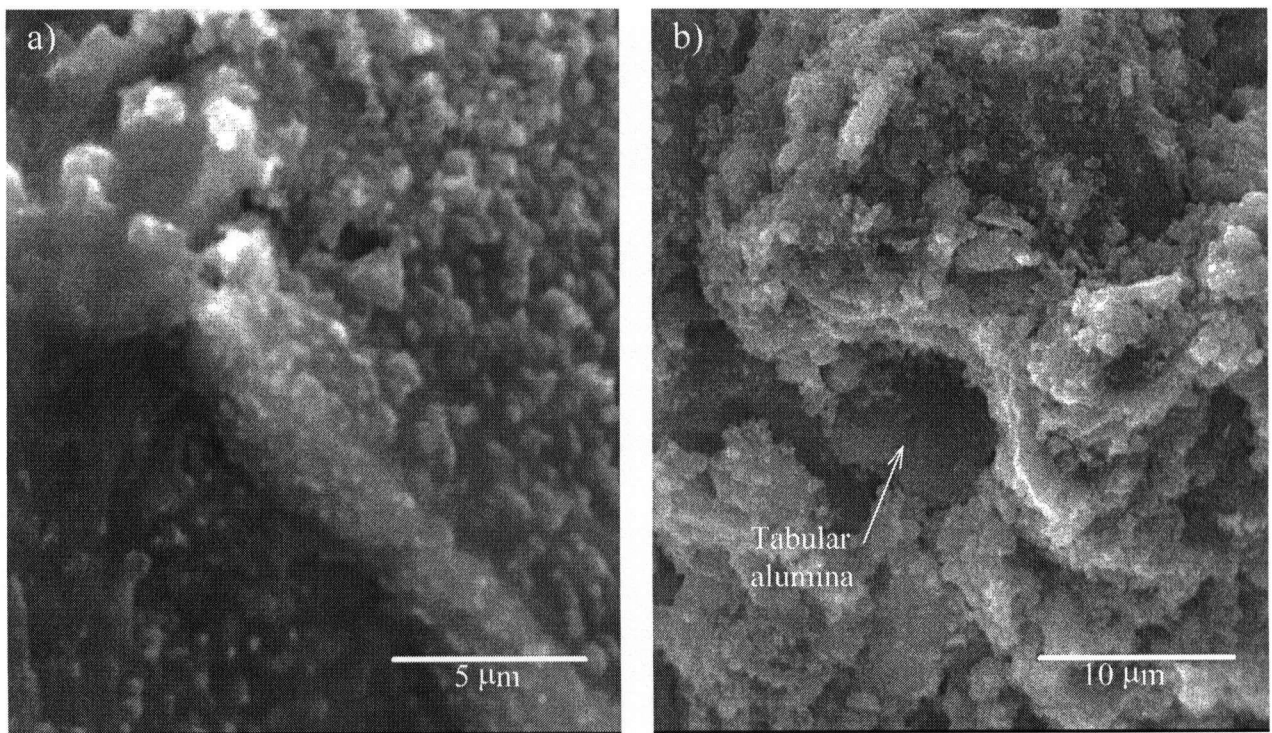
Figure 4.4-14. SEM of NCC specimens based on: a) SF1, and b) SF3, fractured at 816°C.

SEM analysis of self-flowing ULCC fractured at 1093°C shows some important evolution if compared to 816°C:

- there is a general development of the fracture through refractory aggregate grains (Figure 4.4-15 a) ;

- there are present isolated zones of refractory aggregate covered by a film of molten phase (4.4-15 b) ;

- there are present interlocking needle like structures having a chemical composition, determined by EDS, in the range of 56-62% SiO_2, 31-38% Al_2O_3 , 6-8% CaO, 1-4%Na_2O.
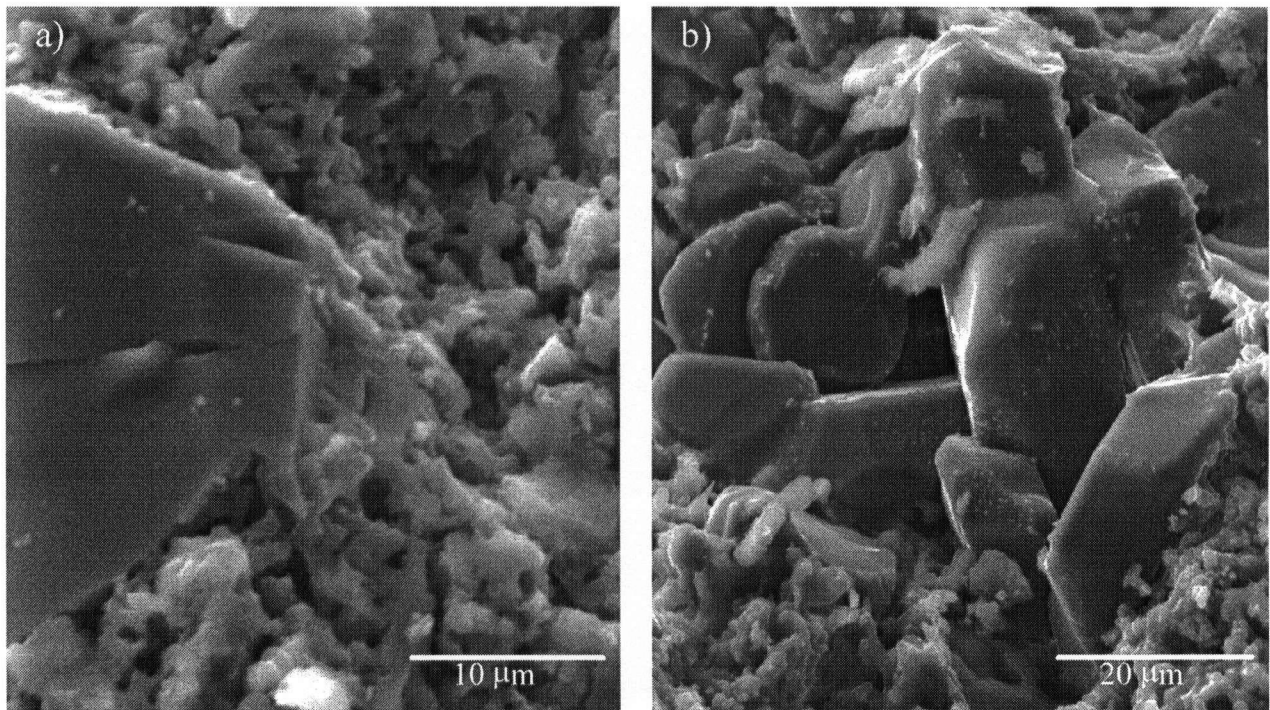
Figure 4.4-15. SEM of ULCC specimens based on: a) SF1, and b) SF3, fractured at 816°C.

The development of the fracture path through refractory aggregate grains reveals that at 1093°C the toughness of the binding system is higher than that of the mullite calcines, and there is a strong bond formed between the aggregate grains and the binding system.

The presence of zones of refractory aggregate covered by a molten film demonstrates that at 1093°C a metastable liquid starts to form by interaction between the agglomerations with high calcia and alkali content (resulted from the final stage of hydration of calcium aluminate

181

cement) and the rest of the matrix. At 1093°C the molten zones extended on the surface refractory grains still have a isolated topology and there is a clear delimitation between the molten zones and silica fume matrix.

X-ray diffraction performed on ULCC compositions and on their binding systems showed that no mullite or other aluminosilicate crystalline phase is formed up to 1093°C. It is well known that, due to the hydraulic interaction within the binding system, traces of mullite may develop at temperatures as low as 1085°C but probably due to diffusional hindrances significant amounts are rarely found below 1300-1400°C.

The interlocking needle shape structures that were found at the fracture surface at 1093°C (Figure 4.4-16) could not be attributed to any new formed crystalline phase. Due to their non-parallel orientation this structures cannot be identified as a low crystallinity phase formed by thermal decomposition of kyanite. It is more likely that the needle structures that were
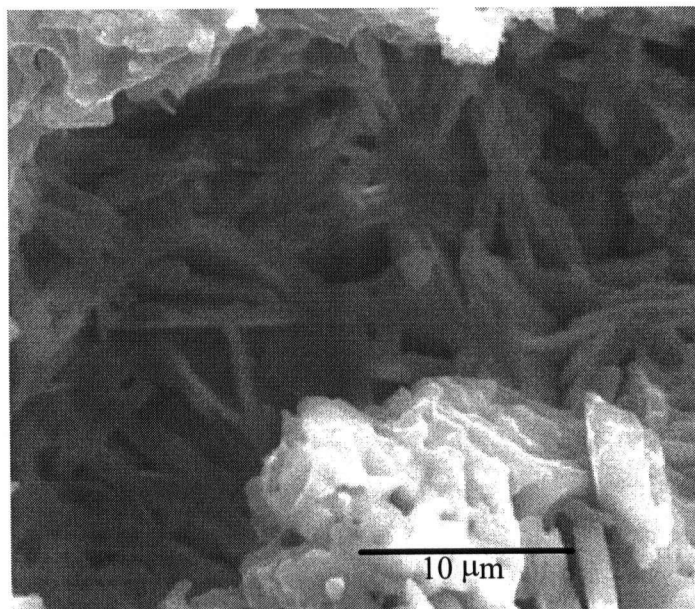
Figure 4.4-16. Aluminosilicate interlocking needle shaped structures in ULCC based on SF1 fractured at 1093°C.

background interference of the film that covers all the crystals. For ULCC specimens the EDS analysis of these needle shape structures were in the range of 40-75% Al_2O_3 , 30-60% SiO_2 0.5-2.2% CaO (Figure 4.4-17).

According to SEM analysis of the ULCC specimens fractured at 1371°C the process governing the fracture is represented by the pull-out of mullite crystals from the binding system matrix. There is no important difference in the size-aspect ratio characteristics of mullite crystals developed in ULCC based on SF1 and SF3.

Only in the case of NCC compositions fractured at 1370°C is there still present a fracture path through refractory aggregate particles. Mullite is present at the fracture surface, but no pull-out mechanism could be identified (Figure 4.4-18 a). This may be explained by a higher viscosity of the molten film surrounding the component particles of NCC. At the fracture

Figure 4.4-18 Mullite crystals in the fracture surface of specimens based on SF1 a), and b) large particle of SF3 transformed by interaction with the matrix, in NCC fractured at 1370°C.

background interference of the film that covers all the crystals. For ULCC specimens the EDS analysis of these needle shape structures were in the range of 40-75% Al_2O_3 , 30-60% SiO_2 0.5-2.2% CaO (Figure 4.4-17).

According to SEM analysis of the ULCC specimens fractured at 1371°C the process governing the fracture is represented by the pull-out of mullite crystals from the binding system matrix. There is no important difference in the size-aspect ratio characteristics of mullite crystals developed in ULCC based on SF1 and SF3.

Only in the case of NCC compositions fractured at 1370°C is there still present a fracture path through refractory aggregate particles. Mullite is present at the fracture surface, but no pull-out mechanism could be identified (Figure 4.4-18 a). This may be explained by a higher viscosity of the molten film surrounding the component particles of NCC. At the fracture

Figure 4.4-18 Mullite crystals in the fracture surface of specimens based on SF1 a), and b) large particle of SF3 transformed by interaction with the matrix, in NCC fractured at 1370°C.

surface of NCC specimens based on SF3, large particles of silica fume may be observed (Figure 4.4-18 b). The aspect of their surface and the EDS analysis (62-72% ZrO_2) indicate an interaction with the surrounding matrix

The different behavior of large particles of SF3 in BS and castable specimens of NCC demonstrates that at 1371°C there is a significant interaction of large particles of tabular alumina refractory aggregate grains with the SiO_2 containing layer. The interaction of large particles of SF3 with the surrounding matrix in NCC specimens is due to a higher concentration of Al_2O_3 in the molten or glassy matrix and not to the presence of a rich calcia low viscosity liquid as in the case of ULCC BS based on SF3.

4.4.3. Correlation of microstructure with mechanical strength

The increase in strength at the first heat up of self-flowing castables in the temperature range of 540-1093°C can be attributed to a process of "inter-particle bonding" of the high purity silica fume particles, rather than liquid phase formation. In order to explain the nature of this apparent sintering process and the influence of water for casting on strength development, a few experiments were performed to determine the compositions of the interstitial solution of concentrated pastes of binding system (during the dormant period). This solution was separated by vacuum filtration of binding system water suspensions. After drying at 110°C the solid residue was analyzed by SEM and EDS. The results showed (taking ULCC as an example) that crystals of calcium-aluminum-alkali phosphate grow from an amorphous material containing more than 97% SiO_2. No crystalline form of SiO_2 was found up to 1093°C. This result demonstrates that during the dormant period, there is an interaction between the fume silica and the water solution of dispersants, causing the superficial hydration of silica fume particles and release of silicic acid. At the end of the hydraulic setting, silica fume particles are covered

by a partially hydrated amorphous layer, onto which the calcium ions and the dispersant are adsorbed. These particles interact physically and chemically with each other and all the other solid species present in the binding system, through this hydroxylated layer. Being predominantly chemical, this inter-particle bonding will exist as long as the hydroxylated layer exists on silica fume particles and probably to a lower extent on alumina particles.

During the first heat up the chemical bonds will disappear, while the de-hydroxylation advances, but the inter-particle bond does not weaken, as proven by retention of strength with temperature. A reactivity increase of the particle surface during the de-hydroxylation process could be the only factor to determine the inter-particle bonding, up to the temperature where the hydraulic bond is completely destroyed. If the inter-particle distances are somehow increased, or the number of particles with good contacts with each other is decreased (i.e. at higher amounts of water for casting), strength at a certain temperature shows a proportional decrease. However, variation of strength with the temperature follows the same continuous increase in strength pattern.

Although this inter-particle evolution can successfully explain the influence of water content and dispersant admixtures on early strength development and the strength increase and densification at temperatures below 816°C, it cannot explain the strength increase in the temperature range of 816-1093°C when no chemically bonded water is present. The theory developed by Chaklader [140, 141] suggests "super-plasticity of oxidic amorphous phases", in the range of temperatures where the de-hydroxylation or de-carbonation takes place. It is hypothesized that similar behavior could be found in binding systems of refractory castables, having all the silica fume particles covered with an amorphous layer of silicic acid. According to this theory, it is possible to use the high reactivity of a solid, during a decomposition reaction or a phase transformation, in order to enhance the densification and inter-particle bonding. The broken bonds re-link across the reactive interface without necessarily producing significant

elimination of pores or voids from the matrix. Transient instability of the atom positions during the decomposition reaction would also produce a super-plastic state that could be used for densification. Experiments on deformation under load of silica fume specimens, prepared by drying concentrated pastes of silica fume and dispersant admixture, showed plastic deformation at 870°C for SF1 and 900°C for SF3. Also the coalescence of silica fume particles to form a "glassy" looking phase, identified by SEM on binding systems, cannot be attributed to a diffusion process but rather to a plastic deformation of the amorphous silica gel deposited on the silica fume particles at the end of the de-hydroxylation process. The significant deformation under load experimentally evident at temperatures between 816-1093°C should be attributed only to the super-plastic amorphous phase surrounding the silica fume particles. Due to the fact that at these temperatures there is no significant crystalline development, it can be assumed that the strength development is due to an amorphous to glassy phase transition rather than amorphous to crystalline transition.

4.5. Pilot scale experiment : pumping and spray-gunning of advanced castable refractories

One of the objectives of the research program was to verify the laboratory results with a spray gunning pilot scale experiment performed using a self-flowing LCC composition based on mullitic refractory aggregate. Prior to this, laboratory work was necessary to select the castable formulation and to design the accelerator admixture. The main difficulty encountered during preparation of the pilot scale experiment was related to the design of the accelerator admixture. As presented in Chapter 2.5, the mechanism of setting acceleration of self-flowing castables for spray gunning applications is not yet well understood, and the selection of accelerator admixtures is made only on trial and error basis.

Taking into account that a spray-gunning trial requires at least several hundred kilograms of material for one run, it is understandable that laboratory experiments should allow the selection of the proper accelerator admixture without room for error. Therefore, it was necessary to setup of a laboratory method to allow for an accurate evaluation of the accelerator admixture and the assessment of the properties of the spray-gunned castable.

Two pilot scale experiments were performed. During the first experiment (performed using sodium aluminate accelerator), an accidental clogging of the spray nozzle occurred and only half of the required quantity of the castable was installed. While preparing the second experiment, both the castable formulation and the laboratory evaluation method were refined. This resulted in the design of a new class of chemical admixtures for spray-gunning and made possible a successful pilot scale experiment. A new Flash Flocculation (FF) process was discovered, which allowed to preserve the mix plasticity during spray gunning

4.5.1. Experimental castable compositions

The following details were considered in the design of the experimental LCC compositions:

- the use of mullite refractory aggregate (Mulcoa 60 or Mulcoa 70),

- maximum content of silica fume, set at 8%,

- 50-100% flow at 5.5% water,

- maximum content of CAC (Secar 71), set at 5%.

For the first pilot scale experiment the use of Mulcoa 60 refractory aggregate and a maximum setting time of 4 hours was required. At the time of the second experiment the Mulcoa 70 refractory aggregate (with a large content of a continuous -4 mesh fraction) was used and the -100 mesh Mulcoa 90 fraction was replaced with a similar fraction of calcined bauxite. A minimum working time of 2 hours and a maximum setting time of 12 hours were required.

The knowledge accumulated during the study of the rheology of binding systems of

Table 4.5-1. Composition of LCC 34.

Component	wt%
Kyanite-325 mesh	8
CA Aluchem	8
Silica Fume Elkem 971	8
CAC SECAR 71	4
Mulcoa 60, -4+8 mesh	16
Mulcoa 60, -8+20 mesh	24
Mulcoa 60, -35 mesh	14
Mulcoa 90, -100 mesh	18
Sodium Aluminate	0.01
Sodium Tripolyphosphate	0.08
Sodium Lignosulphonate	0.0096
Water	5/5.5
Flow (%)	55/100

Table 4.5-2. Composition of LCC 83.

Component	wt%
Kyanite-325 mesh	4
CA Aluchem	10
Silica Fume Duralum AB	8
CAC SECAR 71	4
Mulcoa 70, -4 mesh	45
Mulcoa 70, -8+20 mesh	9
Mulcoa 70, -35 mesh	14
Alphastar, -100F	16
Sodium Aluminate	0.005
Sodium Tripolyphosphate	0.08
Sodium Lignosulphonate	0.0096
Citric Acid	0.01
Water	5/5.5
Flow (%)	45/70

refractory castables and its correlation with flow facilitated the composition design. Table 4.5-1 shows the experimental composition LCC 34 used for the first plant trial and Table 4.5-2 the experimental composition LCC 83 used for the second plant trial. Both composition are characterized by very good self flowing values. If compared to the early LCC 34, the latter composition LCC 83 has the following features:

- The main refractory aggregate fraction is of a continuous particle size distribution, -4 mesh. All the other fractions of refractory aggregate were needed to adjust the particle size distribution to an Andreassen distribution;

- It has higher content of CA and lower content of kyanite in order to improve the flow;

- Contains a lower purity (cheaper) silica fume SF3;

- Contains a mixture of sodium aluminate and citric acid in order to obtain the desired working and setting characteristics (LCC 83, at 5.5% water has a flow of 70% at 2 hours after mixing and a setting time of 8 hours).

Table 4.5-3 presents some of the properties of LCC 34 and, for comparison, the properties of Versaflow 60, a commercial LCC produced by Harbison Walker Refractories.

Table 4.5-3. Properties of LCC 34 and Versaflow 60

Property	LCC 34	Versaflow 60 ADTECH
Self Flow at 5.5% water (%)	100	no self flow @ 6.5% water
CAC content (wt.%)	4.00	7.00
MOR after drying 230°F (MPa)	14.0	10.7*
MOR after firing 1500°F (MPa)	22.0	17.7*
MOR after firing 2000°F (MPa)	25.1	12.6*
CCS after drying 230°F (MPa)	48.3	113.7*
CCS after firing 1500°F (MPa)	76.0	63.2*
HMOR @ 1500°F	26.7	8.31
Permanent Linear Change (%)		
after drying (230°F)	-0.05	negligible*
after firing (1500°F)	-0.056	-0.200*
Apparent Porosity after 1500°F	10.48	18.5

* catalog data

Mechanical properties are shown for 5.5% water for LCC 34 (self-flowing) and for 6.5% water for Versaflow 60 ADTECH (vibcasting). Except the CCS after drying, LCC 34 is superior to Versaflow 60 in every aspect, but the most important difference is the self-flowing value and HMOR.

4.5.2. Design of the spray gunning admixture

A simple method for laboratory assessment of the properties of spray gunned castables was developed. After mixing in a Hobart mixer for 5 minutes, the chemical admixture for spray-gunning was added, the castable was mixed again for 30 seconds and a slump test was performed by turning the mixer bowl upside down. The slump was considered satisfactory if no flow occurred. The plasticity of the mix was evaluated visually. If the castable had no slump and maintained a plastic consistency the material was molded and the resulting specimens were cured and subjected to mechanical testing (CCS, MOR and HMOR).

During spray-gunning, due to the turbulence in the spraying hose, and due to the fact that the admixture is injected through a high pressure nozzle, the mixing is almost instantaneous. These conditions cannot be fully reproduced in the laboratory by mixing the castable in a planetary mixer. The value of 30 seconds, for mixing the castable with spray-gunning admixture, was chosen because it is the minimum time that allows for homogenization of the material in the mixing bowl. Shorter mixing time (i.e. 20 seconds) results in the coexistence of non-slumping and self-flowing material. The plasticity of the mix was evaluated qualitatively. Four levels of plasticity were defined:

0. self-flowing (highest plasticity and cohesiveness);

1. high plasticity (the castable has no slump, it is cohesive and can be subjected to plastic deformation without cracking or separation surfaces);

2. low plasticity (the castable has no slump and if subjected to plastic deformation, cracking or separation surfaces are observed);

3. no plasticity (the material has no cohesiveness, and has the appearance of a dry gravel and there is a separation between the binding system and the refractory aggregate).

Material with high plasticity (level 1 and 2) could be molded by hand ramming in molds, and mechanical test specimens were obtained.

During preliminary laboratory experiments several observation were made:

- some admixture solutions triggered strong flash setting even at low levels of admixture, and the resulting material had no plasticity. These mixtures included calcium chloride and lithium chloride solutions.

- some admixture solutions produced a flash setting effect at a certain level of addition but an over dosage of solution resulted in regaining the self-flowing behavior. This indicates that flash setting depends not only on the amount of solid active substance added to the castable, but also on the total amount of additional water brought by the solution of the admixture. These admixtures included potassium aluminum phosphate and aluminum sulfate.

As in the field applications a precise control of the flow of spray-gunned mix is difficult to achieve the process has to be robust; i.e. tolerant to dosage variations. Several possible scenarios may occur:

a) an under-dosage of the admixture solution would translate to insufficient quantity of active solid substance and flow or slump of the lining;

b) an over-dosage of the admixture solution would result in :

- loss of plasticity (due to over-dosage of the active solid substance in the accelerator mix)

- return to self-flow behavior regime (due to over-dosage of water)

Accordingly, an optimum accelerator admixture should have the following properties:

- high solubility, to minimize the supplementary amount of water introduced to the castable;

- suppress self-flowing behavior, at low levels of addition, to minimize both the supplementary amount of water and unwanted impurities (such as alkalis, chlorine, etc.);

- produce, after addition to the castable, a high plasticity non flowing material, in order to avoid delaminations or other macrodefects in the refractory lining;

- have a stable effect over a wide range addition levels, in order to be tolerant to the variable field conditions.

Ideally, after spray gunning, the castable should remain in a thickened but plastic state for a reasonable length of time. This facilitates troweling, finishing and checking for proper installation. Accelerators which cause rapid setting or stiffening of the castable are not acceptable, as they cause laminations and in some cases nozzle clogging. The initial focus of the laboratory experiments was to identify spray-gunning admixtures that could suppress the slump at low levels of admixture. As initial target, the maximum level of admixture was fixed at 0.8%. This is because, for a generic case of 50% solid load (of solid active substance in solution), the amount of water inducing segregation in the LCC 34 castable is 5.5%.

The investigation was performed among the chemicals that are well known to have an accelerating effect on CAC. Some of the chemicals, which could not suppress the flow at an addition level of 0.8%, were not considered for further examination. In this category were: magnesium hydroxide, potassium silicofluoride, calcium hydroxide, potassium chloride, lithium carbonate, and cupric sulphate. Although having a strong accelerating effect (confirmed by laboratory tests), lithium chloride was not considered for pilot scale experiments due to its high toxicity.

The chemicals which proved to be effective for admixture levels equal or less than 0.8%, were used as saturated solutions with the exception of calcium chloride. $CaCl_2$ having solubility of 74.5g in 100 cm^3 water at room temperature, produced a total loss of plasticity at almost any concentration.
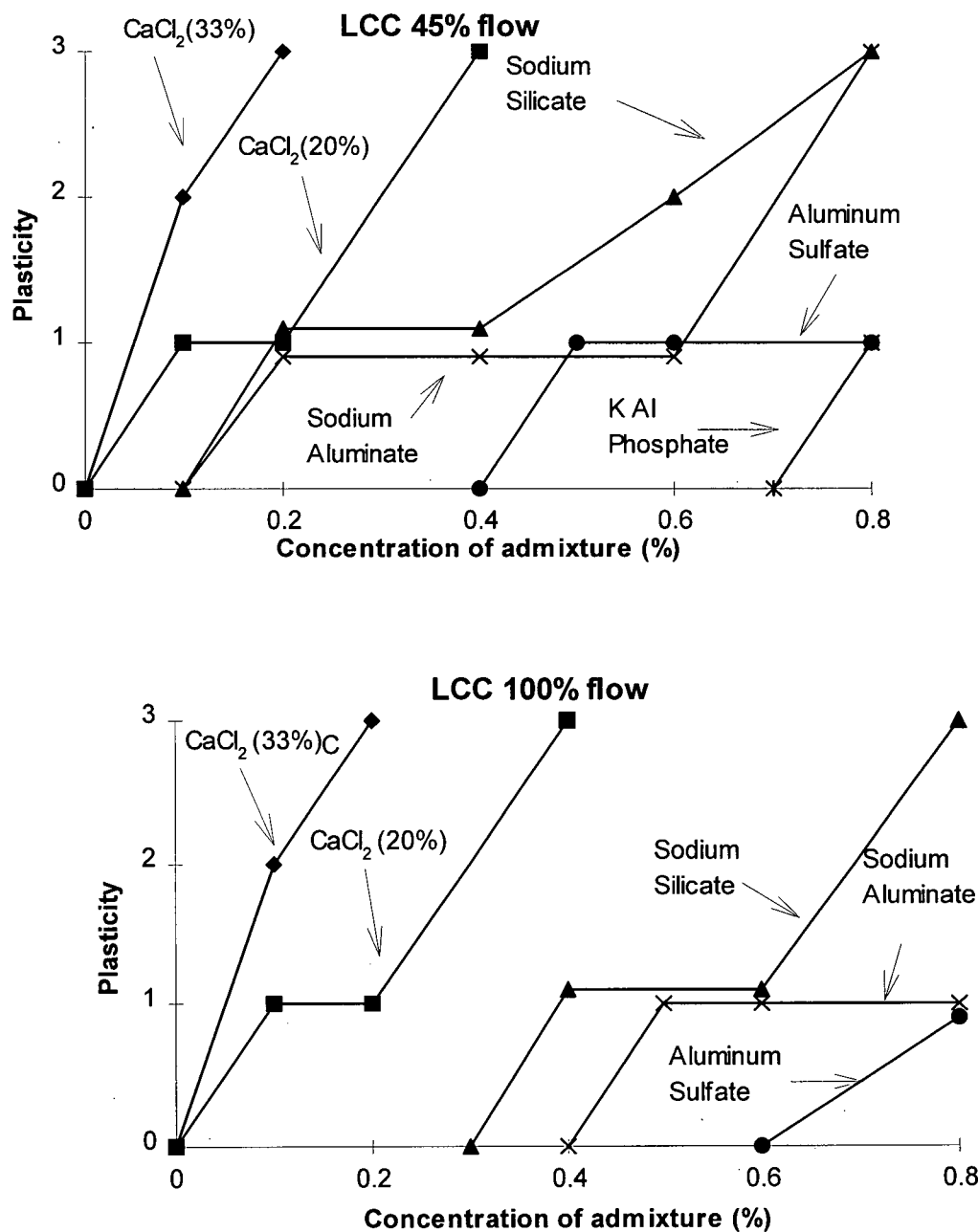
Figure 4.5-1. The effect of accelerator admixtures for LCC 34, at 45% and 100% flow, on mix plasticity.

In order to study the influence of castable composition and water content, a group of experiments was performed for LCC and ULCC compositions, at flow values corresponding to consistencies for pumping (45-50% flow) and self-leveling (80-100% flow). The experimental
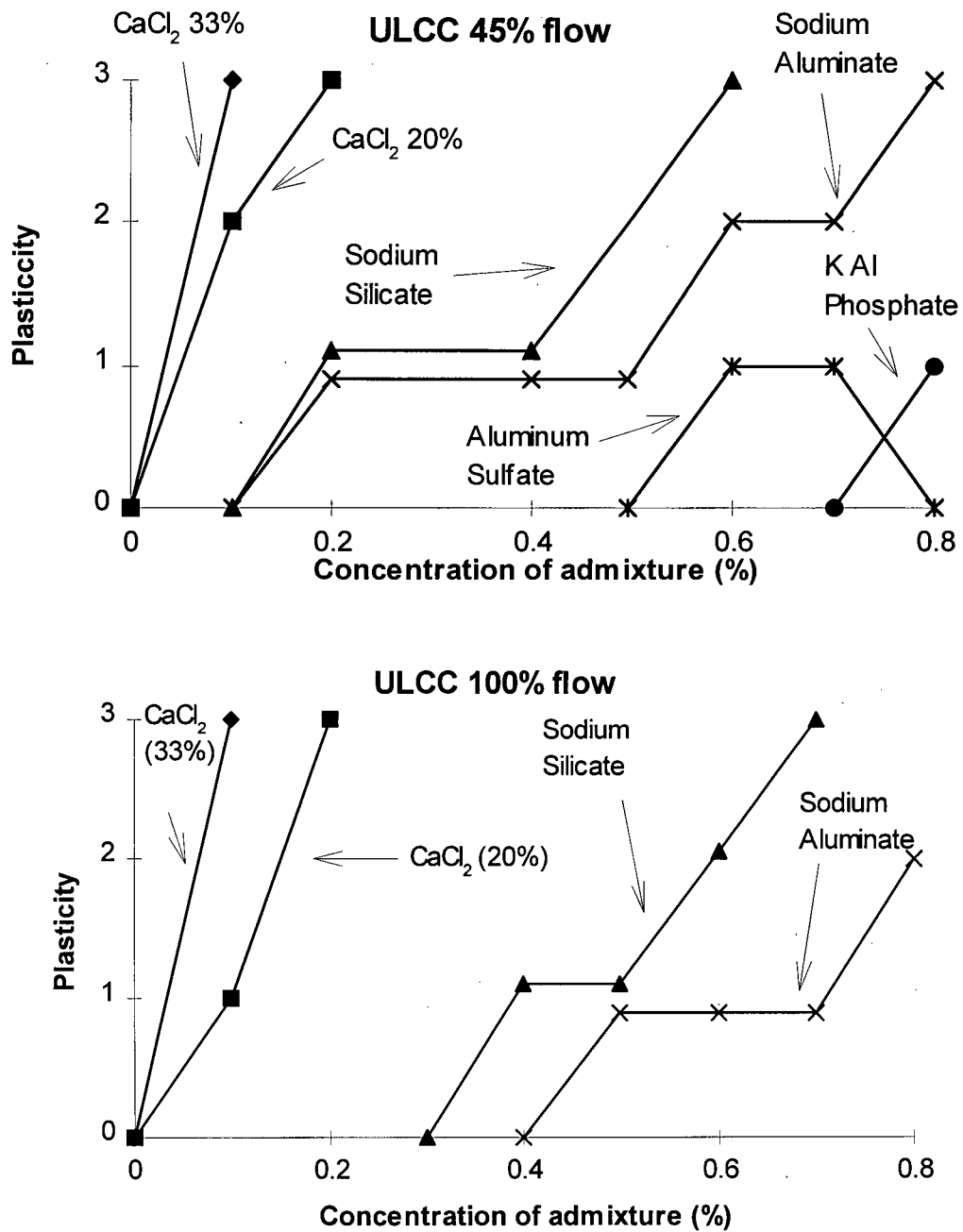
Figure 4.5-2. The effect of accelerator admixtures on plasticity for ULCC composition based on Mulcoa 60 (Table 4.2-5), at 45% and 100% flow.

results (Figure 4.5-1 and 4.5-2) showed that the use of strong setting accelerators, such as $CaCl_2$ solution, results in a rapid loss of plasticity. Weak accelerators, such as aluminum sulfate and potassium phosphate, may loose their effect at certain water levels or some compositional characteristics of the castable. The best options seemed to be the use of sodium aluminate and sodium silicate. However, during molding, the specimens prepared from the castable mixes accelerated with sodium aluminate and sodium silicate, it was found that sodium silicate induces a rapid setting for both LCC and ULCC formulations, making its use disadvantageous. Also, during the hand molding of the castables with these accelerators, it was found that sodium silicate induces a rapid setting for both LCC and ULCC formulations, making its use disadvantageous. It was considered that none of the admixtures mentioned represents a perfect solution for spray-gunning of refractory castables.

4.5.3. The Flash Flocculation (FF) concept

It may be considered, that a typical setting accelerator suppresses the flow due to a sudden release of Ca^{2+} ions through CAC hydration. If the accelerator system is too effective, an excess of Ca^{2+} ions results and a loss of plasticity occurs through flocculation of the matrix.

This proposed mechanism for flash setting is schematically presented in Figure 4.5-3. The main impediment in obtaining an effective acceleration combined with a good plasticity was identified in the autocatalytic character of the hydration reaction of calcium aluminate cement. An increased concentration of Ca^{2+} ions in the binding system removes the amorphous layer of calcium aluminates, and produces a sudden termination of the induction period. Accelerated hydration results in a massive release of Ca^{2+} ions, which triggers the flocculation of the binding system. The hydration completion causes the consumption of the interstitial water from the

binding system, which is producing the loss of plasticity. This mechanism explains the sensitivity flash setting accelerators to the water levels, and the content and type of hydraulic binder of the castable.

In order to avoid the sudden release of Ca^{2+} ions and the consumption of the interstitial water, it was necessary to use an admixture that suppresses the flow (by flocculation of the binding system) and simultaneously suppresses the flash setting of CAC. The effect of such a system consists just of a 'Flash Flocculation' of the binding system without triggering an accelerated hydration process and, subsequently, the loss of plasticity that is associated with the consumption of interstitial water.

The proposed mechanism for Flash Flocculation (FF) is presented in Figure 4.5-4. The initial experiments were conducted using binary mixtures of $CaCl_2$ and citric acid. The action of these admixtures proved to be difficult to control resulting in complete loss of plasticity or in low plasticity at levels of addition above 1%. Analysis of the correlation between viscosity of binding systems, setting time and content of plasticizer admixture, allowed to retard the setting time by using excess levels of plasticizers. Also by using an excess of plasticizer, the ionic strength of the interstitial solution increases, the double layer of fine reactive ceramic powders is compressed, zeta potential decreases and a supplementary flocculation effect occurs.

Additional experiments showed that SNFC cannot be used in the presence of sodium aluminate, calcium hydroxide, or sodium silicate because at high pH it transforms to an amorphous and viscous precipitate, but it can be used with calcium chloride.
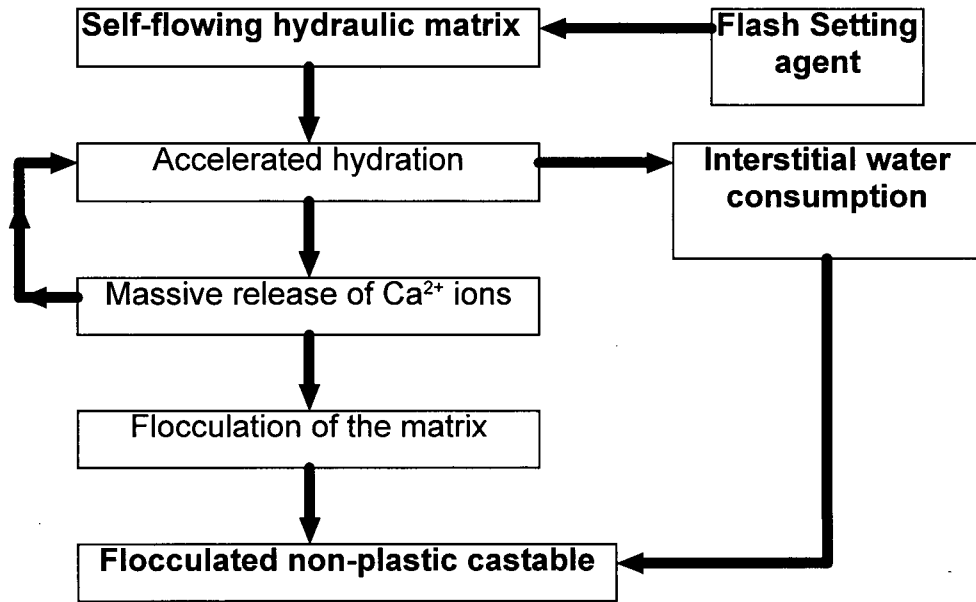
Figure 4.5-3. Flash setting mechanism.
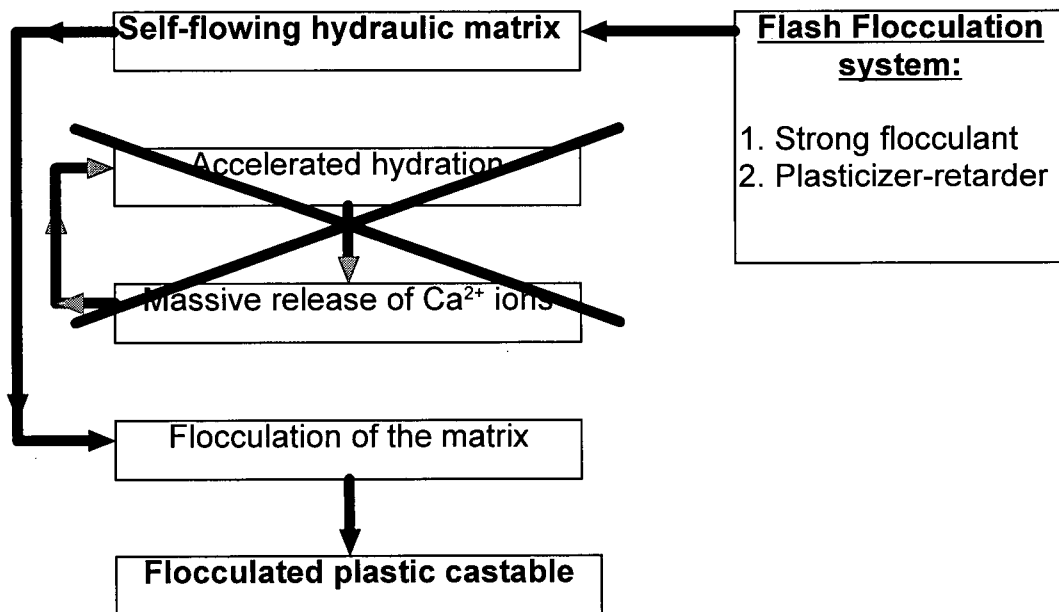
Figure 4.5-4. Flash Flocculation mechanism.

198

Two flash-flocculating admixture solutions (FFAS) were designed. One was a mixture of calcium chloride, STPP and SNFC, and the other one is a mixture of calcium chloride and SNFC. The compositions of the two solutions are presented in Table 4.5-4.

Table 4.5-4. Compositions of FF solutions.

Component (g/ml)	A1	A2
Calcium Chloride	0.25	0.25
STPP	0.1	0
SNFC	0.25	0.25

The first experiments were performed on LCC 34 compositions. Both FFAS proved to be very effective and very stable in suppressing the slump while maintaining the plasticity for a large range of concentration and for different initial amounts of water used for casting (Table 4.5-5). Composition A2 was more effective that A1 and this could be due to the fact that STPP is not an essential component for setting time retardation and its excess does not provide a major decrease in flow.

Table 4.5-5. Flash Flocculation tests using A1 and A2 solutions.

FFAS	Concentration (wt.%)	LCC 34 5% water	LCC 34 5.5% water
A1	0.2	flow	flow
A1	0.3	no flow / plastic	flow
A1	0.4	no flow / plastic	no flow / plastic
A1	0.6	no flow / plastic	no flow / plastic
A1	0.8	no flow / plastic	no flow / plastic
A2	0.2	no flow / plastic	no flow / plastic
A2	0.3	no flow / plastic	no flow / plastic
A2	0.4	no flow / plastic	no flow / plastic
A2	0.6	no flow / plastic	no flow / plastic
A2	0.8	no flow / plastic	no flow / plastic

FFAS agents do not induce fast setting and stiffening and, as a result, after mixing the castable remained plastic and trimming was possible. The plasticity of the fresh mixed material was in fact better that the one given by sodium silicate solution. From the results presented in Table 4.5-5 it may be concluded that the use of Flash Flocculants and in particular A2 solution bring the following advantages :

- it has a stable effect over a very large range of addition (0.2-0.8%);

- it is effective at very low levels of addition (0.2%);

- it gives good plasticity of the castable mix;

- it prevents immediate hardening/apparent drying of the castable ;

- it is not sensitive to the level of water used for preparing the self-flowing castable mix.
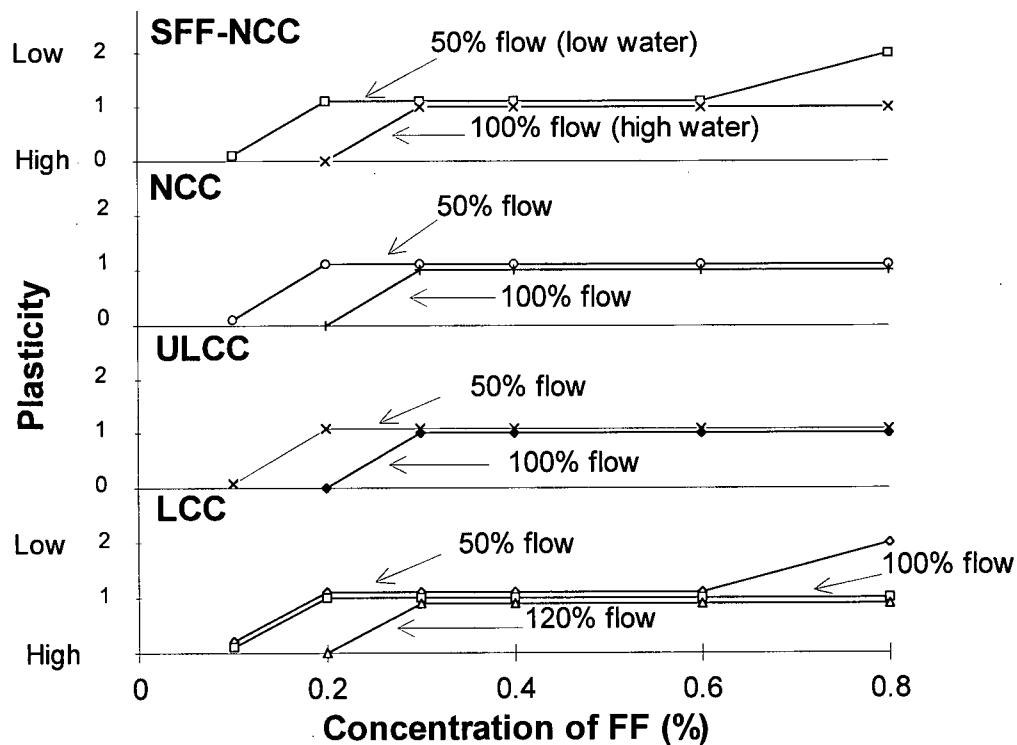
Figure 4.5-5. Plasticity rating versus concentration of A2 as FF admixture.

Further experiments tested the composition A2 with LCC (LCC 34), ULCC, NCC and SFF-NCC compositions (Figure 4.5-5). For all these compositions the experiments indicated that, if compared to flash setting, the Flash Flocculation offers not only a better solution for spray-gunning of self-flowing castables, but also has the advantage of acting independently of the hydraulic setting and therefore it can be used with the same effect for LCC, ULCC, NCC and NCC-SFF.
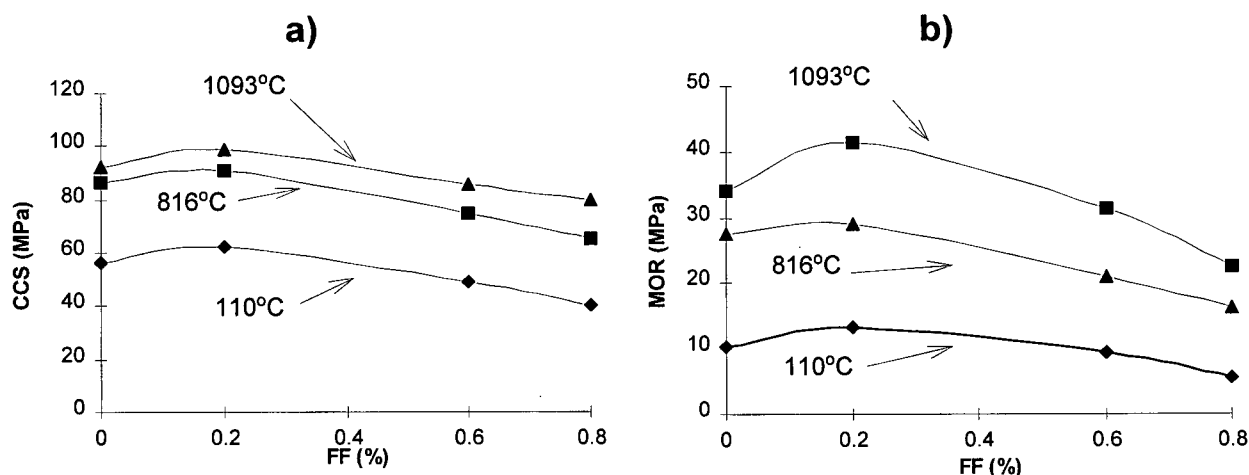
Figure 4.5-5. Laboratory testing of: a) MOR, and b) CCS, of LCC 34 formulation, for different levels of admixture of FF agent (0% FF corresponds to casting without vibration).

Further experiments were performed in order to study the influence of the FF admixture on the mechanical properties of refractory castables. Figure 4.5-6 shows the laboratory testing of MOR and CCS of LCC SFR 34 formulation, for different levels of FF admixture solutions.

The strength of LCC specimens molded at minimum level of admixture (0.2% FF) was higher than in the case of specimens without addition of FF. This is explained by the fact that at this level of admixture, the Flash Flocculated castable has a high plasticity and the compaction during molding translates into a better homogeneity. Even for a 0.8% admixture level, when the mix has a low plasticity, the strengths of Flash Flocculated castable represented 60-80% of the castable strength, molded by casting (i.e. at 0%FF).

Even for high concentration of FF agent, there is no negative effect on mechanical properties of the castable, due to formation of low melting point phases. This aspect is better presented by the HMOR data. The trend of variation of HMOR is similar to that of MOR. Figure 4.5-7 presents a comparison between the HMOR of LCC without admixture and LCC with admixtures of FF agent, sodium silicate and sodium aluminate. For the same level of admixture and the same level of plasticity, the Flash Flocculation is superior to the flash setting process. The lower HMOR values obtained for flash setting admixtures, and the higher relative difference between the HMOR at 816°C and 1093°C, indicate that even at the minimum concentration, these agents have a negative effect on strength of the castable because they induce a lower plasticity and consequently structural defects in the castable.
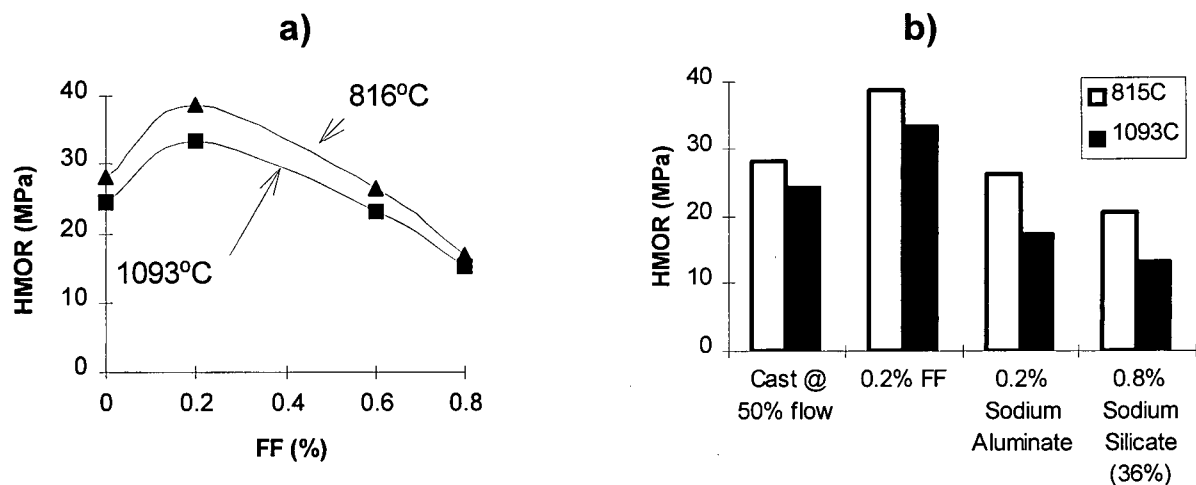
Figure 4.5-7. Variation of HMOR of LCC a) with concentration of FF , and b) for different spray gunning admixtures.

4.5.4. Pilot scale experiment

The first spray gunning pilot scale experiment was performed with LCC 34 accelerated with sodium aluminate. However, a short time after beginning spraying the accelerator nozzle was clogged, and only half of the required quantity of castable was installed. Although the castable showed a good flow in the hose and the material that was installed on the spraying target showed no slump, the experiment was only partially successful. The main cause for the accelerator nozzle clog was identified to be the fast stiffening and setting produced by sodium aluminate and insufficient pressure in the accelerator line. This resulted in the reflux of the castable from high pressure spraying hose into the accelerator line.

For the second pilot scale experiment (Figure 4.5-8), several improvements were made:

- the injection system of the spray-gunning admixture was redesigned in order to avoid nozzle clogging;

- an FF agent was used, in order to avoid clogging and fast setting of the castable;

- the castable formulation, LCC 83, had improved setting characteristics (i.e. the same flow value for 2 hours after mixing, for a setting time of 8 hours).

Before the pilot scale experiment, the composition LCC 83 was subjected to laboratory testing in order to asses its flow mechanical properties. Because LCC 83 was made with a low grade silica fume SF3 (Duralum AB, Washington Mills), more test specimens containing high purity silica fume (Elkem 971, Elkem, Norway) were prepared. The results of the laboratory testing made on LCC 83 and on similar compositions, LCC 83E, based on high purity silica fume, are presented in Table 4.5-6. The data presented in Table 4.5-6 demonstrates that both

Table 4.5-6. Mechanical properties of Flash Flocculated specimens (laboratory data).

MOR(MPa)	LCC 83	LCC 83 + 0.2% FF	LCC 83 + 0.8% FF	LCC 83E	LCC 83E + 0.2% FF	LCC 83E + 0.8% FF
after 5H at 110°C	10.34	13.44	5.69	12.93	11.89	10.86
after 5H at 1093°C	27.66	26.12	16.22	31.22	34.03	14.97
HMOR (MPa)						
at 1093°C	24.3	25.86	15.51	28.44	33.09	14.48

LCC compositions have high mechanical strengths, and are compatible with the Flash Flocculating agent.

An Aliva III machine was used for the gunniting plant trial (Figure 4.5-8). This machine is a revolving pump, consisting in a drum with six cells, that are filled one by one with the wet castable and then the cylinders are discharged on a stream of compressed air (5 atm in the secondary circuit, and 7 atm in the primary circuit), and pushed through a special designed nozzle, into the gunning hose. While one cylinder is discharging, the next cylinder is filled with fresh material from the hopper above it. A swing tube valve automatically positions in front of the discharging cylinder, to avoid the air pressure to enter through the cylinder and the hopper. With proper cylinder filling, this allows an almost continuous flow of material to the outlet. Because an admixture dosing pump was not available in UBC, the injection unit was built in house, using a gas pressured tank containing the liquid solution of FFAS. This designed assured a maximum reliability of the system, and flexibility for handling the possible pressure transients at the spraying nozzle.

After mixing, the castable was poured into the vibrating hopper of the Aliva pump. The existence of the vibrator hopper allows the feeding of the pump with the castable, which has no free flow or very low flow values. The material fills the cylinder cells of the revolving drum, and arrives in a jet of compressed (secondary) air. The mixture of high velocity compressed air and castable is injected through the hose. On the main hose, the secondary air and FFAS is
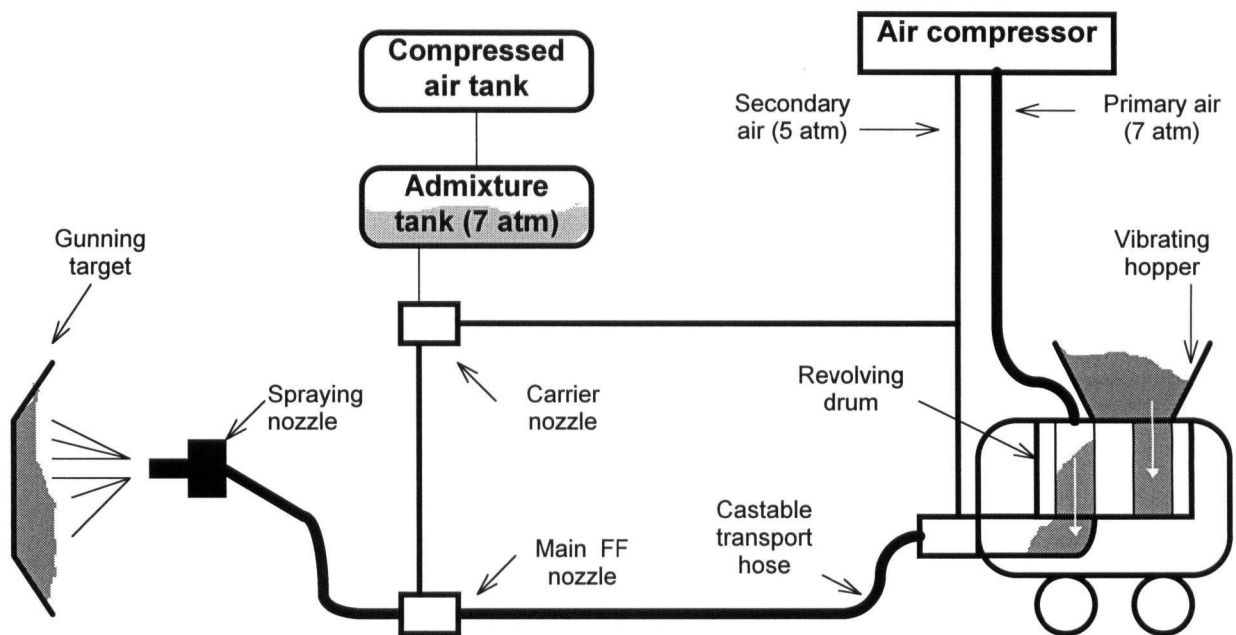
Figure 4.5-8. The design of the spray-gunning experimental setup.

injected through the main accelerator nozzle and forms a fine mist that is mixed with the castable. The castable is finally ejected through the spraying nozzle to the target panel. The admixture solution was stored in the pressurized tank. The pressure above the liquid was provided by the compressed air tank, which was equipped with a pressure regulator. A needle valve allowed the solution of Flash Flocculating agent to be injected through the carrier nozzle into the secondary air stream.

This setting had the following advantages:

• The feeding of the admixture solution from the pressure vessel avoided any overflow problems that might occurred in the case of the high pressure liquid pumps. Also due to the buffer effect of the gas pressure, a stable and easy flow control of admixture was possible;

- The use of the secondary air carrier allowed for the injection of a fine mist of admixture. Due to its relatively high pressure (5 at.) and constant flow it prevented the clogging of the main FFAS nozzle, at the start-up or at the end of the gunning process.

- The injection of the admixture at 5 meters before the spraying nozzle allowed for a better mixing and a longer reaction time between the castable and the FF agent.

A quantity of 240 kg of LCC 83 mix, prepared at Clayburn Refractories, was divided into two equal batches and sprayed on the vertical wooden target panels. The first batch of 120kg of castable, was sprayed without any addition of accelerator, in order to test the pumping capability of the mix. The pumping experiment was successful, the mix SFR 83 at 5.5% water showed a stable high flow rate of 240kg/min, even for secondary air pressures 40% lower than the nominal value (3 atm instead of 5 atm).

The second batch was sprayed with the addition of FF agent (A2). Due to an operating mistake the spraying started with a high excess of admixture. By reducing the FFAS flow, the material adhered to the target panel, proving no slump and a very good plasticity that remained at the same level for more than 2 hours. Also due to the high plasticity provided by A2 there was no rebound during the gunning process.

After demolding and drying, the test specimens were cut from the gunned pannels, using a diamond saw. The specimens were subjected to mechanical testing (CCS, MOR and HMOR) and to open porosity and permanent linear change measurements.

Table 4.5-7 presents a summary of the properties of self-flowing LCC 83 and LCC 34 compositions, and also the properties of the material resulted from pilot scale experiments. Both castable compositions are characterized by self flow behavior at low water levels. With the exception of the MOR after drying LCC 83 has better properties than LCC 34. The results of the pilot plant experiments confirmed the fact if compared to casting the Flash Flocculation does is not produce an important decrease in the strength of the spray gunned castable. Both LCC compositions show a continuous increase in strength in the 110-1093°C temperature range.

The plant trial showed that:

Table 4.5-7. Properties of SFR 83 and SFR 34 compositions.

Property	LCC 83	LCC 34
Dry weight required for installing, (t/m^3)	2.88	2.72
Amount of water required for pumping/casting, (%)	5.25-5.75	5.25-5.75
Bulk density, (t/m^3)	3.03*	2.86
Cold Modulus of Rupture (MOR) after		
Drying at 110°C, (MPa)	11.4* (10.34)	14.04
Heating at 816°C, (MPa)	39.9*	22.08
Heating at 1093°C, (MPa)	26.89* (27.66)	25.18
Cold Crushing Strength (CCS) after		
Drying at 110°C, (MPa)	60.21*	48.32
Heating at 816°C, (MPa)	94.92*	76.05
Heating at 1093°C, (MPa)	105.26*	98.02
Hot Modulus of Rupture (HMOR)		0
at 816°C, (MPa)	41.88*	26.72
at 1093°C, (MPa)	38.52* (24.3)	17.16** (28.43)
Permanent linear change after		0
Heating at 816°C, (%)	-0.07*	-0.056
Heating at 1093°C, (%)	-0.1*	-0.1

* gunned with A2
** gunned with sodium aluminate

- The composition LCC 83 is suitable for gunning applications at 5.0 to 5,5 wt% water. There was no segregation or dilatant behavior during the transport of the castable through the hoses;

- Spray-gunning of self-flowing refractory castables can be successfully performed using FFAS;

- By gunniting LCC 83 with FFAS, a highly homogeneous material was obtained, any segregation or laminations were avoided;

- The material resulted from the spray-gunning pilot scale experiment showed exceptional mechanical properties, similar to the materials installed by casting.

Based on the laboratory experiments and on the results of the pilot scale experiments it may be concluded that both compositions LCC 83 and LCC 34, are suitable for pumping and spray-gunning applications, using the newly developed Flash Flocculating admixture, containing calcium chloride and sodium naftalene-sulphonate formaldehyde-condensate (SNFC).

5. Conclusions

Based on the experimental and theoretical work carried out in this study, the following conclusions are drawn:

1. The flow properties of low, ultra low and no cement castables are determined by the rheological properties of the binding system and the particle size distribution of the refractory aggregate:

   - For castable compositions containing silica fume, the Andreassen model (with the Andreassen exponent q=0.21-0.25) provides particle size distributions characterized by goof self-flow properties. For silica fume free castable compositions the self-flow behavior was achieved using a particle size distribution characterized by an Andreassen exponent having a low value (q=0.22) for particles above 10μm and a high value (q=0.56) for particles below 10μm. It results that the Andreassen model is not the only solution for designing self-flowing compositions because the colloidal interactions between the ultrafine particles cannot be treated by a simple geometrical (mechanical) approach;

   - The binding system is a complex fluid for which the rheological and hydraulic properties are closely interconnected, and each individual component of the binding system has multiple effects on rheological and hydraulic interactions.

2. The viscometric study of the binding system is an important tool for a scientific and accurate investigation of hydraulic and rheological properties of self-flowing castables during the dormant period for the following reasons:

   - it is able to reproduce the shear conditions to which the hydraulic binder is subjected during the processing and application of Advanced Refractory Castables;

- compared to the flow measurement (which is a single point empirical measurement) it is more accurate, has a wider measuring range (often more than ten times), and provides a full rheological characterization with respects to the non-Newtonian aspects of flow;

- allows for the study of the hydraulic bond evolution during the dormant period and therefore, allows for the study of both rheological and hydraulic effects of chemical admixtures;

- provides a complete information on the effect of ultrafine reactive particles on the evolution of the hydraulic bond;

- for a given particle size distribution of the refractory aggregate, the viscosity of the binding system has a good correlation with the flow of the corresponding castable composition and, as a result, it provides a new and unique capability of correlating a macroproperty of a non-homogeneous fluid-solid mixture (the flow of the castable) with the fundamental rheological hydraulic properties of the binding system;

- from a technical point of view it has and unmatched capability for the multifactorial study and optimization of the content and nature of chemical admixtures.

3. The evolution of the hydraulic bond during the dormant period determines the early stages of the ceramic bond development. Solid experimental evidence showed that in favorable hydraulic and rheological conditions (such as low content of water and hydraulic binder and high reactivity of ultrafine particles), the ceramic matrix development occurs at temperatures as low as 500°C, which are well below the temperatures corresponding to the thermodynamic equilibrium solid-state reactions. In comparison with the existing concepts on the ceramic matrix formation in Advanced Refractory Castables, this new identified type of ceramic matrix development has several distinctive features:

- it is determined by the reactivity and quality of the ultrafine components of the binding system;

- the early strength development associated with the formation of the ceramic matrix takes place with no new crystalline phase development, as proved by the microstructural study and mechanical properties measurements for ultra low and no cement castables;

- the evolution of mechanical strength and open porosity with temperature, as well as the microstructural evolution with temperature, demonstrates that the early strength development cannot be attributed to a sintering process assisted by the formation of a metastable liquid, but rather to mechanism similar to that postulated by the "Superplasticity Theory";

- a proper compositional design of the binding system (high reactivity of ultrafine fraction and an optimized content of chemical admixtures) can trigger the development of the ceramic matrix before the total decomposition of the hydraulic bond and this is reflected in a significant increase in the mechanical strength of Advanced Refractory Castables.

4. The control of the hydraulic and colloidal interactions existing in the binding system is a key factor for the improvement of the application technology of Advanced Refractory Castables. A novel concept for spray-gunning, the Flash Flocculation concept, was developed using the knowledge generated by the present work. Compared to the existing technology of Flash Setting that relies on an uncontrolled accelerated hydration, in the Flash Flocculation process the colloidal suspension of the binding system losses its fluidity without interfering with the hydraulic setting. The novelty of the Flash Flocculation concept relies on the possibility of obtaining a colloidal flocculation of the binding system without triggering an accelerated hydration. The possibility of separation of hydraulic and colloidal interactions within the binding system was demonstrated for the first time, being the most important technical application generated during the present work, with an exceptional impact on the development of spray-gunning technology. From a scientific point of view the Flash

Flocculation concept represents the first approach of phenomenological design and optimization for Advanced Refractory Castables. As demonstrated by laboratory experiments and pilot plant trial, the Flash Flocculation concept brings a major improvement over the current spray-gunning technology based on Flash Setting, for the following reasons:

- The sprayed-gunned material using Flash Flocculation is characterized by an unprecedented plasticity as demonstrated by the pilot plant experiment. After the spray-gunning, the refractory installation maintained a high plasticity, that allowed trimming and indentation without cracking, for more than 30 minutes. This exceptional plasticity also resulted in the total absence of defects such as voids and laminations.

- Due to the fact that the Flash Flocculation does not depend on the hydraulic interactions and acts only on the repulsive interactions in the colloidal suspension of the binding system, it is effective for the spray-gunning of self-flowing castables regardless of their nature and content of hydraulic binder, ultrafine powders or chemical admixtures.

- By acting at colloidal level only on the rheology of the binding system the Flash Flocculation is very tolerant to processing errors. It is known that small variations in the dosage of Flash Setting agents can completely compromise the spray-gunning process. The experimental results showed that up to 200% overdosage of Flash Flocculation agent has no major impact on the spray gunning process or on the mechanical properties of the installed castable.

- Due to the low amount of Flash-Flocculation agents required for spray-gunning and the exceptional plasticity of the installed material, the Flash Flocculation process produces

high quality refractory installations, having similar properties to those obtained by casting.

Based on the results of the laboratory experiments and pilot plant trial it may be concluded that the Flash Flocculation agents are superior in every aspect to any Flash Setting agents that are currently in industrial use.

Due to the complexity of the Advanced Refractory Castables, most of the current research efforts in this field are hindered by the employment of an empirical and "trial-and-error" approach. During the present work, it was demonstrated that the development of scientific and accurate measurement methods, combined with a better understanding of the correlation of colloidal, chemical and solid-state phenomena are the key issue for achieving further significant advances.

6. Future work

As a result of the present study several direction for further investigation on the self-flowing castables are recommended:

1. In order to improve the performance of no cement castables the design of new hydraulic alumina binders with enhanced setting and flow properties is required. Particular attention should be focused on the hydration behavior of high alumina binders and the compatibility of these binders with plasticizer and accelerator admixtures.

2. The development of new binding systems based on magnesia spinel fine powders should result in further improvement of silica fume free no cement castables. The use of magnesia spinel as major constituent of the silica fume free no cement castables should result in increased thermal shock resistance, HMOR and corrosion resistance to basic slags.

3. The investigation of the possibilities of hydraulic activation of silica fume particles is of particular importance. This research is important to better understand the colloidal interactions existing in the binding systems.

4. The study of the effects of aluminum non-wetting additives (such as CaF_2 , $BaSO_4$, metakaolin etc.) on flow and mechanical properties of low cement castables would bring an opportunity for improving corrosion resistance of self-flowing refractory castables used in the aluminum industry.

5. Pilot scale experiments of spray gunning of no cement castables and silica fume free no cement castables with flash flocculating admixtures would validate the conclusions of the laboratory experiments. Also further refinement of the Flash Flocculation concept by the design of Flash Flocculation Admixture Systems for specific use in castables containing high alumina binders is recommended.

References :

[1]   W. E Lee and R. E. Moore, *"Evolution of In Situ Refractories in the 20th Century"*, J. Am. Cer. Soc., 81 (6) 1385-1410, 1998

[2]   L.P. Krietz, et al., *"Evolution and Status of Refractory Castable Technology Entering the 1990s"*, Am, Cer. Soc. Bull.,69 (10),1690-1693, 1990

[3]   E. Criado, et al., *"Database on Refractory Materials for Iron and Steelmaking "* " Refractories for the Steel Industry", R. Amavis, Ed. Elsevier. Appl. Sci., 118-129,1989

[4]   G. Klages et al., *"Requirements for Refractory Materials in Modern Steel Production"* " Refractories for the Steel Industry", R. Amavis, Ed. Elsevier. Appl. Sci.,133-141 , 1989

[5]   R. Baker, *"Future Steelmaking Requirements and Implications on Refractories"*, " Refractories for the Steel Industry", R. Amavis, Ed. Elsevier. Appl. Sci., 112-151, 1989

[6]   D.R.Lancard, *"Evolution of Monolithic Refractory Technology in United States"*, "Advances in Ceramics", R.E. Fisher, (13), Ed. Am. Cer. Soc., Columbus, Oh., 46-66, 1985

[7]   C.E. Semler,*"Overview of Refractory problems In Industry"*, Interceram 40,(7), 534-539,1991

[8]   T. Imay, *" Future Trends in Steelmaking Process in Japan"* Proc. of UNITECR '93, Sao Paolo, Brasil, 95-130, 1993

[9]   P. Jeschke et al., *"Recent Tendencies in Refractories for Iron and Steel Production"* Proc. of UNITECR '93, Sao Paolo, Brasil, 95-130, 1993

[10]   X. C. Zong,*"China's Refractories Industry on the Advance"* Interceram 44, (2), 105-110, 1995

[11]   E. S. Wright, *" Manufacturing and Market Trends in the U.S. Refractory Industry"* , Am, Cer. Soc. Bull.,69, (7), 1155-1162, 1990

[12]   G. Oprea, *" Advanced Refractory Castables"*, Proceedings of the International Symposium on Advanced Ceramics for Structural and Tribological Applications, CIM, Vancouver, BC, Canada, 93-106, 1995

[13]   P. White et. al., *"Use of Silica Fume and other Ultrafine Particles in Low Cement Castables "*, Proceedings of the UNITECR '91, Aachen, Germany, 181-185, 1991

[14] T.A., Bhier, " *Admixtures and their Interaction with Range Calcium Aluminate Cements* ",Proceedings of the UNITECR '95, Kyoto, Japan, 357-364, 1995

[15] H.F.W. Taylor, "The Chemistry of Cements", Academic Press, London, 1964

[16] Y Sasagawa et al., *"Role of Alumina Cement in Castable Refractories"*, Proceedings of the UNITECR '91, Aachen, Germany, 301-308, 1991

[17] D. A. Fumo et. Al., *Calcium Aluminates for Refractory Castables: Synthesis and Hydration Behavior*", Proceedings of the UNITECR '91, Aachen, Germany, 329-336, 1991

[18] A. Capmas and D. Menetrier-Sorrentino, "*The Effect of Temperature on the Hydration of Calcium Aluminate Cement*", Proceedings of UNITECR '89, Anaheim, California, 1157-70, 1989

[19] C. M. Freitas et al., *"Hydration Conditions and Microstructure Development in Calcium Aluminate Cements' Pastes"*, Proceedings of UNITECR '93, Sao Paulo, Brasil, 684-696, 1993

[20] K. Fujii, et al.,*"Kinetics of Hydration of Monocalcium Aluminate"*, J. Am. Cer. Soc., 69 (4), 361-364, 1986

[21] D. Mentrier-Sorentino et. al.,*" Hydration of Amorphous and Crystallized Compounds Based on Monocalcium Aluminate"* Proceedings of the UNITECR '91, Aachen, Germany, 267-271, 1991

[22] D. A. Fumo et. al., " *Effect of Silica Fume Additions on the Hydration Behavior of Calcium Aluminates*", Proceedings of the UNITECR '97, New Orleans LA, USA, 1325-1333, 1997

[23] Y. Hongo, *"ρ-Al$_2$O$_3$ Bonded Castable Refractories"*, Taikabutsu Overseas, 9, 35-38, 1989

[24] M.W. Vance and K.J. Moody *"Use of Hydratable Alumina Binders in Refractory Castables and Related Applications* ", paper presented at the 97th ACERS Annual Meeting and Exposition, May 1, 1995, Cincinnati, Ohio.

[25] F. Azizian and M.A. Azam, *"Development of alumina-based binders for no cement castables"*, paper presented at The 97th ACERS Annual Meeting and Exposition, Cincinnati, Oh, 1995

[26] S. Mohmel et al., *Investigations on the Hydration Behaviour of Clinker Phases of High Alumina Cements,* Proceedings of the UNITECR '91, Aachen, Germany, 147-50,1991

[27] S. M., Busnell-Watson, and J.H., Sharp, *'"Further Studies of the Effect of Temperature upon the Setting Behavior of Refractory Calcium Aluminate Cements"*, Cem.& Concr. Res., 20, 623-635, 1990

216

[28] S. M., Busnell-Watson, and J.H., Sharp," *On the Cause of Anomalous Setting Behavior with Respect to Temperature of Calcium Aluminate Cements",* Cem.& Concr. Res., 20, 677-686, 1990

[29] D. R. Lankhard and L. E. Hackman, *"Use of Admixtures in Refractory Concretes",* Am. Cer. Soc. Bull., 62, 1019-1025, 1983

[30] J. H. Sharp et. al., *"The Effect of Admixtures on Hydration of Calcium Aluminate Cements",* Calcium Aluminate Cements, Chapmann and Hall, London , 127-141, 1990

[31] N. Bunt et. al., *"Additives in Calcium Aluminate Cement Containing Castables",* Proceedings of the UNITECR '97, New Orleans LA, USA, 1347-1354, 1997

[32] W. Gessner et. al.," *On the Influence of Specific Surface Area and Na_2O Content of Aluminas on the Hydration process in $CaO•Al_2O_3$ / Al_2O_3 Mixes",* Proceedings of the UNITECR '95, Kyoto, Japan, 313-320, 1995

[33] T. A. Bier, et. al.,*"Admixtures and their Interactions with High Range calcium Aluminate Cement",* Proceedings of the UNITECR '95, Kyoto, Japan, 357-367, 1995

[34] S.A. Rodger and D. D. Double, *"The Chemistry of Hydration of High Alumina Cement in the Presence of Accelerating and Retarding Admixtures",* Cem. & Concr. Res., 14, 73-82, 1984

[35] T. Matusovic and D. Curlin," *Lithium Salts as Set Accelerators for High Alumina Cement".* Cem. & Concr. Res., 23, 885-895, 1993

[36] T. A. Bier et al., *"The Use of Conductimetry to Characterize the Reactivity of Calcium Aluminate Cements",* Advances in Ceramics, Vol. 13, R. E. Fisher, Ed.Am. Cer. Soc., Columbus, Oh, 705-16 ,1985

[37] T. Kondo et. al., *"Relationships Between Setting Time and Additives in Castables",* Taikabutsu Overseas, 17 (2), 47-52, 1997

[38] B. Myhre and K. Sunde, *"Alumina based castables with very low contents of hydraulic compound. Part II."* Proc. of UNITECR '95 , Kyoto, Japan, 317-324, 1995

[39] J. P. Bayoux et al., *"Theory and Practice of Fume Silica-Aluminous Cement Interaction-Part I ".* Paper presented at UNITECR '89, Anaheim, California, 1989

[40]   P. White et al., *"Use of Fume Silica and other Ultrafine Particles in Low Cement Castables",* Proceedings of the UNITECR '91, Aachen, Germany, 181-185, 1991

[41] B. Monsen, A. Seltveit, *"Effect of Microsilica on Physical Properties and Mineralogical Composition of Refractory Concretes",* Advances in Ceramics, Vol. 13, R. E. Fisher, Ed. Am. Cer. Soc., Columbus, Oh, 201-210,1985

217

[42] R. C. da Silveira et al., *"Silica Fume - CCM Production and Application*
Proceedings of UNITECR '93, Sao Paulo, Brasil, 717-727,1993

[43] P. C. Aitcin et al., *Physical and Chemical Characterization of Condensed Silica Fumes,* Am.   Ceram. Soc. Bull., , 63, (12), 1487-1491, 1984

[44]   V. Yogendran et. al.,*" Hydration of Cement and Silica Fume Paste",*
Cem. & Concr. Res., 21, 691-708, 1991

[45] S. Urhan, *"Alkalii Silica and Pozzolanic Reaction in Concrete",*
Cem. & Concr. Res., 17, 141-152, 1987

[46] S. Bentsen et. al.,*" Calcium Aluminate Cements",* Chapmann and Hall, London,
294-317,1990

[47] J. P. Bayoux et al., *"Theory and Practice of Fume Silica-Aluminous Cement Interaction-Part II"*, May 1990

[48] J. P. Bayoux et al., *"Theory and Practice of Fume Silica-Aluminous Cement Interaction-Part III"*,

[50] W. Gessner et. al., *"On the Influence of Alumina on the Hydration Behavior of Monocalcium Aluminate",* Proceedings of UNITECR '93, Sao Paulo, Brasil, 265-273,1993

[51] A. Mathieu et al., *"Calcium Aluminates Cements And Reactive Aluminas"*,
Proceedings of UNITECR '93, Sao Paulo, Brasil, 672-682,1993

[52] T. A. Bier et al., *"The Use of Conductimetry to Characterize the Reactivity of Calcium Aluminate Cements,* Proceedings of UNITECR '93, Sao Paulo, Brasil, 705-682,1993

[53] B. Myhre, *The Effect of Particle-Size Distribution on Flow of Refractory Castables",* Paper presented at ACERS 30th Annual Refractories Symposium,
St Louis, 1994

[54] B. Myhre, *"Particle Size Distribution and its Relevance in Refractory Castables"*,
Paper presented at the 2nd India International Congress, New Delhi, 8-9
February, 1996

[55] J. Chappuis, *"Rheological Measurements with Cement Pastes in Viscometers: a Comprehensive Approach"*, Proceedings of the International Conference of British Society of Rheology , Liverpool, UK, March 16-29 1990, p3-12, 1990

[56] V. S. Ramachadran and R. F. Feldman, *"Effect of Calcium Lignosulfonate on Tricalcium Aluminate and its Hydration Products"*, Mater. Cons., 26 (5), 67-76,
1972

[57]   E. Nagele, "*The Zeta Potential of Cement*", Cement and Concrete Research,15, ,
         453-462, 1985

[58]   E. Nagele, " *The Zeta-Potential of Cement. Part III : The Non-Equilibrium Double
         Layer On Cement*" Cem. & Conc. Res.,17 , 573-580, 1987

[59]   E. Nagele,"*The Zeta Potential of Cement: Part II Effect of pH-value*", Cement
         and Concrete Research,16, 853-863, 1986

[60]   E. Nagele, "*The Zeta Potential of Cement: Part IV Effect of Simple Salts*",
         Cement and Concrete Research,17, 977-982, 1987

[61]   P. J. Andersen et al., " *The Effect of Calcium Sulfate on the Adsorption of a
         Superplasticizer on Cement* " Cem. & Conc. Res., 16, 255-259 , 1986

[62]   E. Nagele, " *The Zeta-Potential of Cement. Part V : Effect of Surfactants*"
         Cem. & Conc. Res.,18 , 257-264, 1988

[63]   P. J. Andersen et al., " *The Effect of Superplasticizers and Air-Entraining Agents
         on the Zeta Potential of Cement Particles*" Cem. & Conc. Res., 16, 931- 940,
         1986

[64]   E. Nagele, "*Correlation Between Zeta-Potential and Mechanical Properties of
         Cementitious Materials* ", Cem. & Conc. Res.,18 , 257-264, 1988

[65]   F. Massazza et al.,"*Interaction Between Superplasticizers*", J. Am. Ceram. Soc.,
         65 (4), 203-207,1982

[66]   L. Nachbaur et. al., "*Electrikinetic Properties which Control the Coagulation of
         Silicate Cement Suspensions during Early Age of Hydration*", Journal of Colloid
         and Interface Science, 202, 261-268, 1998

[67]   H. Uchikawa et. al.,"*The Role of Steric Repulsive Force in the Dispersion of
         Cement Particles in Fresh Paste Prepared with Organic Admixture*", Cem. &
         Conc. Res., 27 , 37-50, 1997

[68]   M. Yang and H.M. Jennings, "*Influence of Mixing Methods on the Microstructure
         and Rheological Behavior of Cement Paste*", Adv. Cem. Based Mat., 2, 70-78,
         1995

[69]   R. Lapasin et. al., "*Flow Behavior of Fresh Cement Pastes. A Comparison of
         Different Rheological Instruments and Techniques*", Cem. Conc. Res., 13,
         349-356, 1983

[70]   P. Banfill and D.C. Saunders, "*Viscometric examination of cement pastes*",
         Cement and Concrete Research, 11 (3), 363-70, 1981

[71]   R. Lapasin, "*Rheology of Cement Pastes*", Il Cemento, 79 (4), 217-226, 1982

[72]   R. Shaughnessy and P.E. Clark, *"The Rheological Behavior of Fresh Cement Pastes"*, Cem. Conc. Res., 18, 327-341, 1988

[73]   Y. E. Pivinskii, *"Refractory Concretes of New generation. General Characteristics of the Binder System"* , Ogneupory, 12, 1-8, 1991

[74]   J. Chappuis and J. P. Bayoux, *"A Comprehensive Study of Rheology of Aluminous Cement Pastes",* Proceedings of UNITECR '89, Anaheim, California, 1171-82, 1989

[75]   A. Papo, B. Caufin, *"A rheological study of cement pastes by oscillatory means"* Cem. & Concr. Res. 21, 1111-17, 1991

[76]   Y. E. Pivinskii, *"Refractory Concretes of New generation. General Rheological Aspect"* , Ogneupory, 35, 116-125, 1994

[77]   Y.P. Ivanov and T. T. Roshavelov, *"Flow Behavior of Modified Cement Pastes",* Cem. & Concr. Res. 23, 803-810, 1991

[78]   K. Watanabe et. al., *Rheology of Castable Refractories"*, Taikabutsu Overseas, 9, 41-53, 1981

[79]   W. Gessner et. al., *"On the Change in Microstructure During Hydration of Monocalcium Aluminate at 20ºC and 50ºC"*, Calcium Aluminate Cements, Chapmann and Hall, London , 96-110, 1990

[80]   H. Fryda et. al., *"Relations Between Setting Properties of Low Cement Castables and Interactions Within the Binder System (CAC-Fillers-Admixtures-Water)"*, Proceedings of the UNITECR '97, New Orleans LA, USA, 1315-1323, 1997

[81]   H. Nakashima, *'Application of Self-Flow Type Castable Refractories in NKK"*, Proc. of UNITECR '95 , Kyoto, Japan, 205-213, 1995

[82]   D.R. Dinger and J.E. Funk *"Particle Packing. Part 4: Computer Modeling of Particle Packing Phenomena"*, Interceram, 42 (3), 150-152, 1993

[83]   D.R. Dinger and J.E. Funk, *"Particle packing: II[B]: Review of packing of polydisperse particle systems"*, Interceram, 41 (3), 176-179, 1992

[84]   B. Myhre, *"Microsilica in Alumina Based Castables . The Effect of Additions on Flow."*, Proceedings of XXIII Congreso ALAFAR, Mexico, 160-171, 1994

[85]   B. Myhre and K. Sunde, *"Alumina based castables with very low contents of hydraulic compound. Part I."* Proc. of UNITECR '95 , Kyoto, Japan, 19-22, 1995

[86]   J. S. Masaryk et al., *"Development And Use Of Low Cement, Self-Flow Castables",* Proceedings of UNITECR '93, Sao Paulo, Brasil, 527-538,1993

[87] E.S. Octaviano, *"A Model Anaysis of Refractory Castables Self-Flow for Testing Optimization"*, Proceedings of the UNITECR '97, New Orleans LA, USA, 605-601, 1997

[88] A.M. Hundere and B. Myhre, *"Effect of Different Finest Fractions in Alumina Based Ultralow Cement Castables'*, paper presented at ACERS' 98th annual meeting and exposition, Indianapolis April 14-17, 1996

[89] B. Myhre and A.M. Hundere, *"Substitution of Reactive Alumina with Microsilica in Low Cement and Ultra Low Cement Castables"* , Proceedings of the UNITECR '97, New Orleans LA, USA, 43-52, 1997

[90] G.W. Kriechbaum, et. al., *'The Matrix Advantage System"*, Proceedings of the UNITECR '97, New Orleans LA, USA, 645-655, 1997

[91] R.A. Marra, *"Compositional Variables and Their Effect on Steel Slag Resistance and Hot Strength of High Alumina Spinel Castables"*, paper presented at UNITECR '97, New Orleans LA, USA, 1997

[92] H.F.W. Taylor, *"Cement Chemistry"*, Thomas Telford Publishing, London, 331, 1997

[93] Z. Li, et. al., *" Difference in Dispersing Effects Between Organic and Inorganic Deflocculants in Castables"*, Proceedings of the UNITECR '97, New Orleans LA, USA, 1355-1359, 1997

[94] J.R. Baldo and A.C. Morelli, *"The Effect of the Matrix Mass Fraction and the Defloculant Type on the Development of a Self-Flowing Low Cement Refractory Castable"*, Proc. of UNITECR '95 , Kyoto, Japan, 19-22, 1995

[95] F. Azizian, *"A Review of Actibond Binders in No Cement Castables"*, paper presented at ACERS' 100 anual meeting and exposition, Cincinnati, OH, 1998

[96] F. Azizian, *"Development of No-Cement Castables"*, paper presented at the 98th ACERS Annual Meeting and Exposition, April, 1995, Indianapolis, Indiana.

[97] B. Sandberg and B. Myhre, *"Microsilica. A Versatile Raw Material."*, paper presented at the Indian Refractories Congress, Jamshedpur, India, February, 1994

[98] J.L. Larosa-Thompson and M.W. Grutzeck, *"C-S-H, Tobermorite and Coexisting Phases in the Ssystem CaO-Al2O3-SiO2-H2O"*, J. Am. Cer. Soc. 79, (4), 967-971,1996

[99] K. Mohan and H.W.F. Taylor, *Analytical Electron Microscopy of Cement Pastes. Part IV"*, J. Am. Cer. Soc. 65, (3), 717-719,1982

[100] D. Viehland et al., *" Mesostructure of CSH Gels in Portland Cement Paste"*, J. Am. Ceram. Soc. 79, (7), 1731-1744,1996

[101]   G.W. Groves et. al., *"Transmission electron Microscopy and Microanalytical Studies of Ion-Beam-Thinned Sections of Tricalcium Silicates"*, J. Am. Ceram. Soc. 69 , 353-356,1996

[102]   K. Fujii and W. Kondo, *"estimation of Thermochemical Data for Calcium Silicate Hydrate"*, J. Am. Ceram. Soc.66, C 220-221,1983

[103]   X.D. Cong and R.J. Kirkpatrick, *"Introduction to ^{27}Al and ^{29}Si NMR Spectroscopy of Cements and Concretes"*, Appl. NMR Spectrosc. Cem Sci., pp. 55-75, 1994

[104]   H.F.W. Taylor, *"Proposed Structure for CSH Gel"*, J. Am. Ceram. Soc. 69, 464-467,1986

[105]   E.M. Gartner, *"A Proposed Mechanism for the Growth of CSH During the Hydration of Tricalcium Silicate"*, Cem. & Concr. Res.27, 665-672, 1997

[106]   B. Myhre, *"Cement-Free Castables in the System MgO-SiO_2"*, paper presented at ACERS' 93rd Annual Meeting and Exposition, Cincinnati, OH, May, 1991

[107]   J. Temuujin et. al., *"Formation of Layered Magnesium Silicate during the Aging of Magnesium Hydroxide-Silica Mixtures"*, J. Am. Cer. Soc. 81, 754-756,1998

[108]   H.F.W. Taylor, *"Nanostructure of CSH"*, Advn. Cem. Bas. Mat., 1, 38-46, 1993

[109]   I.G. Richardson and G.W. Groves, *"Incorporation of Minor and Trace Elements into Calcium Silicate Hydrate (CSH) Gel in Hardened Cement Paste'*, Cem .& Concr. Res.23, 131-138, 1993

[110]   S. Kwan et. al., *"Structures and Phase Relations of Aluminum-Substituted Calcium Silicate Hydrate'*, J. Am. Cer. Soc., 80, 967-971,1997

[111]   S. Kwan et. al., *" ^{29}Si and ^{27}Al MASNMR Study of Strtatlingite"*, J. Am. Cer. Soc.79, 1921-1926,1996

[112]   S. Kwan et. al., *"Structures and Phases Relations of Aluminum-Substituted Calcium Silicate Hydrate"*, J. Am. Cer. Soc. 80, 967-971,1997

[113]   P.S. de Silva and F.P. Glasser, *Phase Relations in the System CaO-SiO_2-Al_2O_3-H_2O Relevant to Metakaolin - Calcium Hydroxide Hydration"*, Cem. & Concr. Res.23, 627-639, 1993

[114]   M. Daimon et. al., *"Rheological Properties of Cement Mixes: II Zeta Potential and Preliminary Viscosity Studies"* , Cem. & Concr. Res., 9, 103-109, 1979

[115]   Y. Naruse, et al, *"Progress of Additives in Monolithic Refractories* "Advances in Ceramics", R. E. Fisher, (13), Ed. Am. Cer. Soc., Columbus, Oh., 245-256, 1985

[116]   I. Meland ,*"Influence of Condensed Silica Fume and Fly Ash on the Heat Evolution in Cement Paste"*, Proc. of ICUFASF, Montebello, Canada, 665-679, 1986

[117] D. L. Hipps, et. al., *"Internal Pressure Measurements for Control of Explosive Spalling in Refractory Castables"*, Cer. Bull.,63 (7), 905-910, 1984

[118] B. Myre , *"Development of a Bauxite Based Ultra-Low Cement Castable"*. Br. Ceram. Trans. J. , 90, 149-152, 1991

[119] E. P. Weaver et al., *"High-Tech Castables"*, Advances in Ceramics", R. E. Fisher,(13), Ed. Am. Cer. Soc., Columbus, Oh., 219-229,1985

[120] S. Banerjee, et al., *"Low-Moisture Castables: Properties and Applications "* Advances in Ceramics, R. E. Fisher, (13), Ed. Am. Cer. Soc., Columbus, Oh., 257-273,1985

[121]   C. Richmond and C.E. Chaille, *"High Performance Castables for Severe Applications"*, Advances in Ceramics, R.E. Fisher,(13), Ed. Am. Cer. Soc., Columbus, Oh.,230-244,1985

[122] B. Myhre and K. Sunde, *"Tabular Alumina Based Castables Part I"*, technical paper, Elkem Refractories , Norway, 1993

[123] J.M. Roy and L.R. Tingley, *"High-Performance Aluminas for Refractories"*, Interceram, 43, (5), 360-365, 1994

[124] E.M. Levin et.al, *"Phase Diagrams for Ceramists"*, Amertican Ceramic Society, Columbus, OH, 1964

[125] B. Myhre and K. Sunde, *"Tabular Alumina Based Castables Part II"*, technical paper, Elkem Refractories , Norway, 1993

[126] S. Banerjee, *"Monolithic Refractories"*, World Scientific Publishing, Singapore, 1998

[127] B. Myhre , *"Development of a Bauxite Based Ultra-Low Cement Castable"*. Br. Ceram. Trans. J. , 90, 149-152, 1991

[128] T. Eguchi, *"Low-Cement Bonded Castable Refractories"*, Taikabutsu Overseas, 9,10-25, 1989

[129] B. Myhre, *"Hot Strength and Bond-Phase Reactions in Low and Ultra-Low Cement Castable"*, Proceedings of UNITECR '93, Sao Paolo, Brasil, 583-594, 1993

[130] *"Refractories Handbook"*, The Technical Association of Refractories, Japan, 1988

[131] W.G. Allen, *"Advanced Equipment for Refractory Placement"*, Proceedings of the UNITECR '97, New Orleans LA, USA, 523-530, 1997

[132] S. Banerjee, *"Spray-Gunning Refractories"*, Proceedings of the UNITECR '97, New Orleans LA, USA, 553-562, 1997

[133] B. Myhre and A.M. Hundere, *"Free Flowing Castables- A prerequisite for Wet-Gunning of Refractory Castables"* , Proceedings of the UNITECR '97, New Orleans LA, USA, 43-52, 1997

[134] N. Cassens et. al., *"Shortcreting Self-Flow Refractory Castables"*, Proceedings of the UNITECR '97, New Orleans LA, USA, 531-544, 1997

[135] R.J. Scharf, *"Shortcreting Ultralow Cement Castable Refractories"*, Proceedings of the UNITECR '97, New Orleans LA, USA, 43-52, 1997

[136] B. Myhre and K. Sunde, *"Alumina based castables with very low contents of hydraulic compound. Part I."* Proc. of UNITECR '95 , Kyoto, Japan, 309-316, 1995

[137] H.A. Barnes and K. Walters, *"The Yield Stress Myth"*, Rheol. Acta, 25, 323-326, 1985

[138] D. Chen, *"Yield Stress: a Time Dependent Property and How to Measure It,"*, Rheol. Acta, 25, 542-554

[139] B. Myhre and B. Sandberg, *"Mullite Formation in Tabular Alumina Based Castables"*, paper presented at ACERS' 97th annual meeting, Cincinnati, OH, May 2nd, 1995

[140] A.C.D Chaklader, *"Reactive Hot-Pressing of Clays and Alumina"*, J. Am. Ceram. Soc., 49 (9), 479-483, 1966

[141]- A.C.D Chaklader, *"Flow Behavior of Hydroxides during Decomposition"*, Mat. Res. Bull., 4, 161-164, 1969

APPENDIX

Hot modulus of rupture (HMOR) Testing Apparatus

As a part of the research program, a Hot Modulus of Rupture Testing Apparatus was constructed in the Ceramics Laboratory of Metals and Materials Engineering Department of University of British Columbia. The apparatus was designed to comply to the requirements of ASTM C 583 for testing of HMOR of refractory castables, to utilize as much as possible the resources already existent in the department, and to allow an easy and efficient operation.

The apparatus consists of an electric furnace placed inside the frame of an Instron Universal Testing Machine. The main characteristics of operation are:

- maximum testing temperature: 1500°C.
- maximum heating rate: 400°C/h.
- maximum number of specimens (15x2.5x2.5 cm) loaded in a single run: 12.
- maximum force load: 15 kN.
- cross head speed 0.25 -0.0025 cm/min.

There are three major constituent parts of the Hot Modulus of Rupture Testing Apparatus:

1. High temperature furnace .
2. Force loading system.
3. Power supply, heating elements and temperature controller

High temperature furnace

The high temperature furnace is a light insulation board furnace placed inside the frame of an Instron Universal Testing Instrument. The thermal insulation consist of: a 2.5 cm inner layer of fiberboard Rath KVS 184 and a 5 cm outer layer of fiberboard Fiberfrax Duraboard 3000.

There are two doors to the furnace :

- main front door for loading the test specimens. This door has a quartz window protected by a refractory shield in order to allow the operator to view and correct, if necessary, the position of the samples in the furnace. There are also two alumina positioning rods that allows the correction any possible misalignment or blockage of the test specimens.

- bottom swinging door that allows the removal of the specimens immediately after testing.

Up to 12 test specimens may be loaded in the furnace in one run. The specimens are placed on two horizontal alumina tube rods (1.25 cm diameter) and pushed one by one under the load bearings, after testing, evacuated from the furnace through the bottom swinging door.

The components of the high temperature furnace are presented in Table 5-1.

Table 5-1. The characteristics of the components of the high temperature furnace.

Item	Type
Inner lining	1" refractory fiberboard Rath KVS 184
Outer lining	2" refractory fiberboard Fiberfrax Duraboard 3000
Lining support	hanger rods Zircar HR-2 with stainless steel shaft collars Zircar SC-1
Bottom door lining	2" refractory fiberboard Rath KVS 184 (two layers)
Insulating element holders	Zircar Type H-2
Strapping element holders	Zircar Type K-3
Guiding rods	1/2 " diameter 99.9% alumina rod
Pusher rod	1/2 " diameter 99.9% alumina rods
Pusher head	Part made using castable N1

The specimens are positioned one by one on the guiding rods under the load system. In between two specimens there are placed two refractory "T"-shaped spacers, to maintain a distance of about 1cm between specimens, and between the first specimen and the pusher head. The swinging door has a counterbalance that allows opening with a load corresponding to a half of the specimen weight (<0.12 kgf).
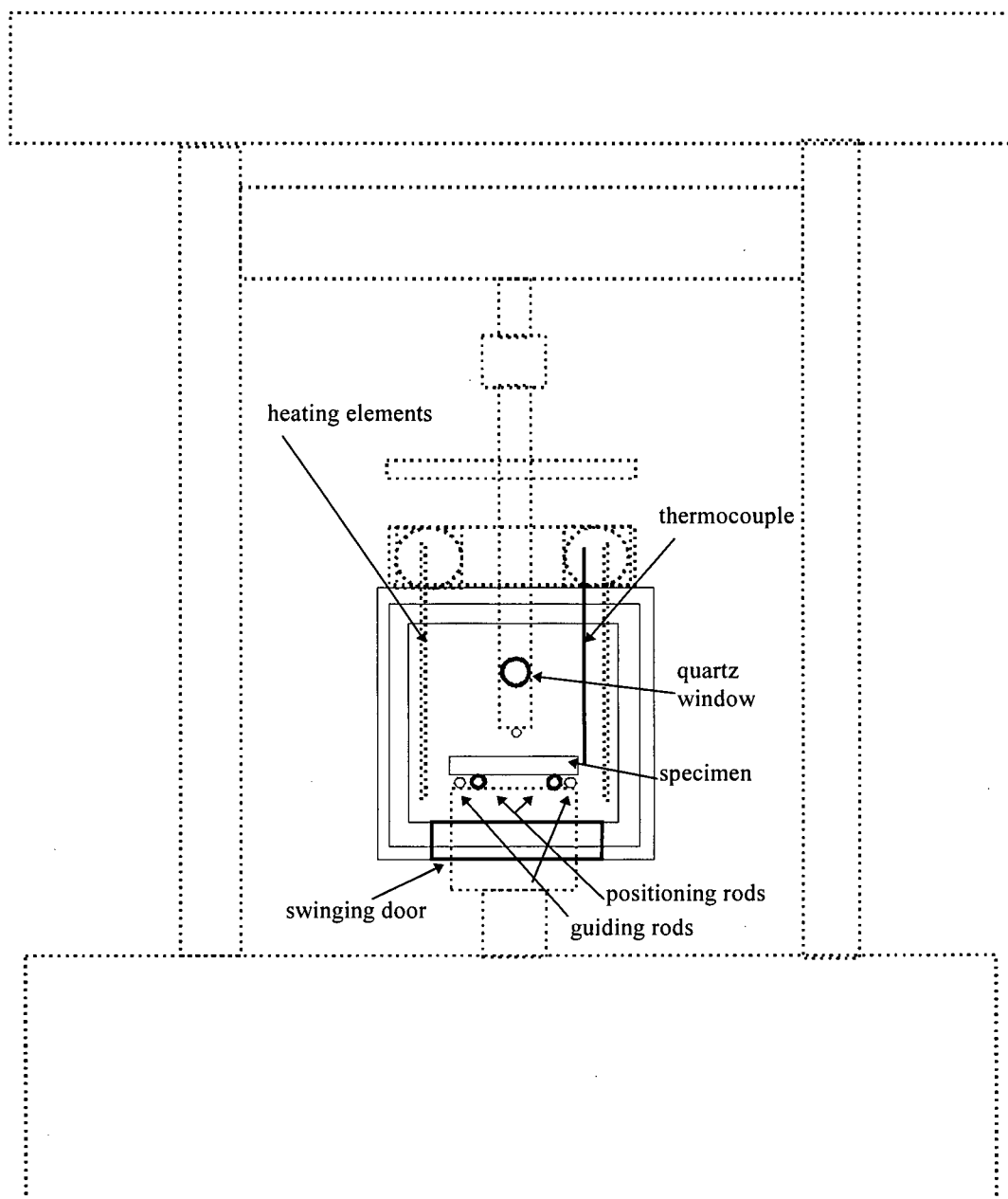
Figure 5-1. Front view of the high temperature furnace

The specimens, after testing, are pushed one by one by the new specimens, off the bottom load plate, and together with the two corresponding spacers, are evacuated through the swinging door out of the furnace (Figure 5-1). This design allows the evacuation of each specimen to be done by opening the swinging door for less than 1 second, and this translates to a stable thermal environment during testing.

Force loading system

The force loading system (Figure 5-2) is composed of:

- Instron Universal Testing Instrument (model FCL).

- load cell Omega LCCB-3K.

- upper cooling part.

- convection shield.

- force applying alumina rod (5cm diameter).

- upper load bearing (1.25 cm alumina rod).

- lower load bearings (1.25 cm alumina rods).

- bottom load plate (N1 castable).

- insulating bricks (Thermal Ceramics K-26).

- bottom cooling part.

The load cell is attached directly on the cross head of the Instron Testing Instrument, in a compressive fixture, and is continued by the upper cooling part. The upper cooling part consists of a brass cylinder (5 cm diameter) having copper cooling coils. Between the upper cooling part and the metallic fixture of the force applying rod, there is a convection cooling shield, directing the air flow generated by two cooling fans. This design is necessary in order to maintain the temperature of the load cell below 50°C degrees, and to allow a better cooling of the heating element ends. The bottom part of the force applying rod is grooved horizontally and the upper bearing rod is inserted. The lower load bearing rods, having a 12.5 cm span, sit on the bottom load plate, that sustains the ends of the guiding rods. Under the bottom load plate there are two insulating bricks (Thermal Ceramics K-26), sitting on the bottom water cooling system.

After testing more than 100 specimens, none of the parts of the force loading system had a breakdown or misalignment.

During measurements at temperatures above 1093°C and at high flow rate of water in the upper cooling system, water droplets may condense. This condensation should be avoided by reducing the flow rate of the water for cooling.
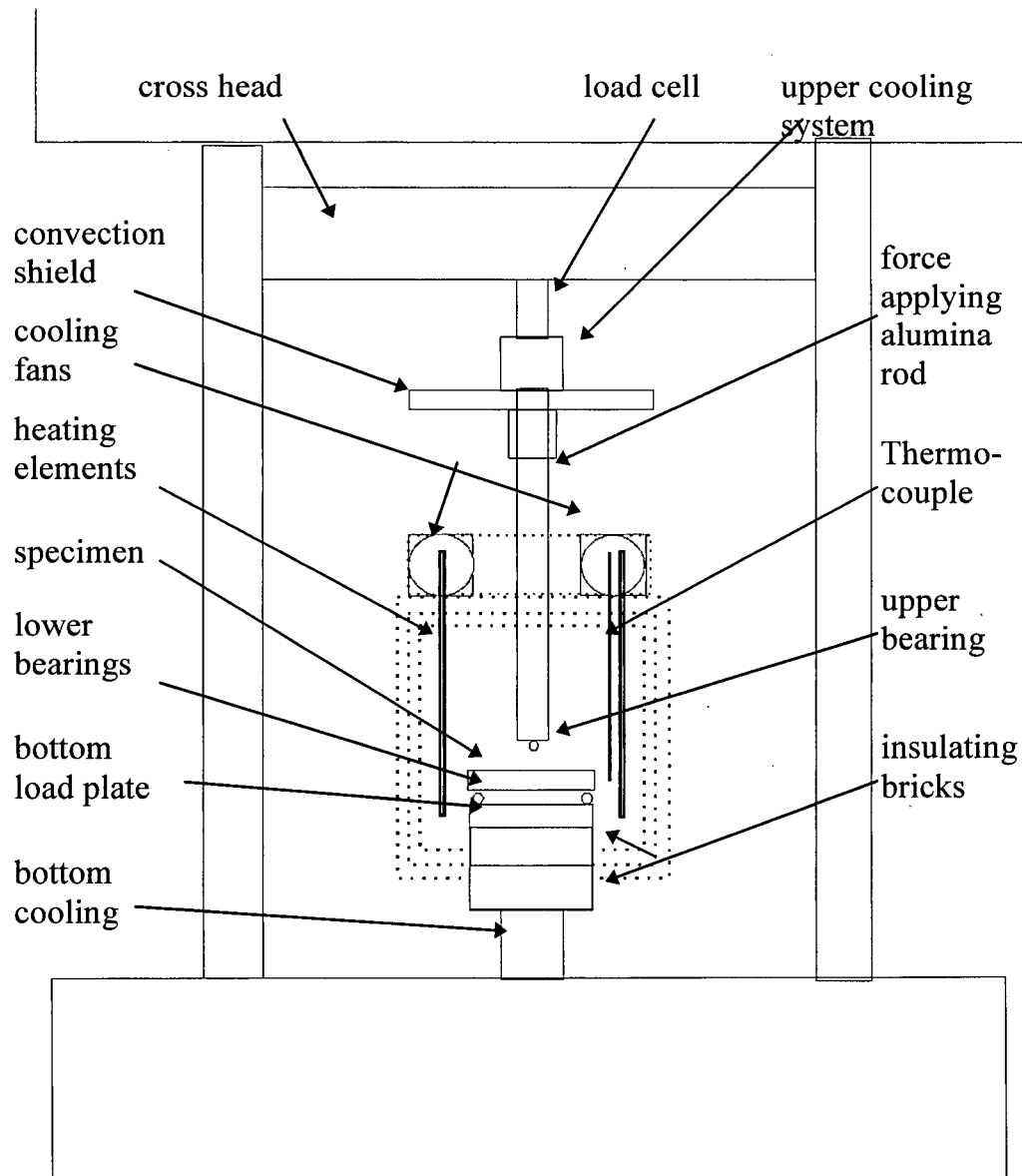

Figure 4.1-4. Design of the force loading system.

Power supply, heating elements, and temperature controller

The high temperature furnace is heated by eight $MoSi_2$ heating elements type Super Kantal 17-6/12-5-5-2. The elements have the maximum service temperature of 1700°C and the maximum power of 1000W. The eight elements (as shown in Figure 5-3) are connected in two parallel series, with 250A aluminum straps.

The temperature control unit consist of a Pt/Pt-13%Rh thermocouple connected to a programmable temperature controller (type Omega CN2011J-DCI) which commands a solid state relay (type SSR240DC75).

The variable power source consists of a high voltage variable tension source (220V 75A VARIAC) that allows the continuous variation of voltage in the range of 0-220V. The secondary coil of the VARIAC is connected through the solid state relay to the primary circuit of a low voltage transformer. As a result, at the secondary circuit the low can be continuously adjusted in the range of 0-40V for maximum currents up to 500A. This design was necessary because the resistivity of $MoSi_2$ elements varies with temperature, while the maximum power density remains constant. For safe operation of the furnace, the maximum current through the heating elements should be below 125A.

After several runs of the furnace it resulted that the thermal steady state in ramp up to temperatures of 1500°C is obtained for intensities of 80-100A. Currents of about 80A are recommended during the soaking time or specimen testing.
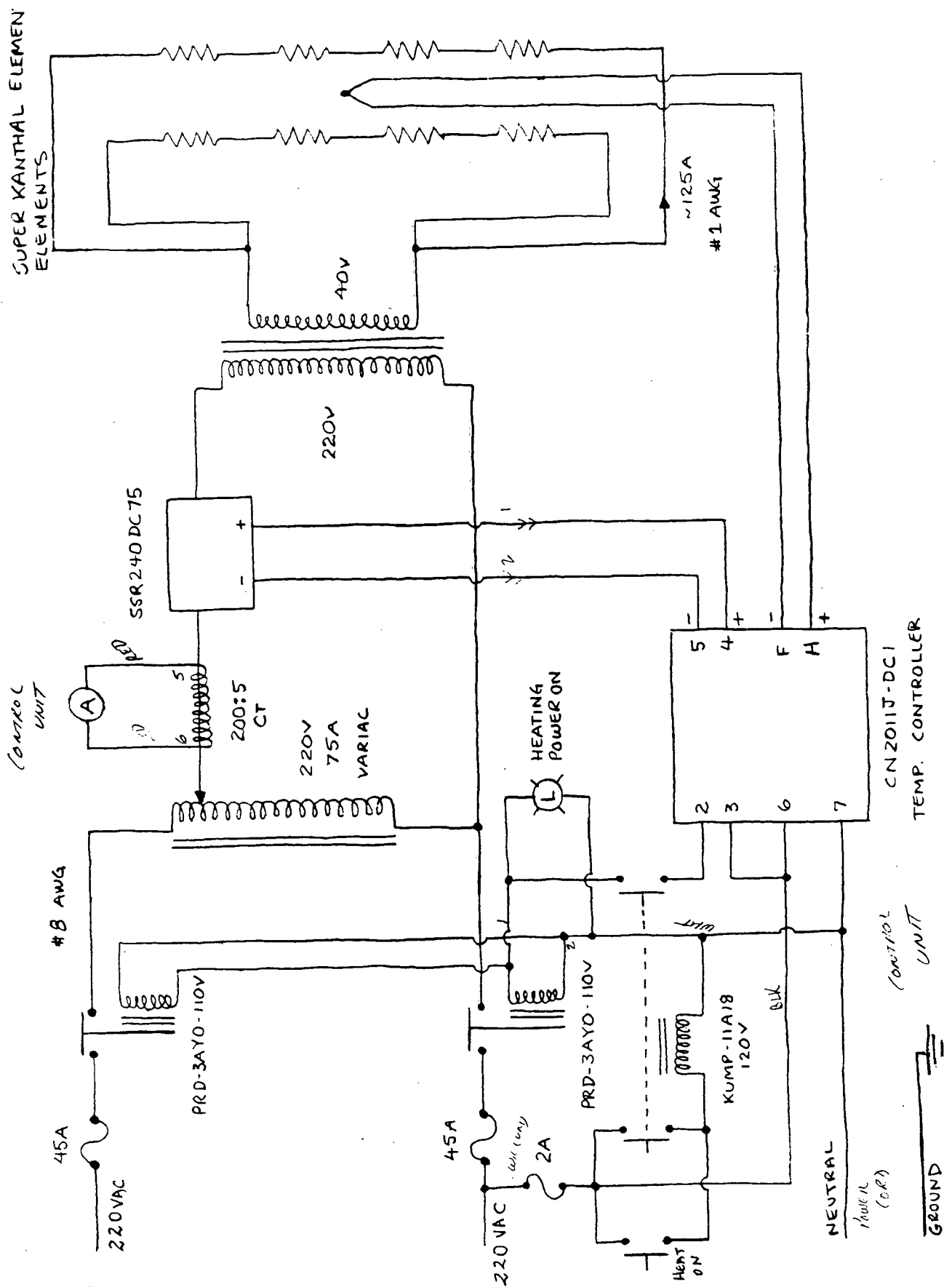
Figure 5-3. Electric design of the high HMOR furnace.